

**Human Carbonic Anhydrase II:
a Novel Scaffold for Artificial Metalloenzymes**

Inauguraldissertation

zur Erlangung der Würde eines Doktors der Philosophie

vorgelegt der

Philosophisch-Naturwissenschaftlichen Fakultät
der Universität Basel

von

Fabien Wilhelm MONNARD

aus Attalens (FR)

Basel, 2013

Genehmigt von der Philosophisch-Naturwissenschaftlichen Fakultät auf Antrag von:

Prof. Dr Thomas R. Ward

Prof. Dr Karl Gademann

Basel, den 11. Dezember 2012

Prof. Dr Jörg Schibler

Dekan

Acknowledgements

I would first like to thank Prof. Dr Thomas R. Ward for his support, guidance and contagious enthusiasm during my Ph.D. thesis. I am also grateful to Prof. Dr Karl Gademann for agreeing to co-referee this thesis.

I would like to thank all of my lab-colleagues, present and past, for their advice and the good times we shared. And, more particularly, extended thanks to Elisa, Jeremy & Thibaud.

Sincerest thanks go to Elisa Nogueira, Maurus Schmid and Tillmann Heinisch, who worked together with me on the Carbonic Anhydrase project.

I am grateful to Prof. Dr Daniel Häussinger and Kaspar Zimmermann for NMR measurements of human Carbonic Anhydrase. I would like also to thank Prof. Dr Markus Meuwly and Dr. Tristan Bereau for their computational work related to my project.

Furthermore, I would like to thank all of the members of the technical staff, from the “Werkstatt” and the “Materialausgabe” as well as the secretaries, for their highly efficient and friendly service, without which the chemical institute would not run smoothly.

I gratefully acknowledge Novartis as well as the Swiss National Science Foundation and the University of Basel for their financial support.

Special thanks also go to all of my students.

I wish to express a special thank you to those who have played music with me in recent years in the orchestra of Basel region and, more especially Christina, Lucia and Marius.

Acknowledgements

I would like to say a big thank you to those who have shared my life throughout these last four years of Ph.D.: Lea, Silvia, Lucienne, Anita, Kathrin, Stefanie, Susanne, Nicolas, Michel, Tobias, ...

Finalement j'aimerais remercier mes parents et mes frères pour leur soutien infaillible durant ces quatre années de thèse. Merci à eux !

Summary

The development of efficient biocatalysts for industry remains a challenge. Over the past decade, the group of Professor Thomas R. Ward (University of Basel, Switzerland) has developed various artificial metalloenzymes for enantioselective catalysis. For this purpose, a biotinylated organometallic catalyst is incorporated in (Strept)avidin, thereby providing a hybrid catalyst that displays attractive features, reminiscent of both chemo- and biocatalysts.

Relying on knowledge acquired within the group, the main objective of my research was to rationally design and study a novel class of artificial metalloenzymes centered on an alternative biomolecular scaffold: human Carbonic Anhydrase II (hCA II). The interest in hCA II is motivated by the possibility to use this protein as a target, because it is overexpressed in various forms of cancers. This feature may be exploited to accumulate a catalytic drug in cells requiring therapeutic action. A library of ruthenium piano-stool complex bearing a sulfonamide anchor was designed *in silico*, synthesized and tested as organometallic hCA II inhibitor.

An additional second recognition motif was subsequently introduced to further fine-tune the binding affinity of the metal complex for the hCA II. In parallel with these synthetic efforts, we developed widely applicable force field parameters amenable to molecular dynamics simulations of hCA II-inhibitor interactions. These were experimentally validated and used to predict the affinity of fluorinated arylsulfonamide inhibitors for hCA II.

Based on computational results, a second generation of inhibitors with improved binding affinities for wild-type hCA II (10 nM) were designed *in silico*. Coupled to a second recognition element, which ensured precise localization of catalytic metals within the hCA II binding pocket, a well-defined chiral environment was tailored to provide a favourable environment for enantioselective catalysis. A chemogenetic optimization strategy (*i.e.* genetic variation of the hCA II combined with chemical fine-tuning of the piano-stool moiety) allowed for improving the catalytic performance of the artificial metalloenzyme for the reduction of prochiral imines.

Summary

During my PhD thesis, I gained expertise in the *in-silico* design, synthesis and biophysical characterization of organometallic inhibitors and their interaction with a model protein: human Carbonic Anhydrase II. The multidisciplinary environment provided in the group of Professor Thomas R. Ward gave me a unique opportunity to collaborate on a daily basis with molecular biologists, computational chemists, protein crystallographers etc.

The work presented herein was initiated and guided by Prof. Dr Thomas R. Ward at the Chemistry Department of the Philosophic-Scientific Faculty of the University of Basel, during the time period from October 2008 to September 2012.

Excerpts from this work have been published in the following journals:

Fabien W. Monnard, Tillmann Heinisch, Elisa S. Nogueira, Tilman Schirmer, and Thomas R. Ward “Human Carbonic Anhydrase II as Host for Piano-stool Complexes Bearing a Sulfonamide Anchor”, *Chem. Commun.*, **2011**(47), 8238.

Maurus Schmid, Elisa S. Nogueira, Fabien W. Monnard, Thomas R. Ward, and Markus Meuwly “Arylsulfonamides as Inhibitors for Carbonic Anhydrase: Prediction & Validation”, *Chem. Sci.*, **2012**(3), 690. + Front cover

Fabien W. Monnard, Elisa S. Nogueira and Thomas R. Ward “Artificial Imine Reductase Based on Human Carbonic Anhydrase as Host Protein”, in preparation.

Tristan Bereau, Christian Kramer, Fabien W. Monnard, Elisa S. Nogueira, Thomas R. Ward, and Markus Meuwly “Scoring multipole electrostatics in atomistic protein-ligand binding simulations”, in preparation.

Keywords: artificial metalloenzymes, asymmetric catalysis, chemogenetic optimization, human Carbonic Anyhydrase II, transfer hydrogenation, imine reduction.

Table of contents

Acknowledgements	i
Summary	iii
Table of contents	v
Abbreviations	xi
I Generalities	1
1 Introduction	3
1.1 Preamble	3
1.2 Introduction to catalysis	3
1.2.1 Catalyst performance	5
1.2.2 Chirality and the importance of enantioselectivity	6
1.2.3 Homogeneous asymmetric catalysis	7
1.2.4 Enzymatic catalysis	8
1.2.5 Artificial metalloenzymes	10
1.3 Artificial metalloenzymes: Background	11
1.3.1 General anchoring strategies within macromolecular scaffolds	12
1.3.2 Previous technology: Biotin-streptavidin	14
1.3.3 Human Carbonic Anhydrase II, a protein scaffold for the creation of artificial metalloenzymes	16
1.3.4 Human Carbonic Anhydrase II anchoring strategy	17
1.4 Catalytic system: imine reduction by transfer hydrogenation	22
1.5 Catalyst optimization: biological and chemical diversity	26

Table of contents

1.6	Research project	28
1.7	References	29
2	Results and discussion	37
2.1	Suitable catalytic systems for hCA II	38
2.2	Design and Synthesis	39
2.2.1	Introduction to rational ligand design	39
2.2.2	First ligand generation: bipyridine derivatives	42
2.2.3	Second ligand generation: picolyamine derivatives	47
2.2.4	Carbene ligand	50
2.2.5	Complex synthesis	52
2.3	Protein inhibitor interactions	54
2.3.1	Circular dichroism	54
2.3.2	Thermodynamics of hCA II-inhibitor binding	56
2.3.3	Crystallographic studies	67
2.3.4	NMR studies	69
2.4	Catalysis	71
2.4.1	Imine transfer hydrogenation	71
2.4.2	Michaelis-Menten kinetic experiments	79
2.5	References	81
3	Conclusion and outlook	85
II	Experimental	87
4	Experimental section	89
4.1	General experimental conditions	89
4.1.1	Solvents and reagents	89
4.1.2	Separation and purification methods	89
4.1.3	Spectroscopic methods	90

4.1.4	Spectrometric methods	90
4.1.5	Other methods	91
4.2	Ligand synthesis	92
4.2.1	2,2'-Bipyridine-5-sulfonamide (1)	92
4.2.2	4-(Di-2-pyridinylamino)-benzenesulfonamide (2)	94
4.2.3	4-((2,2'-Bipyridine)4-yl)benzenesulfonamide (3)	98
4.2.4	<i>N</i> -(Di(2-pyridyl)methyl)-amidobenzene-4-sulfonamide (4)	104
4.2.5	4-(2-(Aminomethyl)pyridin-4-yl)benzenesulfonamide (5)	112
4.2.6	<i>N</i> -((4-(4-Sulfamoylphenyl)pyridin-2-yl)methyl)benzenesulfonamide (6)	116
4.2.7	1,3-Dimesityl-5-((4-sulfamoylbenzamido)methyl)-4,5-dihydro-1 <i>H</i> -imidazol-3-ium (7)	125
4.3	Complex synthesis	130
4.3.1	General procedure for complex synthesis	130
	Synthesis of ruthenium complexes 8, 9, 10, 11, 12	132
	Synthesis of iridium complexes 13, 14, 15, 16, 17, 18	137
4.4	General procedure for hCA II inhibition profiling	143
4.4.1	Esterase activity screening assay	143
4.4.2	Competitive displacement assay	144
4.5	General procedure for circular dichroism measurements	145
4.5.1	Sample preparation and data analysis	145
4.6	Catalytic experiments: transfer hydrogenation	146
4.7	Sample work up and analysis	146
4.7.1	1-Methyl-6,7-dimethoxy-3,4-dihydroisoquinoline	146
4.7.2	1-Methyl-3,4-dihydroisoquinoline	146
4.7.3	Phenylpyrrolone	147
4.7.4	2-Cyclohexylpyrrolidine	147
4.8	Michaelis-Menten experiments	148
4.9	Protein purification: resin preparation	149

Table of contents

4.10 Table of molecules	150
4.11 References	158
III Annexes	159
Curriculum vitae	257

Abbreviations

δ	chemical shift in parts per million (ppm)
\subset	included in
Å	Angstrom
ACN	acetonitrile
Ala (A)	L-alanine
BuLi	<i>n</i> -butyllithium
CD	circular dichroism
CH ₂ Cl ₂	dichloromethane
Cys (C)	L-cysteine
d	day(s)
DCC	<i>N,N'</i> -dicyclohexylcarbodiimide
DIPAMP	1,2-bis(<i>o</i> -anisylphenylphosphinyl)ethane
DIPEA	<i>N,N</i> -diisopropylethylamine
DMF	<i>N,N</i> -dimethylformamide
DMSO	dimethyl sulfoxide
DNA	deoxyribonucleic acid
DNSA	dansylamide
<i>E</i>	enzyme
EA	elementary analysis
EDAC	1-(3-dimethylaminopropyl)-3-ethylcarbodiimide hydrochloride
<i>ee</i>	enantiomeric excess
ESI	electron spray ionisation
EtOAc	ethyl acetate
EtOH	ethanol
FAB	fast atom bombardment
Gln (Q)	L-glutamine
Glu (E)	L-glutamate
h	hour(s)
H ₂ KPO ₄	potassium phosphate
hCA II	human Carbonic Anhydrase II
HCl	hydrogen chloride
His (H)	L-histidine

Abbreviations

HPLC	high performance liquid chromatography
HRMS	high resolution mass spectrometry
Ile (I)	L-isoleucine
<i>i</i> PrOH	2-propanol
ITC	isothermal titration calorimetry
<i>J</i>	coupling constant in hertz
K ₂ CO ₃	potassium carbonate
Leu (L)	L-leucine
Lys (K)	L-lysine
Maldi-TOF	matrix-assisted laser desorption/ionization - time of flight
MeOH	methanol
MgSO ₄	magnesium sulfate
min	minute(s)
mL	milliliter
MS	mass spectrometry
Na ₂ CO ₃	sodium carbonate
Na ₂ SO ₄	sodium sulfate
NaN ₃	sodium azide
NaOH	sodium hydroxide
NH ₃	ammonia
NMR	nuclear magnetic resonance
NOESY	nuclear Overhauser effect spectroscopy
<i>P</i>	product
pcs	pseudocontact chemical shift
PDB	Protein Data Bank
Phe (F)	L-phenylalanine
ppm	parts per milliom
Pro (P)	L-proline
R _f	retention factor (TLC)
r.t.	room temperature
<i>S</i>	substrate
Ser (S)	L-serine

TBAF	tetrabutylammonium fluoride
TFA	trifluoroacetic acid
THF	tetrahydrofuran
Thr (T)	L-threonine
TLC	thin layer chromatography
TON	turnover number
Tris	tris(hydroxymethyl)aminomethane hydrochloride
Ts	tosyl
TsDPEN	<i>N-p</i> -tosyl-1,2-diphenylethylenediamine
UV	ultraviolet
v/v	volume/volume ratio
Val (V)	L-valine
WT	wild-type

Abbreviations

Part I

Generalities

*Il est bon de savoir que l'utopie n'est jamais rien
d'autre que la réalité de demain et que la réalité
d'aujourd'hui était l'utopie d'hier.*

Le Corbusier



Introduction

1.1 Preamble

Enzymes are involved in most chemical transformations in Nature.^[1] Due to their high architectural complexity, folded polypeptides are able to perform a variety of complex tasks. Moreover, enzymes containing metallic ion cofactors in their active sites possess the ability to perform complex biological transformations (*e.g.* photosynthesis, respiration, water oxidation, molecular oxygen reduction and nitrogen fixation, *etc.*). Such natural biocatalysts have been studied and improved for the purpose of industrial synthesis over the past 30 years. Nowadays, biocatalytic steps using fine-tuned biological scaffolds are implemented in industry in order to synthesize complex molecules, *e.g.* advanced pharmaceutical or insecticide intermediates.^[2-4] For this purpose, (bio)chemists have worked on genetic optimization of enzymes in order to reach high chemo-, regio- and stereoselective biotransformations under environmentally friendly conditions.^[5,6]

1.2 Introduction to catalysis

Catalysis plays an important role in green technologies and is one of the most important chemical tools. Its continued development will certainly contribute in the future to solve important energy and environmental challenges.^[7] Historically, in 1836, Berzelius and other

scientists observed that certain substances added to (or coming into contact with) other compounds were able to accelerate the transformation of those compounds. In 1909, Ostwald was awarded the Nobel Prize in Chemistry for his work on catalysis. His search led him to a contemporary definition of catalysis:^[8] catalysis (from Greek *katalusis*: dissolution) is a phenomenon by which a substance, called a catalyst, modifies the reaction profile of a reaction without itself undergoing any permanent chemical change, *i.e.* it must be regenerated at the end of the reaction. It should be noted that the catalyst participates in a reaction by providing an alternative reaction mechanism involving various transition states (Figure 1.1, red line) and decreasing the energy of activation ($\Delta G_{cat}^{\ddagger} < \Delta G_{uncat}^{\ddagger}$), although the thermodynamic equilibrium (ΔG_r) of the reaction is not altered.^[9]

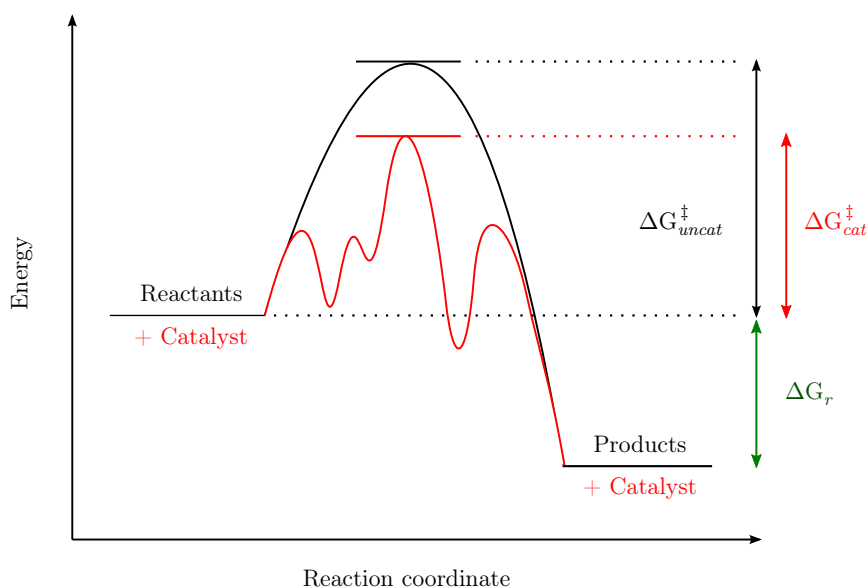


Figure 1.1. Reaction profile of a catalyzed (red line) and uncatalyzed (black line) reaction.

In the early 20th century, the emphasis was placed on heterogeneous catalysis for the production of ammonia. Since 1909, the Haber-Bosch process has been based on an inexpensive iron catalyst and has been used by BASF for large scale production of ammonia. Chemists have also focused on the synthesis of hydrocarbons from carbon monoxide (Fischer-Tropsch process) which was used on a large scale during World War II to produce petrol.^[7] In 1965, Wilkinson revolutionized the world of catalysis presenting the first homogeneous catalyst used for the hydrogenation of alkenes.^[10] Since the 1970s, Rachel Carson's book "Silent Spring"

changed the perception of the chemical industry in the general population, and sparked an environmental movement, which had a significant impact on government policies requiring stricter regulation of produced chemical substances, especially pesticides. As a result, chemical companies have had to develop environmentally sustainable solutions, leading in Europe to the REACH legislation in 2006 (Registration, Evaluation, Authorization and Restriction of Chemicals) managed by the European Chemicals Agency.^[11]

Finally, to illustrate the importance of catalysis in chemistry in recent years, several Nobel Prizes have been awarded for breakthroughs in this field, *e.g.* for metal catalyzed asymmetric transformations (2001),^[12–14] the development of the metathesis reaction (2005),^[15–17] the studies of chemical processes on solid surfaces (2007),^[18] and for metal-catalyzed cross coupling reactions (2010).^[19–21]

1.2.1 Catalyst performance

The successful application of a catalytic transformation depends on several key parameters such as temperature, pH, solvents, etc. The activity of a catalyst is defined as the amount of product produced per mole of catalyst in a defined time (TOF), while for biocatalysts the specific activity is defined as the amount of product transformed per unit mass of enzyme per unit of time.^[7] For the study of artificial metalloenzymes, the theory developed by Michaelis-Menten for enzyme kinetics was applied. The catalytic reactions were divided into two steps (equation 1.1). First, the enzyme (E) and the substrate (S) associate in a rapid and reversible step to form a complex ES (dissociation constant K_S in equation 1.1). Then, the chemical processes take place during the second step when the ES complex is converted into the product (P) and the enzyme (E) is recovered (rate constant k_2).^[22]



The simple Michaelis-Menten kinetic is described by equation 1.2, where K_M can be treated as the overall dissociation constant of all enzyme-bound species (if $k_2 \ll k_{-1}$).^[23] In

this model, it is also assumed that the binding steps are fast, thus k_2 can be assimilated to the overall catalytic rate constant k_{cat} .

$$v = \frac{[E]_0 \cdot k_{\text{cat}} \cdot [S]}{K_M + [S]} \quad (1.2)$$

The catalytic rate constant of the enzyme k_{cat} [1/s] and the dissociation constant K_M [1/M] can be determined experimentally (section 2.4.2). The k_{cat}/K_M constant determines the specificity of the enzyme for competing substrates. In the ideal case for catalysis, an enzyme shows high specific activity and should be subject to minimal substrate inhibition.

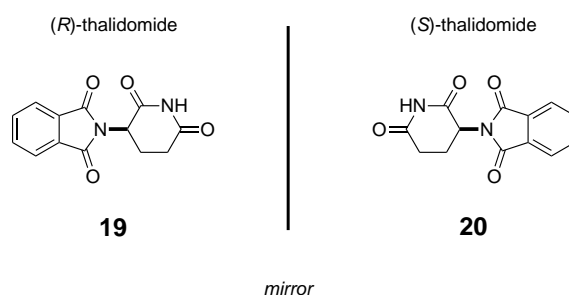
1.2.2 Chirality and the importance of enantioselectivity

A chiral (from Greek *kheir* : Hand) object is defined as an object that is not superposable with its mirror image.^[24] Chirality is an intrinsic propriety of matter. Nature contains many different types of chiral molecules such as amino acids, carbohydrates, lipids or DNA, which are essential building blocks for all organisms.

Chiral technology has taken an important place in the fine chemicals and therapeutic industries, and it is expected that biocatalysts able to transform prochiral substrates to highly enantiopure pharmaceutical intermediates will reach \$354 million in 2013 (\$198 million in 2006).^[4] The two enantiomers present the same physical and chemical properties in an achiral environment. However, because living systems are chiral, each of the enantiomers of a chiral drug can behave very differently *in vivo*, and thus display different pharmacological activities.^[25] The importance of controlling drug chirality can be illustrated by thalidomide. Thalidomide was used in racemic form for the treatment of morning sickness in pregnant women in the 60s. While (*R*)-thalidomide (**19**) acts as a sedative, (*S*)-thalidomide (**20**) induced fetus deformations because of its teratogenic properties (Scheme 1.1).^[26]

Therefore, control of the enantioselectivity of catalytic reaction is crucial to enable the production of the desired enantiomer. In addition, the synthesis of enantiopure compounds catalyzed by chiral catalysts reduces chemical waste produced during the production process. An enantiopure

Scheme 1.1. Structure of thalidomide. The two enantiomers of thalidomide display different biological activities: the (*R*)-thalidomide is a sedative, while the (*S*)-thalidomide has teratogenic properties.



compound is in opposition to a racemate, which consists of equimolar amounts of both enantiomers. The degree of enantiomeric enrichment of a non racemic mixture can be determined by polarimetry, spectroscopy (NMR) or chromatographic techniques (GC, or HPLC). Enantiomeric excess (*ee*) is defined as:

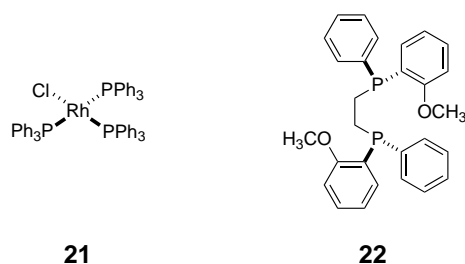
$$ee = \frac{|([R] - [S])|}{([R] + [S])} \cdot 100 \quad (1.3)$$

1.2.3 Homogeneous asymmetric catalysis

In 1966, Wilkinson and Osborn reported the first generation of homogeneous hydrogenation catalysts based on a rhodium complex (**21**, Scheme 1.2).^[10] To induce a higher degree of stereoselectivity in asymmetric catalysis, Kagan and Dang proposed to use a bidentate ligand. This ligand was accessible from the natural product, L-(+)-tartaric acid.^[27] This pioneering work was extended by Knowles and co-workers,^[28] whereby a rhodium complex bearing enantiopure phosphorus ligands was reported for the asymmetric hydrogenation of dehydro amino acids. The synthesis of L-DOPA was achieved in high *ee* (94 %) with the enantiopure biphosphane ligand DIPAMP (**22**, Scheme 1.2).^[12] L-DOPA is used as drug for the treatment of Parkinson's disease.

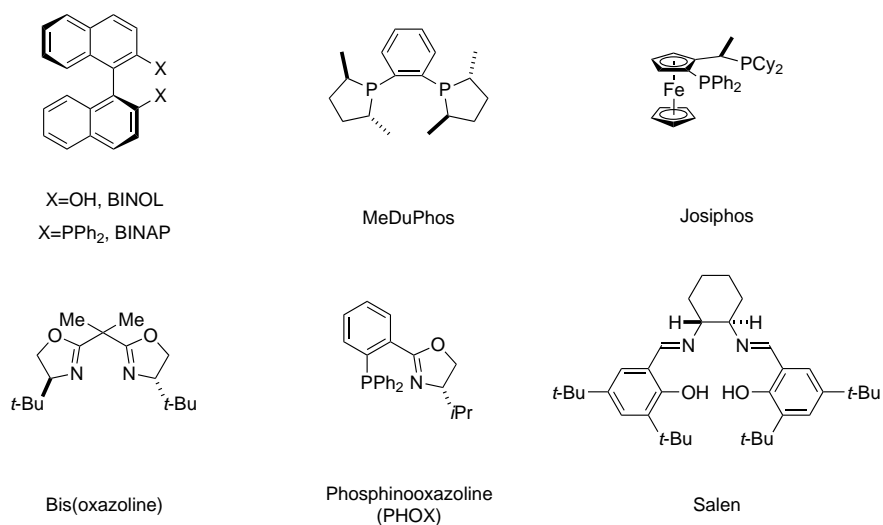
During the past decade, asymmetric catalysis has been one of the most active research fields in chemistry.^[29] Numerous enantiopure catalysts have been reported in literature, but only a few of them, the so-called "privileged chiral catalysts", present good enantioselectivity over a wide range of transformations and bear ligands presented in Scheme 1.3.^[30] However,

Scheme 1.2. Wilkinson's catalyst **21** ($[\text{RhCl}(\text{PPh}_3)_3]$) for hydrogenation of functionalized olefins and DIPAMP enantiopure ligand (**22**) used for asymmetric hydrogenation of dehydro amino acids.



rational modifications of these ligands (*i.e.* the first coordination sphere) in order to improve the reaction selectivity remain a very challenging task for chemists. Indeed numerous interactions such as weak and non-bonding contacts with solvent, buffer, salts can influence the selectivity of the reaction.^[31] It is noteworthy that a difference in energy of 2 kcal/mol in the transition state energies results in an enantiomeric excess of 95%.

Scheme 1.3. Examples of ligands used for the synthesis of “privileged chiral catalysts”.

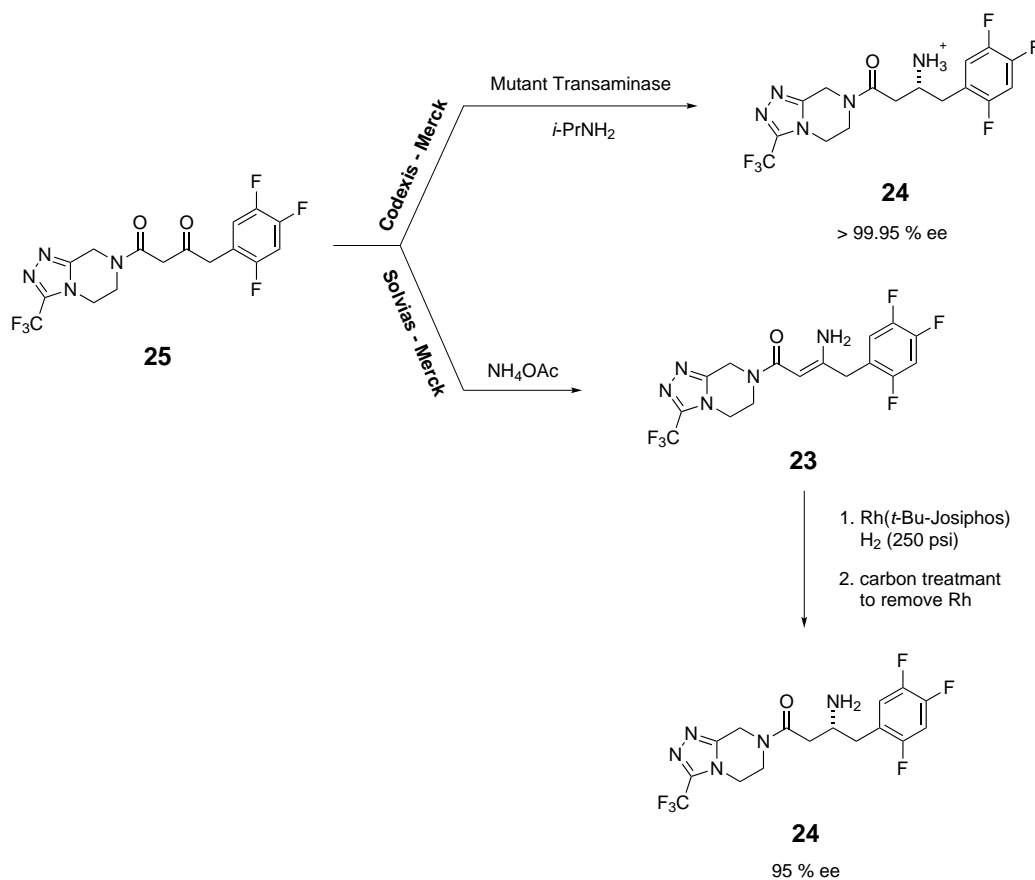


1.2.4 Enzymatic catalysis

Compared to homogeneous catalysts, enzymes provide an environmentally friendly route to synthesize enantiopure chemicals. To illustrate the advantages of enzyme catalysis over classical synthetic methods, development of the industrial synthesis of sitagliptin, which is used for the treatment of type 2 diabetes, is of particular interest.^[32] Indeed, using traditional cata-

lysts for the industrial synthesis of pharmaceuticals, many problems arise such as the removal of metal traces from the product or the high hydrogen pressure required for the asymmetric hydrogenation of the enamine intermediate product **23** (Scheme 1.4, Solvias-Merck pathway).^[33] Therefore synthesis of pharmaceuticals using “fine-tuned” enzymes presents many advantages. Coupled to *in silico* design, a directed evolution strategy used by Codexis and Merck led to the development of an (*R*)-selective transaminase for the synthesis of compound **24**.^[34] The enzymatic process can be achieved at high substrate concentration (220 g · L⁻¹, substrate/catalyst 2600 mol/mol, and TOF 163 h⁻¹) and in the presence of DMSO (50%). β -Ketoamide (**25**) was converted to sitagliptin in 92% yield and >99.95% *ee* (Scheme 1.4) under mild conditions (40 °C). Compared to the rhodium catalyzed reaction, sitagliptin was obtained in a 13% increased overall yield and with an improved enantiomeric excess.

Scheme 1.4. Synthesis of enantiopure sitagliptin (**24**) using a homogeneous (Solvias-Merck) or an enzymatic (Codexis-Merck) route.



1.2.5 Artificial metalloenzymes

Considering the number of chemical transformations catalyzed by transition metals which have not been observed to occur enzymatically and the ability of macromolecules to selectively discriminate substrates, the Ward group and others reasoned that a hybrid catalyst may combine some of the most attractive features of homogeneous and enzymatic catalysts previously presented.^[32,35] Since the 70's, chemists have designed many hybrid catalyst, so called "artificial metalloenzymes", that exhibit high selectivity for the synthesis of enantiomerically enriched compounds in aqueous media (Section 1.3). The artificial metalloenzyme concept dates back to 1978 when Whitesides and Wilson postulated:

"A globular protein modified by introduction of a catalytically active metal at an appropriate site could, in principle, provide an exceptionally well-defined steric environment around that metal, and should do so for considerably smaller effort than would be required to construct a synthetic substance of comparable stereochemical complexity."^[36]

They proved this theory by incorporation of biotinylated metal catalysts into avidin, achieving conversion of α -acetamidoacrylic acid in 44% *ee*. Whitesides and co-workers also proposed a hybrid catalyst based on hCA II for the hydrogenation of α -acetamidoacrylic acid. However, only a small amount of hydrogenated product was observed (without any enantiomeric excess) and it was concluded that hCA II was a severe poison for the catalytic reaction.^[37]

1.3 Artificial metalloenzymes: Background

The pioneering work of Whitesides and Wilson was based on incorporating one biotinylated phosphine-rhodium(I) complex within avidin, for the hydrogenation of α -acetamidoacrylic acid, yielding a modest chiral induction (44% *ee*).^[36] In more general terms, the development of a hybrid catalyst results from the combination of a biomolecular scaffold (*e.g.* proteins,^[38,39] DNA^[40] or peptides^[41]) with an active catalytic moiety. To ensure the precise localization of the organometallic catalyst precursor embedded within the biomolecular host, a very strong guest \subset host interaction (*e.g.*, a protein inhibitor) is required (anchor, Figure 1.2).

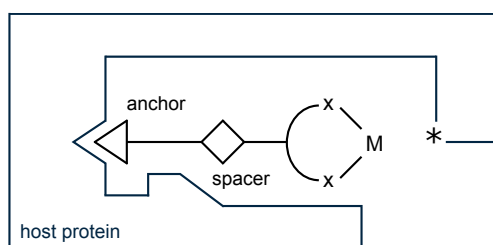


Figure 1.2. General scheme of an artificial metalloenzyme using supramolecular anchoring strategy to incorporate a catalytically active metal within the host protein. Chemical optimization can be achieved either by modification of the spacer or the metal ligand scaffold (x). Site-directed mutagenesis allows a genetic optimization of the protein near the catalytic metal center (*) to further optimize the enantioselectivity.

To create new artificial metalloenzymes, two different approaches can be envisaged: a catalytically active metal center within a biomolecular scaffold can be created from scratch, the so-called *de novo* design,^[42,43] or, alternatively, by modification of an existing natural enzyme or protein.^[44] The design of an artificial metalloenzyme based on a wild-type protein has many advantages compared to the *de novo* approach.^[45] Indeed, our understanding of protein folding is still lacunar for the purpose of designing complex proteins with well-defined catalytic sites. This problem can be overcome with the recent advances in computational protein design.^[46] However, this approach requires extensive efforts and is limited to simple catalytic transformations.^[47] Interestingly, Pecoraro and co-workers recently reported a *de novo* designed metalloprotein (Figure 1.3a) able to hydrolyse *p*-nitrophenyl acetate ($k_{\text{cat}}/K_{\text{m}} \approx 2500 \text{ M}^{-1} \text{ s}^{-1}$) with an efficiency only ~ 100 -fold lower than wild-type human Carbonic Anhydrase II (Figure 1.3b and Section 1.3.3).^[48]

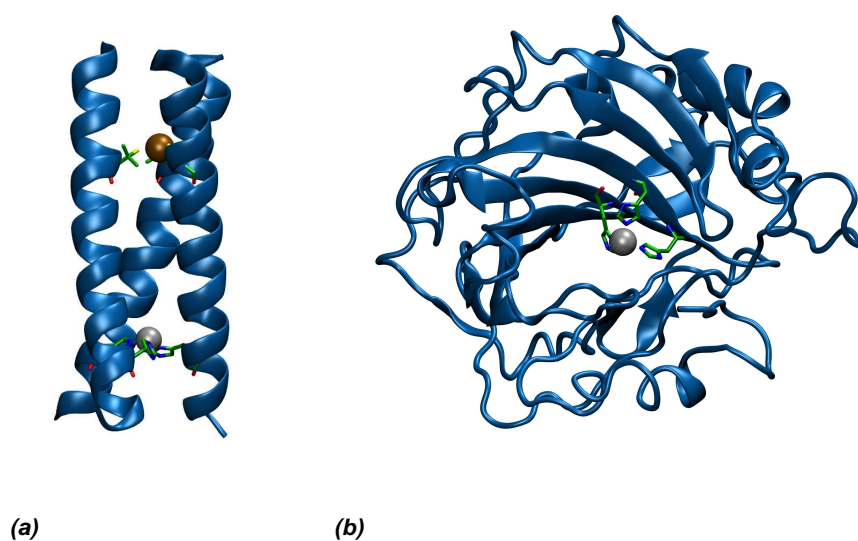


Figure 1.3. **a)** *de novo*-designed scaffold (PDB code 3PBJ) with a Zn binding site (gray) used as catalytic metal and a Hg binding site (brown) for structural stabilization, **b)** native protein scaffold: human Carbonic Anhydrase II (PDB code 1G54).

1.3.1 General anchoring strategies within macromolecular scaffolds

Currently, different strategies are exploited for the localization of an organometallic moiety within macromolecular scaffolds: dative, covalent or supramolecular anchoring (Figure 1.4)^[49] or a combination of them.^[50]

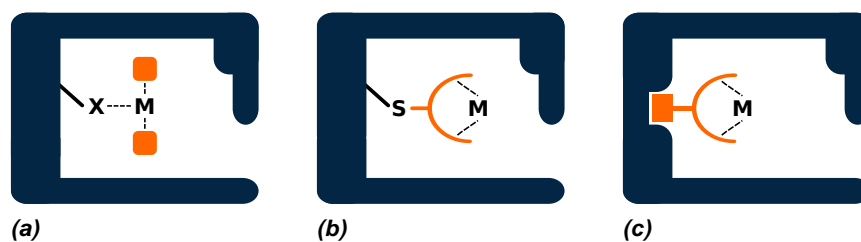


Figure 1.4. Anchoring strategies for the localization of a catalyst precursor within macromolecular scaffolds (blue): **a)** dative, **b)** covalent, and **c)** supramolecular. M denotes the catalytically active transition metal and the chemically synthesized first coordination sphere is highlighted in orange.^[45]

The dative anchoring strategy relies on the coordination of a catalytic metal by chemical functionalities present directly on the surface of the macromolecular scaffold or an inhibitor which coordinate to the metal present within a protein pocket, *e.g.* sulfonamide ligands that bind hCA II zinc (Section 1.3.4).^[51–53] In the case of hCA II, this anchoring technique was

previously used by Kazlauskas *et al.* to modify the catalytic activity of the protein. For this purpose, Zn^{II} was substituted by Mn^{II} to obtain a novel peroxidase able to enantioselectively epoxidize olefins conjugated to an aromatic or aliphatic carbon (Figure 1.5b).^[54–56] Moreover, metal ions can also be accommodated into specific binding sites of certain non-metalloproteins to obtain catalytically active metalloproteins.^[57,58] In the further development, as opposed to simply exchanging the bound metal ion or binding metal at exposed coordinating residues, Ward *et al.* identified through a PDB search, metal-free two-histidines one-carboxylate binding motifs in proteins amenable to facial coordination of metals.^[59]

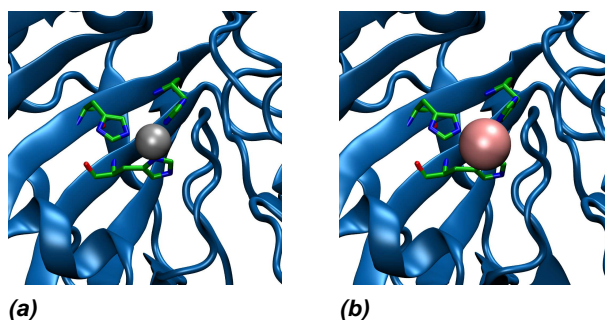


Figure 1.5. a) Native hCA II with Zn^{II} as active metal (PDB code 1G52) b) Modified hCA II with Mn^{II} as active metal (PDB code 1RZD).

The covalent approach^[6,60–63] commonly uses a cysteine as an anchoring residue, a method proposed by Kaiser *et al.*^[64] This method allows for precise localization of a metal complex within or on the surface of a biological scaffold. Recently, Häussinger *et al.* used this strategy to localize lanthanide tags on protein surfaces for solution NMR studies (Section 1.3.4).^[65]

The supramolecular anchoring method preferred in the Ward group and by others has been investigated.^[66,67] In this approach, a strong and highly specific non-covalent interaction between a biomacromolecule and a small molecule derived from specific ligand/inhibitor structures is observed (Section 1.3.2). This technique allows for easy chemical optimization of metal ligand features (first coordination sphere) and avoids uncertainties concerning the localization of the metal within the macromolecular scaffold.^[68]

1.3.2 Previous technology: Biotin-streptavidin

The first generation of metalloenzymes developed in the Ward group relied on the high affinity of (+)-biotin (also known as vitamin H) towards two proteins, streptavidin and avidin. To introduce the catalytic metal within the host protein, the biotin, used as anchor, is derivatized through the valeric acid side chain. Despite the modifications brought to the valeric acid side chain of biotin, the affinity towards the host protein remains high.^[69] This artificial metalloenzyme remains remarkably stable even under harsh catalytic conditions, *e.g.* 55 °C and mixture of water and organic solvents.^[70]

As previously mentioned, the first example of a hybrid catalyst based on biotin-avidin technology was developed by Whitesides and Wilson in 1978.^[36] A biotinylated Wilkinson's catalyst was embedded into avidin to obtain 44% *ee* for the reduction of α -acetamidoacrylic acid. Subsequently, rational chemogenetic modifications of the hybrid catalyst enabled the Ward group to improve the enantioselectivity of the reaction up to 91% *ee* (*R*) as well as reversed of the enantioselectivity 75% *ee* (*S*) for the reduction of 4'-bromoacetophenone.^[71,72] In contrast to the rational design strategy proposed by the Ward group, an alternative approach focused on directed evolution of hybrid catalysts was implemented by Reetz and co-workers.^[73] They were able to enhance or invert the selectivity for the transfer hydrogenation of α -acetamidoacrylate. This Darwinian approach to create novel artificial metalloenzymes faced, however, screening problems due to *e.g.* low protein expression levels in miniaturized systems (96 well plates). Moreover, the metals are extremely sensitive to cellular debris and the activity of the catalysts decrease if the protein is not adequately purified.^[74] Compared to the results obtained by chemogenetic optimization for the reduction of α -acetamidoacrylate, the directed evolution strategy yielded only 65% *ee* (*R*) or 7% *ee* (*S*) under optimized conditions.

Having demonstrated the potential of artificial metalloenzymes for enantioselective transformations of prochiral substrates, other catalytic systems have been successfully investigated within the Ward group.^[71,72] They focused on reactions for which the substrate does not bind to the catalytic metal center in the transition state.^[38] In such cases, the second coordination

sphere is expected to have a strong influence on the enantioselectivity of the reaction. For this purpose, asymmetric transfer hydrogenation, dihydroxylation, and sulfoxidation were studied. A summary of the different artificial metalloenzymes developed within the Ward group is reported in Table 1.1.

Table 1.1. Catalytic reactions using artificial metalloenzymes implemented in the Ward group.^[38,49]

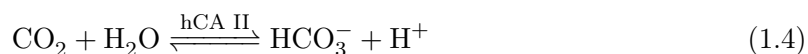
Entry	Reaction Type	General catalytic conditions
1	Hydrogenation ^[75]	H ₂ O buffer, H ₂ (5 bar), r.t., 15 h
2	Ketone reduction ^[76,77]	H ₂ O buffer/DMF, formic acid (pH 6.25), 55 °C, 64 h
3	Alcohol oxidation ^[78]	H ₂ O/DMF/acetone (5/1), TBHP ^a , r.t., 90 h
4	Allylic substitution ^[72]	H ₂ O/DMSO (10/1), DMB ^b , K ₂ CO ₃ , r.t., 16 h
5	Imine reduction ^[22]	H ₂ O buffer, sodium formate (pH 7.5), 5 °C, 48 h
6	Olefin metathesis ^[79]	H ₂ O/DMSO (5/1), pH 7 or 4, 40 °C, 16 h
7	Enantioselective Sulfoxidation ^[57]	H ₂ O buffer/DMF/EtOH, pH 2.2, r.t., 48 h
8	Enantioselective <i>cis</i> -dihydroxylation ^[58]	H ₂ O, K ₂ CO ₃ , r.t., 24 h
9	C-H activation ^[80]	H ₂ O buffer/MeOH, 23 °C, 72 h

^a *tert*-butylhydroperoxide. ^b didodecyldimethylammonium bromide.

Nowadays, a major challenge in bioinorganic chemistry is the development of new artificial metalloenzymes that catalyze *in vivo* the conversion of drug precursors into an active form to treat diseases in a targeted manner.^[32] Towards this goal, it may be possible to exploit proteins that are overexpressed in certain forms of disease in order to accumulate active catalysts within the cells that require therapeutic action. During our research, a biological scaffold candidate with the required characteristics drew our attention: human Carbonic Anhydrase II.^[53]

1.3.3 Human Carbonic Anhydrase II, a protein scaffold for the creation of artificial metalloenzymes

Carbonic Anhydrase isozymes are metalloenzymes that catalyze the reversible hydration of carbon dioxide into bicarbonate with remarkable efficiency ($k_{\text{cat}}/K_{\text{M}} \approx 1.5 \times 10^8 \text{ M}^{-1} \text{ s}^{-1}$, Equation 1.4). These are critical enzymes and any deficiency or mutation can result in diseases such glaucoma, ureagenesis and lipogenesis.^[81] Additionally, overexpression of hCA IX and hCA XII are found in certain forms of cancers^[82] and inhibitors have been designed for diagnosis and therapy.^[83,84]



Wild-type human Carbonic Anhydrase II (hCA II, EC 4.2.1.1, M [g·mol⁻¹] = 29227, pI 7.4, 259 amino acids) is a globular protein, see Table 2.1.^[53] The active site of hCA II comprises a catalytic Zn^{II} ion coordinated tetrahedrally to three histidines (His94, His96 and His119, Figure 1.6a) and a solvent molecule. The Zn-cofactor is located at the base of a funnel-shaped cavity measuring roughly 15 Å in diameter at its mouth and 15 Å deep.^[85] This cavity is characterized by three major domains: (i) the primary coordination sphere around the Zn-cofactor (gray, Figure 1.6b); (ii) the primary and secondary hydrophobic faces involved in secondary recognition of inhibitors (yellow, Figure 1.6b); and (iii) the hydrophilic face that is located around His64 responsible for the catalytic activity of the protein (blue, Figure 1.6b).

Table 1.2. hCA II structural stability parameters.

Parameters	
Temperature ^[86,87]	up to 55 °C
pH ^[53]	5.7—8.4
Metal ^[88]	low exchange rate
Organic solvent ^[89]	less than 20 % (DMSO)

Human Carbonic Anhydrase II is particularly attractive for the development of a new artificial metalloenzyme for many reasons: (i) hCA II is a monomeric protein with a large

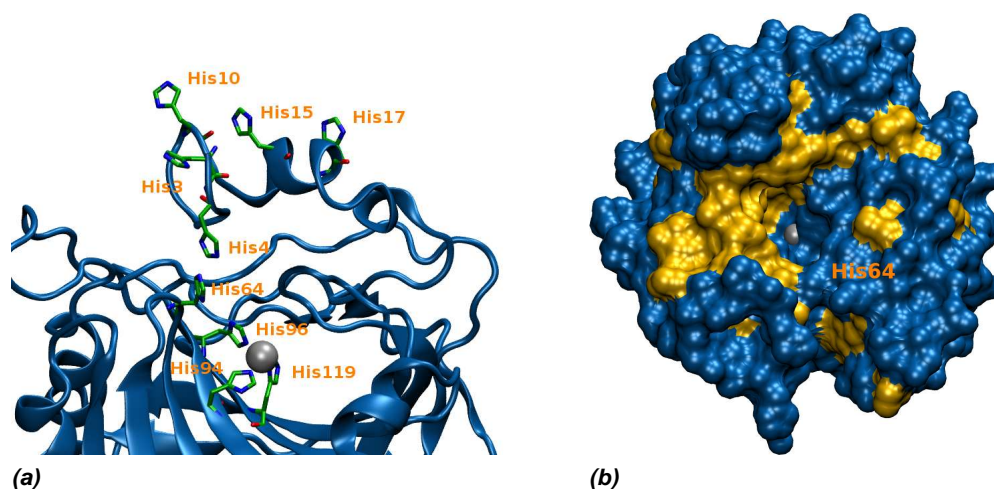


Figure 1.6. a) Zinc atom coordinated with three histidine residues (His94, His96 and His119) and the histidine cluster involved in the proton-shutting process for reversible hydration of carbon dioxide (His64, His4, His3, His17, His15 and His10) b) hCA II surface rendering showing hydrophobic residues (yellow), polar residues (blue) and Zn-cofactor (gray).^[81]

binding pocket able to accommodate metal complexes; (ii) it is possible to apply computational design for rational tailoring of the active site to accommodate inhibitors compatible with soft transition metals;^[90,91] (iii) this monomeric protein is easy to overexpress in *E. coli* and to purify;^[85] (iv) since hCA II also has promiscuous esterase activity, it is possible to monitor the rate of *p*-nitrophenylacetate hydrolysis, allowing inhibition to be monitored (Section 1.3.4); (v) the X-ray determination of hCA II structure is well established (Section 2.3.3)^[53] and NMR may provide the structure of the protein-inhibitor complex in solution (Section 2.3.4).^[65]

1.3.4 Human Carbonic Anhydrase II anchoring strategy

In the spirit of Fischer's lock-and-key model,^[92] molecules analogous to the transition state of carbon dioxide (CO₂) hydration (Figure 1.7a and c) should be effective hCA II ligands.^[93] Based on this consideration, sulfonamide derivatives were proposed in 1940 by Keilen *et al.* as specific inhibitors of human Carbonic Anhydrase isozymes.^[94]

The sulfonamide nitrogen anion coordinates to the Zn^{II} cofactor (Figure 1.7b), and two hydrogen bonds are established with the protein scaffold. The first of those is between the O_γ of Thr199 and the sulfonamide NH, and the second between the sulfonamide oxygen and the

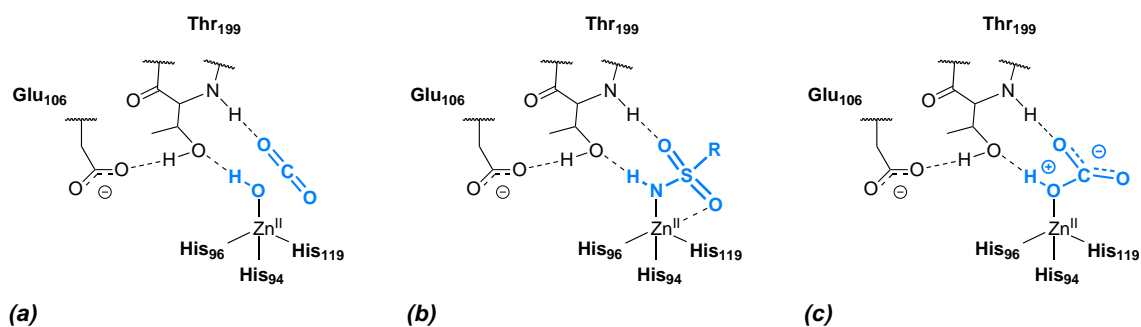


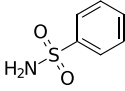
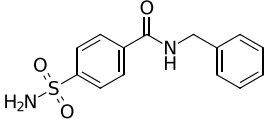
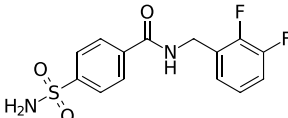
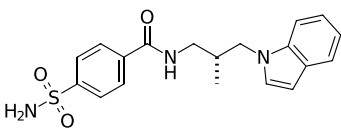
Figure 1.7. Diagram comparing **a**) carbon dioxide (putative interactions), **b**) an arylsulfonamide, and **c**) bicarbonate bound to the active site of hCA II. The arylsulfonamide can be viewed as a transition state analogue of the hydratase reaction.^[53]

NH of the Thr199 backbone. Moreover, the second sulfonamide oxygen coordinates weakly to Zn^{II} . To complete this sulfonamide interaction, aromatic moieties were found to interact significantly with the primary hydrophobic faces inside the funnel-shaped cavity (Figure 1.6b, yellow surface).^[95] In the case of benzenesulfonamide (Table 1.3 entry **1**, $K_d = 200\text{--}1500$ nM) the bonds to the Zn^{II} cofactor represent approximately 65% of the free energy of binding, while hydrogen bonds and hydrophobic interaction represent approximately 10% and 25%, respectively.^[96] To further increase the binding affinity between ligands and protein, secondary recognition elements may be exploited.

Jain *et al.* reported that *para*-substituted benzenesulfonamides bearing benzyl moieties (Table 1.3, entries **2** to **4**) can interact with the hydrophobic upper rim of the funnel-shaped cavity of hCA II. Indeed *N*-(4-sulfamylbenzoyl)benzylamine establishes an edge-to-face contact with Phe131, and the affinity observed for hCA II is approximately 100-fold higher ($K_d = 2.1$ nM)^[97] than for the corresponding non-substituted *para*-carboxybenzenesulfonamide ($K_d = 270$ nM).^[98] In the same spirit, Whitesides and co-workers computationally designed *para*-benzenesulfonamide derivatives able to interact bivalently with the protein scaffold (Figure 1.8b). In 2002, they reported an inhibitor with the highest known affinity for hCA II ($K_d \approx 30$ pM, Table 1.3 entry **4**).^[99] To further increase the affinity of inhibitors, Fierke introduced fluorine substituents on the molecular scaffold. Another benefit of fluorine is the metabolic stabilization of inhibitors when used as drugs. (Table 1.3, entry **2**).^[100,101]

1.3. Artificial metalloenzymes: Background

Table 1.3. hCA II dissociation constants (K_d) of selected ligands.

Entry	Structure	Dissociation constant (nM)
1		200-1500 ^[102,103]
2		2.1 ^[104]
3		0.29 ^[100]
4		0.03 ^[99]

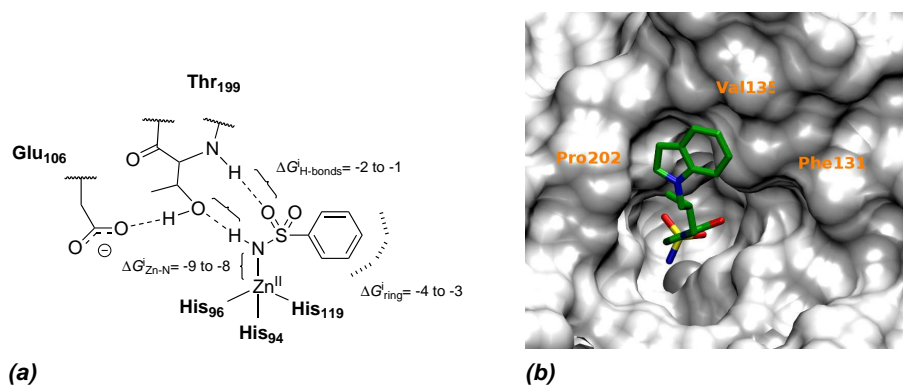


Figure 1.8. a) Estimated free energies between the benzenesulfonamide anion and hCA II (in kcal·mol⁻¹)^[96] b) hCA II complexed with (*R*)-*N*-(3-indol-1-yl-2-methyl-propyl)-4-sulfamoylbenzamide, the strongest inhibitor reported to date (PDB: 1IF7).^[99] Pro202, Val135, and Phe131 of the hydrophobic surface as second recognition element.

There are several convenient assays to quantify interactions (K_d or K_i) between hCA II and inhibitors. An exhaustive review was published by Whitesides and co-workers^[53] and the four most popular are reported in Table 1.4. Two of the most commonly used methods to determine affinities (Section 2.3.2 for results) between hCA II and inhibitors are: i) the hydrolysis of *p*-nitrophenylacetate, which can be determined by measuring the appearance of nitrophenolate (λ_{\max} 348 nm). This method is most appropriate for weak inhibitors, whereby the hydrolysis can still be measured over a reasonable time frame; ii) competition experiments with dansylamide (DNSA). This is best achieved by determining the fluorescence signal caused by bound DNSA (unbound DNSA does not fluoresce). This method is most appropriate for strong inhibitors.

ITC offers perhaps the widest K_d window ($K_d = 10^{-3} - 10^{-9}$ M) between hCA II and its inhibitors. Unfortunately, the use of metal complexes as inhibitors leads to the observation of multiple events, which we assumed to be caused by interactions with residues on the surface of the protein. This renders the interpretation of measurements difficult.^[105]

Table 1.4. Techniques used to determine affinities of inhibitors for hCA II.

Technique	Observable	Detectable K_d (M)
Dansylamide competition ^[106–108]	bound dansylamide	$10^{-4} - 10^{-8}$
Spectrophotometry ^[85,109]	hydrolysis of <i>p</i> -nitrophenylacetate	$10^{-4} - 10^{-7}$
CD ^[110]	aromatic residues	$10^{-3} - 10^{-5}$
ITC ^[53]	heat change during binding	$10^{-3} - 10^{-9}$

In 1996 Spicer *et al.* reported the first 2D NMR assignment of hCA II but the three-dimensional (3D) hCA II structure determination in solution remains challenging because of the size of hCA II (29 kD).^[53,111] Nevertheless, recent advances in NMR spectroscopy show that pseudocontact chemical shift provide information about long distance influences due to their $1/r^3$ dependences (up to ~ 50 Å, hCA II dimension $46 \cdot 56$ Å). For this purpose, methylated DOTA (DOTA-M8, Figure 1.9) is complexed with a lanthanide, and this macro-

molecule is covalently linked to the surface of a protein, as demonstrated by Häussinger and co-workers.^[65] Moreover, this technique allows the precise location of the inhibitors/complexes inside the funnel-shaped cavity, in solution.

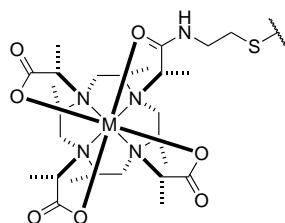


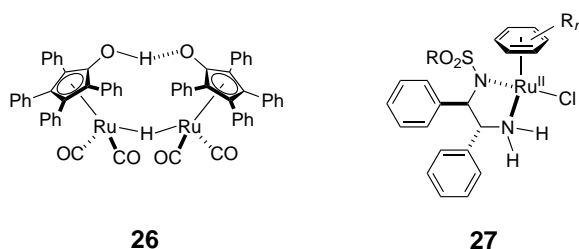
Figure 1.9. Structure of DOTA-M8.^[65] M denotes a lanthanide ion.

1.4 Catalytic system: imine reduction by transfer hydrogenation

Asymmetric reduction of compounds with C=N bonds is relatively underdeveloped although enantiomerically pure amines play an important role in the pharmaceutical, agrochemical, and chemical industries.^[112] In the last 30 years, organometallic catalysts were developed to address this problem. Imine reduction by transfer hydrogenation is commonly carried out using isopropanol, formic acid or formate salts as the hydrogen source and most widely employed catalytic metals are ruthenium, rhodium, and iridium.^[113,114]

The first examples of asymmetric transfer hydrogenation were reported in the 1970s from the groups of Ohkubo^[115] and Sinou^[116] who used Wilkinson's based catalyst for the reduction of prochiral ketones. They were able to induce enantioselectivity relying on enantiopure ligands (monosaccharides) bound to catalytically active metals. In 1981, Grigg *et al.* proposed C=N transfer hydrogenation, using Wilkinson's catalyst, $[\text{RhCl}[\text{P}(\text{C}_6\text{H}_5)_3]_3]$, in isopropanol to reduce aldimines into secondary amines.^[117] Six years later, in 1987, a ruthenium catalyst, $\text{Ru}_3(\text{CO})_{12}$, for transfer hydrogenation of imines was reported by Jones *et al.*^[118] who successfully used it for the reduction of benzylideneaniline. Nevertheless, the efficiency (conversion and enantioselectivity) of such catalysts remained generally low. The 1990's brought improved catalysts including Shvo's diruthenium catalyst (**26**)^[119] and Noyori's ruthenium (II) based catalyst (**27**, Scheme 1.5).^[120]

Scheme 1.5. Shvo (**26**) and Noyori (**27**) complexes used for transfer hydrogenation.

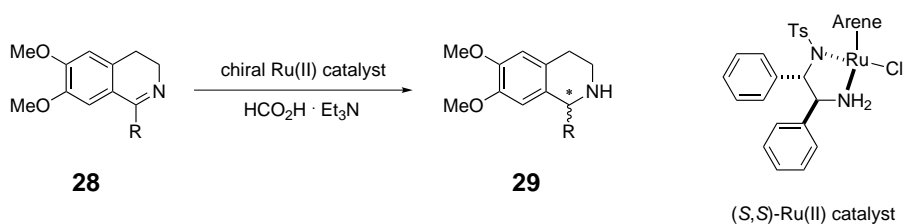


The Shvo diruthenium complex has been extensively investigated by Bäckvall^[121,122] and Casey^[123] as a transfer hydrogenation catalyst. Shvo's catalyst was found to have high turnover frequencies even at low loadings (0.3%) for the transfer hydrogenation of imines. Noy-

1.4. Catalytic system: imine reduction by transfer hydrogenation

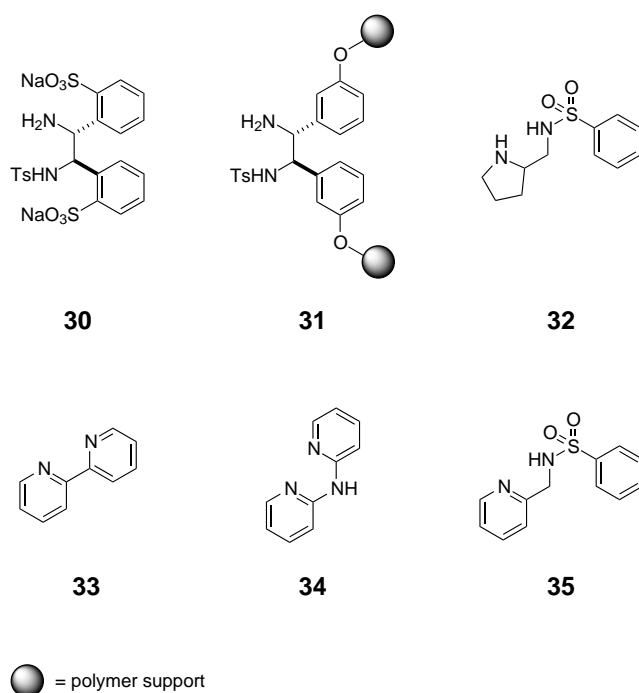
ori's ruthenium (II) based catalyst uses the *N-p*-tosyl-1,2-diphenylethylenediamine (TsDPEN) enantiopure ligand previously developed for ketone reduction.^[120] In addition, catalysts bearing TsDPEN derivative ligands have been used for the reduction of a wide range of substrates, such as C=O and C=N bonds, under mild conditions, *i.e.* room temperature and no hydrogen gas, and provide excellent *ee*'s (up to 99%).^[124] By using Noyori's catalyst, cyclic imines bearing alkyl or benzyl groups were enantioselectively reduced, and applied for the synthesis of isoquinoline or β -carboline alkaloids. In 1996, Noyori published, as a model for the asymmetric transfer hydrogenation of imines, the synthesis of salsolidine (quant., 95% (*R*), (*S,S*)-Ru catalyst, Scheme 1.6).^[125] For this purpose, formic acid/triethylamine azeotrope was used as hydrogen source. The reactivity of the catalyst was much higher (>1000-fold) for the imine reduction when compared to the ketone reduction. Moreover, Noyori highlighted the structural importance of the Ru(II) arene cap along with the sulfonamide moiety (Scheme 1.6) for the successful enantioselective reduction of imines.^[113] Carreira *et al.* recently demonstrated that the iridium catalyst containing TsDPEN ligands bearing strongly electron deficient sulfonamides (*e.g.* perfluorosulfonamide) have enhanced selectivity and reactivity for the ketone reduction.^[126] The first industrial application for imine reduction using an iridium ferrocenyl diphosphine catalyst was announced in 1996 for the synthesis of the herbicide (*S*)-metolachlor.^[127]

Scheme 1.6. Asymmetric transfer hydrogenation of a cyclic imine.



In the interest of developing environmentally friendly water soluble organometallic complexes, Noyori's ruthenium (II) based catalyst was modified to be water soluble. In 2006, Deng *et al.* reported the first asymmetric transfer hydrogenation of cyclic imines and iminiums in water. Catalysis was performed with a water-soluble Ru(II)-catalyst and NaHCO₂ as hydrogen source (Scheme 1.7). The observed *ee*'s were improved by addition of CTAB (cetyltrimethylammonium), a surfactant which increased the solubility of the substrate, product, and catalyst.^[128,129] At the same time, different systems for transfer hydrogenation of ketones and imines in water were reported from the labs of Ogo,^[130,131] Renaud^[132] and Süß-Fink.^[133] Many routes to increase the water solubility of organometallic complexes have been reported (Scheme 1.7): i) by increasing the TsDPEN hydrophilicity (ligand **30**);^[128] ii) the use of polymer-supported catalyst (ligand **31**);^[134] iii) incorporation of the catalyst in a biomolecular scaffold;^[135] and iv) use of other types of ligand, *e.g.* based on a pyridine moiety (ligands **32**, **33**, **34** and **35**).^[130–133]

Scheme 1.7. Selected ligands for imine transfer hydrogenation.

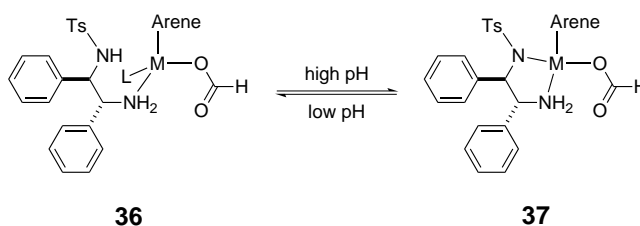


In 2005, Xiao *et al.* reported that, for asymmetric transfer hydrogenation, the pH of the reaction solution affects the catalyst performance in the aqueous-phase.^[134] The observed

1.4. Catalytic system: imine reduction by transfer hydrogenation

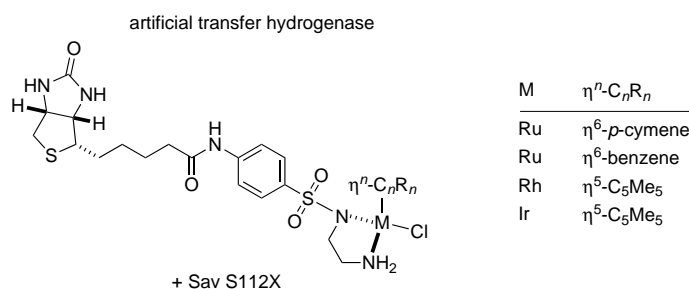
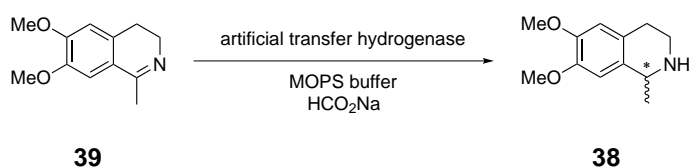
variations of enantioselectivity according to the pH may be explained by the protonation of TsDPEN ligand under acidic conditions.^[124] Depending on the nature of the aromatic sulfonamide moieties, the pK_a of the corresponding N-H group varies between 4.5 (Ar = C₆F₅) and 7.6 (Ar = *p*-toluene).^[136] The change in the sulfonamide protonation leads to an “on-and-off” catalyst state observed by Xiao, as illustrated in Scheme 1.8.^[137]

Scheme 1.8. Metal-TsDPEN ligand proposed states under acid (complex **36**) or basic (complex **37**) conditions. L may be a water molecule.^[124]



Combining the fields of homogeneous and enzymatic catalysis, Ward *et al.* were able to integrate known catalysts within a protein scaffold in order to render them water-soluble. A novel artificial transfer hydrogenase for the enantioselective reduction of cyclic imines was reported in 2011.^[22] Imines were reduced under mild conditions (Scheme 1.9) using formate as hydrogen source. Chemogenetic optimization of the hybrid catalyst resulted in a system that yielded both enantiomers (*S*, 78% and *R*, 96 % *ee*) of salsolidine (**38**).

Scheme 1.9. Artificial transfer hydrogenase for the reduction of 1-methyl-6,7-dimethoxy-3,4-dihydroisoquinoline into salsolidine based on biotin-streptavidin technology.^[22]



1.5 Catalyst optimization: biological and chemical diversity

To further enhance the activity and selectivity of hybrid catalysts, several methods have been developed.^[73,138–140] Directed evolution is one of the most powerful, and it involves the introduction of random mutations into the genes, thus creating a library of mutant proteins. These enzymes variants are screened for catalytic activity and selectivity, and the best candidates taken forward to another round of random mutagenesis. In the case of hybrid catalysts, this process turns out to be complicated as for the need to use purified (or semi-purified) protein for screening.

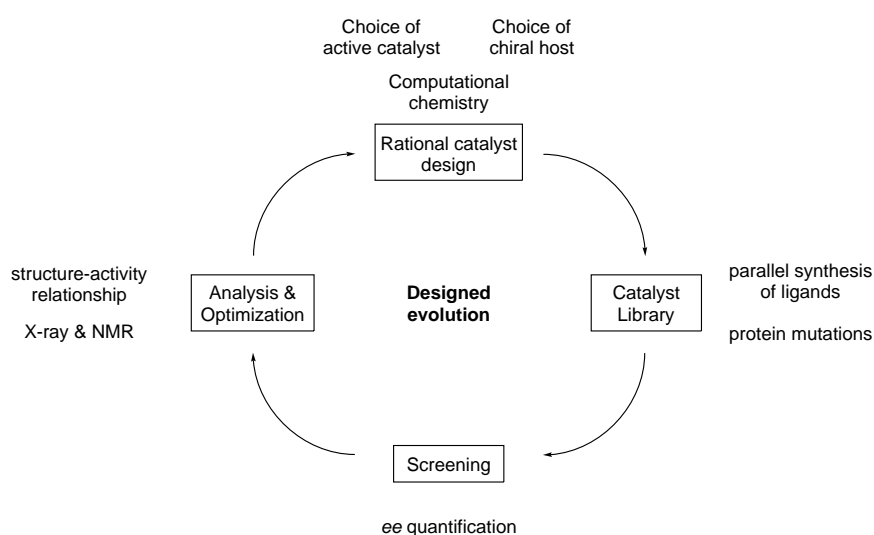


Figure 1.10. Optimization of artificial metalloenzymes.^[1]

To address this problem and to optimize hybrid catalysts, the chemogenetic approach, previously described by Ward and co-workers, was found to be the most suitable solution.^[141,142] As the name indicates, the chemogenetic approach relies on two distinct optimizations: i) genetic modification of the protein scaffold, based on computational calculations and X-ray structures. Particular attention is given to the active site of enzyme ($<10 \text{ \AA}$ around the catalytic metal center);^[143,144] and ii) chemical fine-tuning of the catalytic moiety, to adjust

1.5. Catalyst optimization: biological and chemical diversity

the localization of the catalytic moiety inside the funnel-shaped cavity of the protein. These combined techniques allow the design of a small collection of hybrid catalysts with improved activity and selectivity. One advantage of this approach is that the chemogenetically optimized library of hybrid catalysts is produced and screened on a relatively short time frame.

This operation can also be performed iteratively as shown in Figure 1.10 resulting in a process which has been called “designed evolution”.^[145]

1.6 Research project

The objectives of this thesis are to strengthen and expand the concept of artificial metalloenzymes in the direction of developing new hybrid catalysts. Relying on the knowledge acquired within the Ward group, human Carbonic Anhydrase II has been selected as a potential biomolecular scaffold for the creation of artificial metalloenzymes.

With this goal in mind, three challenges were identified:

1. based on *in silico* docking and X-ray information, hCA II inhibitors that could potentially act as bidentate ligands for piano stool complexes were designed, synthesized, and characterized.
2. the most promising ligands were used to create and optimize an artificial transfer hydrogenase (ATHase) for the enantioselective reduction of imines.
3. these ATHases were characterized both structurally and in terms of catalytic performances.

1.7 References

- [1] Thomas, C. M.; Ward, T. R. *Appl. Organomet. Chem.* **2005**, *19*, 35.
- [2] Bornscheuer, U. T.; Huisman, G. W.; Kazlauskas, R. J.; Lutz, S.; Moore, J. C.; Robins, K. *Nature* **2012**, *485*, 185.
- [3] DeSantis, G.; Wong, K.; Farwell, B.; Chatman, K.; Zhu, Z.; Tomlinson, G.; Huang, H.; Tan, X.; Bibbs, L.; Chen, P.; Kretz, K.; Burk, M. J. *J. Am. Chem. Soc.* **2003**, *125*, 11476.
- [4] Thayer, A. M. *Chem. Eng. News* **2012**, *12*, 13.
- [5] Jing, Q.; Okrasa, K.; Kazlauskas, R. J. *Chem. Eur. J.* **2009**, *15*, 1370.
- [6] Qi, D.; Tann, C. M.; Haring, D.; Distefano, M. D. *Chem. Rev.* **2001**, *101*, 3081.
- [7] Hagen, J. *Industrial Catalysis*; Wiley-VCH Verlag GmbH & Co. KGaA: 2006.
- [8] Lindström, B.; Pettersson, L. J. *CATTECH* **2003**, *7*, 130.
- [9] Crabtree, R. H. *The organometallic chemistry of the transition metals*; Wiley New York: 2009.
- [10] Osborn, J. A.; Jardine, F. H.; Young, J. F.; Wilkinson, G. *J. Chem. Soc. A* **1966**, *1966*, 1711.
- [11] Margossian, N. *Le Règlement REACH*; Dunod: 2007.
- [12] Knowles, W. S. *Angew. Chem. Int. Ed.* **2002**, *41*, 1999.
- [13] Noyori, R. *Angew. Chem. Int. Ed.* **2002**, *41*, 2008.
- [14] Sharpless, K. B. *Angew. Chem. Int. Ed.* **2002**, *41*, 2024.
- [15] Chauvin, Y. *Angew. Chem. Int. Ed.* **2006**, *45*, 3740.
- [16] Grubbs, R. H. *Angew. Chem. Int. Ed.* **2006**, *45*, 3760.
- [17] Schrock, R. R. *Angew. Chem. Int. Ed.* **2006**, *45*, 3748.
- [18] Ertl, G. *Angew. Chem. Int. Ed.* **2008**, *47*, 3524.
- [19] Suzuki, A. *Angew. Chem. Int. Ed.* **2011**, *50*, 6722.
- [20] Negishi, E.-I. *Angew. Chem. Int. Ed.* **2011**, *50*, 6738.
- [21] Johansson Seechurn, C. C. C.; Kitching, M. O.; Colacot, T. J.; Snieckus, V. *Angew. Chem. Int. Ed.* **2012**, *51*, 5062.
- [22] Dürrenberger, M. *et al.* *Angew. Chem. Int. Ed.* **2011**, *50*, 3026.
- [23] Fersht, Alan, *Structure and Mechanism in Protein Science: A Guide to Enzyme Catalysis and Protein Folding*; W. H. Freeman: 1st ed.; 1998.

- [24] Nic, M.; Jirat, J.; Kosata, B. "IUPAC Compendium of Chemical Terminology – The Gold Book", 2009.
- [25] Lin, G.-Q.; You, Q.-D.; Cheng, *Chiral Drugs: Chemistry and Biological Action*; Wiley ed.; 2011.
- [26] Maier, W. A. *Arch. Dis. Child.* **1965**, *40*, 154.
- [27] Kagan, H. B.; Dang, T.-P. *J. Am. Chem. Soc.* **1972**, *94*, 6429.
- [28] Vineyard, B. D.; Knowles, W. S.; Sabacky, M. J.; Bachman, G. L.; Weinkauff, D. J. *J. Am. Chem. Soc.* **1977**, *99*, 5946.
- [29] Zhou, Q.-L. *Privileged Chiral Ligands and Catalysts*; Wiley-VCH Verlag GmbH & Co. KGaA: 2011.
- [30] Yoon, T. P.; Jacobsen, E. N. *Science* **2003**, *299*, 1691.
- [31] Vogl, E. M.; Gröger, H.; Shibasaki, M. *Angew. Chem. Int. Ed.* **1999**, *38*, 1570.
- [32] Ringenbreg, M. R.; Ward, T. R. *Chem. Commun.* **2011**, *47*, 8470.
- [33] Hansen, K. B. *et al. J. Am. Chem. Soc.* **2009**, *131*, 8798.
- [34] Savile, C. K.; Janey, J. M.; Mundorff, E. C.; Moore, J. C.; Tam, S.; Jarvis, W. R.; Colbeck, J. C.; Krebber, A.; Fleitz, F. J.; Brands, J.; Devine, P. N.; Huisman, G. W.; Hughes, G. J. *Science* **2010**, *329*, 305.
- [35] Ward, T. R. *Bio-inspired Catalysts*; Springer Verlag: 2009.
- [36] Wilson, M.; Whitesides, G. *J. Am. Chem. Soc.* **1978**, *100*, 306.
- [37] Wilson, M. E. *Asymmetric homogeneous hydrogenation utilizing enzyme-Rhodium conjugates*, Thesis, Massachusetts Institute of Technology, 1977.
- [38] Ward, T. R. *Acc. Chem. Res.* **2011**, 788.
- [39] Yamaguchi, H.; Hirano, T.; Kiminami, H.; Taura, D.; Harada, A. *Org. Biomol. Chem.* **2006**, *4*, 3571.
- [40] Boersma, A. J.; Feringa, B. L.; Roelfes, G. *Org. Lett.* **2007**, *9*, 3647.
- [41] Megens, R. P.; Roelfes, G. *Chem. Eur. J.* **2011**, *17*, 8514.
- [42] Zastrow, M. L.; Peacock, A. F. A.; Stuckey, J. A.; Pecoraro, V. L. *Nat. Chem.* **2012**, *4*, 118.
- [43] Hill, R. B.; Raleigh, D. P.; Lombardi, A.; DeGrado, F. W. *Acc. Chem. Res.* **2000**, *33*, 745.
- [44] Reetz, M. T.; Zonta, A.; Schimossek, K.; Jaeger, K.-E.; Liebeton, K. *Angew. Chem. Int. Ed.* **1997**, *36*, 2830.

- [45] Rosati, F.; Roelfes, G. *ChemCatChem* **2010**, *2*, 916.
- [46] Heinisch, T.; Ward, T. R. *Curr. Opin. Chem. Biol.* **2010**, *14*, 184.
- [47] Bazzoli, A.; Tettamanzi, A. G. B.; Zhang, Y. *J. Mol. Biol.* **2011**, *407*, 764.
- [48] Kiefer, L. L.; Paterno, S. A.; Fierke, C. A. *J. Am. Chem. Soc.* **1995**, *117*, 6831.
- [49] Steinreiber, J.; Ward, T. R. *Coord. Chem. Rev.* **2008**, *252*, 751.
- [50] Meggers, E. *Chem. Commun.* **2009**, 1001.
- [51] Ueno, T.; Koshiyama, T.; Abe, S.; Yokoi, N.; Ohashi, M.; Nakajima, H.; Watanabe, Y. *J. Organomet. Chem.* **2007**, *692*, 142.
- [52] Fernández-Gacio, A.; Codina, A.; Fastrez, J.; Riant, O.; Soumillion, P. *ChemBioChem* **2006**, *7*, 1013.
- [53] Krishnamurthy, V. M.; Kaufman, G. K.; Urbach, A. R.; Gitlin, I.; Gudiksen, K. L.; Weibel, D. B.; Whitesides, G. M. *Chem. Rev.* **2008**, *108*, 946.
- [54] Okrasa, K.; Kazlauskas, R. J. *Chem. Eur. J.* **2006**, *12*, 1587.
- [55] Jing, Q.; Okrasa, K.; Kazlauskas, R. J. *Chem. Eur. J.* **2009**, *15*, 1370.
- [56] Jing, Q.; Kazlauskas, R. J. *ChemCatChem* **2010**, *2*, 953.
- [57] Pordea, A.; Creus, M.; Panek, J.; Duboc, C.; Mathis, D.; Novic, M.; Ward, T. R. *J. Am. Chem. Soc.* **2008**, *130*, 8085.
- [58] Köhler, V.; Mao, J.; Heinisch, T.; Pordea, A.; Sardo, A.; Wilson, Y. M.; Knörr, L.; Creus, M.; Prost, J.-C.; Schirmer, T.; Ward, T. R. *Angew. Chem. Int. Ed.* **2011**, *50*, 10863.
- [59] Amrein, B.; Schmid, M.; Collet, G.; Cuniasse, P.; Gilardoni, F.; Seebeck, F. P.; Ward, T. R. *Metallomics* **2012**, *4*, 379.
- [60] Carey, J. R.; Ma, S. K.; Pfister, T. D.; Garner, D. K.; Kim, H. K.; Abramite, J. A.; Wang, Z.; Guo, Z.; Lu, Y. *J. Am. Chem. Soc.* **2004**, *126*, 10812.
- [61] Deuss, P. J.; Popa, G.; Botting, C. H.; Laan, W.; Kamer, P. C. J. *Angew. Chem. Int. Ed.* **2010**, *49*, 5315.
- [62] Rutten, L.; Wiczorek, B.; Mannie, J.-P. B. A.; Kruithof, C. A.; Dijkstra, H. P.; Egmond, M. R.; Lutz, M.; Gebbink, R. J. M. K.; Gros, P.; van Koten, G. *Chem. Eur. J.* **2009**, *15*, 4270.
- [63] Haquette, P.; Talbi, B.; Canaguier, S.; Dagorne, S.; Fosse, C.; Martel, A.; Jaouen, G.; Salmain, M. *Tetrahedron Lett.* **2008**, *49*, 4670.
- [64] Kaiser, E. T.; Lawrence, D. S. *Science* **1984**, *226*, 505.
- [65] Häussinger, D.; Huang, J.; Grzesiek, S. *J. Am. Chem. Soc.* **2009**, *131*, 14761.

- [66] Davies, C. L.; Dux, E. L.; Duhme-Klair, A.-K. *Dalton Trans.* **2009**, 10141.
- [67] Letondor, C.; Ward, T. R. *ChemBioChem* **2006**, *7*, 1845.
- [68] Krämer, R. *Angew. Chem. Int. Ed.* **2006**, *45*, 858.
- [69] Pordea, A.; Ward, T. R. *Chem. Commun.* **2008**, 4239.
- [70] Creus, M.; Ward, T. R. *Progress in Inorganic Chemistry*; John Wiley & Sons, Inc.: 2011.
- [71] Creus, M.; Pordea, A.; Rossel, T.; Sardo, A.; Letondor, C.; Ivanova, A.; LeTrong, I.; Stenkamp, R.; Ward, T. R. *Angew. Chem. Int. Ed.* **2008**, *47*, 1400.
- [72] Pierron, J.; Malan, C.; Creus, M.; Gradinaru, J.; Hafner, I.; Ivanova, A.; Sardo, A.; Ward, T. R. *Angew. Chem. Int. Ed.* **2008**, *47*, 713.
- [73] Reetz, M. T.; Peyralans, J. J.-P.; Maichele, A.; Fu, Y.; Maywald, M. *Chem. Commun.* **2006**, 4318.
- [74] Köhler, V.; Wilson, Y. M.; Lo, C.; Sardo, A.; Ward, T. R. *Curr. Opin. Biotechnol.* **2010**, *21*, 744.
- [75] Collot, J.; Gradinaru, J.; Humbert, N.; Skander, M.; Zocchi, A.; Ward, T. R. *J. Am. Chem. Soc.* **2003**, *125*, 9030.
- [76] Letondor, C.; Humbert, N.; Ward, T. R. *Proc. Natl. Acad. Sci. U.S.A.* **2005**, *102*, 4683.
- [77] Letondor, C.; Pordea, A.; Humbert, N.; Ivanova, A.; Mazurek, S.; Novic, M.; Ward, T. R. *J. Am. Chem. Soc.* **2006**, *128*, 8320.
- [78] Thomas, C. M.; Letondor, C.; Humbert, N.; Ward, T. R. *J. Organomet. Chem.* **2005**, *690*, 4488.
- [79] Lo, C.; Ringenberg, M. R.; Gnanndt, D.; Wilson, Y.; Ward, T. R. *Chem. Commun.* **2011**, *47*, 12065.
- [80] Hyster, T. K.; Knörr, L.; Ward, T. R.; Rovis, T. *Science* **2012**, *338*, 500.
- [81] Supuran, T. C. *Nat. Rev. Drug Discovery* **2008**, *7*, 168.
- [82] Beasley, N. J.; Wykoff, C. C.; Watson, P. H.; Leek, R.; Turley, H.; Gatter, K.; Pastorek, J.; Cox, G. J.; Ratcliffe, P.; Harris, A. L. *Cancer Res.* **2001**, *61*, 5262.
- [83] Can, D.; Spingler, B.; Schmutz, P.; Mendes, F.; Raposinho, P.; Fernandes, C.; Carta, F.; Innocenti, A.; Santos, I.; Supuran, T. C.; Alberto, R. *Angew. Chem. Int. Ed.* **2012**, *51*, 3354.
- [84] Salmon, A. J.; Williams, M. L.; Wu, Q. K.; Morizzi, J.; Gregg, D.; Charman, S. A.; Vullo, D.; Supuran, C. T.; Poulsen, S.-A. *J. Med. Chem.* **2012**, *55*, 5506.

- [85] Nair, S. K.; Calderone, T. L.; Christianson, D. W.; Fierke, C. A. *J. Biol. Chem.* **1991**, *266*, 17320.
- [86] Matulis, D.; Kranz, J.; Salemme, F.; Todd, M. *Biochemistry* **2005**, *44*, 5258.
- [87] Avvaru, B.; Busby, S.; Chalmers, M.; Griffin, P.; Venkatakrishnan, B.; Agbandje-McKenna, M.; Silverman, D.; McKenna, R. *Biochemistry* **2009**, *48*, 7365.
- [88] Cusanelli, A.; Frey, U.; Richens, D. T.; Merbach, A. E. *J. Am. Chem. Soc.* **1996**, *118*, 5265.
- [89] Vullo, D.; Franchi, M.; Gallori, E.; Antel, J.; Scozzafava, A.; Supuran, C. *J. Med. Chem.* **2004**, *47*, 1272.
- [90] Siegel, J. B.; Zanghellini, A.; Lovick, H. M.; Kiss, G.; Lambert, A. R.; Clair, J. L. S.; Gallaher, J. L.; Hilvert, D.; Gelb, M. H.; Stoddard, B. L.; Houk, K. N.; Michael, F. E.; Baker, D. *Science* **2010**, *329*, 309.
- [91] Ward, T. R. *Angew. Chem. Int. Ed.* **2008**, *47*, 7802.
- [92] Fischer, E. *Ber. Dtsch. Chem. Ges* **1894**, *27*, 2985.
- [93] Huc, I.; Lehn, J. M. *Proc. Natl. Acad. Sci. U.S.A.* **1997**, *94*, 2106.
- [94] Mann, T.; Keilin, D. *Nature* **1940**, *146*, 164.
- [95] Supuran, C. T.; Casini, A.; Scozzafava, A. *Med. Res. Rev.* **2003**, *23*, 535.
- [96] Krishnamurthy, V. M.; Bohall, B. R.; Kim, C. Y.; Moustakas, D. T.; Christianson, D. W.; Whitesides, G. M. *Chem. Asian J.* **2007**, *2*, 94.
- [97] Kim, C. Y.; Chang, J. S.; Doyon, J.; Jr, T. T. B.; Fierke, C. A.; Jain, A.; Christianson, D. W. *J. Am. Chem. Soc.* **2000**, *122*, 12125.
- [98] Taylor, P. W.; King, R. W.; Burgen, A. S. *Biochemistry* **1970**, *9*, 2638.
- [99] Grzybowski, B. A.; Ishchenko, A. V.; Kim, C.-Y.; Topalov, G.; Chapman, R.; Christianson, D. W.; Whitesides, G. M.; Shakhnovich, E. I. *Proc. Natl. Acad. Sci. U. S. A.* **2002**, *99*, 1270.
- [100] Doyon, J. B.; Hansen, E. A. M.; Kim, C. Y.; Chang, J. S.; Christianson, D. W.; Madder, R. D.; Voet, J. G.; Baird Jr, T. A.; Fierke, C. A.; Jain, A. *Org. Lett.* **2000**, *2*, 1189.
- [101] Böhm, H.-J.; Banner, D.; Bendels, S.; Kansy, M.; Kuhn, B.; Müller, K.; Obst-Sander, U.; Stahl, M. *ChemBioChem* **2004**, *5*, 637.
- [102] King, R. W.; Burgen, A. S. V. *Proc. R. Soc. London, Ser. B* **1976**, *193*, 107.
- [103] Schmid, M.; Nogueira, E. S.; Monnard, F. W.; Ward, T. R.; Meuwly, M. *Chem. Sci.* **2012**, *3*, 690.

- [104] Jain, A.; Whitesides, G. M.; Alexander, R. S.; Christianson, D. W. *J. Med. Chem.* **1994**, *37*, 2100.
- [105] Zimbron, J. M.; Sardo, A.; Heinisch, T.; Wohlschlager, T.; Gradinaru, J.; Massa, C.; Schirmer, T.; Creus, M.; Ward, T. R. *Chem. Eur. J.* **2010**, *16*, 12883.
- [106] Iyer, R.; Barrese III, A. A.; Parakh, S.; Parker, C. N.; Tripp, B. C. *J. Biomol. Screening* **2006**, *11*, 782.
- [107] Baird Jr, T. T.; Waheed, A.; Okuyama, T.; Sly, W. S.; Fierke, C. A. *Biochemistry* **1997**, *36*, 2669.
- [108] Wang, S. C.; Zamble, D. B. *Biochem. Mol. Biol. Educ.* **2006**, *34*, 364.
- [109] Srivastava, D. K.; Jude, K. M.; Banerjee, A. L.; Haldar, M.; Manokaran, S.; Kooren, J.; Mallik, S.; Christianson, D. W. *J. Am. Chem. Soc.* **2007**, *129*, 5528.
- [110] Freskgaard, P.-O.; Maartensson, L.-G.; Jonasson, P.; Jonsson, B.-H.; Carlsson, U. *Biochemistry* **1994**, *33*, 14281.
- [111] Venters, R. A.; Farmer II, B. T.; Fierke, C. A.; Spicer, L. D. *J. Mol. Biol.* **1996**, *264*, 1101.
- [112] Höhne, M.; Bornscheuer, U. T. *ChemCatChem* **2009**, *1*, 42.
- [113] Wills, M. *Modern Reduction Methods*; Wiley-VCH Verlag GmbH & Co. KGaA: 2008.
- [114] Blaser, H.-U.; Spindler, F. . In *Organic Reactions*; John Wiley & Sons, Inc.: 2004.
- [115] Ohkubo, K.; Hirata, K.; Yoshinaga, K.; Okada, M. *Chem. Lett.* **1976**, *5*, 183.
- [116] Descotes, G.; Sinou, D. *Tetrahedron Lett.* **1976**, *17*, 4083.
- [117] Grigg, R.; Mitchell, T. R. B.; Tongpenyai, N. *Synthesis* **1981**, *6*, 442.
- [118] Basu, A.; Bhaduri, S.; Sharma, K.; Jones, P. G. *J. Chem. Soc., Chem. Commun.* **1987**, 1126.
- [119] Shvo, Y.; Czarkie, D.; Rahamim, Y.; Chodosh, D. F. *J. Am. Chem. Soc.* **1986**, *108*, 7400.
- [120] Hashiguchi, S. I.; Fujii, A.; Takehara, J.; Ikariya, T.; Noyori, R. *J. Am. Chem. Soc.* **1995**, *117*, 7562.
- [121] Samec, J. S. M.; Bäckvall, J.-E. *Chem. Eur. J.* **2002**, *8*, 2955.
- [122] Samec, J. S. M.; Ell, A. H.; Bäckvall, J.-E. *Chem. Commun.* **2004**, 2748.
- [123] Casey, C. P.; Johnson, J. B. *J. Am. Chem. Soc.* **2005**, *127*, 1883.
- [124] Zhou, X.; Wu, X.; Yang, B.; Xiao, J. *J. Mol. Catal. A: Chem.* **2012**, *357*, 133.
- [125] Uematsu, N.; Fujii, A.; Hashiguchi, S.; Ikariya, T.; Noyori, R. *J. Am. Chem. Soc.* **1996**, *118*, 4916.

- [126] Soltani, O.; Ariger, M. A.; Vázquez-Villa, H.; Carreira, E. M. *Org. Lett.* **2010**, *12*, 2893.
- [127] Blaser, H.-U. *Adv. Synth. Catal.* **2002**, *344*, 17.
- [128] Wu, J.; Wang, F.; Ma, Y.; Cui, X.; Cun, L.; Zhu, J.; Deng, J.; Yu, B. *Chem. Commun.* **2006**, 1766.
- [129] Wang, F.; Liu, H.; Cun, L.; Zhu, J.; Deng, J.; Jiang, Y. *J. Org. Chem.* **2005**, *70*, 9424.
- [130] Ogo, S.; Abura, T.; Watanabe, Y. *Organometallics* **2002**, *21*, 2964.
- [131] Abura, T.; Ogo, S.; Watanabe, Y.; Fukuzumi, S. *J. Am. Chem. Soc.* **2003**, *125*, 4149.
- [132] Romain, C.; Gaillard, S.; Elmkaddem, M. K.; Toupet, L.; Fischmeister, C.; Thomas, C. M.; Renaud, J.-L. *Organometallics* **2010**, *29*, 1992.
- [133] Canivet, J.; Süß-Fink, G. *Green Chem.* **2007**, *9*, 391.
- [134] Wu, X.; Li, X.; King, F.; Xiao, J. *Angew. Chem. Int. Ed.* **2005**, *44*, 3407.
- [135] Ward, T. R. *Acc. Chem. Res.* **2011**, *44*, 47.
- [136] Mohar, B.; Valleix, A.; Desmurs, J.-R.; Felemez, M.; Wagner, A.; Mioskowski, C. *Chem. Commun.* **2001**, 2572.
- [137] Lowe, M. P.; Parker, D.; Reany, O.; Aime, S.; Botta, M.; Castellano, G.; Gianolio, E.; Pagliarin, R. *J. Am. Chem. Soc.* **2001**, *123*, 7601.
- [138] Reetz, M. T.; Bocola, M.; Carballeira, J. D.; Zha, D.; Vogel, A. *Angew. Chem. Int. Ed.* **2005**, *44*, 4192.
- [139] Turner, N. J. *Nat. Chem. Biol.* **2009**, *5*, 567.
- [140] Jäckel, C.; Hilvert, D. *Curr. Opin. Biotechnol.* **2010**, *21*, 753.
- [141] Creus, M.; Ward, T. R. *Org. Biomol. Chem.* **2007**, *5*, 1835.
- [142] Häring, D.; Distefano, M. D. *Bioconjugate Chem.* **2001**, *12*, 385.
- [143] Morley, K. L.; Kazlauskas, R. J. *Trends Biotechnol.* **2005**, *23*, 231.
- [144] Reetz, M. T.; Carballeira, J. D.; Peyralans, J.; Höbenreich, H.; Maichele, A.; Vogel, A. *Chem. Eur. J.* **2006**, *12*, 6031.
- [145] Petrounia, I. P.; Arnold, F. H. *Curr. Opin. Biotechnol.* **2000**, *11*, 325.

La première vertu d'une pensée active sera donc de s'attacher aux problèmes qui se posent et non pas à ceux que l'on suppose.

D. de Rougemont

2

Results and discussion

The framework of the second chapter of this thesis is built around the development of a new, artificial metalloenzyme capable of enantioselective catalysis, and based on human Carbonic Anhydrase II scaffold (hCA II). For this purpose, several scientific fields, represented by chemists, biologists and protein crystallographers, have joined forces. The discussion that follows focuses particularly on issues related to the chemistry (*i.e.* synthesis, catalysis, ...) of the project.

In the first section, the choice of a suitable catalytic system for the new protein is briefly discussed (section 2.1). The preparation of different ligands and complexes previously designed using computational tools are presented in sections 2.2.2, 2.2.5 and 2.2.1, respectively. Section 2.3 focuses on the interaction of the protein and the different inhibitors previously synthesized. This is then followed by the analysis of the interaction between inhibitor and hCA II using X-ray (section 2.3.3) and NMR (section 2.3.4) imaging. Finally, as an illustrative example of an enantioselective catalytic reaction, the transfer hydrogenation of cyclic imines using artificial metalloenzymes is presented and discussed in section 2.4.

2.1 Suitable catalytic systems for hCA II

A number of recent reviews have introduced preparative methods for new artificial metalloenzymes.^[1–3] In this context, and with the experience gained by the research group of Prof. Ward in the field of hybrid catalysts, the first point to be addressed is the selection of potential catalytic systems compatible with the new biomolecular scaffold, human Carbonic Anhydrase II (hCA II).

Having chosen human Carbonic Anhydrase II as a biomolecular scaffold for the development of a new, enantioselective artificial metalloenzyme, it is important to recall the various constraints imposed by the protein scaffold, as summarized in Table 2.1.

Table 2.1. hCA II structural stability parameters.

Parameters	
Temperature ^[4,5]	up to 55 °C
pH ^[6]	5.7–8.4
Metal ^[7]	low exchange rate
Organic solvent ^[8]	less than 20 % (DMSO)

With these constraining parameters in mind, different catalytic systems suitable for the host protein were selected: 1,4-addition,^[9,10] imine reduction^[11] (and/or reductive amination) and metathesis.^[12] The advantage of using a bioorthogonal chemical reaction, such as metathesis cross-coupling, is that it avoids any interfering reaction with the plethora of functions present on the surface of hCA II.^[12–14] Indeed, the 26 lysine residues found in hCA II makes the use of ketone substrates difficult, due to the formation of imines by Schiff base.

Having defined the different catalytic systems that can be used with hCA II, the development of a specific ligand and -inhibitor combination for each type of catalytic reactions was planned. Such ligands are based on a bipyridine pattern for the 1,4-addition, and, in our case, it was completed by 2-picolylamine derivative ligands for the transfer hydrogenation of cyclic imines. Carbene ligands were synthesized for the preparation of metathesis catalysts.

2.2 Design and Synthesis

2.2.1 Introduction to rational ligand design

With the lock-and-key model in mind, many different approaches have been envisaged for the identification of new, potent hCA II ligands.^[15] In our case, a rational approach involving computational tools was envisaged by exploiting the arylsulfonamide moiety as a transition-state analogue for the hydratase reaction (section 1.3.4). The first aim of this investigation was to parameterize zinc-sulfonamide interactions in order to predict the binding free energy between hCA II and model ligands.^[16] This calculation method was validated by studying the influence of protein mutations on the inhibitor affinity (section 2.3.2). Subsequently, a library of fluorinated inhibitors was studied in order to assess the influence of fluorine atoms on protein-inhibitor interactions. Results are presented in the following sections 2.2.2 and 2.3.2.

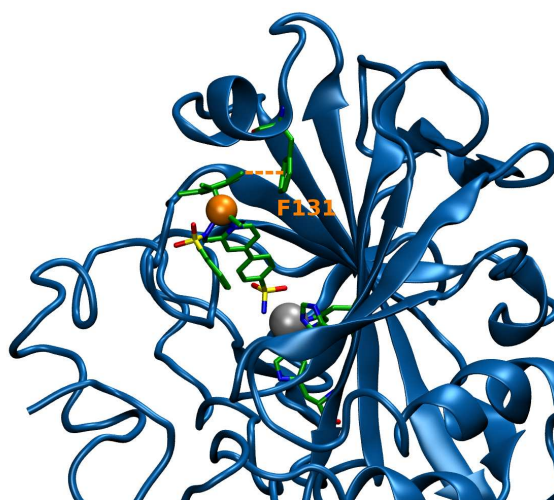


Figure 2.1. Close up view of the structure of $[(cp^*)Ir(5)Cl]Cl$ (**16**) \subset WT hCA II (PDB code 1G54). Position F131 is highlighted and can interact with the complex (orange dashes). (Maurus Schmid calculations)

Furthermore, catalytic centers were parameterized and the first calculation results for hCA II hybrid catalyst are presented in Figure 2.1. In the absence of crystallographic information on the exact location of the catalytic center, computational tools provided a qualitative model of the hybrid catalyst. This theoretical model was used to predict the amino acid

residues to be mutated. Mutations at positions I91 and K170 were found to be relevant for genetic optimization.

Because our computational resources were limited, information gained from existing crystal structures as well as published affinity constants for specific ligands were exploited to successfully create new *in silico* designed inhibitors. To validate the designed structures, inhibitors were manually docked into the funnel-shaped cavity of hCA II. The advantage of this technique was to rapidly provide an overview of the interactions between the protein scaffold and the potential inhibitor-ligands. For this purpose, computer tools including Maestro, and VMD^[17] were used.

The first generation of ligands was based on a report by Fierke *et al.*^[18] They provided a tight-binding (down to nM, see Table 1.3) library of fluorinated compounds that come into contact with the protein scaffold at multiple points, including a CH/ π bond between the upper part of the inhibitor and the residue F131 (highlighted in orange, Figure 2.2a). The first generation of ligands bearing pyridine residues that can interact with the F131 residue was thus conceived. As an illustrative example, Figure 2.2b shows the ligand **4** docked into the hCA II pocket with a possible interaction with residue F131 as anticipated. The newly designed inhibitor-ligands are shown in Scheme 2.1.

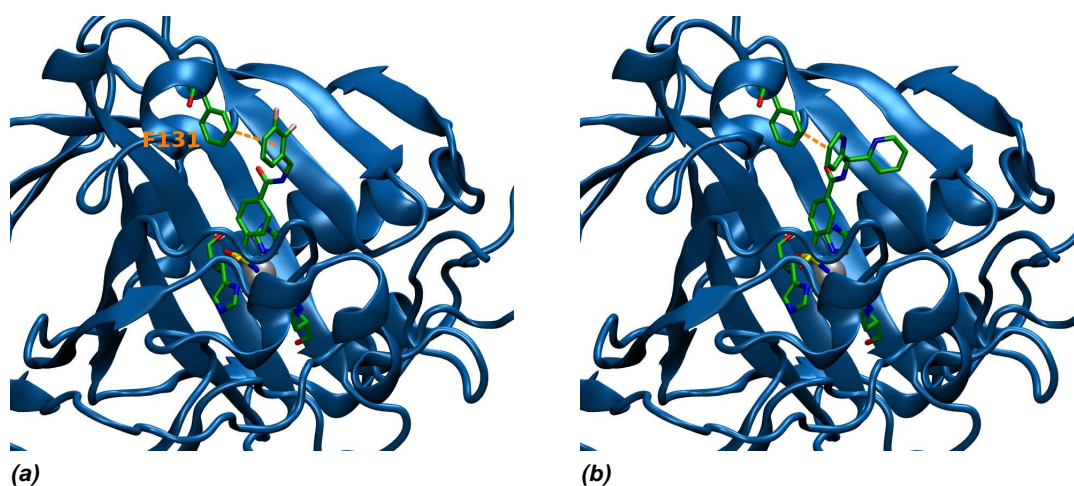
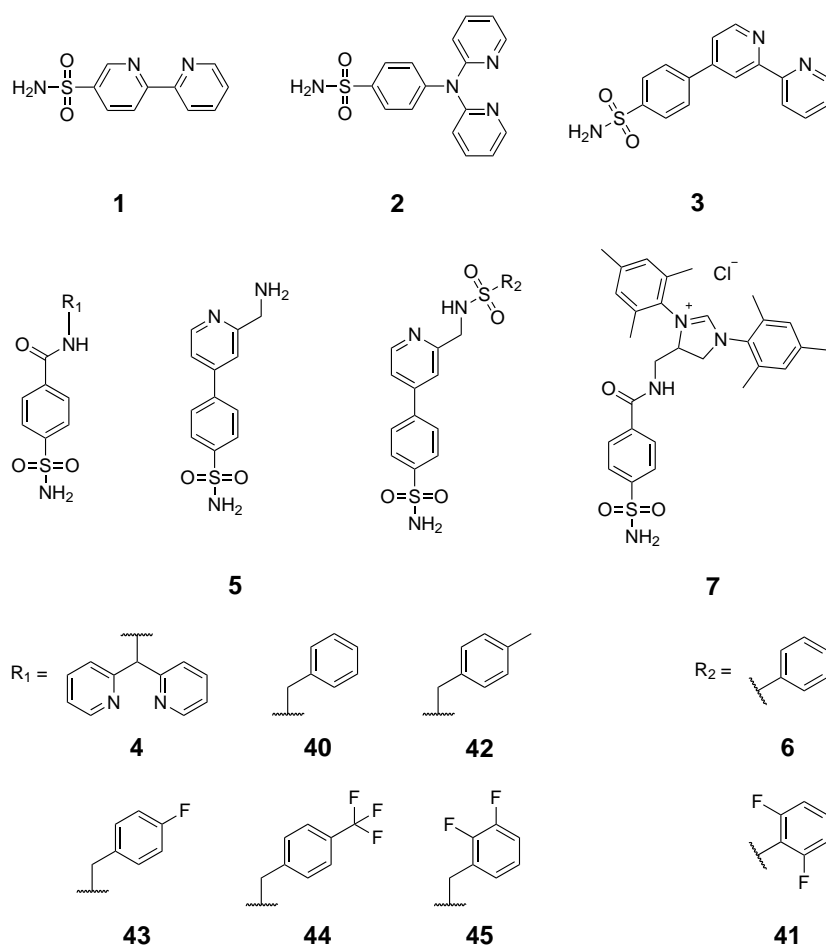


Figure 2.2. a) Close up view of the structure of *N*-(2,3-difluorobenzyl)-4-sulfamoylbenzamide \subset WT hCA II (PDB code 1G52). CH/ π interaction between F131 and the ligand phenyl ring is highlighted in orange. b) From the same point of view, *N*-(di(2-pyridyl)methyl)-amidobenzene-4-sulfonamide (**4**) was manually docked into wild type hCA II (PDB code 1G52).

The first generation of ligands was based on bipyridine type ligands, such as **2**, **3** and **4**. The shorter ligand **1** was also part of this library. With ligand **1**, the metal is located more deeply in the hCA II funnel-shaped cavity, leading to a greater number of interactions between the first and second coordination sphere and the substrate. This may induce higher enantioselectivity during catalytic reactions. Inhibitor **40** and its derivatives have been designed for the study of interactions between inhibitors and protein. Ligands **6** and **41** complement the library and have been specifically conceived for the transfer hydrogenation reactions. The carbene ligand **7** was designed for metathesis reactions.

In section 2.2.2 and following, the various syntheses required to obtain the inhibitor-ligands presented in Scheme 2.1 are reported in detail.

Scheme 2.1. Structure of sulfonamide ligand-inhibitors used in this study.

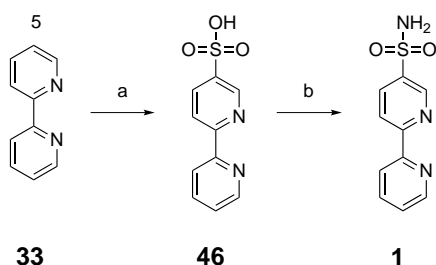


2.2.2 First ligand generation: bipyridine derivatives

2,2'-Bipyridine-5-sulfonamide (**1**)

For the synthesis of 2,2'-bipyridine-5-sulfonamide (**1**), the proposed two step synthesis is presented in Scheme 2.2. Access to compound **46** was gained by sulfonation of the 2,2'-bipyridine (**33**). The subsequent activation of the sulfonic acid bipyridine **46** with PCl_5 , followed by treatment with aqueous NH_3 , resulted in the substitution reaction to 2,2'-bipyridine-5-sulfonamide (**1**).

Scheme 2.2. Synthesis of ligand **1**.



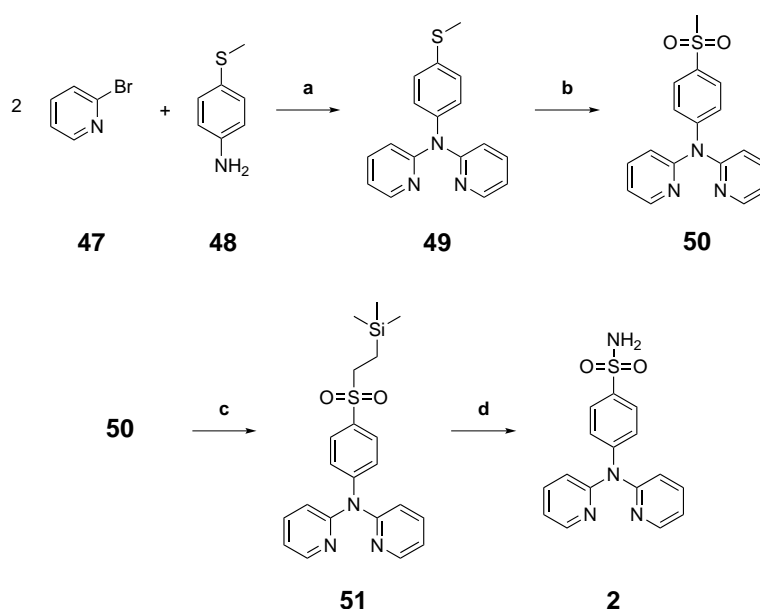
Reagents and conditions: **a)** HgSO_4 , oleum, 220 °C, 24 h **b)** i) PCl_5 , toluene, 120 °C, 30 min ii) conc. aqueous NH_3 , r.t., overnight.

The standard ligand synthesis procedure to obtain sulfonic acid derivative **46** from commercially available 2,2'-bipyridine (**33**) was previously described by Kuchler *et al.*^[19] Transformation of **33** into **46** was achieved in the presence of a catalytic amount of mercury(II), which allows for the activation of position 5 of bipyridine ring (Scheme 2.2). Two purification methods were proposed in the literature in order to obtain the compound **46**. Pilling *et al.*^[20] proposed an easy, rapid method for purification by crystallization of the product after removing mercury traces using activated charcoal; however, this method could not be reproduced. Kuschler and co-workers were able to isolate the product by ion exchange extraction of the tetra(*N*-butyl)ammonium salt in CH_2Cl_2 . The synthesis of 2,2'-bipyridine-5-sulfonamide (**1**) was achieved using PCl_5 , leading to a sulfonyl chloride intermediate followed by sulfonamide group formation in concentrated NH_3 aqueous solution. Due to the low overall yield (11 %), the last step synthesis was carried out on a gram scale.

4-(Di-2-pyridinylamino)-benzenesulfonamide (**2**)

The ligand **2** was prepared according to Scheme 2.3. Preparation of ligands containing sulfonamide moieties remains a major challenge to synthetic chemists because it is not always possible to obtain a sulfonamide group from a sulfonic acid intermediate, as demonstrated for the synthesis of compound **1**. To circumvent the use of sulfonic acids, the route shown in Scheme 2.3, using a thiomethyl group, was envisioned. The advantage of this route over the sulfonic acid method is that a cross-coupling reaction, such as Buchwald-Hartwig amination, can be applied (Scheme 2.3, reaction a).

Scheme 2.3. Synthesis of ligand **2**.



Reagents and conditions: a) tris(dibenzylideneacetone)dipalladium, 1,1'-bis(diphenylphosphino)ferrocene, sodium *tert*-butoxide, toluene, under N₂, 100 °C, 24 h b) KMnO₄/MnO₂ (1/1), CH₂Cl₂, r.t., 3 d c) i) BuLi, THF, -78 °C, 1 h ii) chloromethyltrimethylsilane, THF, r.t., 2 d d) i) TBAF, THF, r.t., 1 h ii) hydroxylamine-*O*-sulfonic acid, sodium acetate, THF, H₂O, r.t., overnight.

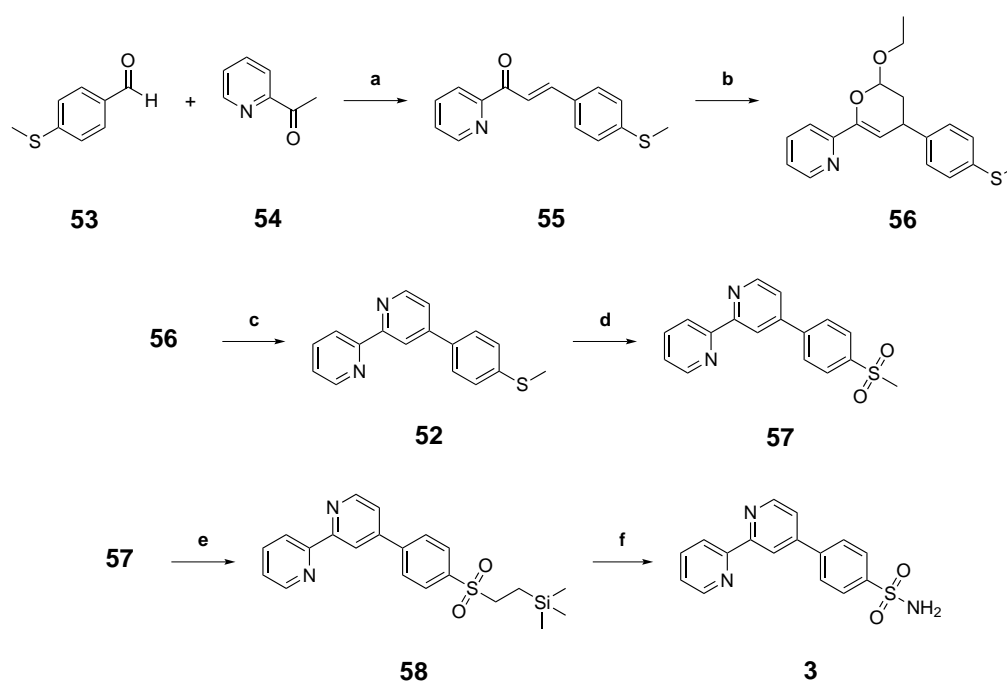
A four-step synthesis was envisioned: Buchwald-Hartwig amination^[21] leading to compound **49**, followed by sulfonamide group preparation as demonstrated by Zhang *et al.*^[22] Commercially available compounds **47** and **48** were reacted under Buchwald-Hartwig^[21] conditions in the presence of a palladium catalyst. This cross coupling reaction generated the key intermediate product, **49**, after flash chromatography. The thiomethyl group had to be fully

oxidized using a mixture of $\text{KMnO}_4/\text{MnO}_2$ that was removed by filtration to obtain product **50** according to Lee.^[23] Product **2** was obtained in a two-step synthesis, first compound **50** was protected with chloromethyltrimethylsilane to obtain compound **51**, which can be reduced to the corresponding sulfone using TBAF. Sulfonamide formation using hydroxylamine-*O*-sulfonic acid results in the formation of product **2** (overall yield 12%).

(4-((2,2'-Bipyridine)4-yl)benzenesulfonamide (**3**))

A class of bipyridine ligand containing longer spacers was also envisaged. The synthesis of (4-((2,2'-bipyridine)4-yl)benzenesulfonamide (**3**) was achieved by minor modification of the procedure published by Bergman and co-workers^[24] to first obtain (4-(4-(methylthio)phenyl)-2,2'-bipyridine (**52**). A synthetic pathway described in the previous section (Scheme 2.3) was applied to transform the thiomethyl to sulfonamide, resulting in ligand **3** (Scheme 2.4).

Scheme 2.4. Synthesis of ligand **3**.

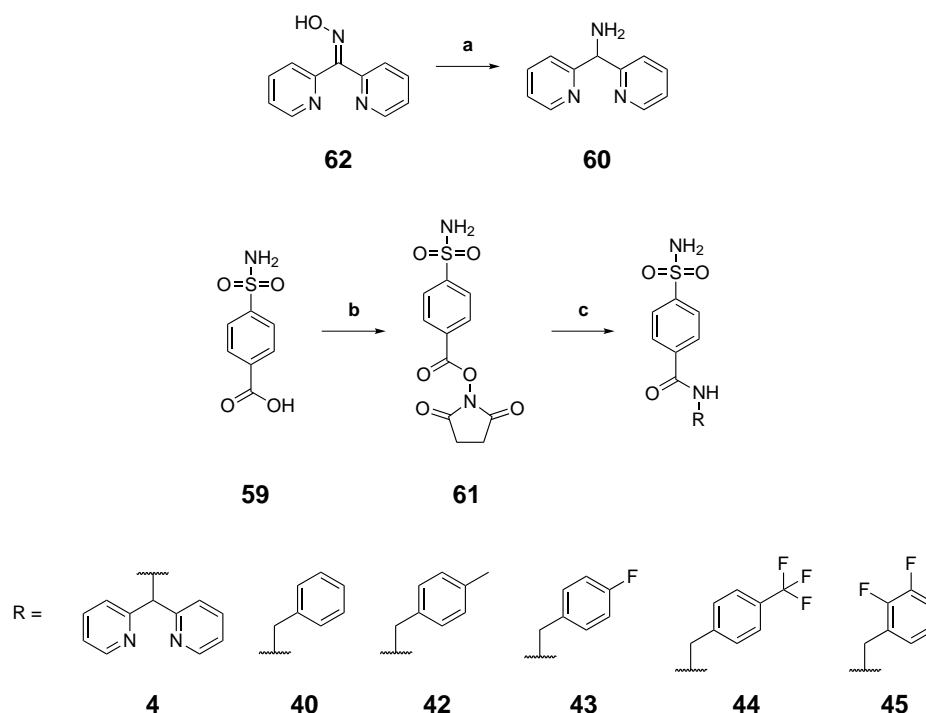


Reagents and conditions: a) NaOH aq. solution, MeOH, r.t., 3 h b) ethyl vinyl ether, yttrium hexafluoroacetylacetonate, 4 Å molecular sieves, THF, under N_2 , r.t., 3 d c) $\text{H}_2\text{NOH}\cdot\text{HCl}$, ACN, reflux, 6 h d) $\text{KMnO}_4/\text{MnO}_2$ (1:1), CH_2Cl_2 , r.t., 3 d e) i) BuLi, THF, $-78\text{ }^\circ\text{C}$, 1 h ii) chloromethyltrimethylsilane, THF, r.t., 2 d f) i) TBAF, THF, r.t., 1 h ii) Hydroxylamine-*O*-sulfonic acid, sodium acetate, THF, H_2O , r.t., overnight.

Following the route published by Bergman and co-workers^[24] with only minor modifications, commercially available 2-acetylpyridine (**53**) was reacted with 4-(methylthio)benzaldehyde (**54**) under Michael conditions to obtain the heterodiene product **55**, which was purified by crystallization from a saturated MeOH solution. The synthesis of **56** was achieved by aldol condensation of **55** with ethyl vinyl ether, using yttrium hexafluoroacetylacetonate instead of the typical copper catalyst.^[25] Following the work of Ciufolini and co-workers, who developed the synthetic pathway to obtain pyridine from dihydropyrans, the intermediate compound **52** was synthesized using $\text{H}_2\text{NO} \cdot \text{HCl}$ as the nitrogen source.^[25] Subsequently, thioether **52** was oxidized to the sulfone **57** under heterogeneous conditions with $\text{KMnO}_4/\text{MnO}_2$.^[23] The synthesis of (4-((2,2'-bipyridine)4-yl)benzenesulfonamide was completed by transformations of precursors **57** to the corresponding sulfonamide **3** using the standard method illustrated in the previous section (overall yield 8%).

***N*-(Di(2-pyridyl)methyl)-amidobenzene-4-sulfonamide (4)**

The synthesis of **4** relies on two key steps, comprising oxime reduction followed by amide bond formation. The oxime reduction was previously described by Meunier using zinc as the reducing agent.^[26] 4-Carboxybenzenesulfonamide (**59**) activation was achieved using the method described by Whitesides and co-workers.^[27] Compound **60** was directly reacted with **61** without purification to avoid any decomposition of the primary amine. Ligand **4** was isolated as a white powder (overall yield 59%). Following the same strategy, a library of inhibitors (**40**, **42**, **43**, **44** and **45**) was prepared (overall yield 15-44%).

Scheme 2.5. Synthesis of inhibitors **4**, **40**, **42**, **43**, **44** and **45**.

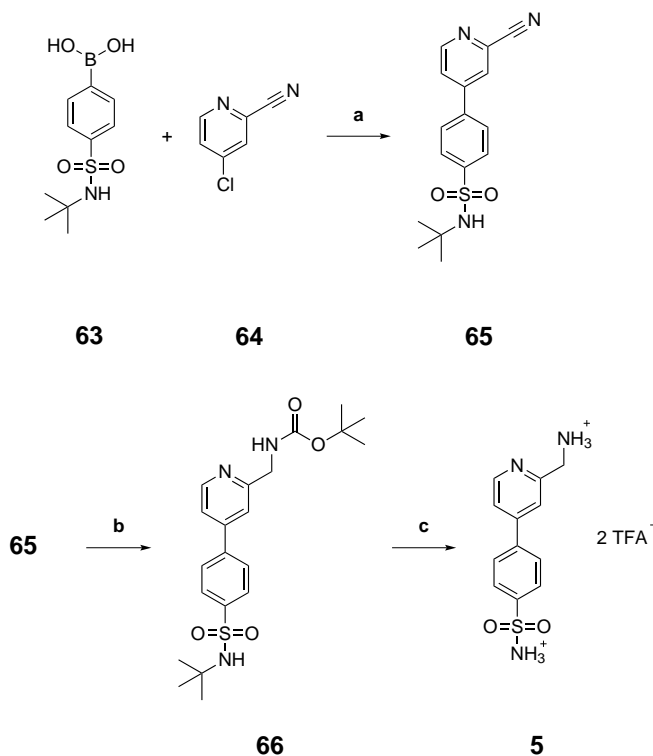
Reagents and conditions: a) ammonium acetate, Zn, H₂O/MeOH/NH₃, 80 °C, 5 h b) NHS, DCC, DMF, r.t., overnight c) **60** or benzylamine derivatives, H₂KPO₄, H₂O/acetone, r.t., overnight.

2.2.3 Second ligand generation: picolyamine derivatives

4-(2-(Aminomethyl)pyridin-4-yl)benzenesulfonamide (**5**)

A second generation of ligand-inhibitors was envisaged based on the 2-picolyamine class of ligands. As previously reported, this type of ligand was successfully applied for reduction of ketones in water.^[28,29] A three-step synthesis of **6** was proposed according to Scheme 2.6. First, commercially available 4-(*tert*-butylaminosulfonyl)benzeneboronic acid (**63**) was coupled to 4-chloropyridine-2-carbonitrile (**64**) by the Suzuki method, followed by two deprotection steps; the nitrile was reduced with $(\text{AlCl}_3) \cdot \text{LiAlH}_4$ ^[30] and *tert*-butylaminosulfonyl was cleaved using TFA.^[31] This three-step synthesis led to 4-(2-(aminomethyl)pyridin-4-yl)benzenesulfonamide (**5**).

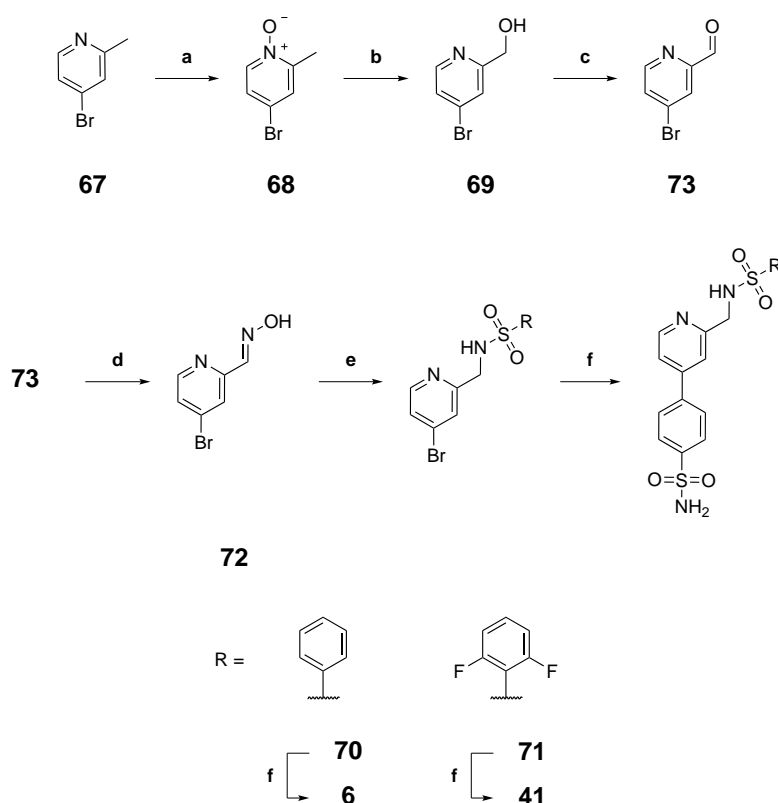
Scheme 2.6. Synthesis of ligand **5**.



Reagents and conditions: **a**) $[\text{Pd}(\text{PPh}_3)_4]$, Na_2CO_3 , THF, reflux, 3 h **b**) i) LiAlH_4 , AlCl_3 , THF, r.t., 5 h ii) Boc_2O , CH_2Cl_2 , r.t., overnight **c**) TFA, anisole, r.t., overnight.

The synthesis presented in Scheme 2.6 was centered on the coupling of **63** and **64** under Suzuki-Miyaura conditions to obtain compound **65**. Subsequently, the nitrile group was reduced with $(\text{AlCl}_3) \cdot \text{LiAlH}_4$. Reduction of the nitrile followed by precipitation of the amine from diethyl ether did not generate a clean product but, by generating the Boc protected amine **66**, the product could be purified by column chromatography. The ligand **5** was obtained by double deprotection with TFA to produce **6** as a colorless solid (overall yield 39%).

Considering the promise held by ligand **5** as a scaffold for new catalysts,^[29,32] an investigation in the direction of a new approach to the synthesis of **6** (Scheme 2.7) was proposed in order to avoid purification problems encountered during the preparation of **5**. Moreover this second methodology allowed for large scale synthesis. The synthesis started with commercially available 4-bromo-2-methylpyridine (**67**), which was readily oxidized with 3-chloroperoxybenzoic acid to compound **68**. Treatment of molecule **68** with trifluoroacetic anhydride (Boekelheid reaction) led to the alcohol function present in molecule **69**.^[33,34] The alcohol function was oxidized to the corresponding aldehyde with MnO_2 .^[35] The aldehyde function was transformed into oxime^[36] and reduced to amine using TFA and Zn, and the obtained primary amine was reacted with sulfonylchloride derivatives, leading to picolylamine ligand **70** and **71**.^[37] Finally, 4-sulfamoylphenylboronic acid, pinacol ester was coupled to the different bromo pyridine derivatives under microwave irradiation^[38] to obtain inhibitor ligands **6** and **41**.

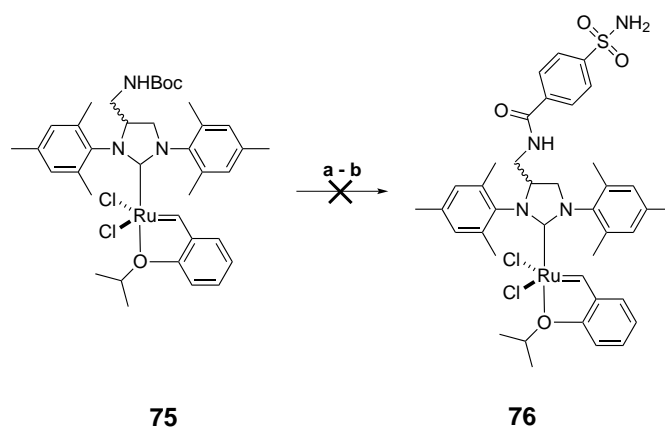
Scheme 2.7. Synthesis of ligands **6** and derivatives.

Reagents and conditions: **a)** 3-chloroperoxybenzoic acid, CH_2Cl_2 , r.t., overnight **b)** trifluoroacetic anhydride, reflux, 30 min **c)** MnO_2 , chloroform, reflux, 2 h **d)** hydroxylamine hydrochloride, NaHCO_3 , MeOH, r.t., overnight. **e)** i) TFA, zinc dust, r.t., 1 h ii) arylsulfonylchloride derivatives, DIPEA, CH_2Cl_2 , r.t., overnight **f)** $[\text{Pd}(\text{PPh}_3)_4]$, Na_2CO_3 , water/dioxane (1/1), microwave (150°C), 15 min.

2.2.4 Carbene ligand

The synthesis of the carbene ligand **74** (Scheme 2.9) was also envisioned. Following the work published by Hoveyda and Grubbs, who reported the synthesis of a carbene ligand that could be bound to a solid support.^[39,40] The strategy was also applied by Ward *et al.*^[12] to synthesize a biotinylated carbene complex (Scheme 2.8). In our case this synthetic strategy did not work, as the activated *para*-carboxysulfonamide will not react with the deprotected carbene **75**. Therefore, a multi-step synthesis was proposed to first prepare the sulfonamide protected ligand **74** (Scheme 2.9), which can react with the 1st generation Hoveyda-Grubbs catalyst. Finally, as previously discussed in section 2.2.3, the sulfonamide group can be deprotected under acid conditions.

Scheme 2.8. Proposed synthesis of carbene complex.

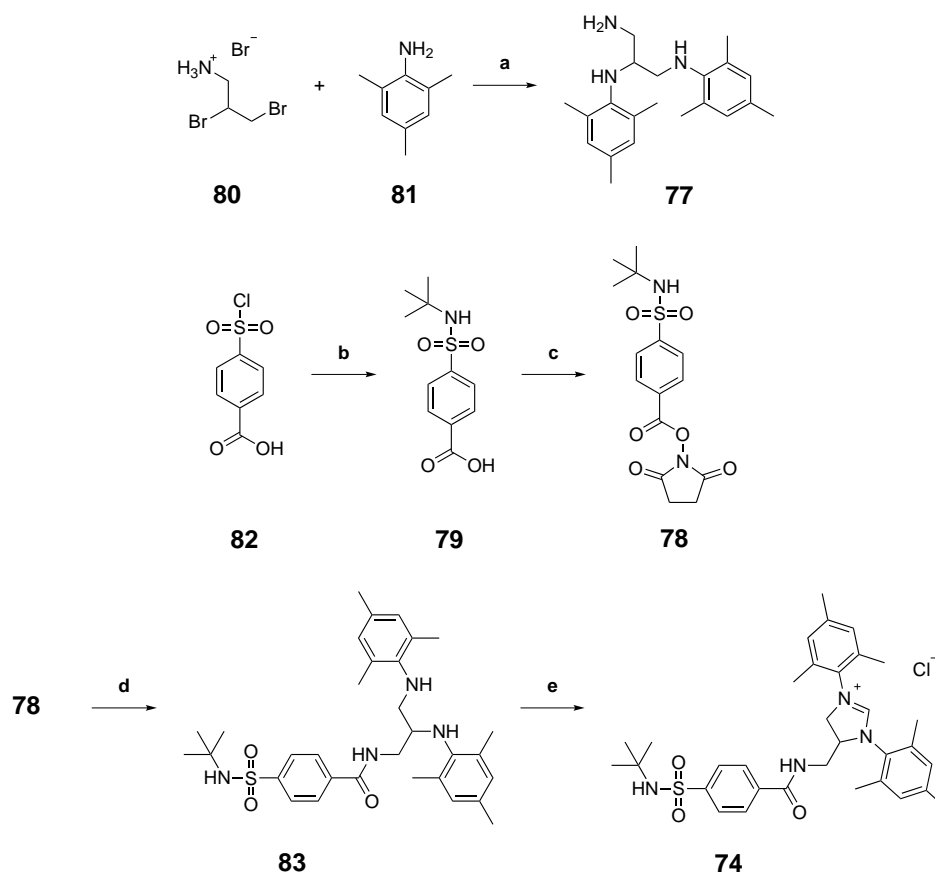


Reagents and conditions: **a)** HCl (g), CH₂Cl₂ **b)** **61**, NEt₃, DMF, r.t. or reflux, overnight.

A five-step synthesis was envisaged for the preparation of the carbene precursor (**74**, Scheme 2.9). The two building blocks **77** and **78** were prepared separately. First, *tert*-butylamine was reacted with 4-(chlorosulfonyl)benzoic acid to obtain the *tert*-butyl protected sulfonamide **79**. At the end of the synthesis, this protecting group is easily removed under acidic conditions, *i.e.* conc. HCl. The use of HCl is important to prevent chloride ligand displacement on the carbene Ru complex.^[31] Compound **79** was sub-

sequently activated with *N*-hydroxysuccinimide in order to obtain intermediate compound **78**. The second building block, **77**, was prepared by a slightly modified procedure published by Ward *et al.*^[12] Compound **80** was reacted with 2,4,6-trimethylaniline (**81**), leading to molecule **77** without Boc protection; compound **77** was directly coupled to compound **78**. The synthesis of ligand **74** was finally achieved using triethylorthoformate (overall yield 23%). Unfortunately, after many attempts it was not possible to obtain the carbene precursor **76**. The hygroscopicity of the imidazolium salt is one possible explanation for the non-reactivity (the deprotonation does not occur under basic conditions). This may be avoided by modifying the counterion and choosing, for example, PF_6^- , which is less hygroscopic than chloride.

Scheme 2.9. Synthesis of carbene ligand **74**.



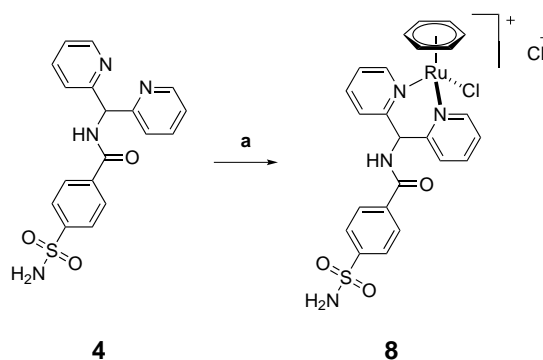
Reagents and conditions: a) 120 °C, overnight b) *tert*-butylamine, MeOH, r.t., overnight c) NHS, DCC, DMF, r.t., overnight. d) **77**, DMF, r.t., 72 h e) triethylorthoformate, NH_4Cl , 120 °C, 48 h.

2.2.5 Complex synthesis

Ruthenium, rhodium and iridium complexes

Two strategies were used for the synthesis of complexes. First, ruthenium, rhodium and iridium dimers were coupled with bipyridine-type ligands in acetonitrile (Scheme 2.10). Acetonitrile was used due to its characteristic lability when used as a ligand. Bipyridine type complexes were insoluble in acetonitrile and could be purified by filtration followed by a repeated washes. Most metal dimers used for this study were commercially available except for $[(\eta^6\text{-C}_6\text{Me}_6)\text{RuCl}_2]_2$, which was synthesized according to the procedure by Mann *et al.*^[41]

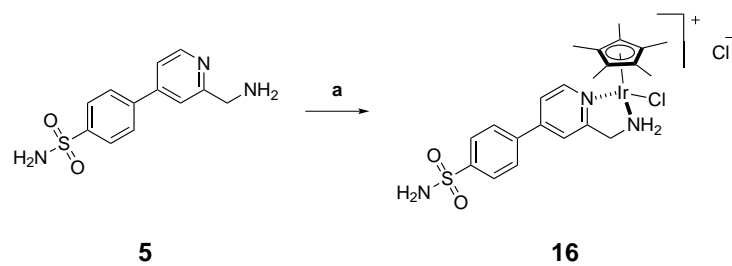
Scheme 2.10. Synthesis of bipyridine-type complexes.



Reagents and conditions: a) $[(\eta^6\text{-C}_6\text{H}_6)\text{RuCl}_2]_2$, ACN, reflux, 4 h.

For the synthesis of complexes based on the 2-picolylamine pattern, the protocol described by Oro and co-worker was followed.^[42] The reaction was performed in ethanol and the product was purified by precipitation with diethyl ether (Scheme 2.11). NMR analysis of complexes $[(\text{cp}^*)\text{Ir}(\mathbf{6})\text{Cl}]\text{Cl}$ (**17**) and $[(\text{cp}^*)\text{Ir}(\mathbf{41})\text{Cl}]\text{Cl}$ (**18**) indicated the presence of two states of coordination in solution according to the pH. The sulfonamide amine binds to the metal, as previously described by Xiao, Section 1.4.

Scheme 2.11. Synthesis of 2-picolyamine-type complexes.



Reagents and conditions: **a**) [(cp*)IrCl₂]₂, EtOH, reflux, 2 h.

2.3 Protein inhibitor interactions

2.3.1 Circular dichroism

The circular dichroism (CD) spectrum of wild type hCA II in the near-UV region (from 240 nm to 350 nm) is diagnostic of its tertiary structure, as previously reported by Carlsson *et al.*^[43] The spectrum contains a characteristic, large, positive band at 246 nm and a deep, broad negative band in the region between 260 and 300 nm, which displays a fine structure. The observed signal can be attributed to the seven tryptophan residues (Trp 97, 123, 192, 209 and 245) located in the central β -sheet region of hCA II scaffold (see Figure 2.3).

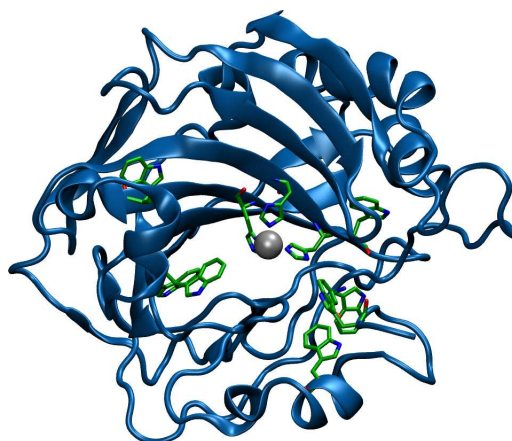


Figure 2.3. Human Carbonic Anhydrase II with the seven Trp residues highlighted in green (PDB code 1G54). Trp residues are mainly localized in the funnel-shaped cavity and the presence of a catalyst inside the pocket alters the three-dimensional structure of the protein, resulting in CD spectra modification.

As catalytic conditions required small amounts of organic solvent to dissolve complexes and/or substrates, hCA II structural stability was investigated by circular dichroism in the presence of varying DMSO concentrations (0 to 50%, v/v) in phosphate buffer solution. The asymmetric environment around the various aromatic amino acid residues of WT hCA II was slowly disrupted, upon unfolding, when the DMSO concentration in the phosphate buffer exceeded 50% (Figure 2.4).

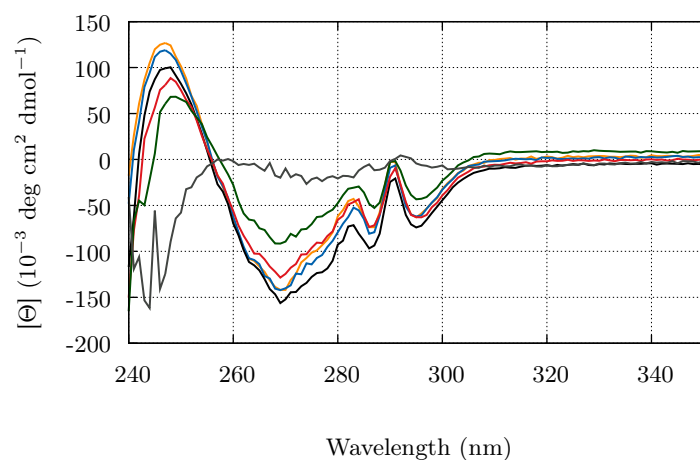


Figure 2.4. The near-UV CD spectrum of WT hCA II. WT hCA II was dissolved in 50 mM phosphate buffer, pH 7.4. Cell path lengths and protein concentration were 1 cm and 1 mg/mL, respectively. Percentage of DMSO: 0% (○), 10% (●), 20% (●), 30% (●), 40% (●), 50% (●).^[44]

The presence of complex [(cp*)Ir(**6**)Cl]Cl (**17**) inside the hCA II the funnel-shaped cavity induced a rise in the signal in the first part of the CD spectra (240 to 300 nm, Figure 2.5). The change in the spectra indicated a change in the asymmetric environment of the hCA II scaffold, due to an inhibitor located inside the funnel-shape of the protein that disturbed Trp residues. The increasing signal reached a maximum at 0.8 equivalents of added complex. An inhibitor-protein ratio of 0.8 was therefore used for the catalytic reaction.

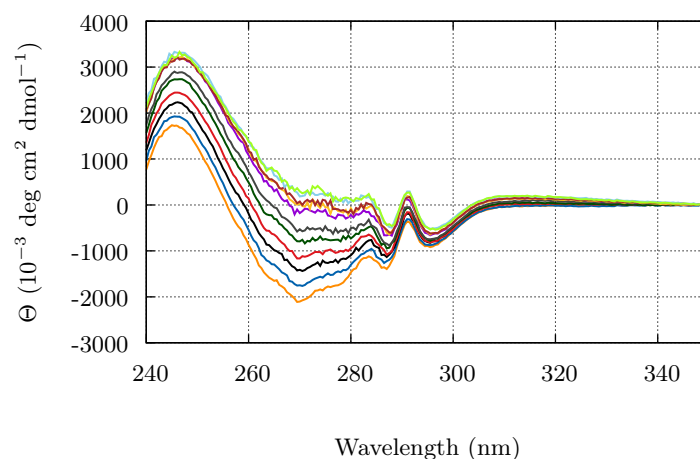


Figure 2.5. Near-UV CD spectrum of WT hCA II (○) and [(cp*)Ir(**6**)Cl]Cl (**17**) ⊂ WT hCA II (0.1 equiv. (●), 0.2 equiv. (●), 0.3 equiv. (●), 0.4 equiv. (●), 0.5 equiv. (●), 0.6 equiv. (●), 0.7 equiv. (●), 0.8 equiv. (●), 0.9 equiv. (●), 1.0 equiv. (●)). The protein was dissolved under imine catalytic condition of 1.2 M MOPS buffer containing 3 M sodium formate, pH 7.5, 22 °C. Cell path lengths and protein concentration were 0.1 cm and 1 mg/100μL, respectively.

2.3.2 Thermodynamics of hCA II-inhibitor binding

To determine the thermodynamics of protein-inhibitor binding in solution, two popular techniques were used based on ease of observation, as explained in Section 1.3.4. The inhibition constant (K_i) and the equilibrium dissociation constant (K_d) are introduced in the following sections. It should be noted that the lowercase letter, *i.e.* i and d , refers to the type of experimental approach used to determine the equilibrium dissociation constant K , and thus are directly comparable.^[45]

Esterase activity screening assay

Steady-state kinetic experiments were used to determine the inhibition constant K_i . Ligands or complexes with inhibition constants on the order of mM were titrated against hCA II (experimental details in Section 4.4). Binding experiments were performed in HEPES buffer (pH 8) containing 10% DMSO to solubilize the inhibitors as well as the substrate (*p*-nitrophenyl acetate).

For easy comparison of hydrolysis of *p*-nitrophenyl acetate (constant concentration), data were presented as % activity of the enzyme as a function of inhibitor concentration. The results were fitted to the function defined by equation 2.1 to determine the inhibition constant K_i .^[16,46,47]

$$v = \frac{v_o \cdot K_i}{K_i + ([I]_t - 0.5\{([I]_t + [E]_t + K_i) - \sqrt{([I]_t + [E]_t + K_i)^2 - 4 \cdot [I]_t \cdot [E]_t}\})} \quad (2.1)$$

Parameters used in the steady-state kinetics equation 2.1 are v_o for the initial velocity of the hCA II catalyzed reaction in the absence of inhibitor, K_i for the binding affinity constant, $[I]_t$ for the total concentration of the inhibitor, and $[E]_t$ for the total concentration of enzyme.

Competitive displacement assay

Competitive displacement of fluorescent hCA II inhibitor, dansylamide (DNSA), was used to determine the dissociation constant K_d . Inhibitors with dissociation constants on the order of nM (experimental details in Section 4.4.2) were titrated using this method. DNSA is a “non-fluorescent” molecule in aqueous solution but, in the presence of hCA II, the fluorescence signal at 470 nm increases (excitation at 280 nm, see Figure 2.6).

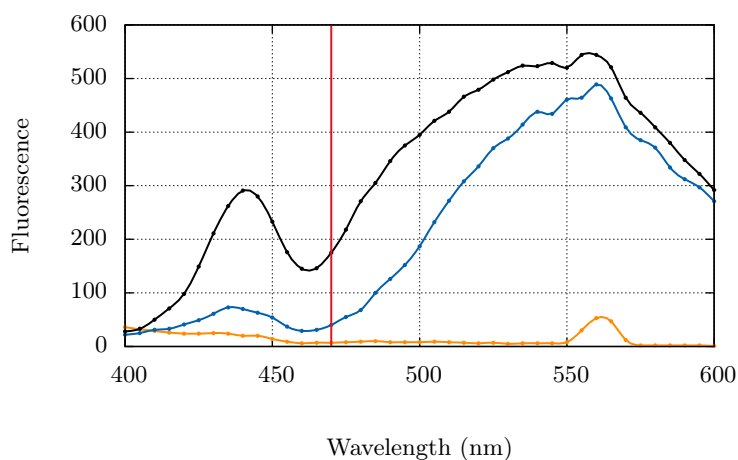


Figure 2.6. Fluorescence spectra of dansylamide (DNSA) \subset hCA II. [Enzyme] = 0.1 μ M, [DNSA] = 2.25 μ M. hCA II (\bullet), DNSA (\bullet), DNSA \subset hCA II (\bullet), 470 nm (\blacksquare).

The dissociation constants (K_d) of screened hits were determined using a slightly modified method proposed by Tripp and coworkers.^[48–50] Screening using a black, flat-bottom 96-well plate (NUNC F96 MicroWell Plates) was realized with excitation at 280 nm and detection at 470 nm. The dissociation constant K_d for DNSA was determined by titrating hCA II with different DNSA concentrations (data reported in Figure 2.7). The equilibrium dissociation constant for DNSA (K_{DNSA}) was determined by fitting the data to equation 2.2

$$F_{\text{tot}} = \frac{F_{\text{obs}} - F_{\text{ini}}}{F_{\text{end}} - F_{\text{ini}}} = \frac{1}{1 + (K_{\text{DNSA}}/[\text{DNSA}])} \quad (2.2)$$

where F_{tot} is the total fluorescence, F_{ini} the initial fluorescence of hCA II in the absence of DNSA, and F_{end} is the end point fluorescence.

Equilibrium dissociation constants for inhibitors were determined by competitive binding

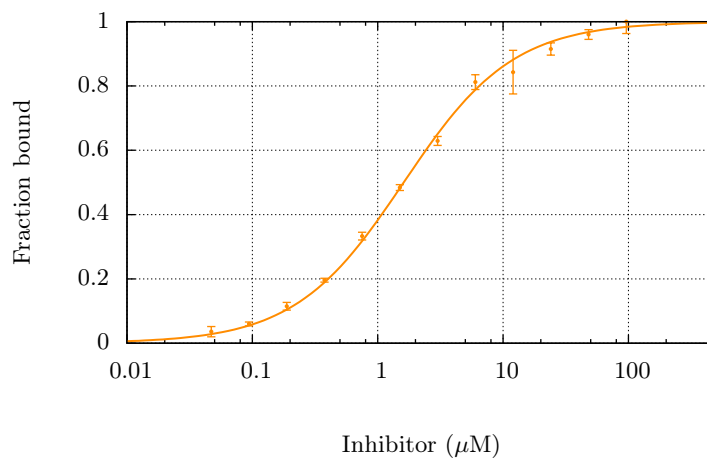


Figure 2.7. Fluorescence titration of dansylamide (DNSA) against hCA II. The increase in the fluorescence emission intensity at 470 nm (●) for a fixed concentration of hCA II ($[\text{Enzyme}] = 0.1 \mu\text{M}$). The solid, smooth line is the best fit of the data according to equation 2.3 for the DNSA dissociation constant (K_d) determination.

with DNSA. A fixed concentration of DNSA ($2.25 \mu\text{M}$) and hCA II (100 nM) was titrated against inhibitors (from $100 \mu\text{M}$ to 25 nM). The K_d value for each inhibitor was determined by fitting the equation 2.3

$$F_{tot} = \frac{F_{obs} - F_{ini}}{F_{end} - F_{ini}} = \frac{1}{1 + (K_{\text{DNSA}}/[\text{DNSA}])(1 + [I]/K_d)} \quad (2.3)$$

where F_{tot} is the fraction of total fluorescence, F_{obs} the fluorescence signal at any concentration of inhibitor, F_{ini} the initial fluorescence of hCA II without DNSA, and F_{end} the end point fluorescence.

First generation inhibitor-ligands

After synthesis of the first generation inhibitors (Scheme 2.12), their respective inhibition constants (K_i , Section 2.3.2) were determined (Figure 2.8) and, as expected, inhibitors **3** and **4** exhibited inhibition constants on the order of nM. (Table 2.2, entry **5** and **6**). However, it was noted that inhibitor **2** was characterized by a low inhibition constant (2900 ± 200 nM), which was probably due to the large size relative to the hCA II cavity. The inhibitor **2** was therefore removed from selection for the synthesis of complexes. Indeed, for the development of a hybrid catalyst, an inhibition constant on the order of magnitude of nM is required. Measurements were validated by comparing the value obtained by titration of inhibitors **84** and **59** with the published values (Table 2.2, entry **1** and **2**).

Scheme 2.12. Structure of arylsulfonamide ligand-inhibitors.

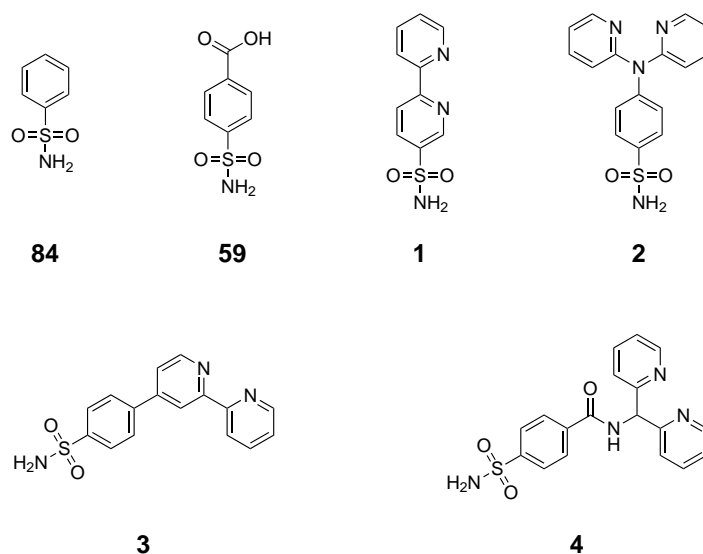


Table 2.2. Final set of parameters for K_i with asymptotic standard error.^[47]

Entry	Inhibitor	Dissociation constant (nM)	Published dissociation constant (nM)
1	84	780 ± 45	200-1500 ^[6]
2	59	570 ± 30	270 ^[6]
3	1	160 ± 15	-
4	2	2900 ± 200	-
5	3	60 ± 16	-
6	4	45 ± 7	-

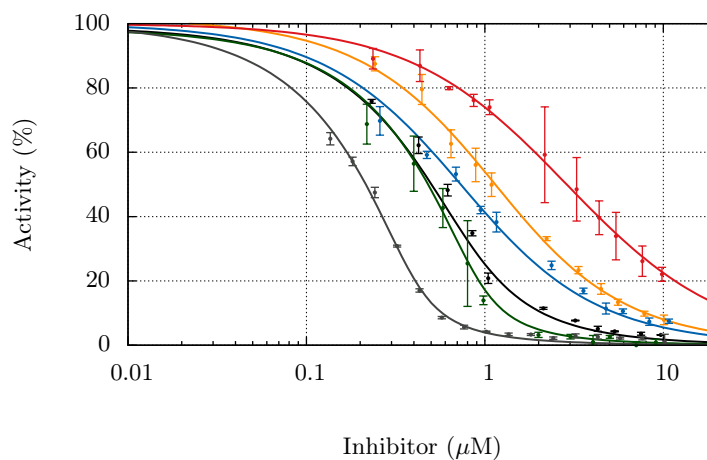


Figure 2.8. Steady-state kinetic data for the inhibition of hCA II first generation ligand-inhibitors. The initial rates of the enzyme-catalyzed hydrolysis of *p*-nitrophenyl acetate were measured as a function of inhibitor concentration. [Enzyme] = 1 μ M, [*p*-nitrophenyl acetate] = 0.5 mM. The solid, smooth lines are the best fits of the data according to equation 2.1 for the K_i of **84** (●), **59** (●), **1** (●), **2** (●), **3** (●), **4** (●).

To investigate more precisely the interactions between hCA II and metal complexes, a collection of ruthenium complexes was synthesized (Section 2.2.5). The first step was to determine the inhibition constant for each complex-inhibitor before moving to the crystallographic analysis (Section 2.3.3). Compared to the parent carboxylic acid 4-carboxybenzenesulfonamide (**59**), all complexes bearing ligands **3** and **4** display increased affinity. Interestingly, $[(\eta^6\text{-biphenyl})\text{Ru}(\mathbf{4})\text{Cl}]\text{Cl}$ (**12**) displays the highest affinity towards hCA II, whereas $[(\eta^6\text{-C}_6\text{H}_6)\text{Ru}(\mathbf{4})\text{Cl}]\text{Cl}$ (**9**) displays a significantly reduced affinity. These data illustrate the subtle complementarity between the piano-stool moiety and the funnel-shaped cavity. Complexes bearing bipyridine ligand **1** were also studied. Titration results of $[(\eta^6\text{-C}_6\text{H}_6)\text{Ru}(\mathbf{1})\text{Cl}]\text{Cl}$ (**8**) against hCA II are reported in Figure 2.9 (●). No reasonable value could be obtained by fitting, due to the linearity of obtained points. This suggests that there was no interaction between the inhibitor-complex **8** and the protein. It is proposed that the metal complex is too big to fit inside the funnel-shaped cavity of the protein; therefore, complex **8** was removed from the library that was used during catalyst implementation. Summary of complex inhibition constants is presented in Table 2.3.

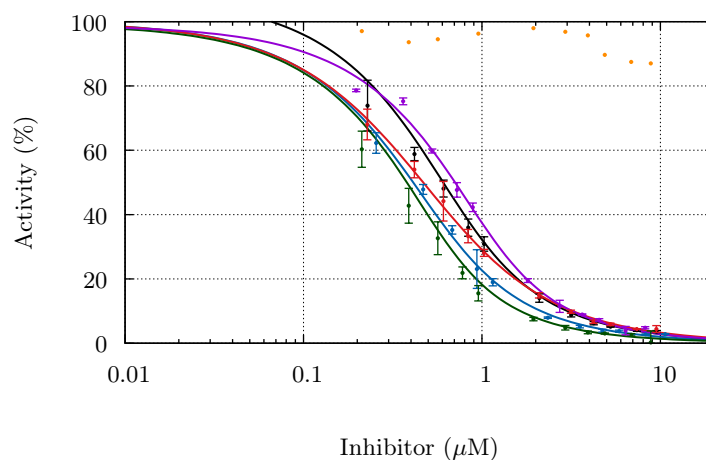


Figure 2.9. Steady-state kinetic data for the inhibition of hCA II ruthenium metal complexes. The initial rates of the enzyme-catalyzed hydrolysis of *p*-nitrophenyl acetate substrate were measured as a function of inhibitor concentration. [Enzyme] = 1 μ M, [*p*-nitrophenyl acetate] = 0.5 mM. The solid, smooth lines are the best fits of the data according to equation 2.1 for the K_i of **8** (●), **9** (●), **10** (●), **11** (●), **12** (●), **15** (●).

Table 2.3. Final set of parameters for K_i with asymptotic standard error.

Entry	Inhibitor	Dissociation constant (nM)	PDB
1	$[(\eta^6\text{-C}_6\text{H}_6)\text{Ru}(\mathbf{1})\text{Cl}]\text{Cl}$ (8)	n.d.	-
2	$[(\eta^6\text{-C}_6\text{H}_6)\text{Ru}(\mathbf{4})\text{Cl}]\text{Cl}$ (9)	194 ± 19	-
3	$[(\eta^6\text{-}i\text{-p-cymene})\text{Ru}(\mathbf{4})\text{Cl}]\text{Cl}$ (10)	275 ± 13	-
4	$[(\eta^6\text{-C}_6\text{Me}_6)\text{Ru}(\mathbf{4})\text{Cl}]\text{Cl}$ (11)	329 ± 16	3PYK
5	$[(\eta^6\text{-biphenyl})\text{Ru}(\mathbf{4})\text{Cl}]\text{Cl}$ (12)	145 ± 12	-
6	$[(\text{cp}^*)\text{Ir}(\mathbf{3})\text{Cl}]\text{Cl}$ (15)	270 ± 40	-

Second generation inhibitor-ligands

Based on a 2-picolyamine pattern, the affinities of the second generation ligand-inhibitors were also determined (Table 2.4). Interestingly, the inhibitor **5** displays a relatively low affinity (150 nM, entry **1**) for the protein compared to inhibitor **6** (11 nM, entry **3**). It should be noted that it is preferable to use the dansylamide method to determine the affinity constant on the nanomolar scale (Section 2.3.2). The determined dissociation constant of 11 nM for ligand-inhibitor **6** suggests an anchoring not only at the level of the zinc-sulfonamide, but also the presence of a secondary recognition element. The arylsulfonyl group can interact with the upper part of the hCA II cavity, as suggested by computational simulation (Figure 2.1). Even

the iridium complex did not significantly affect the observed dissociation constant (15 nM). As the arylsulfonyl group was located near the catalytic center, the metal was located precisely in the funnel-shaped cavity. This feature was used to localize potent mutation sites that could influence the catalytic activity and/or selectivity.

Scheme 2.13. Structure of 2-picolylamine ligand-inhibitors.

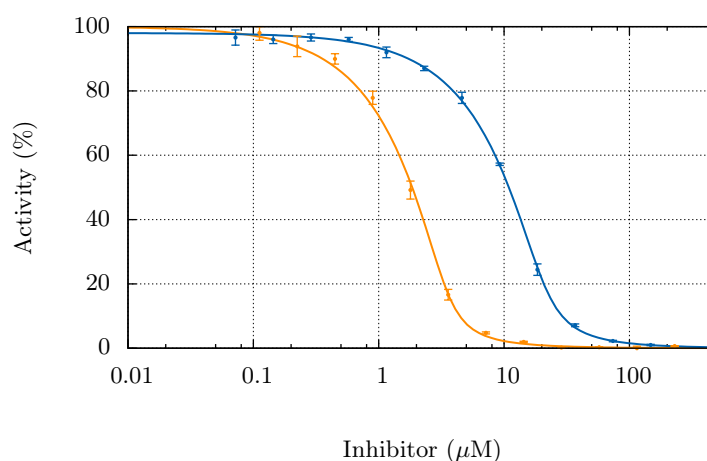
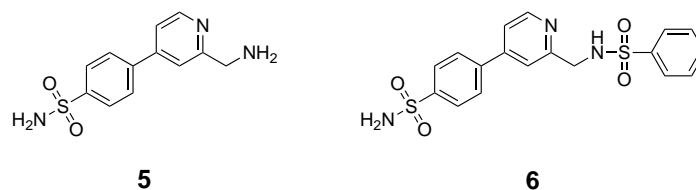


Figure 2.10. Steady-state kinetic data for the inhibition of hCA II second generation ligand-inhibitors. The initial rates of the enzyme-catalyzed hydrolysis of *p*-nitrophenyl acetate substrate were measured as a function of inhibitor concentration. [Enzyme] = 1 μ M, [*p*-nitrophenyl acetate] = 0.5 mM. The solid, smooth lines are the best fits of the data according to equation 2.1 for the K_d of **5** (●), **16** (●).

Table 2.4. Final set of parameters for K_i or K_d with asymptotic standard error.

Entry	Inhibitor	Dissociation constant (nM)	K_i or K_d
1	5	150 ± 35	K_i
2	[(cp*)Ir(5)Cl]Cl (16)	1280 ± 200	K_i
3	6	11 ± 1	K_d
4	[(cp*)Ir(6)Cl]Cl (17)	15 ± 2	K_d

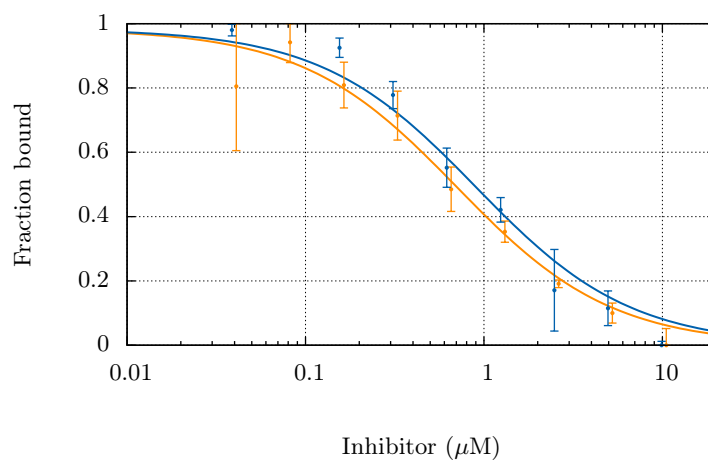


Figure 2.11. Competitive displacement assay data for the inhibition of WT hCA II. The initial rates of the enzyme-catalyzed hydrolysis of *p*-nitrophenyl acetate substrate were measured as a function of inhibitor concentration. [Enzyme] = 1 μ M, [*p*-nitrophenyl acetate] = 0.5 mM. The solid, smooth lines are the best fits of the data according to equation 2.3 for the K_d of **6** (●), **17** (●).

Inhibitors for physical chemistry studies

The computation identified position L198 as a critical site in terms of the thermodynamics of binding for benzenesulfonamide (**84**, Scheme 2.14). Three hCA II mutants were designed and produced recombinantly in *E. coli*: L198A, L198F and L198Q.^[16] The corresponding thermodynamics were determined using the esterase activity assay and fitted raw data are presented in Figure 2.12. This assay yielded $K_i = 1100$ nM for WT hCA II. This value lies well within the reported data ranging from 200–1500 nM.^[6] The experimentally measured inhibition constants of **84** for the L198X mutants are reported in Table 2.5.

Table 2.5. Final set of parameters for dissociation constant, K_d , for benzenesulfonamide **84** with asymptotic standard error for hCA II mutants (see Figure 2.12).^[16]

Entry	Protein	Dissociation constant (nM)	Published dissociation constant (nM)
1	WT	1100 \pm 40	200-1500 ^[6]
2	L198A	5500 \pm 270	-
3	L198F	1700 \pm 130	-
4	L198Q	1800 \pm 100	-

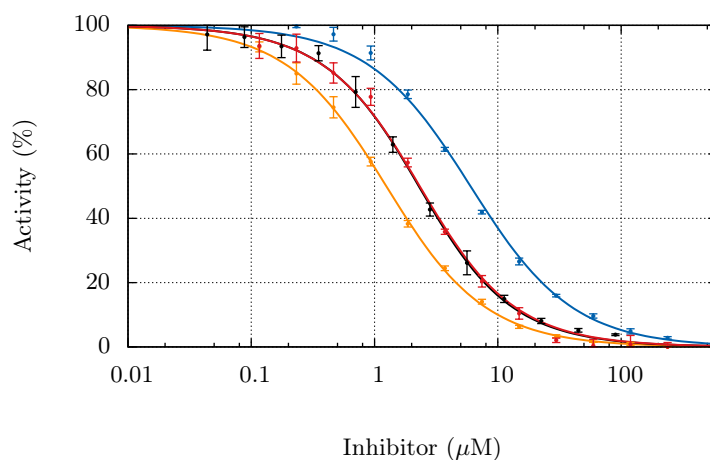
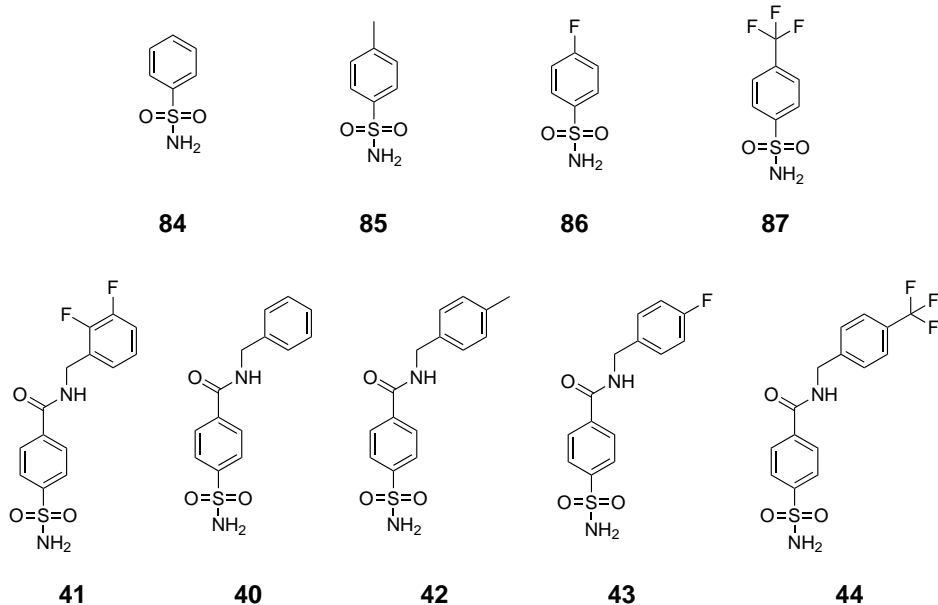


Figure 2.12. Steady-state kinetic data for the inhibition of hCA II mutated proteins by benzenesulfonamide (84). The initial rates of the enzyme-catalyzed hydrolysis of *p*-nitrophenyl acetate substrate were measured as a function of inhibitor concentration. [Enzyme] = 1 μ M, [*p*-nitrophenyl acetate] = 0.5 mM. The solid, smooth lines are the best fits of the data according to equation 2.1 for the K_i of WT (\bullet), L198A (\bullet), L198F (\bullet), L198Q (\bullet).

Scheme 2.14. Structure of arylsulfonamide inhibitors used for computational studies.



In a second phase, five fluorinated inhibitors were studied (Scheme 2.14). The thermodynamic binding constants were determined for inhibitors **84**, **85**, **86** and **87** using esterase activity screening. A difference in K_i was observed (800–300 nM, Table 2.6) due to the interaction of the fluorine atoms with the funnel-shaped cavity of hCA II. The inhibitor **87**, bearing the trifluoromethyl group, binds to the protein with the lowest dissociation constant (30 nM), as previously noted. This was probably due to enhanced hydrophobic interactions inside the protein cavity. Due to the observed, high inhibition constant for **87** (nM range), a competitive displacement test was employed to determine the K_d of inhibitors **87**, **40**, **42**, **43**, **44** and **45**. In this case, the analysis of the data shows little difference between the observed dissociation constants K_d (Table Scheme 2.14, entry **6** to **9**). Indeed, the modifications brought to the inhibitors have little impact, because the fluorine atoms are located too far outside the cavity of the protein. To validate these measurements, the obtained K_d for DNSA, **40**, and **43** were compared to published values and were in agreement (Table 2.6, entries **5**, **7** and **10**).^[6]

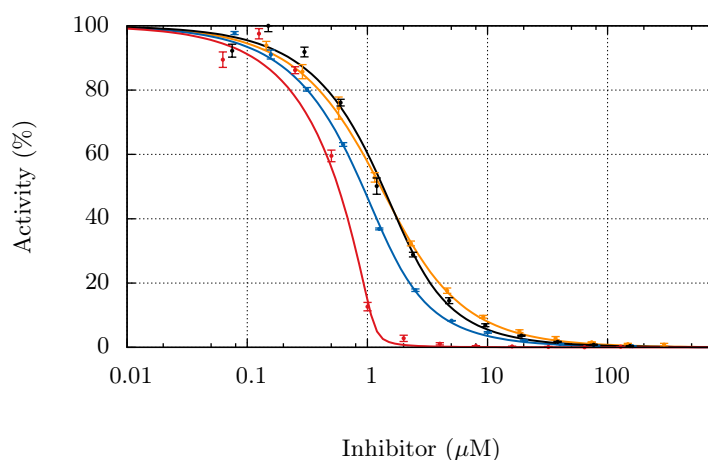


Figure 2.13. Steady-state kinetic data for the inhibition of WT hCA II. The initial rates of the enzyme-catalyzed hydrolysis of *p*-nitrophenyl acetate substrate were measured as a function of inhibitor concentration. [Enzyme] = 1 μ M, [*p*-nitrophenyl acetate] = 0.5 mM. The solid, smooth lines are the best fits of the data according to equation 2.1 for the K_i of **84** (○), **85** (●), **86** (●), **87** (●).

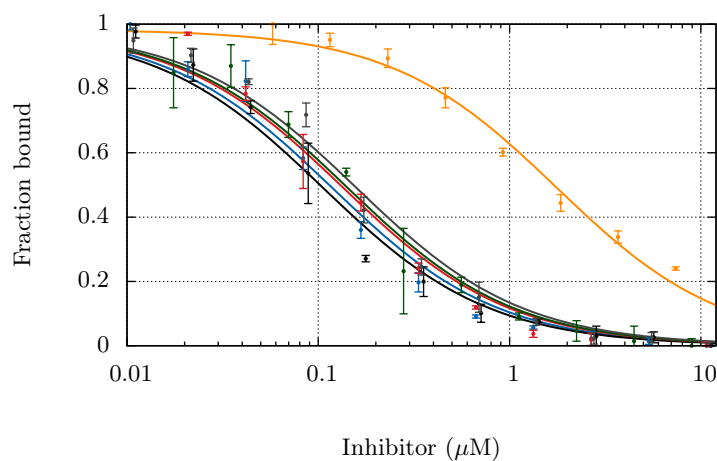


Figure 2.14. Competitive displacement assay data for the inhibition of WT hCA II. The initial rates of the enzyme-catalyzed hydrolysis of *p*-nitrophenyl acetate substrate were measured as a function of inhibitor concentration. [Enzyme] = 1 μM , [*p*-nitrophenyl acetate] = 0.5 mM. The solid, smooth lines are the best fits of the data according to equation 2.3 for the K_d of 87 (●), 40 (●), 42 (●), 43 (●), 44 (●), 45 (●).

Table 2.6. Final set of parameters for K_i or K_d with asymptotic standard error.

Entry	Inhibitor	Dissociation constant (nM)	K_i or K_d	Published dissociation constant (nM)	PDB
1	84	780 ± 45	K_i	200-1500 ^[51,52]	-
2	85	330 ± 30	K_i	82 ^[52]	-
3	86	490 ± 10	K_i	590 ^[53]	1IF4
4	87	30 ± 3	K_i	-	-
5	40	1.9 ± 0.2	K_d	1.1 ^[54]	1G4O
6	42	1.7 ± 0.2	K_d	-	-
7	43	2.2 ± 0.2	K_d	3.3 ^[55]	-
8	44	2.3 ± 0.2	K_d	-	-
9	45	2.5 ± 0.2	K_d	0.29 ^[56]	1G52
10	DN5A	1600 ± 60	K_d	826 ^[57]	1OKL

2.3.3 Crystallographic studies

(in collaboration with Tillmann Heinisch)

An X-ray structure analysis was used to gain insight on the host-guest interactions of ruthenium complexes bearing the bispy **4** ligand.^[47] Complementary NMR analysis of $[(\eta^6\text{-C}_6\text{H}_6)\text{Ru}(\mathbf{4})\text{Cl}]\text{Cl}$ (**9**) indicated the existence of a single diastereomer, as evidenced by an NOE cross-peak between the η^6 -benzene and $\text{HC}_{\text{bridge}}$ (Figure 2.15).

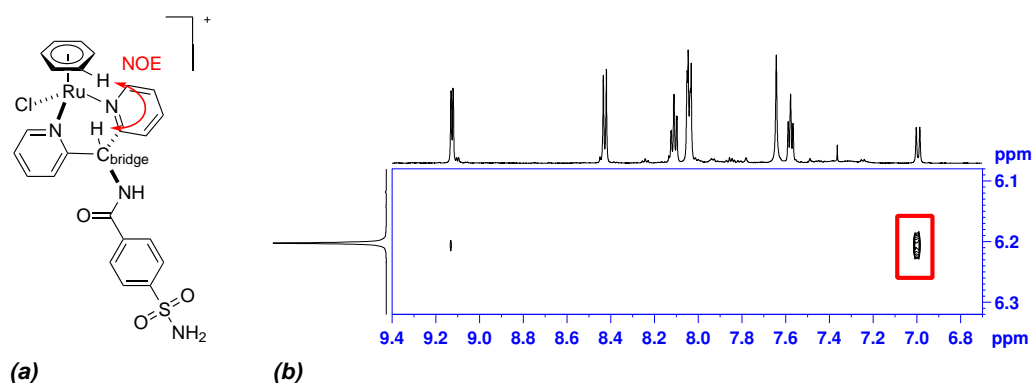


Figure 2.15. Cross correlation (NOE) 6.21 ppm (η^6 -benzene) - 7.00 ppm ($\text{HC}_{\text{bridge}}$) normalized integral 6.22 (1.35/H), confirming the assignment of diastereomer.

Human Carbonic Anhydrase II crystals were soaked in a solution of $[(\eta^6\text{-C}_6\text{Me}_6)\text{Ru}(\mathbf{4})\text{Cl}]\text{Cl}$ (**11**) and diffraction data were collected at a synchrotron to 1.3 Å resolution. After refinement of the protein structure, strong residual positive- and anomalous difference densities were apparent in the funnel-shaped sulfonamide-binding cavity. This was modeled as $[(\eta^6\text{-C}_6\text{Me}_6)\text{Ru}(\mathbf{4})\text{Cl}]\text{Cl}$ (**11**). The various interactions between the anchoring group (benzene-sulfonamide) and the protein are reminiscent of related hCA II-sulfonamide complexes (Figure 2.16). As expected, by computational design, the upper part of complex **11** interacts with the upper edge of the funnel-shaped cavity (residues V121, F131, V135, L141, L198, P202, and L204, Figure 2.16b).

The piano-stool moiety is localized at the entrance of the funnel-shaped cavity. The chlorine atom is exposed to the solvent, as expected from the NMR, while the refinement of the *N*-(di(2-pyridyl)methyl)-amidobenzene-4-sulfonamide (**4**) part of the Ru-ligand gave the best results, with an occupancy of 100%. For ruthenium, hexamethylbenzene, and chlorine.

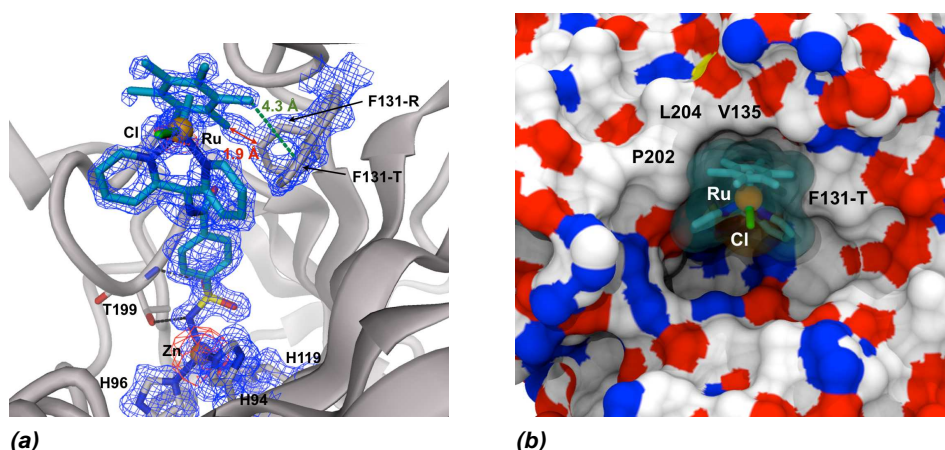


Figure 2.16. Crystal structure of complex $[(\eta^6\text{-C}_6\text{Me}_6)\text{Ru}(\text{bispy } \mathbf{3})\text{Cl}]^+ \subset \text{hCA II}$ (PDB code 3PYK). **a)** Close-up view of the sulfonamide binding cavity. Interactions between the sulfonamide group and protein are indicated. Residue F131 adopts two conformations, as explained in the text. The 2Fo-Fc map is shown in blue at 1.0 Å, the anomalous difference density map in red at 3.0 Å. **b)** Interactions between the piano-stool moiety and residues of the “hydrophobic wall” at the entrance of the ligand binding site.^[47] (Pictures Tillmann Heinisch)

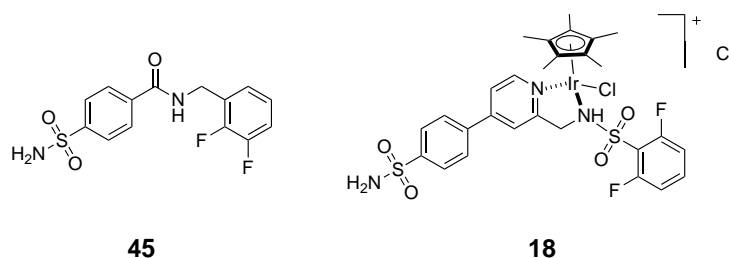
the occupancy was set to 50%. We assume that a partial dissociation of the metal from bispy **4** and the 10-fold increased affinity of the latter fragment for hCA II may explain this observation (Table 2.2 and Table 2.3). Interestingly, the phenyl group of residue F131, which is also involved in the Fierke’s studies,^[18] was found to adopt two conformations (Figure 2.16a). The conformation with a dihedral angle $\chi_2 = 93^\circ$ is not compatible with ligand binding (F131-R side chain contact indicated by a red arrow, Figure 2.16a), whereas the conformation ($\chi_2 = 16^\circ$) is stabilized by a CH/ π interaction between one methyl of the hexamethylbenzene cap and the F131-T phenyl side chain (green dotted line, Figure 2.16a).

2.3.4 NMR studies

(in collaboration with Kaspar Zimmermann and Prof. Dr Daniel Häussinger)

NMR spectroscopy was used to further investigate interactions in solution between the protein host hCA II and the catalyst. For this purpose, pseudocontact chemical shift (pcs) were recorded for fluorinated inhibitors. To validate the method developed by Häussinger^[58] on a 30 kDa protein-like hCA II, *N*-(2,3-difluorobenzyl)-4-sulfamoylbenzamide (**45**) was used as a test inhibitor (Scheme 2.15).

Scheme 2.15. Structure of ligand-inhibitors used for NMR studies.



The complex **45** ⊂ hCA II S166C C206S was chosen as a model system because the X-ray structure was previously reported by Christianson (PDB code 1G52).^[18] The 1D ¹⁹F-NMR experiment was recorded (Figure 2.17) and observed pcs of **45** ⊂ hCA II S166C C206S ([TmM8] labeled) were in good agreement with the published X-ray structure. Indeed, initial calculations from the obtained pcs (Figure 2.17, red highlighted) indicate a 5 Å deviation for the fluorine position.

At this stage of research, a fluorinated active catalyst (**18**, Scheme 2.15) was synthesized (Section 2.2.3) to determine the position and the orientation of the catalyst inside the funnel-shaped cavity of hCA II. Ultimately, this may lead to precious information about the solution structure of the novel hybrid catalyst.

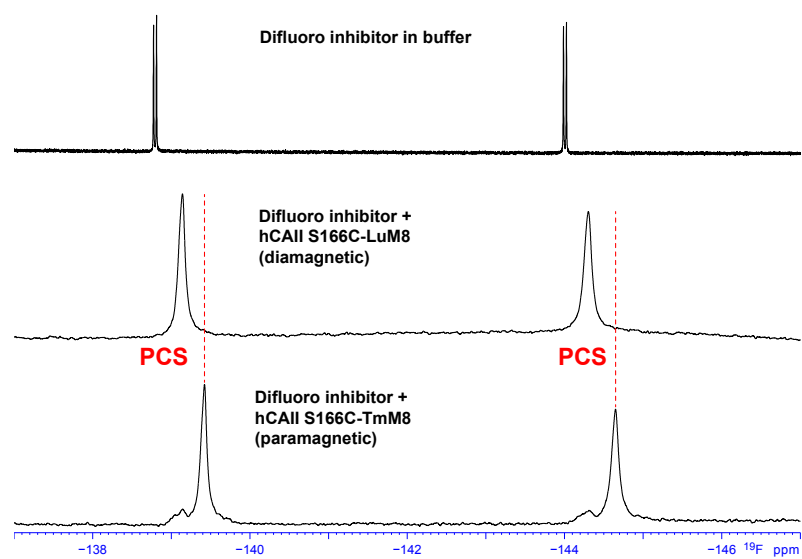


Figure 2.17. 1D ^{19}F spectra of inhibitor 45: a) without protein, b) with double mutant hCA II S166C C206S, c) with labeled hCA II S166C C206S with [TmM8]. PCS are highlighted in red. (Picture Kaspar Zimmermann)

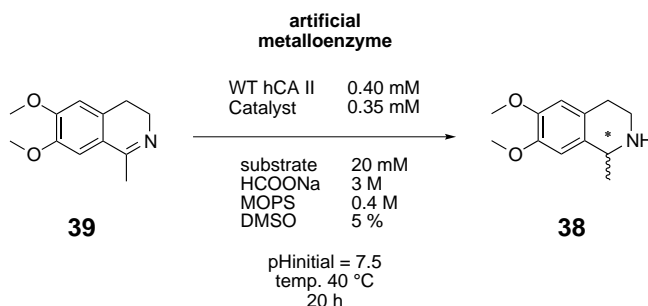
2.4 Catalysis

This last section of this Chapter 2 aims to identify an active and selective artificial metalloenzyme using hCA II as a well-defined second coordination sphere. For this purpose, different catalytic systems were envisaged (Section 2.1). In investigations using palladium (II) complexes bearing bipyridine-derivative ligands for 1,4-addition, it was not possible to reduce the reaction temperature below 45 °C, which corresponds to the denaturation temperature of hCA II.^[10,59] Additionally, in 2011 Cadierno *et al.* reported the instability of Pd(II)/bipy complexes under aqueous catalytic conditions leading to the formation of palladium (0) nanoparticles.^[60] The results presented below focus on successful asymmetric transfer hydrogenation of cyclic imines as a model reaction for hCA II. Chemical and genetic modifications were implemented for the optimization of the system. Previous results concerning activity and selectivity of hybrid catalysts are provided.

2.4.1 Imine transfer hydrogenation

Asymmetric transfer hydrogenation was chosen as a model reaction because of its compatibility with protein environments (Section 2.1). In 2008, efforts by Ward and co-workers identified an artificial transfer hydrogenase for the enantioselective reduction of cyclic imines.^[11] Hybrid catalysts used for this study were created by a combination of various arylsulfonamide complexes with hCA II. For this purpose, two types of ligands were synthesized based on bipyridine or aminopyridine patterns (Sections 2.2.2 and 2.2.3). Cyclic imine reduction was tested under conditions previously described by the Ward group (Scheme 2.16).^[11]

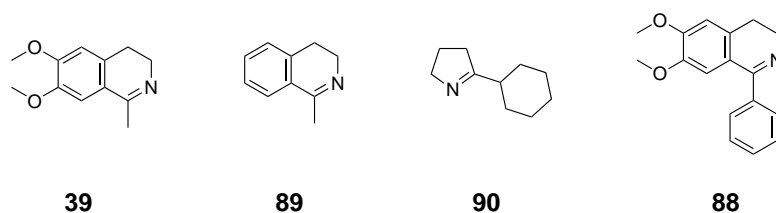
Scheme 2.16. Typical reaction conditions for the enantioselective reduction of cyclic amines.^[11]



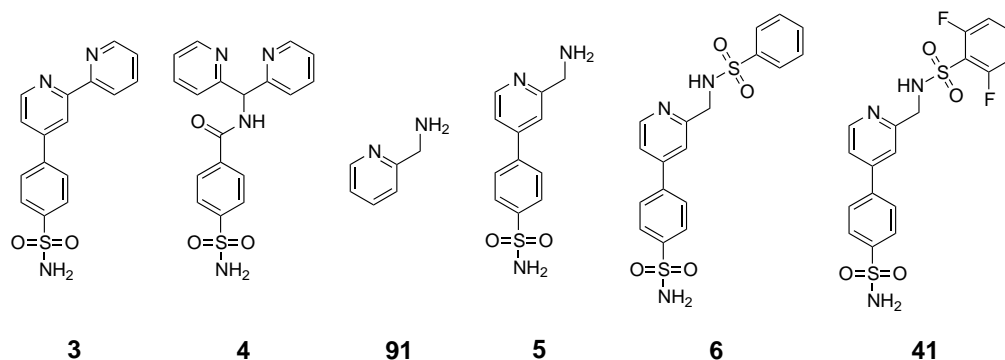
First round of screening

Iridium protein hybrid catalysts were reported as the most active by Ward and co-workers.^[11] Screening results with different substrates (Scheme 2.17) are reported in Table 2.7. It is noteworthy that after 20 h of reaction time, conversion of substrate was observed. An enantiomeric excess of up to 30% (*S*) was reached by the hybrid catalyst [(cp*)Ir(**6**)Cl]Cl (**17**) \subset WT hCA II for the reduction of cyclic imine **39** (Table 2.7 entry **14**). Complexes bearing ligand **6** were therefore further investigated for the reduction of substrate **39**. In the absence of hCA II, all complexes presented in Table 2.7 catalyzed the aqueous transfer hydrogenation of cyclic imines to yield racemic mixtures. Bulky substrate **88** was also tested in presence of [(cp*)Ir(**5**)Cl]Cl catalyst, but no conversion was observed, and we speculate that low water solubility of **88** may be the cause.

Scheme 2.17. Substrate diversity for imine reduction.



In order to obtain improved activity and enantiomeric excess, different strategies were implemented. We focused our attention on modifications at the active catalytic site affecting the reaction outcome by making use of: a chemical diversity (1st sphere of coordination, *e.g.* ligands, Scheme 2.18), a genetic diversity (2nd sphere of coordination), and a substrate diversity (Scheme 2.17).^[61,62]

Scheme 2.18. Ligand diversity for imine reduction.**Table 2.7.** Results obtained for co-catalyst screening.^a

Entry	Ligand (Complex)	Metal	η^n -(arene)	Substrate	Protein	Conv. ^b	TON	ee (%)
1	91 (13)	Ir	η^5 -C ₅ Me ₅	39	-	98	54	0
2	91 (13)	Ir	η^5 -C ₅ Me ₅	39	WT	93	52	0
3	91 (13)	Ir	η^5 -C ₅ Me ₅	89	-	99	55	0
4	91 (13)	Ir	η^5 -C ₅ Me ₅	89	WT	99	55	0
5	91 (13)	Ir	η^5 -C ₅ Me ₅	90	-	quant.	55	0
6	91 (13)	Ir	η^5 -C ₅ Me ₅	90	WT	85	47	0
7	5 (16)	Ir	η^5 -C ₅ Me ₅	39	-	quant.	55	0
8	5 (16)	Ir	η^5 -C ₅ Me ₅	39	WT	20	11	5 (<i>S</i>)
9	5 (16)	Ir	η^5 -C ₅ Me ₅	89	-	99	55	0
10	5 (16)	Ir	η^5 -C ₅ Me ₅	89	WT	46	25	6 (<i>S</i>)
11	5 (16)	Ir	η^5 -C ₅ Me ₅	90	-	quant.	55	0
12	5 (16)	Ir	η^5 -C ₅ Me ₅	90	WT	36	20	5 (<i>S</i>)
13	6 (17)	Ir	η^5 -C ₅ Me ₅	39	-	61	34	1 (<i>S</i>)
14	6 (17)	Ir	η^5 -C ₅ Me ₅	39	WT	41	23	30 (<i>S</i>)
15	6 (17)	Ir	η^5 -C ₅ Me ₅	89	-	43	24	3 (<i>S</i>)
16	6 (17)	Ir	η^5 -C ₅ Me ₅	89	WT	26	15	3 (<i>S</i>)
17	6 (17)	Ir	η^5 -C ₅ Me ₅	90	-	40	22	2 (<i>S</i>)
18	6 (17)	Ir	η^5 -C ₅ Me ₅	90	WT	22	12	24 (<i>S</i>)
19	-	-	-	39	WT	0	0	0
20	-	-	-	89	WT	0	0	0
21	-	-	-	90	WT	0	0	0

^a *Reaction conditions:* The reaction was carried out at 40 °C for 20 h using 1.8 mol% complex (0.35 mM final concentration), 20 mM substrate, 0.4 mM protein, in 0.4 M MOPS buffer (200 μ L total volume, 5% DMSO) containing 3 M formate, pH 7.5.

^b Determined by normal phase HPLC after extraction; the relative response was corrected by the experimentally determined response factor; amine [%] = (amine x 100)/(amine+imine).

Having identified the most efficient hybrid catalyst [(cp*)Ir(**6**)Cl]Cl (**17**)_C WT hCA II, different metal complexes (Ru, Rh and Ir) bearing a bipyridine ligand (**3** and **4**) or picolylamine derivative **6** were tested. Screening results for transfer hydrogenation of 6,7-diethoxy-1-methyl-1,2,3,4-tetrahydroisoquinoline (**39**) are presented in Table 2.8. From this general catalyst screening, the co-catalyst [(cp*)Ir(**6**)Cl]Cl (**17**) emerged as the most active, at 39% conversion (TON = 29, entry **10** in Table 2.8).

Table 2.8. Results obtained for the transfer hydrogenation of 6,7-diethoxy-1-methyl-1,2,3,4-tetrahydroisoquinoline with different hybrid catalysts bearing ligands **6**, **3** or **4**.^a

Entry	Ligand	Metal	η^n -(arene)	Substrate	Protein	Conv. ^b	TON
1	6 ^c	Ru	η^6 -C ₆ H ₆	39	-	48	27
2	6 ^c	Ru	η^6 -C ₆ H ₆	39	WT	4	2
3	6 ^c	Ru	η^6 - <i>p</i> -cymene	39	-	quant.	55
4	6 ^c	Ru	η^6 - <i>p</i> -cymene	39	WT	11	6
5	6 ^c	Ru	η^6 -C ₆ Me ₆	39	-	99	52
6	6 ^c	Ru	η^6 -C ₆ Me ₆	39	WT	21	11
7	6 ^c	Rh	η^5 -C ₅ Me ₅	39	-	97	54
8	6 ^c	Rh	η^5 -C ₅ Me ₅	39	WT	36	20
9	6	Ir	η^5 -C ₅ Me ₅	39	-	quant.	55
10	6	Ir	η^5 -C ₅ Me ₅	39	WT	39	29
13	3	Ir	η^5 -C ₅ Me ₅	39	-	14	8
14	3	Ir	η^5 -C ₅ Me ₅	39	WT	0	0
11	4	Ir	η^5 -C ₅ Me ₅	39	-	3	1
12	4	Ir	η^5 -C ₅ Me ₅	39	WT	1	1

^a *Reaction conditions:* The reaction was carried out at 40 °C for 36 h using 1.8 mol% complex (0.35 mM final concentration), 20 mM substrate, 0.4 mM hCA II, in 1.2 M MOPS buffer (200 μ L) containing 3 M formate, pH 6.5.

^b Determined by normal phase HPLC after extraction; the relative response was corrected by the experimentally determined response factor; amine [%] = (amine x 100)/(amine+imine).

^c Complex *in situ* prepared.

In the absence of crystallographic information on the exact localization of the catalytic center inside the funnel-shaped cavity, docking studies were realized in collaboration with Maurus Schmid to obtain a quantitative model of the hybrid catalyst (Figure 2.18). Based on computational results, mutated proteins were produced and tested in combination with complex **17**. Results for the reduction of substrate **39** are presented in Table 2.9. WT hCA II as well as isozymes K170A and I91A were found to be the most promising protein scaffolds. It is noteworthy that artificial metalloenzyme activity was improved by a single point mutation at

position 91 (full conversion and 29% *ee*), which showed the influence exerted by amino acid localized close to the catalytic center (Figure 2.18).^[61,62]

Table 2.9. Results obtained for the transfer hydrogenation of 6,7-diethoxy-1-methyl-1,2,3,4-tetrahydroisoquinoline (**39**) with hCA II variants.^a

Entry	Complex	Substrate	Protein ^b	Conv. ^c	TON	<i>ee</i> (%)
1	17	39	WT	33	18	27 (<i>S</i>)
2	17	39	H64A	11	6	0
3	17	39	I91A	99	55	29 (<i>S</i>)
4	17	39	K170A	59	33	30 (<i>S</i>)
5	17	39	E106Q - H64A	21	12	3 (<i>S</i>)
6	17	39	F131A	12	6	6 (<i>S</i>)
7	17	39	F131A-A2V	24	13	1 (<i>S</i>)
8	17	39	Q92G	15	8	3 (<i>S</i>)
9	17	39	Q92G - V121G	25	14	1 (<i>S</i>)
10	17	39	L198Q	11	6	23 (<i>S</i>)
11	17	39	L198A	6	3	6 (<i>R</i>)
12	17	39	L198F	13	7	23 (<i>S</i>)
13	17	39	L198H	13	7	23 (<i>S</i>)

^a *Reaction conditions:* The reaction was carried out at 40 °C for 20 h using 1.8 mol% complex (0.35 mM final concentration), 20 mM substrate, 0.4 mM protein, in 0.4 M MOPS buffer (200 μ L total volume, 5% DMSO) containing 3 M formate, pH 7.5.

^b ESI-MS of hCA II isozymes are reported in Part III.

^c Determined by normal phase HPLC after extraction; the relative response was corrected by the experimentally determined response factor; amine [%] = (amine x 100)/(amine+imine).

General conclusions from this second optimization step were: i) genetic modification inside the active pocket does not affect the catalytic reaction, ii) mutation near the catalytic moiety (I91A and K170A) affects only the catalyst activity but with no significant enantiomeric excess modification observed (always \sim 30%). Based on information gained from computational calculations, we speculated that replacing residue isoleucine at position 91 by alanine provides a larger opening at the catalytic center (Figure 2.18). To confirm the location of the catalytic center in the pocket of hCA II and the influences that different mutations can have on catalysis, structural insights on the guest-host interactions need to be gained by X-ray diffraction. Nevertheless, this demonstrates the importance of the environment around the active metal catalyst on performance.

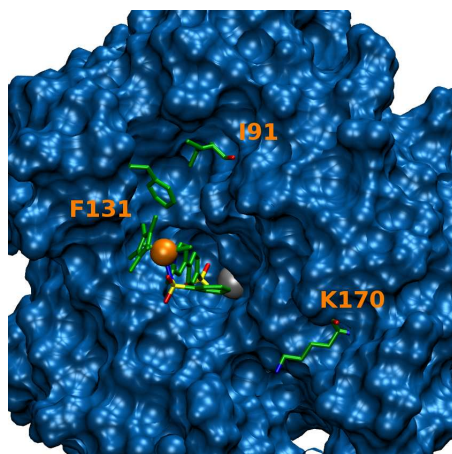


Figure 2.18. Structure of complex $[(cp^*)Ir(6)Cl]Cl$ (**17**) \subset hCA II (PDB code 1G52, Maurus Schmid calculations). Positions I91 and K170 are highlighted.

Complementary to the preliminary study related to the chemogenetic optimization, additional investigations to improve catalyst selectivity by modifying reaction conditions were undertaken.

Catalytic reaction parameter modifications

Reaction conditions were optimized in order to further improve the selectivity of the hybrid catalyst $[(cp^*)Ir(6)Cl]Cl$ (**17**) \subset I91A. Modification to the reaction temperature, catalyst loading, as well as reaction time are presented in Tables 2.10 to 2.12. As previously shown in section 2.3.1, the complex loading into WT hCA II reached a maximum around 0.8 equivalent. For this purpose, different catalyst loadings were also tested. As shown in Table 2.10, it is noteworthy that the conversion at 20 °C in the presence of protein was improved (entries **3** to **6**) compared to the free protein catalysis (entries **1** and **2**). A so-called “protein accelerated catalysis” phenomenon was observed, and this is discussed in Section 2.4.2. In addition, the enantiomeric excess increased up to 56%, but no significant difference between WT and I91A was observed (entries **5** and **8**).

Table 2.10. Results for the transfer hydrogenation of substrate **39** at room temperature.^a

Entry	Complex	Substrate	Protein	equivalent of complex	Conv. ^b	TON	ee (%)
1	17	39	-	0.8	12	7	0
2	17	39	-	0.6	10	8	0
3	17	39	-	0.4	9	9	0
4	17	39	WT	0.8	39	22	52 (<i>S</i>)
5	17	39	WT	0.6	53	39	56 (<i>S</i>)
6	17	39	WT	0.4	30	34	57 (<i>S</i>)
7	17	39	I91A	0.8	59	33	49 (<i>S</i>)
8	17	39	I91A	0.6	75	56	54 (<i>S</i>)
9	17	39	I91A	0.4	74	82	58 (<i>S</i>)
10	-	39	WT	-	0	0	0
11	-	39	I91A	-	0	0	0

^a *Reaction conditions:* The reaction was carried out at r.t. for 20 h, 20 mM substrate, 0.35 mM protein, in 0.4 M MOPS buffer (200 μ L total volume, 5% DMSO) containing 3 M formate, pH 7.5.

^b Determined by normal phase HPLC after extraction; the relative response was corrected by the experimentally determined response factor; amine [%] = (amine x 100)/(amine+imine).

The decrease in temperature to 4 °C afforded an increase in the selectivity of the transfer hydrogenation reaction up to 69% *ee* for compound **38**. This increase was achieved by using [(cp*)Ir(**6**)Cl]Cl \subset WT hCA II as a hybrid catalyst. Again, no marked selectivity difference between WT hCA II and mutant I91A was observed (Table 2.11, entry **3** to **6**). In addition, the activity of the catalyst based on the WT hCA II is lower compared to mutant I91A. By increasing catalyst loading to 5%, the conversion reached 70% (TON = 16, entry **14**).

Furthermore, a decrease in the enantiomeric excess can be expected if the catalyst is no longer bound to the protein. To prevent the release of metal complex into catalytic buffer, the addition of Zn(II) to the catalyst solution was considered. Results are presented in Table 2.10. It should be noted that the addition of zinc does not affect the results obtained for the reduction of **39**.

Finally, hybrid catalyst [(cp*)Ir(**41**)Cl]Cl (**18**) \subset hCA II used for NMR solution studies was tested under the same reaction conditions (Table 2.10, entries **7** to **2**). This catalyst shows a lower activity compared to [(cp*)Ir(**6**)Cl]Cl (**17**) \subset WT hCA II. Nevertheless, the enantiomeric excess observed remains stable for the WT protein (66 % (*S*, entry **7**). We speculate that the catalyst activity depends on the nature of the sulfonamide attached to the 2-picolylamine part of the ligand.

Table 2.11. Results for the transfer hydrogenation of substrate **39** at 4 °C.^a

Entry	Complex	Substrate	Protein	equivalent of complex	Conv. ^b	TON	ee (%)
1	17	39	-	0.8	0	0	0 (<i>S</i>)
2	17	39	-	0.6	0	0	0 (<i>S</i>)
3	17	39	WT	0.8	19	10	67 (<i>S</i>)
4	17	39	WT	0.6	19	14	69 (<i>S</i>)
5	17	39	I91A	0.8	15	8	62 (<i>S</i>)
6	17	39	I91A	0.6	19	14	68 (<i>S</i>)
7	-	39	WT	-	0	0	0
8	-	39	I91A	-	0	0	0

^a *Reaction conditions:* The reaction was carried out at 4 °C. for 20 h, 20 mM substrate, 0.35 mM protein, in 0.4 M MOPS buffer (200 μL total volume, 5% DMSO) containing 3 M formate, pH 7.5.

^b Determined by normal phase HPLC after extraction; the relative response was corrected by the experimentally determined response factor; amine [%] = (amine x 100)/(amine+imine).

Table 2.12. Results for the transfer hydrogenation of substrate **39** at 4 °C with addition of zinc in the reaction buffer.^a

Entry	Complex	Substrate	Protein	Conv. ^b	TON	ee (%)
1	17	39	WT	27	17	68 (<i>S</i>)
2	17	39	I91A	23	14	64 (<i>S</i>)
3	17	39	K170A	18	11	69 (<i>S</i>)
4	17 + Zn	39	WT	35	22	69 (<i>S</i>)
5	17 + Zn	39	I91A	27	17	63 (<i>S</i>)
6	17 + Zn	39	K170A	22	14	66 (<i>S</i>)
7	18	39	WT	7	4	66 (<i>S</i>)
8	18	39	I91A	9	5	23 (<i>S</i>)
9	18	39	K170A	6	4	42 (<i>S</i>)
10	18 + Zn	39	WT	7	5	51 (<i>S</i>)
11	18 + Zn	39	I91A	9	5	21 (<i>S</i>)
12	18 + Zn	39	K170A	6	4	42 (<i>S</i>)
13 ^c	17	39	WT	82	16	70 (<i>S</i>)
14 ^c	17	39	I91A	70	14	66 (<i>S</i>)

^a *Reaction conditions:* The reaction was carried out at 4 °C for 44 h using 1.6 mol% complex (0.3 mM final concentration), 20 mM substrate, 0.4 mM protein, in 0.4 M MOPS buffer (200 μL total volume, 5% DMSO) containing 3 M formate, pH 7.5.

^b Determined by normal phase HPLC after extraction; the relative response was corrected by the experimentally determined response factor; amine [%] = (amine x 100)/(amine+imine). ^c 5% catalyst loading.

2.4.2 Michaelis-Menten kinetic experiments

As previously reported for biotin-streptavidin technology, the host protein is not only responsible for inducing enantioselectivity, but also for increasing the reaction rate of the catalyst. This phenomenon is called “protein accelerated catalysis”.^[63] The kinetic data were collected for different hybrid catalysts at given times with different initial concentrations of substrate. Observed reaction velocity for the reduction of 1-methyl-6,7-dimethoxy-3,4-dihydroisoquinoline (**39**) are reported in Figure 2.19.

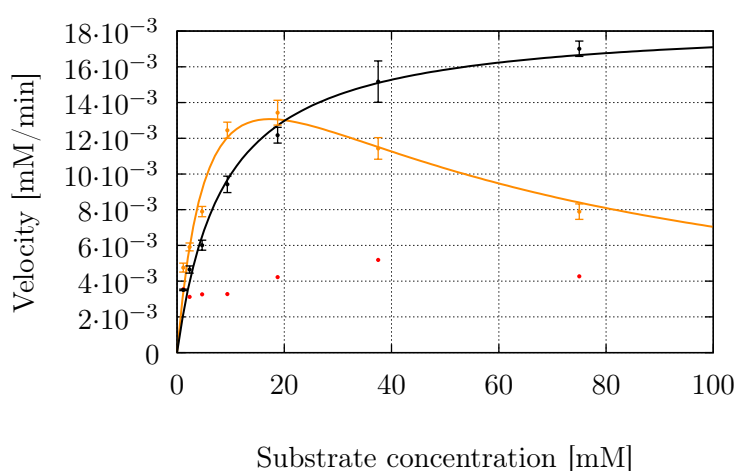


Figure 2.19. Velocity curves for [(cp*)Ir(**6**)Cl]Cl (**17**) or hCA II artificial metalloenzymes as a function of 1-methyl-6,7-dimethoxy-3,4-dihydroisoquinoline (**39**) concentration. 1.8 mol% complex (0.35 mM final concentration), 0.4 mM protein, in 0.4 M MOPS buffer (200 μ L total volume, 5% DMSO) containing 3 M formate, pH 7.5, 25 $^{\circ}$ C. [(cp*)Ir(**6**)Cl]Cl (**17**) (•), [(cp*)Ir(**6**)Cl]Cl (**17**) c WT (◐), [(cp*)Ir(**6**)Cl]Cl (**17**) c I91A (◑).

The Michaelis-Menten kinetic model is one of the simplest models to describe steady-state enzyme kinetics (equation 2.4); however, many proteins show significant deviations, for example due to inhibition.^[64] Calculated values K_m , V_{max} and, if necessary K_i , were obtained from the iteration procedures of equation 2.4 or 2.5 are compiled in Table 2.13. For reactions following the Michaelis-Menten kinetic profile, the rate of product formation is given by

$$v = \frac{V_{max} \cdot [S]}{K_m + [S]} \quad (2.4)$$

where V_{max} is the maximum velocity achieved by the system, and K_m the Michaelis

constant. It follows that $k_{\text{cat}} = V_{\text{max}}/[E]_0$, where $[E]_0$ is the enzyme concentration, *i.e.* the catalyst concentration.

For kinetic studies of $[(\text{cp}^*)\text{Ir}(\mathbf{6})\text{Cl}]\text{Cl}$ (**17**) \subset WT, we assume a simple scenario of substrate inhibition due to a binding event that inhibits the enzyme at high substrate concentration, which can be described by the following equation:^[64]

$$v = \frac{V_{\text{max}} \cdot [S]}{K_{\text{m}} + [S] + \frac{[S]^2}{K_{\text{i}}}} \quad (2.5)$$

Note that other mechanisms of inhibition should also be considered,^[65] requiring much more detailed kinetic exploration beyond the reach of the current studies.

Table 2.13. Kinetics parameters derived from equation 2.4 and 2.5.

Entry	Enzyme	V_{max} (mM/min)	K_{m} (mM)	K_{i} (mM)	k_{cat} (1/min)	$k_{\text{cat}}/K_{\text{m}}$ (1/mM*min)
1	17 \subset WT	$2.31 \cdot 10^{-2}$	6.67	45.08	$6.60 \cdot 10^{-2}$	$9.89 \cdot 10^{-3}$
2	17 \subset I91A	$1.85 \cdot 10^{-2}$	8.63	-	$5.28 \cdot 10^{-2}$	$6.11 \cdot 10^{-3}$

Thus kinetic study shows an increase of reaction rate using artificial metalloenzymes compared to the protein-free catalysis. The presence of a hydrophobic pocket around the catalytic metal may provide a favorable environment for the transfer of hydride to substrate **39**. In addition, transfer hydrogenation catalyzed by complex **17** could not be fitted using equations 2.4 nor 2.5. Further investigation should be carried out to determine the kinetic profile of complex **17**.

Note, however, that a point mutation of hCA II-WT eliminates any inhibition of the hybrid catalyst. One possible reason may be the enlargement of the hydrophobic pocket by substitution of isoleucine by a smaller amino acid (alanine) at position 91. This hypothesis may be explored in the future by NMR studies on the position and orientation adopted by the substrate in the catalytic pocket.

2.5 References

- [1] Rosati, F.; Roelfes, G. *ChemCatChem* **2010**, *2*, 916.
- [2] Steinreiber, J.; Ward, T. R. *Coord. Chem. Rev.* **2008**, *252*, 751.
- [3] Ueno, T.; Abe, S.; Yokoi, N.; Watanabe, Y. *Coord. Chem. Rev.* **2007**, *251*, 2717.
- [4] Matulis, D.; Kranz, J.; Salemme, F.; Todd, M. *Biochemistry* **2005**, *44*, 5258.
- [5] Avvaru, B.; Busby, S.; Chalmers, M.; Griffin, P.; Venkatakrisnan, B.; Agbandje-McKenna, M.; Silverman, D.; McKenna, R. *Biochemistry* **2009**, *48*, 7365.
- [6] Krishnamurthy, V. M.; Kaufman, G. K.; Urbach, A. R.; Gitlin, I.; Gudiksen, K. L.; Weibel, D. B.; Whitesides, G. M. *Chem. Rev.* **2008**, *108*, 946.
- [7] Cusanelli, A.; Frey, U.; Richens, D. T.; Merbach, A. E. *J. Am. Chem. Soc.* **1996**, *118*, 5265.
- [8] Vullo, D.; Franchi, M.; Gallori, E.; Antel, J.; Scozzafava, A.; Supuran, C. *J. Med. Chem.* **2004**, *47*, 1272.
- [9] Lu, X.; Lin, S. *J. Org. Chem.* **2005**, *70*, 9651.
- [10] Lin, S.; Lu, X. *Tetrahedron Lett.* **2006**, *47*, 7167.
- [11] Dürrenberger, M. *et al. Angew. Chem. Int. Ed.* **2011**, *50*, 3026.
- [12] Lo, C.; Ringenberg, M. R.; Gnanndt, D.; Wilson, Y.; Ward, T. R. *Chem. Commun.* **2011**, *47*, 12065.
- [13] Mayer, C.; Gillingham, D. G.; Ward, T. R.; Hilvert, D. *Chem. Commun.* **2011**, *47*, 12068.
- [14] Sletten, E. M.; Bertozzi, C. R. *Angew. Chem. Int. Ed.* **2009**, *48*, 6974.
- [15] Huc, I.; Lehn, J. M. *Proc. Natl. Acad. Sci. U.S.A.* **1997**, *94*, 2106.
- [16] Schmid, M.; Nogueira, E. S.; Monnard, F. W.; Ward, T. R.; Meuwly, M. *Chem. Sci.* **2012**, *3*, 690.
- [17] Humphre, W.; Dalke, A.; Schulten, K. *J. Mol. Graphics* **1996**, *14*, 33.
- [18] Kim, C. Y.; Chang, J. S.; Doyon, J.; Jr, T. T. B.; Fierke, C. A.; Jain, A.; Christianson, D. W. *J. Am. Chem. Soc.* **2000**, *122*, 12125.
- [19] Herrmann, W. A.; Thiel, W. R.; Kuchler, J. G. *Chem. Ber.* **1990**, *123*, 1953.
- [20] Anderson, S.; Constable, E. C.; Seddon, K. R.; Turp, J. E.; Baggott, J. E.; Pilling, M. J. *J. Chem. Soc., Dalton Trans.* **1985**, 2247.
- [21] Yang, J.-S.; Lin, Y.-D.; Lin, Y.-H.; Liao, F.-L. *J. Org. Chem.* **2004**, *69*, 3517.

- [22] Khanna, I. K. *et al. J. Med. Chem.* **2000**, *43*, 3168.
- [23] Shaabani, A.; Mirzaei, P.; Naderi, S.; Lee, D. G. *Tetrahedron* **2004**, *60*, 11415.
- [24] Cordaro, J. G.; McCusker, J. K.; Bergman, R. G. *Chem. Commun.* **2002**, 1496.
- [25] Ciufolini, M. A.; Byrne, N. E. *J. Chem. Soc., Chem. Commun.* **1988**, 1230.
- [26] Renz, M.; Hemmert, C.; Meunier, B. *Eur. J. Org. Chem.* **1998**, *1998*, 1271.
- [27] Jain, A.; Huang, S. G.; Whitesides, G. M. *J. Am. Chem. Soc.* **1994**, *116*, 5057.
- [28] Baratta, W.; Rigo, P. *Eur. J. Inorg. Chem.* **2008**, *2008*, 4041.
- [29] Günnaz, S.; Özdemir, N.; Dayan, S.; Dayan, O.; Çetinkaya, B. *Organometallics* **2011**, *30*, 4165.
- [30] McCalmont, W. F.; Patterson, J. R.; Lindenmuth, M. A.; Heady, T. N.; Haverstick, D. M.; Gray, L. S.; Macdonald, T. L. *Bioorg. Med. Chem* **2005**, *13*, 3821.
- [31] Bourdonnec, B. L.; Meulon, E.; Yous, S.; Goossens, J. F.; Houssin, R.; Henichart, J. P. *J. Med. Chem.* **2000**, *43*, 2685.
- [32] Congreve, A.; Katakay, R.; Knell, M.; Parker, D.; Puschmann, H.; Senanayake, K.; Wylie, L. *New. J. Chem.* **2003**, *27*, 98.
- [33] Jones, R. C.; Canty, A. J.; Deverell, J. A.; Gardiner, M. G.; Guijt, R. M.; Rode-
mann, T.; Smith, J. A.; Tolhurst, V. A. *Tetrahedron* **2009**, *65*, 7474.
- [34] van den Heuvel, M.; van den Berg, T. A.; Kellogg, R. M.; Choma, C. T.; Feringa, B. L. *J. Org. Chem.* **2004**, *69*, 250.
- [35] Yoshiyuki, I.; Masa-aki, I.; Tomonori, I.; Akio, O.; Itaru, H. *Chem. Commun.* **2009**, 2848.
- [36] Negi, S.; Matsukura, M.; Mizuno, M.; Miyake, K.; Minami, N. *Synthesis* **1996**, *1996*, 991.
- [37] Penso, M.; Albanese, D.; Landini, D.; Lupi, V.; Tagliabue, A. *J. Org. Chem.* **2008**, *73*, 6686.
- [38] Christopher, J. A. *et al. J. Med. Chem.* **2009**, *52*, 3098.
- [39] Garber, S. B.; Kingsbury, J. S.; Gray, B. L.; Hoveyda, A. H. *J. Am. Chem. Soc.* **2000**, *122*, 8168.
- [40] Jordan, J. P.; Grubbs, R. H. *Angew. Chem. Int. Ed.* **2007**, *119*, 5244.
- [41] Freedman, D. A.; Evju, J. K.; Pomije, M. K.; Mann, K. R. *Inorg. Chem.* **2001**, *40*, 5711.
- [42] Carmona, D.; Lamata, M. P.; Viguri, F.; Rodríguez, R.; Lahoz, F. J.; Dobri-
novitch, I. T.; Oro, L. A. *Dalton Trans.* **2007**, 1911.

- [43] Freskgaard, P.-O.; Maartensson, L.-G.; Jonasson, P.; Jonsson, B.-H.; Carlsson, U. *Biochemistry* **1994**, *33*, 14281.
- [44] Gianazza, E.; Sirtori, C. R.; Castiglioni, S.; Eberini, I.; Chrambach, A.; Rondanini, A.; Vecchio, G. *Electrophoresis* **2000**, *21*, 1435.
- [45] Neubig, R. R.; Spedding, M.; Kenakin, T.; Christopoulos, A. *Pharmacol. Rev.* **2003**, *55*, 597.
- [46] Qin, L.; Srivastava, D. K. *Biochemistry* **1998**, *37*, 3499.
- [47] Monnard, F. W.; Heinisch, T.; Nogueira, E. S.; Schirmer, T.; Ward, T. R. *Chem. Commun.* **2011**, *47*, 8238.
- [48] Iyer, R.; Barrese III, A. A.; Parakh, S.; Parker, C. N.; Tripp, B. C. *J. Biomol. Screening* **2006**, *11*, 782.
- [49] Baird Jr, T. T.; Waheed, A.; Okuyama, T.; Sly, W. S.; Fierke, C. A. *Biochemistry* **1997**, *36*, 2669.
- [50] Wang, S. C.; Zamble, D. B. *Biochem. Mol. Biol. Educ.* **2006**, *34*, 364.
- [51] Taylor, P. W.; King, R. W.; Burgen, A. S. *Biochemistry* **1970**, *9*, 2638.
- [52] King, R. W.; Burgen, A. S. V. *Proc. R. Soc. London, Ser. B* **1976**, *193*, 107.
- [53] Krishnamurthy, V. M.; Bohall, B. R.; Kim, C. Y.; Moustakas, D. T.; Christianson, D. W.; Whitesides, G. M. *Chem. Asian J.* **2007**, *2*, 94.
- [54] Jain, A.; Whitesides, G. M.; Alexander, R. S.; Christianson, D. W. *J. Med. Chem.* **1994**, *37*, 2100.
- [55] Chu-Young, K.; Pooja, P. C.; Ahamindra, J.; Christianson, D. W. *J. Am. Chem. Soc.* **2001**, *123*, 9620.
- [56] Doyon, J. B.; Hansen, E. A. M.; Kim, C. Y.; Chang, J. S.; Christianson, D. W.; Madder, R. D.; Voet, J. G.; Baird Jr, T. A.; Fierke, C. A.; Jain, A. *Org. Lett.* **2000**, *2*, 1189.
- [57] Grzybowski, B. A.; Ishchenko, A. V.; Kim, C.-Y.; Topalov, G.; Chapman, R.; Christianson, D. W.; Whitesides, G. M.; Shakhnovich, E. I. *Proc. Natl. Acad. Sci. U. S. A.* **2002**, *99*, 1270.
- [58] Häussinger, D.; Huang, J.; Grzesiek, S. *J. Am. Chem. Soc.* **2009**, *131*, 14761.
- [59] Lu, X.; Lin, S. *J. Org. Chem.* **2005**, *70*, 9651.
- [60] Tomas-Mendivil, E.; Diez, J.; Cadierno, V. *Catal. Sci. Technol.* **2011**, *1*, 1605.
- [61] Morley, K. L.; Kazlauskas, R. J. *Trends Biotechnol.* **2005**, *23*, 231.
- [62] Reetz, M. T.; Carballeira, J. D.; Peyralans, J.; Höbenreich, H.; Maichele, A.; Vogel, A. *Chem. Eur. J.* **2006**, *12*, 6031.

- [63] Collot, J.; Humbert, N.; Skander, M.; Klein, G.; Ward, T. R. *J. Organomet. Chem.* **2004**, 689, 4868.
- [64] Reed, M. C.; Lieb, A.; Nijhout, H. F. *BioEssays* **2010**, 32, 422.
- [65] Fersht, Alan, *Structure and Mechanism in Protein Science: A Guide to Enzyme Catalysis and Protein Folding*; W. H. Freeman: 1st ed.; 1998.

The creative 'act' is a process, not a moment.

Unknown

3

Conclusion and outlook

This study dealt with the development of a new hybrid catalyst based on a human Carbonic Anhydrase II scaffold for the reduction of cyclic imines. For this purpose, a first generation of piano-stool hCA II inhibitors incorporating a bidentate ligand bearing an arylsulfonamide anchor was designed *in silico*. To further fine-tune the binding affinity of the metal complex for hCA II, a second recognition motif was developed. X-ray structure analysis revealed a CH/ π interaction between $[(\eta^6\text{-C}_6\text{Me}_6)\text{Ru}(\mathbf{4})\text{Cl}]\text{Cl}$ and the amino acid residue phenylalanine, at position 131 (F131). In parallel with these structural investigations, widely applicable force field parameters amenable to molecular dynamics simulations of hCA II-inhibitor interactions (Maurus Schmid and Tristan Bereau) were experimentally validated.

Based on computational results and X-ray information gained during the first part of my Ph.D., a second generation of catalysts (based on a 2-picolyamine ligand bearing a sulfonamide anchor) was designed *in silico*. Coupled to a second recognition element, which ensures the precise localization of catalytic metals within the hCA II binding pocket, inhibitors show improved binding affinities towards wild-type hCA II (down to level of nM). In this way, a well-defined chiral second coordination sphere was tailored to provide a favorable environment for enantioselective catalysis. A chemogenetic strategy allowed the optimization of $[(\text{cp}^*)\text{Ir}(\mathbf{6})\text{Cl}]\text{Cl}$ (**17**) \subset I91A hCA II as a hybrid catalyst for the enantioselective reduction of prochiral imines. A single point mutation was sufficient to prevent substrate inhibition, and

an enantiomeric excess of 69 % (*S*) was obtained for the synthesis of salsolidine.

A novel artificial metalloenzyme based on hCA II has thus been developed. From this point onward, the goal is to improve the catalytic performance of the artificial metalloenzyme (activity and selectivity). For this purpose, further chemogenetic modifications are necessary, *i.e.* genetic variation of hCA II combined with chemical fine-tuning of the ligand by modifying the arylsulfonyl group.

Part II

Experimental

La première vertu d'une pensée active sera donc de s'attacher aux problèmes qui se posent et non pas à ceux que l'on suppose.

D. de Rougemont

4

Experimental section

4.1 General experimental conditions

4.1.1 Solvents and reagents

Materials and reagents were purchased at the highest commercially available grade and used without further purification.

Solvents used for reactions correspond to the quality “puriss”. For analytical and preparative high performance liquid chromatography (HPLC), HPLC-grade solvents were used. The water used for reactions was filtered using a Barnstead ultrapure water system.

4.1.2 Separation and purification methods

Reactions were monitored by thin layer chromatography (TLC) using Merck silica gel 60 F₂₅₄ plates. Flash chromatography was performed using Merck silica gel 60, particle size 40-63 μm . Compounds were visualized using UV (254 and/or 366 nm) with a UV-lamp from Camag.

High performance liquid chromatography was performed on Agilent 1100 Series with UV-Vis detection.

4.1.3 Spectroscopic methods

^1H , ^{13}C and ^{19}F -NMR spectra were recorded (295 K) on Bruker Avance DRX-500 or DPX-400 MHz spectrometers. Solvents for NMR were obtained from Cambridge Isotope Laboratories, Inc. (Andover, MA, USA). Chemical shifts (δ) are reported in ppm using trimethylsilyane or the residual solvent peaks as a reference and coupling constants (J) are reported in Hertz (Hz). The multiplicity's are abbreviated as: s = singlet, d = doublet, t = triplet, m = multiplet and br = broad.

The NOESY experiment of $[(\eta^6\text{-C}_6\text{H}_6)\text{Ru}(\mathbf{4})\text{Cl}]\text{Cl}$ (**9**) was carried out at 25 °C on a Bruker DRX600 NMR spectrometer, equipped with a z-axis pulsed field gradient dual broadband inverse probehead. The temperature was calibrated using a methanol sample. A phase-sensitive NOESY experiment was performed with 2048 time points in F2 and 512 time increments in the indirect dimension F1, which corresponds to acquisition times of 190 ms in F2 and 47 ms in F1. The mixing time was set to 1.2 s, the recycling delay was 1.5 s and the total experiment time was 1.7 h.

Circular dichroism (CD) spectroscopy analyses were performed on a Chirascan spectrophotometer from Applied Photophysics Ltd (United Kingdom).

The esterase activity screening assay (Section 4.4.1) and competitive displacement assay (Section 4.4.2) were performed using a Tecan Safire spectrophotometer using NUNC 96-well plates. The data were analyzed with gnuplot^[1] (Version 4.2) software using a least-square fitting.

4.1.4 Spectrometric methods

The mass spectra (MS) were recorded on an Esquire 3000 plus (Bruker) for Electron Spray Ionisation (ESI) and/or a Finnigan MAT 8400 for Fast Atom Bombardment (FAB) and/or Voyager-DE PRO bioSpectrometry for Maldi-TOF measurements (matrix: 4-nitroaniline).

High resolution mass spectrometry (HRMS) was recorded on a Bruker FTMS 4.7T BioAPEX II.

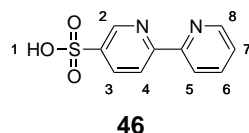
4.1.5 Other methods

The elementary analysis (EA) was measured on a Analysator 240 from Perkin-Elmer or a vario MICRO cube from Elementar.

4.2 Ligand synthesis

4.2.1 2,2'-Bipyridine-5-sulfonamide (1)

2,2'-Bipyridine-5-sulfonic acid (46)^[2]



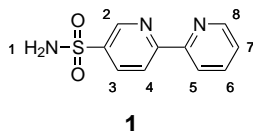
2,2'-Bipyridine (25.00 g, 160.0 mmol, 1.0 eq) was added slowly to oleum (60 mL) maintained at 0 °C, followed by addition of HgSO₄ (818 mg, 2.8 mmol, 0.01 eq). The mixture was stirred for 24 h at 220 °C. The reaction mixture was allowed to cool to room temperature, and the remaining sulfuric acid was removed by distillation. The solid was dissolved in water (125 mL), and activated charcoal (5 g) was added. The solution was refluxed for 15 min, and the mixture was filtered over celite. The pH of the obtained red solution was adjusted with conc. aqueous NH₃ to pH 12-13. The aqueous solution was then washed three times with CH₂Cl₂ in order to remove the starting material. Tetra-*n*-butylammonium bromide (25.0 g) was added, and the solution was extracted with CH₂Cl₂ (3 x 100 mL) and the combined organic layers were washed with water. Hydrobromic acid (48% in H₂O, 5 mL) was added, and the mixture was shaken, washed with CH₂Cl₂ and the volume of the aqueous layer was reduced. The solution was cooled to 0 °C, and cooled isopropanol (20 mL) was added to precipitate the product. The precipitate was filtered and dried to obtain **46** (7.12 g, 29.9 mmol, 19%) as a white powder.

Annex spectra page: 161

¹H NMR (400 MHz, D₂O, 20 °C, δ): 8.85 (d, *J* = 2.2 Hz, 1H, **H**²), 8.47 (dt, *J* = 4.9, 1.3 Hz, 1H, **H**⁸), 8.19 (dd, *J* = 8.3, 2.3 Hz, 1H, **H**³), 7.94 (dd, *J* = 8.4, 0.8 Hz, 1H, **H**⁴), 7.86 (m, 2H, **H**^{5,7}), 7.41 (ddd, *J* = 6.9, 4.9, 1.9 Hz, 1H, **H**⁶).

¹³C NMR (101 MHz, D₂O, 20 °C, δ): 157.4, 153.9, 149.4, 146.3, 139.4, 138.8, 135.9, 125.5, 122.8, 122.3.

MS (FAB, pos.) *m/z*: [M]⁺ calcd for C₁₀H₈N₂O₃S, 236.0; found, 236.0.

2,2'-Bipyridine-5-sulfonamide (**1**)^[2]

Compound **46** (1.51 g, 6.4 mmol, 1.0 eq) was placed in a round-bottom flask and PCl_5 (1.47 g, 7.1 mmol, 1.1 eq) was added. The mixture (calcium chloride protected) was heated at 120 °C for 30 min. The reaction mixture was allowed to cool to room temperature, and toluene (20 mL) was added. The solution was refluxed for 2 h. After cooling, the solution was filtered. The solvent and phosphorylchloride residues were removed under reduced pressure (3 h). A conc. aqueous solution of NH_3 (50 mL) was added to the solid, and the solution was stirred overnight. The solution was concentrated, and the solid was filtered, washed with cooled water and dried under reduced pressure to obtain **1** (0.90 g, 3.8 mmol, 60%) as a pale brown solid.

Annex spectra page: 163

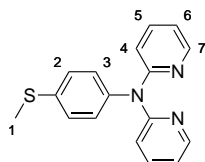
$^1\text{H NMR}$ (400 MHz, $\text{DMSO-}d_6$, 20 °C, δ): 9.07 (d, $J = 2.2$ Hz, 1H, \mathbf{H}^2), 8.74 (ddd, $J = 4.1$, 1.5, 0.8 Hz, 1H, \mathbf{H}^8), 8.57 (d, $J = 8.3$ Hz, 1H, \mathbf{H}^4), 8.44 (d, $J = 7.9$ Hz, 1H, \mathbf{H}^5), 8.34 (dd, $J = 8.4$, 2.4 Hz, 1H, \mathbf{H}^3), 8.00 (td, $J = 7.8$, 1.8 Hz, 1H, \mathbf{H}^6), 7.65 (s, 2H, \mathbf{H}^1), 7.53 (ddd, $J = 7.5$, 4.7, 1.2 Hz, 1H, \mathbf{H}^7).

$^{13}\text{C NMR}$ (101 MHz, $\text{DMSO-}d_6$, 20 °C, δ): 157.7, 153.8, 149.6, 146.3, 140.1, 137.6, 135.0, 125.1, 121.3, 120.6.

MS (ESI, pos.) m/z (relative intensity): $[\text{M}+\text{H}]^+$ calcd for $\text{C}_{10}\text{H}_{10}\text{N}_3\text{O}_2\text{S}$, 236.0; found, 236.0 (100) $[\text{M}+\text{H}]^+$, 258.0 (10) $[\text{M}+\text{Na}]^+$.

EA Anal. calcd for $\text{C}_{10}\text{H}_9\text{N}_3\text{O}_2\text{S}$: C, 51.05%; H, 3.86%; N, 17.86%. Found: C, 50.79%; H, 4.06%; N, 17.45%.

4.2.2 4-(Di-2-pyridinylamino)-benzenesulfonamide (2)

N-(4-(Methylthio)phenyl)-*N*-(pyridin-2-yl)pyridine-2-amine (49)

49

2-Bromopyridine (4.23 mL, 44.2 mmol, 2.2 eq), 4-(methylmercapto)aniline (2.5 mL, 20.1 mmol, 1.0 eq), 1,1-bis(diphenylphosphino)ferrocene (0.83 g, 1.5 mmol, 0.07 eq), tris(dibenzylideneacetone) dipalladium (0.66 g, 0.7 mmol, 0.07 eq) and sodium *tert*-butoxide (5.43 g, 56.5 mmol, 2.8 eq) were dissolved in dry toluene (50 mL). The reaction mixture was flushed with N₂, and heated at 100 °C for 24 h. The solution was cooled to room temperature, and CH₂Cl₂ (50 mL) was added. The solid was removed by filtration and purified by flash gel chromatography (cyclohexane/EtOAc, 1/1). The solvent was removed under vacuum to obtain **49** (5.33 g, 18.2 mmol, 90%) as a pale yellow powder.

Annex spectra page: 165

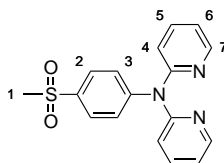
TLC : *n*-hexane/EtOAc (1/1); R_f = 0.10.

¹H NMR (400 MHz, CD₃OD, 20 °C, δ): 8.20 (ddd, *J* = 5.1, 2.0, 0.9 Hz, 2H, **H**⁷), 7.71 (ddd, *J* = 8.4, 7.3, 2.0 Hz, 2H, **H**⁵), 7.31 (d, *J* = 8.6 Hz, 2H, **H**²), 7.07 (m, 4H, **H**^{3,6}), 6.99 (d, *J* = 8.3 Hz, 1H, **H**⁴), 2.49 (s, 3H, **H**¹).

¹³C NMR (101 MHz, CD₃OD, 20 °C, δ): 159.3, 148.9, 143.1, 139.9, 137.7, 129.1, 128.7, 120.0, 118.8, 16.0.

HRMS (ESI-MS, pos.) *m/z*: [M+H]⁺ calcd for C₁₇H₁₆N₃S, 294.1064; found, 294.1053.

EA Anal. calcd for C₁₇H₁₅N₃S · $\frac{1}{5}$ H₂O: C, 68.75%; H, 5.23%; N, 14.15%. Found: C, 68.87%; H, 5.15%; N, 13.99%.

***N*-(4-(Methylsulfonyl)phenyl)-*N*-(pyridin-2-yl)pyridine-2-amine (50)****50**

Compound **49** (500 mg, 1.7 mmol, 1.0 eq) was dissolved in CH₂Cl₂ (25 mL). Finely ground KMnO₄/MnO₂ (4.0 g, 1/1) was added in small portions over a period of 15 min. The mixture was stirred vigorously overnight at room temperature. The product was filtered through celite in order to remove spent oxidant. The residue was then washed with CH₂Cl₂ (2 x 30 mL). The solvent was dried over Na₂SO₄, and removed under reduced pressure to yield **50** (270 mg, 0.8 mmol, 49%) as a white solid.

Annex spectra page: 167

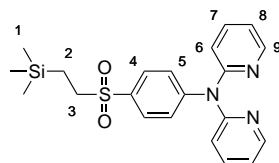
TLC : CH₂Cl₂/MeOH (9/1); R_f = 0.65.

¹H NMR (400 MHz, DMSO-*d*₆, 20 °C, δ): 8.32 (dd, *J* = 4.8, 1.2 Hz, 2H, **H**⁷), 7.84 (d, *J* = 8.7 Hz, 2H, **H**²), 7.77 (td, *J* = 8.2, 1.9 Hz, 2H, **H**⁵), 7.22 (d, *J* = 8.7 Hz, 2H, **H**³), 7.15 (dd, *J* = 7.0, 5.1 Hz, 2H, **H**⁶), 7.04 (d, *J* = 8.2 Hz, 2H, **H**⁴), 3.22 (s, 3H, **H**¹).

¹³C NMR (101 MHz, DMSO-*d*₆, 20 °C, δ): 157.0, 149.5, 148.6, 138.5, 135.3, 128.3, 125.0, 119.8, 118.0, 43.7.

HRMS (ESI-MS, pos.) *m/z*: [M+H]⁺ calcd for C₁₇H₁₆N₃O₂S, 326.0963; found, 326.0952.

EA Anal. calcd for C₁₇H₁₅N₃O₂S: C, 61.52%; H, 4.59%; N, 12.59%. Found: C, 62.09%; H, 4.86%; N, 12.01%.

***N*-(Pyridine-2-yl)-*N*-(4-((2-(trimethylsilyl)ethyl)sulfonyl)phenyl)pyridin-2-amine (51)****51**

To diisopropylamine (156 μL , 1.1 mmol, 1.2 eq) in dry THF (20 mL) at 0 °C *n*-butyllithium (634 μL , 1.6 M solution in *n*-hexane, 1.0 mmol, 1.1 eq) was added. The solution was stirred for 5 min, and then cooled to -70 °C with a dry ice/acetone bath. A solution of **50** (300 mg, 0.9 mmol, 1.0 eq) in dry THF (30 mL) was added over 10 min, and the reaction mixture stirred for 1 h. Chloromethyltrimethylsilane (180 μL , 1.3 mmol, 1.4 eq) was added dropwise, and the mixture was stirred overnight while allowing to warm to room temperature. The reaction was quenched with an aqueous solution of 1 M HCl (50 mL), and the aqueous phase extracted with EtOAc (3 x 60 mL). The combined organic fractions were washed with brine and dried over Na_2SO_4 . The solvent was removed under reduced pressure to obtain **51** (232 mg, 0.6 mmol, 61%) as a white solid.

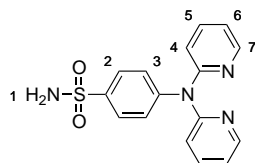
Annex spectra page: 169

TLC : $\text{CH}_2\text{Cl}_2/\text{MeOH}$ (9/1); $R_f = 0.82$.

^1H NMR (400 MHz, CDCl_3 , 20 °C, δ): 8.39 (s, 2H, **H**⁹), 7.81 (d, $J = 7.3$ Hz, 2H, **H**⁴), 7.66 (s, 2H, **H**⁷), 7.24 (d, $J = 7.7$ Hz, 2H, **H**⁵), 7.04 (m, 4H, **H**^{6,8}), 3.00 (m, 2H, **H**³), 1.02 (m, 2H, **H**²), 0.01 (s, 9H, **H**¹).

^{13}C NMR (101 MHz, CDCl_3 , 20 °C, δ): 157.4, 149.8, 149.2, 138.5, 133.6, 129.7, 124.8, 120.0, 118.6, 53.1, 8.88, -1.87.

HRMS (ESI-MS, pos.) m/z : $[\text{M}+\text{H}]^+$ calcd for $\text{C}_{21}\text{H}_{26}\text{N}_3\text{O}_2\text{SSi}$, 412.1515; found, 412.1501.

4-(Di-2-pyridinylamino)-benzenesulfonamide (**2**)**2**

To a solution of **51** (190 mg, 0.5 mmol, 1.0 eq) in dry THF (5 mL) a 1 M solution of TBAF in THF (1.38 mL, 1.4 mmol, 3.0 eq) was added. The mixture was refluxed for 1 h, and cooled to room temperature. A solution of sodium acetate (206 mg, 2.5 mmol, 5.4 eq) in 2 mL of water and hydroxyl-amine-*O*-sulfonic acid (281 mg, 2.5 mmol, 5.4 eq) were added sequentially, and the mixture was stirred overnight at room temperature. The reaction mixture was quenched by adding H₂O (25 mL) and extracted with EtOAc (3 x 30 mL). The combined organic layers were washed sequentially with saturated NaHCO₃ solution, water and brine. The organic layer was dried over Na₂SO₄, and the solvent was removed under vacuum. The product was purified by flash gel chromatography (CH₂Cl₂/MeOH, 5 %) to obtain **2** (71 mg, 0.2 mmol, 47%) as a brown solid.

Annex spectra page: 171

TLC : CH₂Cl₂/MeOH (9/1); R_f = 0.50.

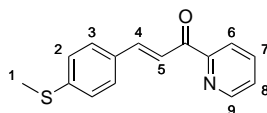
¹H NMR (400 MHz, CDCl₃/CD₃OD, 20 °C, δ): 8.32 (d, *J* = 3.8 Hz, 2H, **H**⁷), 7.79 (d, *J* = 8.7 Hz, 2H, **H**²), 7.63 (td, *J* = 8.2, 1.9 Hz, 2H, **H**⁵), 7.16 (d, *J* = 8.7 Hz, 2H, **H**³), 7.04 (dd, *J* = 7.0, 5.3 Hz, 2H, **H**⁶), 7.00 (d, *J* = 8.2 Hz, 2H, **H**⁴).

¹³C NMR (101 MHz, CDCl₃/CD₃OD, 20 °C, δ): 157.6, 149.0, 148.9, 138.3, 137.6, 128.0, 125.5, 119.7, 118.2.

HRMS (ESI-MS, pos.) *m/z*: [M+H]⁺ calcd for C₁₆H₁₅N₄O₂S, 327.0915; found, 327.0906.

EA Anal. calcd for C₁₆H₁₄N₄O₂S · $\frac{1}{7}$ CH₂Cl₂: C, 57.28%; H, 4.25%; N, 16.55%. Found: C, 57.44%; H, 4.33%; N, 16.19%.

4.2.3 (4-((2,2'-Bipyridine)4-yl)benzenesulfonamide (3)

(E)-3-(4-(Methylthio)phenyl)-1-(pyridin-2-yl)prop-2-en-1-one (55)

55

To 4-(methylthio)benzaldehyde (5.61 mL, 42.0 mmol, 1.1 eq) in a 1.0 M aqueous solution of NaOH (30 mL) and MeOH (90 mL), 2-acetylpyridine (4.49 mL, 40.0 mmol, 1.0 eq) was added. After 3 h of stirring at room temperature, the solution was stored at 4 °C overnight. The yellow precipitate was filtered and washed with H₂O and cold MeOH. The solvent was removed under reduced pressure. The isolated product was recrystallized from MeOH to obtain **55** (5.30 g, 20.8 mmol, 52%) as a yellow-green solid.

Annex spectra page: 173

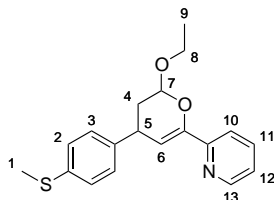
TLC : *n*-hexane/EtOAc (1/1); R_f = 0.51.

¹H NMR (400 MHz, DMSO-*d*₆, 20 °C, δ): 8.80 (ddd, *J* = 4.7, 1.7, 0.9 Hz, 1H, **H**⁹), 8.22 (d, *J* = 16.1 Hz, 1H, **H**⁴), 8.10 (ddd, *J* = 7.9, 1.4, 1.0 Hz, 1H, **H**⁶), 8.05 (ddd, *J* = 7.9, 7.4, 1.7 Hz, 1H, **H**⁷), 7.82 (d, *J* = 16.1 Hz, 1H, **H**⁵), 7.76 (d, *J* = 8.3 Hz, 2H, **H**²), 7.69 (ddd, *J* = 7.4, 4.7, 1.4 Hz, 1H, **H**⁸), 7.32 (d, *J* = 8.4 Hz, 2H, **H**³), 2.53 (s, 3H, **H**¹).

¹³C NMR (101 MHz, DMSO-*d*₆, 20 °C, δ): 188.6, 153.5, 149.1, 143.7, 142.4, 137.7, 130.9, 129.2, 127.6, 125.6, 122.4, 119.6, 14.1.

HRMS (ESI, pos.) *m/z*: [M+H]⁺ calcd for C₁₅H₁₄NOS, 256.0796; found, 256.0793.

EA Anal. calcd for C₁₅H₁₃NOS: C, 70.56%; H, 5.13%; N, 5.49%. Found: C, 70.30%; H, 5.17%; N, 5.59%.

2-(6-Ethoxy-4-(4-(methylthio)phenyl)-5,6-dihydro-2H-pyran-2-yl)pyridine (**56**)**56**

Compound **55** (2.0 g, 7.8 mmol, 1.0 eq) and yttrium (III) hexafluoroacetylacetonate (0.10 g, 0.1 mmol, 0.02 eq) were dissolved in THF (40 mL) and 4 Å molecular sieves (2 g) were added. Ethyl vinyl ether (7.5 mL, 78.3 mmol, 10.0 eq) was added, and the reaction was stirred under nitrogen at room temperature for 3 days. The sieves were removed by filtration over celite. The solvent was removed under reduced pressure, and the brown oil was purified by flash gel chromatography (*n*-hexane/EtOAc, 3/1) to obtain **56** (1.87 g, 5.7 mmol, 73%) as a colorless oil.

Annex spectra page: 175

TLC : *n*-hexane/EtOAc (1/1); $R_f = 0.66$.

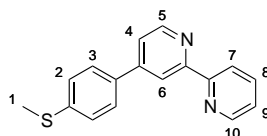
^1H NMR (400 MHz, CD_3OD , 20 °C, δ): 8.46 (ddd, $J = 4.8, 1.8, 0.9$ Hz, 1H, H^{13}), 7.83 (td, $J = 7.8, 1.8$ Hz, 1H, H^{11}), 7.69 (dt, $J = 8.0, 1.1$ Hz, 1H, H^{10}), 7.31 (ddd, $J = 7.6, 4.9, 1.2$ Hz, 1H, H^{12}), 7.21 (m, 4H, $\text{H}^{2,3}$), 6.02 (dd, $J = 2.9, 1.2$ Hz, 1H, H^6), 5.28 (dd, $J = 8.6, 2.0$ Hz, 1H, H^7), 4.10 (dq, $J = 9.6, 7.1$ Hz, 1H, H^8), 3.82 (ddd, $J = 9.9, 6.7, 2.8$ Hz, 1H, H^5), 3.72 (dq, $J = 9.6, 7.1$ Hz, 1H, $\text{H}^{8'}$), 2.44 (s, 3H, H^1), 2.32 (dddd, $J = 13.2, 6.8, 2.1, 1.3$ Hz, 1H, H^4), 1.84 (ddd, $J = 13.2, 10.3, 8.6$ Hz, 1H, $\text{H}^{4'}$), 1.25 (t, $J = 7.1$ Hz, 3H, H^9).

^{13}C NMR (101 MHz, CD_3OD , 20 °C, δ): 153.9, 150.0, 149.8, 142.7, 138.6, 137.9, 129.1, 128.0, 124.4, 120.3, 105.6, 101.8, 65.7, 38.9, 38.4, 16.0, 15.7.

MS (ESI, pos.) m/z (relative intensity): $[\text{M}+\text{H}]^+$ calcd for $\text{C}_{19}\text{H}_{22}\text{NO}_2\text{S}$, 328.1; found, 328.2 (100) $[\text{M}+\text{H}]^+$, 350.0 (6) $[\text{M}+\text{Na}]^+$.

EA Anal. calcd for $\text{C}_{19}\text{H}_{21}\text{NO}_2\text{S}$: C, 69.69%; H, 6.46%; N, 4.28%. Found: C, 69.79%; H, 6.51%; N, 4.29%.

(4-(4-(Methylthio)phenyl)-2,2'-bipyridine (52)

**52**

Compound **56** (1.50 g, 4.5 mmol, 1.0 eq) was dissolved in ACN (10 mL) and $\text{H}_2\text{NOH} \cdot \text{HCl}$ (3.18 g, 45.7 mmol, 10.4 eq) was added. The mixture was refluxed for 6 h, during which time a yellow precipitate formed. The solution was allowed to cool to room temperature, and the ACN was removed under reduced pressure to give an orange solid. A saturated aqueous solution of NaOH/NaCl (30 mL) and CH_2Cl_2 (30 mL) were added to the solid, and the mixture was stirred vigorously until all the solid had dissolved. The organic layer was extracted with CH_2Cl_2 (3 x 20 mL), dried over Na_2SO_4 , and the solvent was removed under reduced pressure. The resulting solid was washed with MeOH to yield **52** (583 mg, 2.1 mmol, 46%) as a white powder.

Annex spectra page: 177

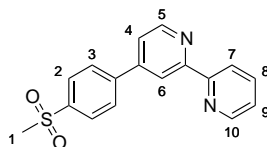
TLC : $\text{CH}_2\text{Cl}_2/\text{MeOH}$ (9/1); $R_f = 0.77$.

^1H NMR (400 MHz, CDCl_3 , 20 °C, δ): 8.72 (m, 3H, $\text{H}^{5,6,10}$), 8.53 (d, $J = 8.0$ Hz, 1H, H^7), 7.88 (td, $J = 7.8, 1.8$ Hz, 1H, H^8), 7.73 (d, $J = 8.5$ Hz, 2H, H^3), 7.57 (dd, $J = 5.2, 1.9$ Hz, 1H, H^4), 7.37 (m, 3H, $\text{H}^{2,9}$), 2.54 (s, 3H, H^1).

^{13}C NMR (101 MHz, CDCl_3 , 20 °C, δ): 156.5, 156.0, 149.6, 149.3, 149.0, 140.5, 137.2, 134.6, 127.5, 126.7, 124.0, 121.5, 121.3, 118.7, 15.9.

HRMS (ESI, pos.) m/z : $[\text{M}+\text{H}]^+$ calcd for $\text{C}_{17}\text{H}_{15}\text{N}_2\text{S}$, 279.0955; found, 279.0951.

EA Anal. calcd for $\text{C}_{17}\text{H}_{14}\text{N}_2\text{S} \cdot \frac{1}{6}\text{H}_2\text{O}$: C, 72.57%; H, 5.13%; N, 9.96%. Found: C, 72.50%; H, 5.23%; N, 10.19%.

(4-(4-(Methylsulfonyl)phenyl)-2,2'-bipyridine (**57**))**57**

Compound **52** (249 mg, 0.9 mmol, 1.0 eq) was dissolved in CH_2Cl_2 (20 mL). Finely ground $\text{KMnO}_4/\text{MnO}_2$ (4.0 g, 1/1) was added to the solution over a period of 0.5 h. The mixture was stirred at room temperature for 3 days. After completion of the reaction, the product was filtered through celite and CH_2Cl_2 was removed under reduced pressure to obtain **57** (220 mg, 0.7 mmol, 79%) as a white powder which was used with no further purification.

Annex spectra page: 179

TLC : $\text{CH}_2\text{Cl}_2/\text{MeOH}$ (9/1); $R_f = 0.83$.

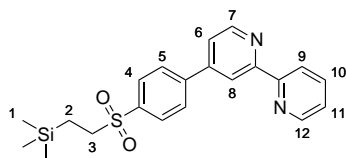
^1H NMR (400 MHz, CDCl_3 , 20 °C, δ): 8.79 (d, $J = 5.1$ Hz, 1H, \mathbf{H}^5), 8.72 (m, 2H, $\mathbf{H}^{6,10}$), 8.50 (d, $J = 8.0$ Hz, 1H, \mathbf{H}^7), 8.08 (d, $J = 8.4$ Hz, 2H, \mathbf{H}^2), 7.96 (d, $J = 8.4$ Hz, 2H, \mathbf{H}^3), 7.88 (td, $J = 7.8, 1.8$ Hz, 1H, \mathbf{H}^8), 7.55 (dd, $J = 5.1, 1.8$ Hz, 1H, \mathbf{H}^4), 7.38 (ddd, $J = 7.6, 4.8, 1.2$ Hz, 1H, \mathbf{H}^9), 3.11 (s, 3H, \mathbf{H}^1).

^{13}C NMR (101 MHz, CDCl_3 , 20 °C, δ): 156.8, 155.4, 150.1, 149.1, 147.6, 143.9, 141.0, 137.6, 128.4, 128.3, 124.4, 121.9, 121.7, 119.5, 44.7.

HRMS (ESI, pos.) m/z : $[\text{M}+\text{H}]^+$ calcd for $\text{C}_{17}\text{H}_{15}\text{N}_2\text{O}_2\text{S}$, 311.0854; found, 311.0850.

EA Anal. calcd for $\text{C}_{17}\text{H}_{14}\text{N}_2\text{O}_2\text{S} \cdot \frac{1}{3}\text{H}_2\text{O}$: C, 64.54%; H, 4.67%; N, 8.85%. Found: C, 64.40%; H, 4.42%; N, 8.81%.

(4-(4-((2-(Trimethylsilyl)ethyl)sulfonyl)phenyl)-2,2'-bipyridine (58)

**58**

Diisopropylamine (0.89 mL, 6.3 mmol, 1.3 eq) in THF (5 mL) was cooled to 0 °C and *n*-butyllithium (2.2 M solution in cyclohexane) (2.6 mL, 5.8 mmol, 1.2 eq) was added. The solution was stirred at 0 °C for 5 min, and cooled to -70 °C with a dry ice/acetone bath. A solution of **57** (1.5 g, 4.8 mmol, 1.0 eq) in dry THF (5 mL) was added dropwise over a period of 10 min. The reaction mixture was stirred for 1 h. Chloromethyltrimethylsilane (0.94 mL, 6.8 mmol, 1.4 eq) was added dropwise and the reaction was stirred at room temperature for 2 d. The reaction was quenched with a 1 M aqueous solution of HCl (2 mL), and the aqueous phase extracted with EtOAc (3 x 50 mL). The combined organic layers were washed with brine and dried over MgSO₄, and the solvent was removed under reduced pressure to obtain **58** (1.61 g, 4.0 mmol, 84%) as a red-brown solid.

Annex spectra page: 181

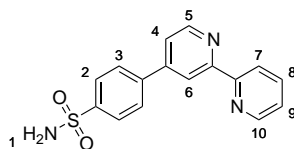
TLC : CH₂Cl₂/MeOH (9/1); R_f = 0.74.

¹H NMR (500 MHz, CDCl₃, 20 °C, δ): 8.79 (d, *J* = 5.1 Hz, 1H, **H**⁷), 8.73 (b, 2H, **H**^{8,12}), 8.48 (d, *J* = 7.9 Hz, 1H, **H**⁹), 8.03 (d, *J* = 8.4 Hz, 2H, **H**⁴), 7.95 (d, *J* = 8.4 Hz, 2H, **H**⁵), 7.90 (td, *J* = 7.7, 1.8 Hz, 1H, **H**¹⁰), 7.58 (dd, *J* = 5.1, 1.8 Hz, 1H, **H**⁶), 7.39 (ddd, *J* = 7.4, 4.8, 1.2 Hz, 1H, **H**¹¹), 3.04 (m, 2H, **H**³), 0.94 (m, 2H, **H**²), 0.01 (s, 9H, **H**¹).

¹³C NMR (101 MHz, CDCl₃, 20 °C, δ): 156.3, 155.1, 149.9, 148.9, 147.8, 143.5, 139.2, 137.9, 129.2, 128.2, 124.5, 122.1, 121.9, 119.7, 53.0, 9.3, -1.9.

HRMS (ESI-MS, pos.) *m/z*: [M+H]⁺ calcd for C₂₁H₂₅N₂O₂SSi, 397.1406; found, 397.1398.

EA Anal. calcd for C₂₁H₂₄N₂O₂SSi · $\frac{2}{3}$ H₂O: C, 61.73%; H, 6.25%; N, 6.86%. Found: C, 61.36%; H, 6.14%; N, 6.56%.

(4-((2,2'-Bipyridine)4-yl)benzenesulfonamide (**3**)**3**

To a solution of **58** (262 mg, 0.7 mmol, 1.0 eq) in dry THF (5 mL) a 1 M solution of TBAF in THF (3.87 mL, 3.9 mmol, 4.3 eq) was added. The mixture was refluxed for 1 h, and cooled to room temperature. A solution of sodium acetate (523 mg, 6.4 mmol, 9.7 eq) in 2 mL of water and hydroxyl-amine-*O*-sulfonic acid (729 mg, 6.5 mmol, 9.8 eq) were added sequentially, and the mixture was stirred overnight at room temperature. The reaction mixture was quenched by adding H₂O (10 mL), and extracted with EtOAc (3 x 30 mL). The organic fractions were washed sequentially with saturated NaHCO₃ solution, water and brine. The organic layer was dried over Na₂SO₄, and the solvent was removed under reduced pressure. The product was purified by flash chromatography (CH₂Cl₂/MeOH, gradient 0 to 5 %) to obtain **3** (149 mg, 0.5 mmol, 72%) as a white solid.

Annex spectra page: 183

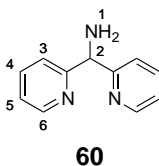
TLC : CH₂Cl₂/MeOH (9/1); R_f = 0.38.

¹H NMR (400 MHz, DMSO-*d*₆, 20 °C, δ): 8.81 (d, *J* = 5.1 Hz, 1H, **H**⁵), 8.74 (d, *J* = 4.0 Hz, 1H, **H**¹⁰), 8.71 (d, *J* = 1.5 Hz, 1H, **H**⁶), 8.45 (d, *J* = 8.0 Hz, 1H, **H**⁷), 8.08 (d, *J* = 8.5 Hz, 2H, **H**²), 7.99 (m, 3H, **H**^{3,8}), 7.85 (dd, *J* = 5.1, 1.9 Hz, 1H, **H**⁴), 7.51 (m, 3H, **H**^{1,9}).

¹³C NMR (101 MHz, DMSO-*d*₆, 20 °C, δ): 156.2, 154.9, 150.2, 149.4, 146.9, 144.7, 140.5, 137.5, 127.6, 126.6, 124.5, 121.9, 120.7, 117.9.

HRMS (ESI, pos.) *m/z*: [M+H]⁺ calcd for C₁₆H₁₄N₃O₂S, 312.0806; found, 312.0803.

EA Anal. calcd for C₁₆H₁₃N₃O₂S · $\frac{1}{3}$ EtOAc: C, 61.11%; H, 4.63%; N, 12.34%. Found: C, 61.02%; H, 4.69%; N, 12.34%.

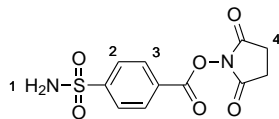
4.2.4 *N*-(Di(2-pyridyl)methyl)-amidobenzene-4-sulfonamide (4)Bis(pyridine-2-yl)methanamine (60)^[3]

Di-2-pyridyl ketoxime (507 mg, 2.5 mmol, 1.0 eq) was dissolved in a mixture of H₂O (7.5 mL), EtOH (12.5 mL) and NH₃ (25% in water, 10.5 mL). Ammonium acetate (369 mg, 4.8 mmol, 1.8 eq) was added and the solution was heated to 80 °C. Zn powder (753 mg, 11.5 mmol, 4.5 eq) was added portionwise over a period of 0.5 h. The reaction mixture was stirred for 5 h at 80 °C. The mixture was allowed to cool and residual Zn powder was removed by filtration. All volatiles were removed under reduced pressure. The solution was basified with a 10 M aqueous solution of NaOH (10 mL). The aqueous layer was extracted with CH₂Cl₂ (3 x 30 mL). The combined organic layers were washed with brine, dried over Na₂SO₄ and the solvent was removed under reduced pressure to afford **60** (340 mg, 1.8 mmol, 72%) as an oil.

Annex spectra page: 185

¹H NMR (400 MHz, CDCl₃, 20 °C, δ): 8.54 (ddd, *J* = 4.8, 1.7, 0.9 Hz, 2H, **H**⁶), 7.60 (td, *J* = 7.7, 1.8 Hz, 2H, **H**⁴), 7.36 (dt, *J* = 8.0, 1.1 Hz, 2H, **H**³), 7.11 (ddd, *J* = 7.5, 4.8, 1.2 Hz, 2H, **H**⁵), 5.30 (s, 1H, **H**²), 2.43 (s, 2H, **H**¹).

MS (ESI-MS, pos.) *m/z* (relative intensity): [M+H]⁺ calcd for C₁₁H₁₂N₃, 186; found, 186 (100) [M+H]⁺, 208 (10) [M+Na]⁺.

2,5-Dioxopyrrolidin-1-yl-4-sulfamoylbenzoate (61)^[4]**61**

4-Carboxybenzenesulfonamide (5.02 g, 24.9 mmol, 1.0 eq) was dissolved in DMF (100 mL) and *N*-hydroxysuccinimide (3.26 mg, 28.4 mmol, 1.1 eq) was added. The mixture was cooled to 0 °C and *N,N'*-dicyclohexylcarbodiimide (5.0 g, 24.2 mmol, 1.0 eq) was added. The solution was stirred at room temperature overnight. The solvent was removed under reduced pressure. The white solid was washed with cooled isopropanol (2 x 50 mL) and dried under reduced pressure to obtain **61** (6.63 g, 22.2 mmol, 89%) as a white powder.

Annex spectra page: 186

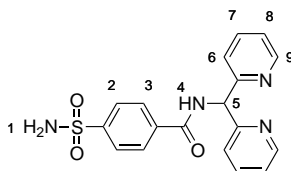
TLC : CH₂Cl₂/MeOH (9/1); R_f = 0.78.

¹H NMR (400 MHz, DMSO-*d*₆, 20 °C, δ): 8.30 (d, *J* = 8.5 Hz, 2H, **H**³), 8.08 (d, *J* = 8.5 Hz, 2H, **H**²), 7.71 (s, 2H, **H**¹), 2.91 (s, 4H, **H**⁴).

¹³C NMR (101 MHz, DMSO-*d*₆, 20 °C, δ): 170.2, 161.0, 149.8, 130.9, 127.2, 126.7, 25.6.

MS (FAB-MS, pos.) *m/z* (relative intensity): [M]⁺ calcd for C₁₁H₁₀N₂O₆S, 298; found, 184 (100) [M-(*N*-Hydroxysuccinimide)]⁺, 299 (52) [M+H]⁺, 452 (27) [M+H+NBA]⁺, 597 (10) [2M+H]⁺.

EA Anal. calcd for C₁₁H₁₀N₂O₆S: C, 44.29%; H, 3.38%; N, 9.39%. Found: C, 44.10%; H, 3.62%; N, 9.52%.

N-(Di(2-pyridyl)methyl)-amidobenzene-4-sulfonamide (4)

Compound **61** (1.09 g, 5.9 mmol, 1.0 eq) was dissolved in acetone (1 mL), H₂O (2 mL), and a 1 M aqueous solution of H₂KPO₄ (4 mL). Compound **60** (1.87 mg, 6.3 mmol, 1.1 eq) was added. The solution was stirred overnight at room temperature. EtOH (10 mL) was added to allow product precipitation, and the mixture was stored in the fridge for 3 d. The solvent was removed by decantation, and the solid was purified by flash chromatography (CH₂Cl₂/MeOH, gradient 1 to 5 %). The solvent was removed under reduced pressure to obtain **4** (2.01 g, 5.4 mmol, 92%) as a white powder.

Annex spectra page: 188

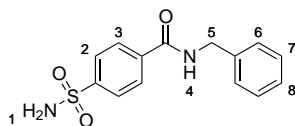
TLC : CH₂Cl₂/MeOH (9/1); R_f = 0.50.

¹H NMR (500 MHz, DMSO-*d*₆, 20 °C, δ): 9.43 (d, *J* = 7.9 Hz, 1H, **H**⁴), 8.53 (dd, *J* = 4.8, 1.6 Hz, 2H, **H**⁹), 8.10 (d, *J* = 8.3 Hz, 2H, **H**³), 7.93 (d, *J* = 8.4 Hz, 2H, **H**²), 7.79 (td, *J* = 7.7, 1.7 Hz, 2H, **H**⁷), 7.54 (b, 4H, **H**^{1,6}), 7.30 (dd, *J* = 7.5, 4.8 Hz, 2H, **H**⁸), 6.47 (d, *J* = 7.9 Hz, 1H, **H**⁵).

¹³C NMR (126 MHz, DMSO-*d*₆, 20 °C, δ): 165.1, 159.5, 148.9, 146.5, 137.0, 136.9, 128.3, 125.7, 122.6, 122.2, 60.1.

HRMS (ESI-MS, pos.) *m/z*: [M+H]⁺ calcd for C₁₈H₁₇N₄O₃S, 369.1021; found, 369.1016.

EA Anal. calcd for C₁₈H₁₆N₄O₃S · ½H₂O · MeOH: C, 55.73%; H, 5.17%; N, 13.68%. Found: C, 55.70%; H, 4.99%; N, 13.87%.

N-Benzyl-4-sulfamoylbenzamide (40)**40**

Benzylamine (202 μL , 1.8 mmol, 1.2 eq) was dissolved in acetone (6 mL), H_2O (12 mL), and a 1 M aqueous solution of H_2KPO_4 (4 mL). Compound **61** (500 mg, 1.7 mmol, 1.0 eq) was added. The solution was stirred at room temperature for 2 h. The solid was extracted with EtOAc (3 x 30 mL). The combined organic layers were washed with brine and dried over Na_2SO_4 . The product was purified by flash chromatography ($\text{CH}_2\text{Cl}_2/\text{MeOH}$, gradient 1 to 5%). The solvent was removed under reduced pressure to obtain **40** (246 mg, 0.8 mmol, 50%) as a white powder.

Annex spectra page: 190

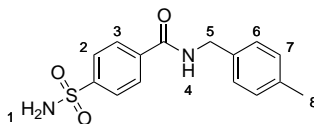
TLC : $\text{CH}_2\text{Cl}_2/\text{MeOH}$ (9/1); $R_f = 0.63$.

^1H NMR (400 MHz, $\text{DMSO}-d_6$, 20 $^\circ\text{C}$, δ): 9.23 (t, $J = 5.9$ Hz, 1H, H^4), 8.04 (d, $J = 8.5$ Hz, 2H, H^3), 7.91 (d, $J = 8.4$ Hz, 2H, H^2), 7.49 (s, 2H, H^6), 7.34 (s, 2H, H^7), 7.33 (s, 2H, H^1), 7.25 (ddd, $J = 8.7, 5.1, 3.7$ Hz, 1H, H^8), 4.50 (d, $J = 6.0$ Hz, 2H, H^5).

^{13}C NMR (101 MHz, $\text{DMSO}-d_6$, 20 $^\circ\text{C}$, δ): 165.2, 146.3, 139.3, 137.2, 128.3, 127.9, 127.2, 126.8, 125.6, 42.7.

MS (FAB-MS, pos.) m/z (relative intensity): $[\text{M}]^+$ calcd for $\text{C}_{14}\text{H}_{14}\text{N}_2\text{O}_3\text{S}$, 290.1; found, 290.1 (100) $[\text{M}]^+$, 184.0 (65) $[\text{M}-\text{C}_7\text{H}_8\text{N}]^+$.

EA Anal. calcd for $\text{C}_{14}\text{H}_{14}\text{N}_2\text{O}_3\text{S}$: C, 57.92%; H, 4.86%; N, 9.65%. Found: C, 57.55%; H, 4.94%; N, 9.66%.

***N*-(4-Methylbenzyl)-4-sulfamoylbenzamide (42)****42**

4-Methylbenzylamine (320 μ L, 2.5 mmol, 1.5 eq) was dissolved in acetone (2 mL), H₂O (6 mL), and a 1 M aqueous solution of H₂KPO₄ (2 mL). Compound **61** (500 mg, 1.7 mmol, 1.0 eq) was added. The solution was stirred at room temperature for 2 h. The solid was extracted with EtOAc (3 x 30 mL). The combined organic layers were washed with brine and dried over Na₂SO₄. The product was purified by flash chromatography (CH₂Cl₂/MeOH, gradient 1 to 5%). The solvent was removed under reduced pressure to obtain **42** (184 mg, 0.6 mmol, 36%) as a white powder.

Annex spectra page: 192

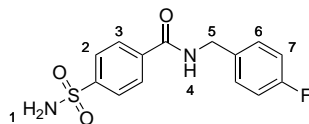
TLC : CH₂Cl₂/MeOH (9/1); R_f = 0.51.

¹H NMR (400 MHz, DMSO-*d*₆, 20 °C, δ): 9.17 (t, J = 6.0 Hz, 1H, **H**⁴), 8.03 (d, J = 8.4 Hz, 2H, **H**³), 7.90 (d, J = 8.4 Hz, 2H, **H**²), 7.47 (s, 2H, **H**¹), 7.22 (d, J = 8.1 Hz, 2H, **H**⁶), 7.14 (d, J = 8.0 Hz, 2H, **H**⁷), 4.44 (d, J = 5.9 Hz, 2H, **H**⁵), 2.27 (s, 3H, **H**⁸).

¹³C NMR (101 MHz, DMSO-*d*₆, 20 °C, δ): 165.1, 146.2, 137.2, 136.3, 135.8, 128.8, 127.8, 127.2, 125.6, 42.5, 20.6.

MS (FAB-MS, pos.) m/z (relative intensity): [M]⁺ calcd for C₁₅H₁₆N₂O₃S, 304.1; found, 304.1 (100) [M]⁺, 184.0 (99) [M-C₈H₁₁N]⁺.

EA Anal. calcd for C₁₅H₁₆N₂O₃S: C, 59.13%; H, 5.33%; N, 9.17%. Found: C, 59.19%; H, 5.30%; N, 9.20%.

***N*-(4-Fluorobenzyl)-4-sulfamoylbenzamide (43)****43**

4-Fluorobenzylamine (289 μ L, 2.5 mmol, 1.5 eq) was dissolved in acetone (2 mL), H₂O (6 mL), and a 1 M aqueous solution of H₂KPO₄ (2 mL). Compound **61** (500 mg, 1.7 mmol, 1.0 eq) was added. The solution was stirred at room temperature for 2 h. The solid was extracted with EtOAc (3 x 30 mL). The combined organic layers were washed with brine and dried over Na₂SO₄. The product was purified by flash chromatography (CH₂Cl₂/MeOH, gradient 5 to 20%). The solvent was removed under reduced pressure to obtain **43** (228 mg, 0.7 mmol, 44%) as a white powder.

Annex spectra page: 194

TLC : CH₂Cl₂/MeOH (9/1); R_f = 0.65.

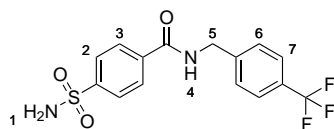
¹H NMR (400 MHz, DMSO-*d*₆, 20 °C, δ): 9.22 (t, *J* = 6.0 Hz, 1H, **H**⁴), 8.03 (d, *J* = 8.4 Hz, 2H, **H**³), 7.91 (d, *J* = 8.4 Hz, 2H, **H**²), 7.48 (s, 2H, **H**¹), 7.37 (dd, *J* = 8.7, 4.0 Hz, 2H, **H**⁶), 7.16 (dd, *J* = 8.7, 6.8 Hz, 2H, **H**⁷), 4.47 (d, *J* = 5.8 Hz, 2H, **H**⁵).

¹³C NMR (101 MHz, DMSO-*d*₆, 20 °C, δ): 165.2, 146.3, 137.1, 135.5, 129.3, 127.9, 125.6, 115.1, 114.9, 42.1.

¹⁹F NMR (376 MHz, DMSO-*d*₆, 20 °C, δ): -116.1.

MS (FAB-MS, pos.) *m/z* (relative intensity): [M]⁺ calcd for C₁₄H₁₃FN₂O₃S, 308.1; found, 308.1 (100) [M]⁺, 184.0 (84) [M-C₇H₇NF]⁺.

EA Anal. calcd for C₁₄H₁₃FN₂O₃S · $\frac{2}{5}$ H₂O: C, 53.29%; H, 4.41%; N, 8.88%. Found: C, 53.08%; H, 4.25%; N, 9.26%.

N-(4-(Trifluoromethyl)benzyl)-4-sulfamoylbenzamide (44)

4-(Trifluoromethyl)benzylamine (359 μL , 2.5 mmol, 1.5 eq) was dissolved in acetone (2 mL), H_2O (6 mL), and a 1 M aqueous solution of H_2KPO_4 (2 mL). Compound **61** (500 mg, 1.7 mmol, 1.0 eq) was added. The solution was stirred overnight at room temperature. The solid was extracted with EtOAc (3 x 30 mL). The combined organic layers were washed with brine and dried over Na_2SO_4 . The product was purified by flash chromatography ($\text{CH}_2\text{Cl}_2/\text{MeOH}$, 10%). The solvent was removed under reduced pressure to obtain **44** (104 mg, 0.3 mmol, 17%) as a white powder.

Annex spectra page: 196

TLC : $\text{CH}_2\text{Cl}_2/\text{MeOH}$ (9/1); $R_f = 0.42$.

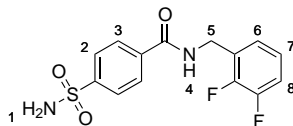
^1H NMR (500 MHz, $\text{DMSO}-d_6$, 20 $^\circ\text{C}$, δ): 9.34 (t, $J = 6.0$ Hz, 1H, H^4), 8.05 (d, $J = 8.4$ Hz, 2H, H^3), 7.92 (d, $J = 8.4$ Hz, 2H, H^2), 7.71 (d, $J = 8.1$ Hz, 2H, H^7), 7.55 (d, $J = 8.0$ Hz, 2H, H^6), 7.50 (s, 2H, H^1), 4.58 (d, $J = 5.9$ Hz, 2H, H^5).

^{13}C NMR (126 MHz, $\text{DMSO}-d_6$, 20 $^\circ\text{C}$, δ): 165.4, 146.4, 144.2, 136.9, 128.0, 127.9, 125.7, 125.3, 125.2, 42.4.

^{19}F NMR (376 MHz, $\text{DMSO}-d_6$, 20 $^\circ\text{C}$, δ): -60.8.

MS (FAB-MS, pos.) m/z (relative intensity): $[\text{M}]^+$ calcd for $\text{C}_{15}\text{H}_{13}\text{F}_3\text{N}_2\text{O}_3\text{S}$, 358.0; found, 358.1 (100) $[\text{M}]^+$, 184.0 (99) $[\text{M}-\text{C}_8\text{H}_{11}\text{N}]^+$.

EA Anal. calcd for $\text{C}_{15}\text{H}_{13}\text{F}_3\text{N}_2\text{O}_3\text{S} \cdot \frac{1}{3}\text{H}_2\text{O}$: C, 49.45%; H, 3.78%; N, 7.69%. Found: C, 49.50%; H, 3.69%; N, 7.76%.

N-(2,3-Difluorobenzyl)-4-sulfamoylbenzamide (45) [5]**45**

2,3-Difluorobenzylamine (470 μ L, 4.1 mmol, 1.2 eq) was dissolved in acetone (6 mL), H₂O (12 mL), and a 1 M aqueous solution of H₂KPO₄ (4 mL). Compound **61** (1.01 mg, 3.4 mmol, 1.0 eq) was added. The solution was stirred overnight at room temperature. The solid was filtered, and washed with EtOH. The product was purified by flash chromatography (CH₂Cl₂/MeOH, gradient 1 to 5%). The solvent was removed under reduced pressure to obtain **45** (155 mg, 0.5 mmol, 14%) as a white powder.

Annex spectra page: 198

TLC : CH₂Cl₂/MeOH (9/1); R_f = 0.59.

¹H NMR (400 MHz, DMSO-*d*₆, 20 °C, δ): 9.26 (t, J = 5.7 Hz, 1H, **H**⁴), 8.04 (d, J = 8.5 Hz, 2H, **H**³), 7.91 (d, J = 8.5 Hz, 2H, **H**²), 7.49 (s, 2H, **H**¹), 7.34 (m, 1H, **H**⁸), 7.19 (m, 2H, **H**^{6,7}), 4.57 (d, J = 5.6 Hz, 2H, **H**⁵).

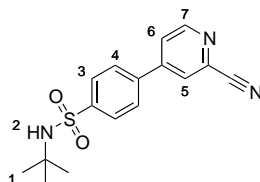
¹³C NMR (101 MHz, DMSO-*d*₆, 20 °C, δ): 165.3, 146.4, 136.8, 128.6, 128.5, 128.0, 125.7, 124.7, 124.6, 116.1, 115.9, 36.5.

¹⁹F NMR (376 MHz, DMSO-*d*₆, 20 °C, δ): -139.7 (d, J = 21.8 Hz, 1F), -144.6 (d, J = 21.8 Hz, 1F).

HRMS (ESI-MS, pos.) m/z : [M+H]⁺ calcd for C₁₄H₁₃F₂N₂O₃S, 327.0614; found, 327.0618.

EA Anal. calcd for C₁₄H₁₃F₂N₂O₃S: C, 51.53%; H, 3.71%; N, 8.58%. Found: C, 51.34%; H, 3.75%; N, 8.48%.

4.2.5 4-(2-(Aminomethyl)pyridin-4-yl)benzenesulfonamide (5)

N-(*tert*-Butyl)-4-(2-cyanopyridin-4-yl)benzenesulfonamide (65)

65

4-Chloro-2-pyridinecarbonitrile (182 mg, 1.3 mmol, 0.7 eq) and 4-(*tert*-butylaminosulphonyl)benzeneboronic acid (496 mg, 1.9 mmol, 1.0 eq) were dissolved in THF (8 mL). Tetrakis(triphenylphosphine)-palladium (136 mg, 0.1 mmol, 0.06 eq) and an aqueous solution (2 mL) of Na₂CO₃ (381 mg, 3.6 mmol, 1.9 eq) were added. The reaction mixture was heated at 80 °C for 6 h. The cooled crude mixture was poured onto water (50 mL), and extracted with CH₂Cl₂ (3 x 50 mL). The combined organic layers were dried over Na₂SO₄. The product was purified by flash chromatography (*n*-hexane/EtOAc 1/1). The solvent was removed under reduced pressure to obtain **65** (325 mg, 1.0 mmol, 80%) as a pale brown powder.

Annex spectra page: 200

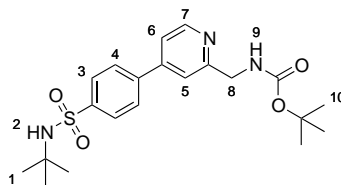
TLC : *n*-hexane/EtOAc (1/1); R_f = 0.54.

¹H NMR (400 MHz, DMSO-*d*₆, 20 °C, δ): 8.85 (d, *J* = 5.2 Hz, 1H, **H**⁷), 8.51 (dd, *J* = 1.9, 0.9 Hz, 1H, **H**⁵), 8.15 (ddd, *J* = 5.2, 1.9, 0.8 Hz, 1H, **H**⁶), 8.10 (d, *J* = 8.2 Hz, 2H, **H**³), 7.97 (d, *J* = 8.4 Hz, 2H, **H**⁴), 7.69 (s, 1H, **H**²), 1.12 (s, 9H, **H**¹).

¹³C NMR (101 MHz, DMSO-*d*₆, 20 °C, δ): 151.9, 147.1, 145.6, 138.3, 133.5, 127.9, 127.0, 126.8, 125.2, 117.5, 53.5, 29.8.

HRMS (ESI-MS, pos.) *m/z*: [M+Na]⁺ calcd for C₁₆H₁₇N₃O₂SNa, 338.0939; found, 338.0941.

EA Anal. calcd for C₁₆H₁₇N₃O₂S · $\frac{1}{3}$ EtOAc: C, 60.39%; H, 5.75%; N, 12.19%. Found: C, 60.31%; H, 5.58%; N, 12.30%.

***N*-(*tert*-Butyl)-4-(2-(aminomethyl)pyridin-4-yl)benzenesulfonamide (66)****66**

LiAlH₄ (104 mg, 2.7 mmol, 2.2 eq) was added to dry THF (10 mL). The reaction mixture was allowed to stir until a homogeneous slurry had formed. AlCl₃ (267 mg, 1.6 mmol, 1.6 eq) was then added, the reaction mixture was cooled to 0 °C, and a solution of **65** (382 mg, 1.2 mmol, 1.0 eq) in THF (10 mL) was added dropwise. The reaction was allowed to warm to room temperature, and was stirred for 2 h. The reaction was quenched with a 2 M aqueous solution of NaOH (10 mL). The product was extracted with EtOAc (3 x 50 mL), and the combined organic layers were washed with brine and dried over Na₂SO₄. The solvent was removed under reduced pressure, and the obtained orange solid was dissolved in CH₂Cl₂ (30 mL) and di-*tert*-butyl dicarbonate (528 mg, 2.4 mmol, 2.0 eq) was added. The solution was stirred overnight at room temperature. The solvent was removed, and the product was purified by flash gel chromatography (*n*-hexane/EtOAc, 1/1) to obtain **66** (328 mg, 0.8 mmol, 65%) as a colorless oil.

Annex spectra page: 202

TLC : *n*-hexane/EtOAc (1/1); R_f = 0.17.

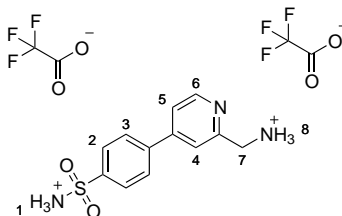
¹H NMR (500 MHz, DMSO-*d*₆, 20 °C, δ): 8.72m, 8.63M (dd, *J* = 5.2, 0.8 Hz, 1H, **H**⁷), 8.00 (d, *J* = 8.7 Hz, 2H, **H**³), 7.72 (d, *J* = 8.7 Hz, 2H, **H**⁴), 7.52m, 7.49M (dd, *J* = 1.8, 0.8 Hz, 1H, **H**⁵), 7.41 (dd, *J* = 5.2, 1.8 Hz, 1H, **H**⁶), 5.57 (s, 1H, **H**⁹), 5.30 (s, 1H, **H**²), 4.62m, 4.52M (d, *J* = 5.5 Hz, 2H, **H**⁸), 1.62m, 1.47M (s, 9H, **H**¹⁰), 1.26 (s, 9H, **H**¹).

¹³C NMR (126 MHz, DMSO-*d*₆, 20 °C, δ): 158.7, 156.2, 150.6, 149.9, 147.6, 144.1, 141.9, 127.8, 127.7, 121.9, 120.5, 119.8, 79.8, 54.9, 45.9, 30.3, 28.5.

Chapter 4. Experimental section

MS (ESI-MS, pos.) m/z : $[M+H]^+$ calcd for $C_{21}H_{30}N_3O_4S$, 420.2; found, 420.2.

EA Anal. calcd for $C_{21}H_{29}N_3O_4S \cdot \frac{1}{4}CH_2Cl_2$: C, 57.81%; H, 6.82%; N, 9.26%. Found: C, 57.87%; H, 6.72%; N, 9.22%.

4-(2-(Aminomethyl)pyridin-4-yl)benzenesulfonamide (**5**)**5**

A few drops of anisole were added to a solution of compound **66** (410 mg, 1.3 mmol, 1.0 eq) in TFA (5 mL). The solution was stirred overnight at room temperature. After removal of TFA under a gentle stream of N₂, the product was dissolved in a mixture of CH₂Cl₂/MeOH, and precipitated with diethyl ether. The solvent was removed by filtration and **5** (545 mg, 1.0 mmol, 76%) was obtained as a pale brown solid.

Annex spectra page: 204

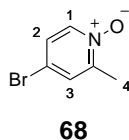
TLC : *n*-hexane/EtOAc (1/1); R_f = 0.17.

¹H NMR (400 MHz, DMSO-*d*₆, 20 °C, δ): 8.73 (d, *J* = 5.2 Hz, 1H, **H**⁶), 8.39 (b, 3H, **H**⁸), 8.02 (d, *J* = 8.6 Hz, 2H, **H**²), 7.98 (d, *J* = 8.6 Hz, 2H, **H**³), 7.92 (s, 2H, **H**⁴), 7.82 (dd, *J* = 5.3, 1.8 Hz, 1H, **H**⁵), 7.50 (s, 2H, **H**¹), 4.29 (d, *J* = 5.8 Hz, 2H, **H**⁷).

¹³C NMR (101 MHz, DMSO-*d*₆, 20 °C, δ): 154.2, 149.7, 146.5, 144.8, 139.8, 127.5, 126.5, 120.9, 120.2, 42.8.

HRMS (ESI-MS, pos.) *m/z*: [M+H]⁺ calcd for C₁₂H₁₄N₃O₂S, 264.0806; found, 264.0802.

EA Anal. calcd for C₁₂H₁₃N₃O₂S · 2 TFA: C, 39.11%; H, 3.08%; N, 8.55%. Found: C, 39.30%; H, 3.24%; N, 8.62%.

4.2.6 *N*-((4-(4-Sulfamoylphenyl)pyridin-2-yl)methyl)benzenesulfonamide (6)4-Bromo-2-methylpyridine-*N*-oxide (68)

4-Bromo-2-methylpyridine (3.00 mg, 17.4 mmol, 1.0 eq) and 3-chloroperoxybenzoic acid (4.80 mg, 27.8 mmol, 1.6 eq) in CH₂Cl₂ (20 mL) were stirred overnight at room temperature. A 2 M aqueous solution of Na₂CO₃ (20 mL) was added, and the reaction mixture was stirred for 1 h. The aqueous layer was extracted with CH₂Cl₂ (3 x 30 mL), and the combined organic layers were washed with brine and dried over Na₂SO₄. The solvent was removed under reduced pressure to obtain **68** (2.40 g, 12.8 mmol, 73%) as a yellow oil.

Annex spectra page: 205

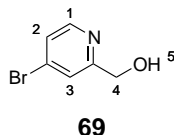
TLC : CH₂Cl₂/MeOH (9/1); R_f = 0.72.

¹H NMR (400 MHz, DMSO-*d*₆, 20 °C, δ): 8.16 (d, *J* = 6.9 Hz, 1H, **H**¹), 7.79 (d, *J* = 2.9 Hz, 1H, **H**³), 7.51 (dd, *J* = 6.9, 3.0 Hz, 1H, **H**²), 2.32 (s, 3H, **H**⁴).

¹³C NMR (101 MHz, DMSO-*d*₆, 20 °C, δ): 149.6, 139.8, 129.2, 126.9, 116.3, 16.9.

HRMS (ESI-MS, pos.) *m/z*: [M+H]⁺ calcd for C₆H₇BrNO, 187.9711; found, 187.9704.

EA Anal. calcd for C₆H₆BrNO · $\frac{1}{4}$ H₂O: C, 37.43%; H, 3.40%; N, 7.28%. Found: C, 37.51%; H, 3.57%; N, 6.96%.

4-Bromo-2-hydroxymethylpyridine (**69**)

Compound **68** (2.40 g, 12.8 mmol, 1.0 eq) was dissolved in dry CH_2Cl_2 (10 mL) and the solution was cooled to 0 °C. Trifluoroacetic acid anhydride (15 mL) was added. When the vigorous thermal reaction had ceased, the orange mixture was stirred at room temperature for 30 min and then refluxed for 3 h. An aqueous saturated solution of NaHCO_3 was carefully added. The aqueous layer was extracted with CH_2Cl_2 (3 x 30 mL), and the combined organic layers were washed with brine, and dried over Na_2SO_4 . The solvent was removed under reduced pressure to obtain **69** (1.90 g, 10.1 mmol, 79%) as a brown oil.

Annex spectra page: 207

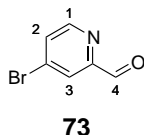
TLC : *n*-hexane/EtOAc (1/1); $R_f = 0.25$.

^1H NMR (400 MHz, CDCl_3 , 20 °C, δ): 8.37 (d, $J = 5.3$ Hz, 1H, **H¹**), 7.49 (d, $J = 1.1$ Hz, 1H, **H³**), 7.38 (dd, $J = 5.4, 1.7$ Hz, 1H, **H²**), 4.75 (s, 2H, **H⁴**).

^{13}C NMR (101 MHz, CDCl_3 , 20 °C, δ): 161.1, 149.5, 133.7, 125.9, 124.1, 64.1.

HRMS (ESI-MS, pos.) m/z : $[\text{M}+\text{H}]^+$ calcd for $\text{C}_6\text{H}_7\text{BrNO}$, 187.9711; found, 187.9704.

EA Anal. calcd for $\text{C}_6\text{H}_6\text{BrNO} \cdot \frac{1}{4}\text{H}_2\text{O}$: C, 37.43%; H, 3.40%; N, 7.28%. Found: C, 37.28%; H, 3.18%; N, 7.13%.

4-Bromo-2-pyridine aldehyde (**73**)

To compound **69** (1.90 g, 10.1 mmol, 1.0 eq) in chloroform (15 mL), MnO_2 (8.78 g, 101.0 mmol, 10.0 eq) was added. The reaction mixture was refluxed for 2 h. Then the solid material was removed by filtration over celite, and the solvent was removed under reduced pressure to obtain **73** (1.07 g, 5.75 mmol, 57%) as a brown oil.

Annex spectra page: 209

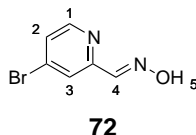
TLC : *n*-hexane/EtOAc (1/1); $R_f = 0.58$.

^1H NMR (400 MHz, CDCl_3 , 20 °C, δ): 10.04 (s, 1H, H^4), 8.61 (d, $J = 5.3$ Hz, 1H, H^1), 8.12 (s, 1H, H^3), 7.70 (d, $J = 3.7$ Hz, 1H, H^2).

^{13}C NMR (101 MHz, CDCl_3 , 20 °C, δ): 192.1, 153.7, 151.0, 134.3, 131.8, 125.3.

MS (FAB-MS, pos.) m/z (relative intensity): $[\text{M}]^+$ calcd for $\text{C}_6\text{H}_4\text{BrNO}$, 184.9; found, 157.0 (100) $[\text{M}-\text{COH}]^+$, 185.0 (12) $[\text{M}]^+$.

EA Anal. calcd for $\text{C}_6\text{H}_4\text{BrNO} \cdot \frac{1}{2}\text{CHCl}_3$: C, 36.96%; H, 2.62%; N, 6.63%. Found: C, 37.27%; H, 2.39%; N, 6.63%.

4-Bromo-2-pyridine ketoxime (**72**)

To compound **73** (1.07 g, 5.8 mmol, 1.0 eq) in MeOH (15 mL), NaHCO₃ (0.77 g, 9.2 mmol, 1.6 eq) and NH₂OH·HCl (1.40 g, 20.1 mmol, 3.5 eq) were added. The reaction mixture was stirred overnight at room temperature before diluting with EtOAc (30 mL), and washing with NaHCO₃ solution and brine. The organic layer was dried over Na₂SO₄, and the solvent was removed under reduced pressure to obtain **72** (0.98 g, 4.9 mmol, 85%) as a yellow solid.

Annex spectra page: 211

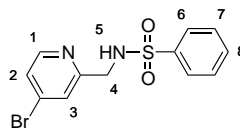
TLC : *n*-hexane/EtOAc (1/1); R_f = 0.50.

¹H NMR (400 MHz, DMSO-*d*₆, 20 °C, δ): 11.90 (s, 1H, **H**⁴), 8.47 (dd, *J* = 5.4, 0.6 Hz, 1H, **H**¹), 8.07 (s, 1H, **H**⁵), 7.93 (dd, *J* = 2.0, 0.6 Hz, 1H, **H**³), 7.66 (dd, *J* = 5.3, 1.9 Hz, 1H, **H**²).

¹³C NMR (101 MHz, DMSO-*d*₆, 20 °C, δ): 153.6, 150.8, 147.7, 132.4, 126.8, 122.5.

MS (FAB-MS, pos.) *m/z*: [M]⁺ calcd for C₆H₅BrN₂O, 199.9; found, 200.0.

EA Anal. calcd for C₆H₅BrN₂O · $\frac{1}{10}$ EtOAc: C, 36.63%; H, 2.79%; N, 13.35%. Found: C, 36.50%; H, 2.77%; N, 13.06%.

N-[(4-Bromopyridin-2-yl)methyl]benzenesulfonamide (70)**70**

Zinc dust (1.37 g, 21.0 mmol, 6.0 eq) was added in several portions to a solution of compound **72** (700 mg, 3.5 mmol, 1.0 eq) in TFA (15 mL) at 0 °C. The reaction mixture was stirred for 15 min, and added to a mixture of a 2 M aqueous solution of NaOH (20 mL) and CH₂Cl₂ (20 mL). The insoluble material was removed by filtration, and the organic layer was separated. The organic layer was washed with water, brine and dried over Na₂SO₄. The solvent was removed under reduced pressure. The reduced product was dissolved in CH₂Cl₂ (15 mL) and DIPEA (0.70 mL, 4.2 mmol, 1.2 eq) was added. The reaction mixture was stirred at 25 °C for 10 min. It was then cooled to 0 °C, and benzenesulfonyl chloride (0.29 mL, 2.2 mmol, 0.7 eq) was added dropwise. The resulting solution was allowed to warm up to 25 °C, and was stirred overnight. The reaction mixture was diluted with CH₂Cl₂ (20 mL), washed with water and brine before drying over Na₂SO₄. The product was purified by flash chromatography (*n*-hexane/EtOAc, 1/1) to afford **70** (280 mg, 0.9 mmol, 25%) as a pale yellow solid.

Annex spectra page: 213

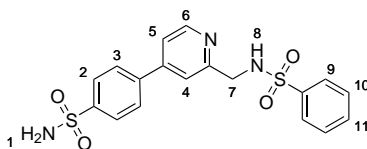
TLC : *n*-hexane/EtOAc (1/1); R_f = 0.32.

¹H NMR (400 MHz, CDCl₃, 20 °C, δ): 8.25 (d, *J* = 5.2 Hz, 1H, **H**¹), 7.84 (dt, *J* = 7.2, 1.4 Hz, 2H, **H**⁶), 7.53 (t, *J* = 7.4 Hz, 1H, **H**⁸), 7.46 (t, *J* = 7.5 Hz, 2H, **H**⁷), 7.34 (d, *J* = 1.4 Hz, 1H, **H**³), 7.31 (dd, *J* = 5.3, 1.7 Hz, 2H, **H**²), 4.25 (s, 2H, **H**⁴).

¹³C NMR (101 MHz, CDCl₃, 20 °C, δ): 156.7, 149.9, 139.7, 132.9, 129.2, 127.3, 126.2, 125.4, 100.1, 47.3.

MS (ESI-MS, pos.) *m/z* (relative intensity): [M+H]⁺ calcd for C₁₂H₁₂BrN₂O₂S, 326.9; found, 327.0 (100) [M+H]⁺, 349.0 (37) [M+Na]⁺.

EA Anal. calcd for C₁₂H₁₁BrN₂O₂S: C, 44.05%; H, 3.39%; N, 8.56%. Found: C, 44.15%; H, 3.47%; N, 8.61%.

***N*-((4-(4-Sulfamoylphenyl)pyridin-2-yl)methyl)benzenesulfonamide (6)****6**

A mixture of 4-sulfamoylphenylboronic acid pinacol ester (207 mg, 0.7 mmol, 1.2 eq), **70** (200 mg, 0.6 mmol, 1.0 eq), tetrakis(triphenylphosphine)palladium (40 mg, 0.03 mmol, 0.05 eq), Na₂CO₃ (191 mg, 1.8 mmol, 2.9 eq), water (1.5 mL) and 1,4-dioxane (1.5 mL) were heated in a sealed vial in a microwave reactor at 150 °C for 15 min. The reaction mixture was diluted with CH₂Cl₂ (30 mL), and washed with water and brine. The organic layer was dried over Na₂SO₄ and the solvent was removed under reduced pressure. The product was purified by flash chromatography (CH₂Cl₂/MeOH, 3%) to obtain **6** (160 mg, 0.4 mmol, 64%) as a colorless solid.

Annex spectra page: 215

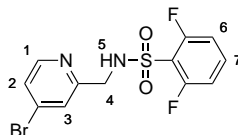
TLC : CH₂Cl₂/MeOH (9/1); R_f = 0.51.

¹H NMR (500 MHz, DMSO-*d*₆, 20 °C, δ): 8.52 (d, *J* = 6.1 Hz, 1H, **H**⁶), 8.35 (t, *J* = 6.3 Hz, 1H, **H**⁸), 7.96 (d, *J* = 8.5 Hz, 2H, **H**²), 7.86 (d, *J* = 8.4 Hz, 2H, **H**³), 7.79 (d, *J* = 6.9 Hz, 2H, **H**⁹), 7.55 (m, 1H, **H**^{1,4,5,10,11}), 4.22 (d, *J* = 6.1 Hz, 2H, **H**⁷).

¹³C NMR (126 MHz, DMSO-*d*₆, 20 °C, δ): 157.8, 149.6, 146.1, 144.6, 140.7, 140.3, 132.3, 129.1, 127.4, 126.5, 126.4, 120.1, 119.3, 48.1.

MS (ESI-MS, pos.) *m/z*: [M]⁺ calcd for C₁₈H₁₈N₃O₄S₂, 404.1; found, 404.1.

EA Anal. calcd for C₁₈H₁₇N₃O₄S₂ · $\frac{1}{3}$ H₂O: C, 52.80%; H, 4.35%; N, 10.26%. Found: C, 52.61%; H, 4.23%; N, 10.42%.

***N*-[(4-Bromopyridin-2-yl)methyl]-2,6-difluorobenzene-1-sulfonamide (**71**)****71**

Zinc dust (1.93 g, 29.5 mmol, 6.0 eq) was added in several portions to a solution of compound **72** (987 mg, 4.9 mmol, 1.0 eq) in TFA (15 mL) at 0 °C. The reaction mixture was stirred for 15 min, and added to a mixture of a 2 M aqueous solution of NaOH (20 mL) and CH₂Cl₂ (20 mL). The insoluble material was removed by filtration, and the organic layer was separated. The organic layer was washed with water, brine and dried over Na₂SO₄. The solvent was removed under reduced pressure. The reduced product was dissolved in CH₂Cl₂ (15 mL) and DIPEA (0.59 mL, 4.3 mmol, 0.9 eq) was added. The reaction mixture was stirred at 25 °C for 10 min. It was then cooled to 0 °C, and 2,6-difluorobenzenesulfonyl chloride (917 mg, 7.3 mmol, 1.1 eq) was added dropwise. The resulting solution was allowed to reach 25 °C, and was stirred overnight. The reaction mixture was diluted with CH₂Cl₂ (20 mL), washed with water and brine before drying over Na₂SO₄. The product was purified by flash chromatography (*n*-hexane/EtOAc, 1/1) to afford **71** (698 mg, 1.9 mmol, 39%) as a pale yellow solid.

Annex spectra page: 217

TLC : *n*-hexane/EtOAc (1/1); R_f = 0.27.

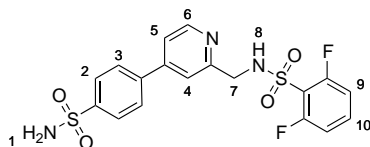
¹H NMR (400 MHz, CDCl₃, 20 °C, δ): 8.32 (d, *J* = 5.5 Hz, 1H, **H**¹), 7.61 (d, *J* = 1.9 Hz, 1H, **H**³), 7.47 (m, 2H, **H**^{2,7}), 6.98 (t, *J* = 8.5 Hz, 1H, **H**⁶), 6.49 (t, *J* = 5.9 Hz, 1H, **H**⁵), 4.52 (d, *J* = 5.8 Hz, 2H, **H**⁴).

¹³C NMR (101 MHz, CDCl₃, 20 °C, δ): 156.1, 149.7, 134.5, 134.4, 134.1, 126.5, 125.7, 113.2, 113.0, 47.5.

¹⁹F NMR (376 MHz, CDCl₃, 20 °C, δ): -107.2.

MS (ESI-MS, pos.) m/z (relative intensity): $[M+H]^+$ calcd for $C_{12}H_{10}BrF_2N_2O_2S$, 363.0; found, 363.0 (100) $[M+H]^+$, 385.0 (100) $[M+Na]^+$.

EA Anal. calcd for $C_{12}H_9BrF_2N_2O_2S$: C, 39.69%; H, 2.50%; N, 7.71%. Found: C, 39.44%; H, 2.65%; N, 7.63%.

2,6-Difluoro-*N*-((4-(4-sulfamoylphenyl)pyridin-2-yl)methyl)benzenesulfonamide (41)**41**

A mixture of 4-sulfamoylphenylboronic acid pinacol ester (147 mg, 0.5 mmol, 1.2 eq), **71** (160 mg, 0.4 mmol, 1.0 eq), tetrakis(triphenylphosphine)palladium (20 mg, 0.02 mmol, 0.05 eq), Na₂CO₃ (136 mg, 1.3 mmol, 2.9 eq), water (1.2 mL) and 1,4-dioxane (1.2 mL) were heated in a sealed vial in a microwave reactor at 150 °C for 15 min. The reaction mixture was diluted with CH₂Cl₂ (30 mL), and washed with water and brine. The organic layer was dried over Na₂SO₄, and the solvent was removed under reduced pressure. The product was purified by flash chromatography (CH₂Cl₂/MeOH, 3%) to obtain **41** (82 mg, 0.2 mmol, 42%) as a colorless solid.

Annex spectra page: 219

TLC : CH₂Cl₂/MeOH (9/1); R_f = 0.45.

¹H NMR (400 MHz, CD₃OD, 20 °C, δ): 8.47 (d, *J* = 5.3 Hz, 1H, **H**⁶), 8.03 (d, *J* = 8.5 Hz, 2H, **H**²), 7.80 (d, *J* = 8.5 Hz, 2H, **H**³), 7.74 (d, *J* = 1.3 Hz, 1H, **H**⁴), 7.52 (dd, *J* = 5.3, 1.9 Hz, 1H, **H**⁵), 7.47 (t, *J* = 8.5 Hz, 1H, **H**¹⁰), 6.98 (d, *J* = 8.6 Hz, 2H, **H**⁹), 4.47 (s, 2H, **H**⁷), 1.19 (s, 2H, **H**¹),

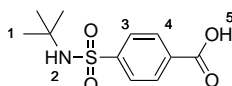
¹⁹F NMR (376 MHz, CD₃OD, 20 °C, δ): -108.9.

MS (ESI-MS, pos.) *m/z*: [M+H]⁺ calcd for C₁₈H₁₆F₂N₃O₄S₂, 440.0; found, 440.1.

EA Anal. calcd for C₁₈H₁₅F₂N₃O₄S₂ · 2H₂O: C, 45.47%; H, 4.03%; N, 8.84%. Found: C, 45.67%; H, 3.86%; N, 8.45%.

4.2.7 1,3-Dimesityl-5-((4-sulfamoylbenzamido)methyl)-4,5-dihydro-1*H*-imidazol-3-ium (7)

4-(*N*-(*tert*-Butyl)sulfamoyl)benzoic acid (79)



79

A solution of *tert*-butylamine in MeOH (50 mL, 3/1) was cooled to 0 °C and 4-(chlorosulfonyl)benzoic acid (2.58 g, 11.7 mmol, 1.0 eq) was slowly added. The reaction mixture was stirred overnight. A 2 M aqueous solution of NaOH (50 mL) was added, and the aqueous layer was washed with CH₂Cl₂ (4 x 100 mL) in order to remove the excess *tert*-butylamine. The aqueous layer was acidified with a 2 M aqueous solution of HCl until pH 1. The product was extracted with CH₂Cl₂ (3 x 100 mL). The combined organic layers were washed with brine, and dried over Na₂SO₄ to obtain **79** (1.58 g, 6.2 mmol, 53%) as a white powder.

Annex spectra page: 221

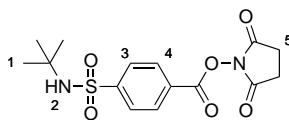
TLC : CH₂Cl₂/MeOH (10%); R_f = 0.25.

¹H NMR (400 MHz, DMSO-*d*₆, 20 °C, δ): 13.38 (s, 1H, **H**⁵), 8.09 (d, *J* = 8.4 Hz, 2H, **H**⁴), 7.93 (d, *J* = 8.6 Hz, 2H, **H**³), 7.72 (s, 1H, **H**²), 1.09 (s, 9H, **H**¹).

¹³C NMR (101 MHz, DMSO-*d*₆, 20 °C, δ): 166.3, 147.9, 133.6, 129.9, 126.5, 53.5, 29.7.

HRMS (ESI-MS, pos.) *m/z*: [M+Na]⁺ calcd for C₁₁H₁₅NO₄SNa, 280.0619; found, 280.0618.

EA Anal. calcd for C₁₁H₁₅NO₄S: C, 51.35%; H, 5.88%; N, 5.44%. Found: C, 51.36%; H, 5.65%; N, 5.45%.

2,5-Dioxopyrrolidin-1-yl-4-(*N*-(*tert*-butyl)sulfamoyl)benzoate (78)**78**

Compound **79** (5.02 g, 25.0 mmol, 1.0 eq) was dissolved in DMF (50 mL) and *N*-hydroxysuccinimide (3.26 g, 28.4 mmol, 1.1 eq) was added. The reaction mixture was cooled to 0 °C, and DCC (5.0 g, 25.0 mmol, 1.0 eq) was added. The solution was stirred overnight at room temperature. The solvent was then removed under reduced pressure, and the white solid was washed with isopropanol (2 x 50 mL). The solid was dried to afford **78** (6.63 g, 22.2 mmol, 89%) as a white powder.

Annex spectra page: 223

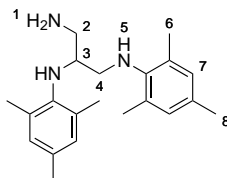
TLC : CH₂Cl₂/MeOH (10%); R_f = 0.25.

¹H NMR (400 MHz, DMSO-*d*₆, 20 °C, δ): 8.28 (d, *J* = 8.6 Hz, 2H, **H**⁴), 8.08 (d, *J* = 8.6 Hz, 2H, **H**³), 7.89 (s, 1H, **H**²), 2.91 (s, 4H, **H**⁵), 1.12 (s, 9H, **H**¹).

¹³C NMR (101 MHz, DMSO-*d*₆, 20 °C, δ): 170.1, 160.9, 150.2, 130.9, 127.3, 127.1, 53.7, 29.7, 25.5.

HRMS (ESI-MS, pos.) *m/z*: [M+Na]⁺ calcd for C₁₅H₁₈N₂O₆SNa, 377.0783; found, 377.0783.

EA Anal. calcd for C₁₅H₁₈N₂O₆S: C, 50.84%; H, 5.12%; N, 7.91%. Found: C, 50.85%; H, 4.98%; N, 7.87%.

***N,N'*-Dimesitylpropane-1,2,3-triamine (77)** [6]**77**

A round-bottom flask equipped with a magnetic stir-bar was charged with 2,3-dibromopropane-1-ammonium bromide (4.20 g, 14.1 mmol, 1.0 eq) and 2,4,6-trimethylaniline (20 mL, 141.0 mmol, 10 eq). After purging with nitrogen, the reaction mixture was stirred overnight at 120 °C. It was then allowed to cool to room temperature, and was dissolved with a 2 M aqueous solution of NaOH (50 mL) and Et₂O (50 mL). The organic and aqueous layers were separated, and the organic layer was washed with water, and brine before drying over Na₂SO₄. The solvent was removed under reduced pressure, and the excess 2,4,6-trimethylaniline was removed by distillation at 100 °C and 0.1 mmHg. The product was purified by flash chromatography (CH₂Cl₂/MeOH 9/1, with 0.1% Et₃N) to obtain **77** (2.00 g, 6.3 mmol, 44%) as a brown oil.

Annex spectra page: 225

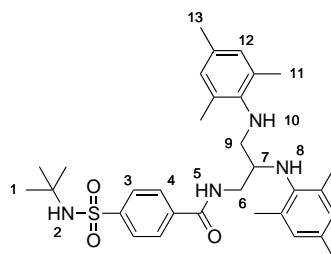
TLC : CH₂Cl₂/MeOH (10%), with 0.1% Et₃N; R_f = 0.37.

¹H NMR (400 MHz, DMSO-*d*₆, 20 °C, δ): 6.72 (s, 2H, **H**⁷), 6.70 (s, 2H, **H**^{7'}), 3.73 (d, *J* = 10.9 Hz, 1H, **H**³), 3.06 (dd, *J* = 11.9, 6.8 Hz, 1H, **H**⁴), 2.77 (d, *J* = 5.2 Hz, 1H, **H**^{4'}), 2.74 (d, *J* = 4.7 Hz, 1H, **H**²), 2.65 (dd, *J* = 12.5, 5.4 Hz, 1H, **H**^{2'}), 2.17-2.12 (m, 18H, **H**^{6,8}).

¹³C NMR (101 MHz, DMSO-*d*₆, 20 °C, δ): 143.9, 142.4, 129.4, 129.2, 129.1, 129.0, 128.9, 128.8, 58.3, 50.0, 48.6, 43.5, 20.2, 20.1, 18.8, 18.2.

HRMS (ESI-MS, pos.) *m/z*: [M+H]⁺ calcd for C₂₁H₃₂N₃, 326.2596; found, 326.2598.

EA Anal. calcd for C₂₁H₃₁N₃ · $\frac{3}{4}$ H₂O: C, 74.40%; H, 9.66%; N, 12.39%. Found: C, 74.33%; H, 9.49%; N, 12.35%.

***N*-(2,3-Bis(mesitylamino)propyl)-4-(*N*-(*tert*-butyl)sulfamoyl)benzamide (83)****83**

Compound **78** (300 mg, 0.8 mmol, 1.0 eq) was dissolved in DMF (5 mL) and compound **77** (304 g, 0.9 mmol, 1.1 eq) was added. The reaction mixture was stirred over the weekend at room temperature, and then the DMF was removed under reduced pressure. The product was purified by flash chromatography (EtOAc/Hexane 1/1) to obtain **83** (415 mg, 0.7 mmol, 87%) as a white powder.

Annex spectra page: 229

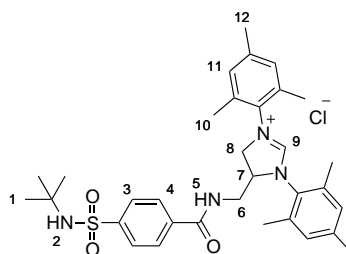
TLC : CH₂Cl₂/MeOH (10%); R_f = 0.49.

¹H NMR (500 MHz, DMSO-*d*₆, 20 °C, δ): 8.67 (t, *J* = 5.7 Hz, 1H, **H**⁵), 7.89 (s, 4H, **H**^{3,4}), 7.66 (s, 1H, **H**²), 6.74 (s, 2H, **H**¹²), 6.69 (s, 2H, **H**^{12'}), 3.91 (m, 1H, **H**¹⁰), 3.79 (d, *J* = 10.8 Hz, 1H, **H**⁷), 3.47 (m, 2H, **H**^{6,8}), 3.36 (m, 1H, **H**^{6'}), 3.05 (m, 1H, **H**⁹), 2.82 (m, 1H, **H**^{9'}), 2.18 (m, 18H, **H**^{11,13}), 1.09 (s, 9H, **H**¹).

¹³C NMR (126 MHz, DMSO-*d*₆, 20 °C, δ): 165.7, 146.4, 143.7, 141.8, 137.4, 129.5, 129.4, 129.3, 129.1, 129.0, 128.8, 127.8, 126.2, 56.6, 53.4, 50.1, 41.9, 29.7, 20.2, 18.8, 18.1.

HRMS (ESI-MS, pos.) *m/z*: [M+H]⁺ calcd for C₃₂H₄₅N₄O₃S, 565.3212; found, 565.3202.

EA Anal. calcd for C₃₂H₄₄N₄O₃S: C, 68.05%; H, 7.85%; N, 9.92%. Found: C, 68.21%; H, 7.81%; N, 9.84%.

5-((4-(*N*-(*tert*-Butyl)sulfamoyl)benzamido)methyl)-1,3-dimesityl-4,5-dihydro-1H-imidazol-3-ium chloride (**74**)**74**

Compound **83** (197 mg, 0.3 mmol, 1.0 eq) was dissolved in triethylorthoformate (5 mL) and NH_4Cl (21 g, 0.4 mmol, 1.1 eq) was added. The mixture was purged with N_2 prior to heating to 120 °C for 48 h. The reaction mixture was allowed to cool to room temperature, and the product precipitated from Et_2O . The white-brown solid was washed three times with Et_2O , and dried under reduced pressure to obtain **74** (121 mg, 0.2 mmol, 57%) as white powder.

Annex spectra page: 229

$^1\text{H NMR}$ (500 MHz, $\text{DMSO-}d_6$, 20 °C, δ): 9.41 (t, $J = 5.4$ Hz, 1H, **H**), 9.14 (s, 1H, **H**), 7.91 (d, $J = 8.6$ Hz, 1H, **H**), 7.86 (s, 4H, **H**), 7.71 (d, $J = 8.0$ Hz, 1H, **H**), 7.09 (d, $J = 10.8$ Hz, 1H, **H**), 7.06 (s, 1H, **H**), 5.19 (dt, $J = 18.8, 7.5$ Hz, 1H, **H**), 4.70 (t, $J = 11.8$ Hz, 1H, **H**), 4.48 (dd, $J = 12.7, 7.6$ Hz, 1H, **H**), 3.67 (dd, $J = 12.3, 5.7$ Hz, 2H, **H**), 3.49 (q, $J = 7.1$ Hz, 6H, **H**), 2.43 (s, 3H, **H**), 2.39 (s, 3H, **H**), 2.35 (s, 3H, **H**), 2.32 (s, 3H, **H**), 2.29 (s, 3H, **H**), 2.24 (s, 3H, **H**), 1.07 (s, 9H, **H**).

$^{13}\text{C NMR}$ (126 MHz, $\text{DMSO-}d_6$, 20 °C, δ): 165.6, 160.4, 146.8, 139.8, 139.4, 136.4, 135.4, 135.3, 130.7, 129.9, 129.8, 129.7, 129.5, 128.0, 126.1, 125.4, 61.5, 58.9, 54.6, 53.4, 53.1, 41.1, 29.7, 20.6, 20.5, 18.2, 17.8, 17.4, 17.1, 15.0.

HRMS (ESI-MS, pos.) m/z : $[\text{M}+\text{H}]^+$ calcd for $\text{C}_{33}\text{H}_{44}\text{N}_4\text{O}_3\text{S}$, 575.3055; found, 575.3050.

EA Anal. calcd for $\text{C}_{33}\text{H}_{43}\text{ClN}_4\text{O}_3\text{S} \cdot 3\text{NH}_4\text{Cl} \cdot \text{H}_2\text{O}$: C, 50.19%; H, 7.27%; N, 12.42%. Found: C, 50.59%; H, 7.09%; N, 12.13%.

4.3 Complex synthesis

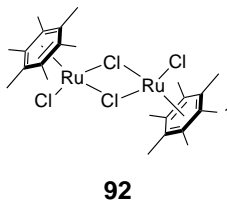
4.3.1 General procedure for complex synthesis

Procedure 1

Bipyridine derivative complexes were synthesized according a modification of the procedure published by Mann.^[7] The ligand (0.28 mmol, 2.0 eq) and the metal dimer (0.14 mmol, 1.0 eq) were dissolved in ACN (5 mL). The resulting solution was purged with nitrogen for 20 min, and then refluxed for 4 h. The volume of the reaction was reduced to 2 mL, and the resulting solid was filtered and washed with a small amount of cold ACN. The solid was dried under vacuum to afford the desired complex.

Procedure 2

The picolyamine-derivative complexes were synthesized according a modification of the procedure published by Çetinkaya.^[8] The ligand (0.28 mmol, 2.0 eq) and the metal dimer (0.14 mmol, 1.0 eq) were dissolved in EtOH (5 mL), and the resulting solution was purged with nitrogen for 20 min. The reaction mixture was refluxed for 2 h and the solvent was removed under reduced pressure. The solid was washed with a small amount of CH₂Cl₂, and dried to afford the desired complex.

$[(\eta^6\text{-C}_6\text{Me}_6)\text{RuCl}_2]_2$ (**92**)

According to the published protocol,^[9] a mixture of di- μ -chlorobis(*p*-cymene)chlororuthenium(II) (0.80 g, 1.3 mmol, 1.0 eq) and hexamethylbenzene (8.75 g, 53.9 mmol, 41.2 eq) were heated to 185 °C for 6 h. The crystals of hexamethylbenzene, which formed on the upper walls of the flask due to sublimation, were periodically melted down with a heat gun. The reaction mixture was cooled to room temperature, and the solid was broken up and transferred to a glass filter containing celite. *p*-Cymene and the excess of hexamethylbenzene were removed by washing with Et₂O. The product was recovered from the celite with CH₂Cl₂ (100 mL). The product was dried under reduced pressure to afford **92** (0.35 g, 0.5 mmol, 40%) as an orange-red solid.

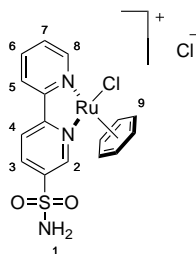
Annex spectra page: 231

¹H NMR (400 MHz, CDCl₃, 20 °C, δ): 2.02 (s, 36H, **H**¹).

¹³C NMR (101 MHz, CDCl₃, 20 °C, δ): 89.1. 16.1.

MS (Maldi-TOF, pos.) *m/z*: [M-Cl]⁺ calcd for C₂₄H₃₆Cl₃Ru₂, 632.9; found, 633.4.

EA Anal. calcd for C₂₄H₃₆Cl₄Ru₂: C, 43.12%; H, 5.43%; N, 0%. Found: C, 43.11%; H, 5.46%; N, 0.39%.

$[(\eta^6\text{-C}_6\text{H}_6)\text{Ru}(1)\text{Cl}]\text{Cl}$ (**8**)**8**

Following procedure 1 (section 4.3.1), compound **8** was obtained as a yellow solid (372 mg, 0.7 mmol, 89%).

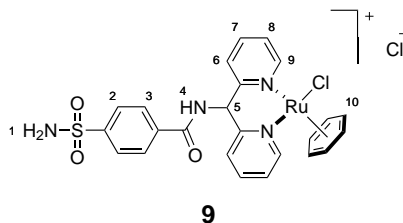
Annex spectra page: 233

$^1\text{H NMR}$ (400 MHz, DMSO- d_6 , 20 °C, δ): 9.95 (d, $J = 1.9$ Hz, 1H, H^2), 9.70 (d, $J = 5.6$, 1.4 Hz, 1H, H^8), 8.85 (d, $J = 8.5$ Hz, 1H, H^4), 8.74 (d, $J = 8.0$ Hz, 1H, H^5), 8.60 (dd, $J = 8.4$, 2.0 Hz, 1H, H^3), 8.34 (m, 3H, $\text{H}^{1,6}$), 7.85 (t, $J = 6.4$ Hz, 1H, H^7), 6.33 (s, 6H, H^9).

$^{13}\text{C NMR}$ (101 MHz, DMSO- d_6 , 20 °C, δ): 156.6, 156.3, 153.3, 152.6, 142.8, 140.2, 136.8, 128.2, 125.0, 124.1, 87.2.

MS (ESI-MS, pos.) m/z : $[\text{M}-\text{Cl}]^+$ calcd for $\text{C}_{16}\text{H}_{16}\text{ClN}_3\text{O}_2\text{RuS}$, 450.9; found, 450.0.

EA Anal. calcd for $\text{C}_{16}\text{H}_{16}\text{Cl}_2\text{N}_3\text{O}_2\text{RuS} \cdot \frac{1}{5}\text{H}_2\text{O} \cdot \frac{3}{20}\text{ACN}$: C, 39.17%; H, 3.42%; N, 9.14%. Found: C, 39.29%; H, 3.24%; N, 9.03%.

$[(\eta^6\text{-C}_6\text{H}_6)\text{Ru}(\text{4})\text{Cl}]\text{Cl}$ (**9**)


Following procedure 1 (section 4.3.1), compound **9** was obtained as a yellow solid (112 mg, 0.2 mmol, 67%).

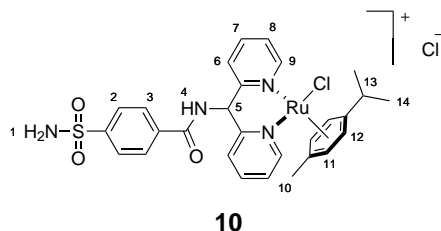
Annex spectra page: 235

$^1\text{H NMR}$ (400 MHz, $\text{DMSO-}d_6$, 20 °C, δ): 10.77 (d, $J = 9.9$ Hz, 1H, \mathbf{H}^4), 9.13 (dd, $J = 5.7$, 1.5 Hz, 2H, \mathbf{H}^9), 8.40 (d, $J = 8.5$ Hz, 2H, \mathbf{H}^2), 8.12 (td, $J = 7.6$, 1.3 Hz, 2H, \mathbf{H}^6), 8.02 (m, 4H, $\mathbf{H}^{3,7}$), 7.63 (s, 2H, \mathbf{H}^1), 7.58 (ddd, $J = 7.4$, 5.7, 1.5 Hz, 2H, \mathbf{H}^8), 6.98 (d, $J = 9.9$ Hz, 1H, \mathbf{H}^5), 6.20 (s, 6H, \mathbf{H}^{10}).

$^{13}\text{C NMR}$ (101 MHz, $\text{DMSO-}d_6$, 20 °C, δ): 166.4, 157.6, 157.5, 147.3, 140.3, 135.9, 128.9, 125.8, 124.5, 122.1, 86.9, 59.2.

HRMS (ESI-MS, pos.) m/z : $[\text{M-Cl}]^+$ calcd for $\text{C}_{24}\text{H}_{22}\text{ClN}_4\text{O}_3\text{RuS}$, 583.0144; found, 583.0139.

EA Anal. calcd for $\text{C}_{24}\text{H}_{22}\text{Cl}_2\text{N}_4\text{O}_3\text{RuS} \cdot \frac{5}{4}\text{H}_2\text{O}$: C, 44.97%; H, 3.85%; N, 8.74%. Found: C, 44.73%; H, 3.76%; N, 9.28%.

$[(\eta^6\text{-}p\text{-Cymene})\text{Ru}(\text{4})\text{Cl}]\text{Cl}$ (10**)**

Following procedure 1 (section 4.3.1), compound **10** was obtained as a yellow solid (122 mg, 0.2 mmol, 64%).

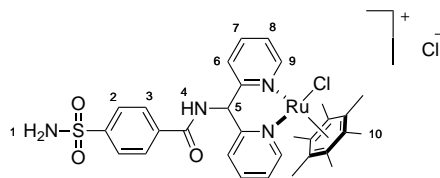
Annex spectra page: 237

$^1\text{H NMR}$ (500 MHz, $\text{DMSO-}d_6$, 20 °C, δ): 10.89 (d, $J = 9.9$ Hz, 1H, \mathbf{H}^4), 9.02 (d, $J = 5.8$ Hz, 2H, \mathbf{H}^9), 8.43 (d, $J = 8.2$ Hz, 2H, \mathbf{H}^2), 8.12 (t, $J = 7.8$ Hz, 2H, \mathbf{H}^7), 8.04 (d, $J = 8.2$ Hz, 4H, $\mathbf{H}^{6,3}$), 7.60 (m, 4H, $\mathbf{H}^{1,8}$), 6.89 (d, $J = 9.5$ Hz, 1H, \mathbf{H}^5), 6.10 (d, $J = 6.1$ Hz, 2H, \mathbf{H}^{12}), 5.95 (d, $J = 6.1$ Hz, 2H, \mathbf{H}^{11}), 2.99 (q, $J = 6.9$ Hz, 1H, \mathbf{H}^{13}), 2.08 (d, $J = 5.1$ Hz, 3H, \mathbf{H}^{10}), 1.18 (d, $J = 6.8$ Hz, 6H, \mathbf{H}^{14}).

$^{13}\text{C NMR}$ (126 MHz, $\text{DMSO-}d_6$, 20 °C, δ): 166.5, 157.2, 147.3, 140.3, 135.8, 129.1, 125.8, 124.7, 122.3, 106.1, 100.0, 85.0, 84.9, 58.9, 30.4, 22.1, 17.5.

HRMS (ESI-MS, pos.) m/z : $[\text{M-Cl}]^+$ calcd for $\text{C}_{28}\text{H}_{30}\text{ClN}_4\text{O}_3\text{RuS}$, 639.0770; found, 639.0767.

EA Anal. calcd for $\text{C}_{28}\text{H}_{30}\text{Cl}_2\text{N}_4\text{O}_3\text{RuS} \cdot \frac{3}{2}\text{H}_2\text{O}$: C, 46.73%; H, 4.90%; N, 7.79%. Found: C, 46.81%; H, 4.71%; N, 8.18%.

$[(\eta^6\text{-C}_6\text{Me}_6)\text{Ru}(\text{4})\text{Cl}]\text{Cl}$ (**11**)
**11**

Following procedure 1 (section 4.3.1), compound **11** was obtained as a yellow solid (125 mg, 0.2 mmol, 66%).

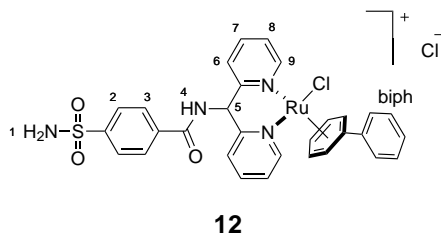
Annex spectra page: 239

^1H NMR (500 MHz, DMSO- d_6 , 20 °C, δ): 10.68 (d, $J = 10.0$ Hz, 1H, H^4), 8.79 (d, $J = 5.0$ Hz, 2H, H^9), 8.40 (d, $J = 8.4$ Hz, 2H, H^2), 8.12 (t, $J = 7.8$ Hz, 2H, H^7), 8.04 (d, $J = 8.4$ Hz, 2H, H^3), 7.98 (d, $J = 8.1$ Hz, 2H, H^6), 7.63 (s, 2H, H^1), 7.59 (t, $J = 6.6$ Hz, 2H, H^8), 6.34 (d, $J = 9.6$ Hz, 1H, H^5), 2.05 (s, 18H, H^{10}).

^{13}C NMR (125 MHz, DMSO- d_6 , 20 °C, δ): 166.6, 156.9, 156.6, 147.3, 140.1, 135.7, 129.1, 125.8, 125.1, 122.5, 94.8, 57.7, 15.2.

HRMS (ESI-MS, pos.) m/z : $[\text{M}-\text{Cl}]^+$ calcd for $\text{C}_{30}\text{H}_{34}\text{ClN}_4\text{O}_3\text{RuS}$, 667.1083; found, 667.1080.

EA Anal. calcd for $\text{C}_{30}\text{H}_{34}\text{Cl}_2\text{N}_4\text{O}_3\text{RuS}$: C, 51.28%; H, 4.88%; N, 7.97%. Found: C, 51.19%; H, 4.86%; N, 8.05%.

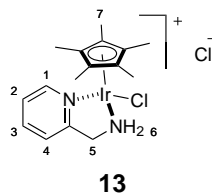
[(η^6 -Biphenyl)Ru(4)Cl]Cl (**12**)

Following procedure 1 (section 4.3.1), compound **12** was obtained as a brown-yellow solid (10 mg, 0.01 mmol, 21%).

Annex spectra page: 241

$^1\text{H NMR}$ (400 MHz, DMSO- d_6 , 20 °C, δ): 10.59 (d, $J = 9.8$ Hz, 1H, \mathbf{H}^4), 8.92 (dd, $J = 5.8$, 1.6 Hz, 2H, \mathbf{H}^2), 8.37 (d, $J = 8.4$ Hz, 2H, \mathbf{H}^3), 8.04 (m, 4H, \mathbf{H}^{7+biph}), 7.89 (d, $J = 8.1$ Hz, 2H, \mathbf{H}^2), 7.78 (dd, $J = 7.2$, 1.7 Hz, 2H, \mathbf{H}^6), 7.62 (s, 2H, \mathbf{H}^1), 7.47 (m, 3H, \mathbf{H}^{biph}), 7.37 (dd, $J = 8.3$, 6.9 Hz, 2H, \mathbf{H}^8), 6.86 (d, $J = 9.6$ Hz, 1H, \mathbf{H}^5), 6.68 (d, $J = 6.1$ Hz, 2H, \mathbf{H}^{biph}), 6.52 (t, $J = 6.0$ Hz, 2H, \mathbf{H}^{biph}), 6.29 (t, $J = 5.9$ Hz, 1H, \mathbf{H}^{biph}).

HRMS (ESI-MS, pos.) m/z : $[\text{M-Cl}]^+$ calcd for $\text{C}_{30}\text{H}_{26}\text{ClN}_4\text{O}_3\text{RuS}$, 659.0457; found, 659.0441.

[(cp*)Ir(2-picolylamine)Cl]Cl (**13**)

Following procedure 2 (section 4.3.1), compound **13** was obtained as a pale orange-yellow solid (24 mg, 0.05 mmol, 42%).

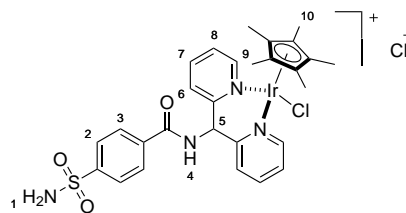
Annex spectra page: 243

$^1\text{H NMR}$ (400 MHz, DMSO- d_6 , 20 °C, δ): 8.65 (d, $J = 5.4$ Hz, 1H, \mathbf{H}^1), 8.03 (td, $J = 7.7$, 1.5 Hz, 1H, \mathbf{H}^3), 7.74 (d, $J = 7.9$ Hz, 1H, \mathbf{H}^4), 7.53 (d, $J = 6.4$ Hz, 1H, \mathbf{H}^2), 6.76 (s, 1H, \mathbf{H}^6), 5.45 (q, $J = 8.7$ Hz, 1H, $\mathbf{H}^{6'}$), 4.47 (dd, $J = 16.4$, 3.4 Hz, 1H, \mathbf{H}^5), 4.12 (dd, $J = 16.2$, 8.4 Hz, 1H, $\mathbf{H}^{5'}$), 1.68 (s, 15H, \mathbf{H}^7).

$^{13}\text{C NMR}$ (101 MHz, DMSO- d_6 , 20 °C, δ): 162.5, 151.4, 139.4, 125.9, 121.7, 86.6, 52.1, 8.4.

MS (ESI-MS, pos.) m/z (relative intensity): $[\text{M-Cl}]^+$ calcd for $\text{C}_{16}\text{H}_{23}\text{ClIrN}_2$, 471.1; found, 471.2 (100) $[\text{M-Cl}]^+$, 435.2 (83) $[\text{M-2Cl-H}]^+$.

EA Anal. calcd for $\text{C}_{16}\text{H}_{23}\text{Cl}_2\text{IrN}_2 \cdot 2\text{H}_2\text{O}$: C, 35.42%; H, 5.02%; N, 5.16%. Found: C, 35.37%; H, 4.73%; N, 5.44%.

$[(cp^*)Ir(4)Cl]Cl$ (**14**)**14**

Following procedure 1 (section 4.3.1), compound **14** was obtained as a yellow solid (45 mg, 0.06 mmol, 49%).

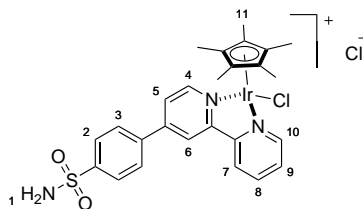
Annex spectra page: 245

$^1\text{H NMR}$ (400 MHz, DMSO- d_6 , 20 °C, δ): 11.00 (d, $J = 9.9$ Hz, 1H, \mathbf{H}^4), 8.87 (m, 2H, \mathbf{H}^9), 8.43 (d, $J = 8.5$ Hz, 2H, \mathbf{H}^2), 8.17 (m, 4H, $\mathbf{H}^{6,7}$), 8.03 (d, $J = 8.5$ Hz, 2H, \mathbf{H}^3), 7.66 (m, 4H, $\mathbf{H}^{1,8}$), 6.27 (d, $J = 9.7$ Hz, 1H, \mathbf{H}^5), 1.62 (s, 15H, \mathbf{H}^{10}).

$^{13}\text{C NMR}$ (100 MHz, DMSO- d_6 , 20 °C, δ): 166.5, 155.5, 155.4, 147.3, 141.1, 135.6, 129.1, 126.2, 125.7, 122.9, 88.8, 59.8, 8.34.

HRMS (ESI-MS, pos.) m/z : $[\text{M}-\text{Cl}]^+$ calcd for $\text{C}_{28}\text{H}_{31}\text{ClIrN}_4\text{O}_3\text{S}$, 731.1; found, 731.2.

EA Anal. calcd for $\text{C}_{28}\text{H}_{31}\text{Cl}_2\text{IrN}_4\text{O}_3\text{S} \cdot 2.1\text{H}_2\text{O}$: C, 41.80%; H, 4.41%; N, 6.96%. Found: C, 41.43%; H, 3.97%; N, 7.06%.

[(cp*)Ir(3)Cl]Cl (15)**15**

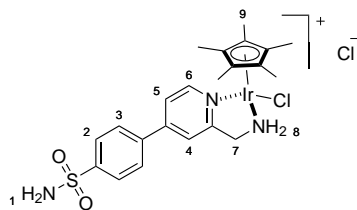
Following procedure 1 (section 4.3.1), compound **15** was obtained as a yellow solid (37 mg, 0.05 mmol, 54%).

Annex spectra page: 247

¹H NMR (400 MHz, DMSO-*d*₆, 20 °C, δ): 9.18 (d, $J = 1.3$ Hz, 1H, **H**⁶), 9.10 (d, $J = 8.1$ Hz, 1H, **H**⁷), 9.03 (t, $J = 5.9$ Hz, 2H, **H**^{4,10}), 8.40 (t, $J = 7.8$ Hz, 1H, **H**⁸), 8.31 (d, $J = 8.4$ Hz, 1H, **H**²), 8.21 (dd, $J = 6.0, 1.7$ Hz, 1H, **H**⁵), 8.06 (d, $J = 8.4$ Hz, 2H, **H**³), 7.90 (t, $J = 6.5$ Hz, 1H, **H**⁹), 7.58 (s, 2H, **H**¹), 1.69 (s, 15H, **H**¹¹).

HRMS (ESI-MS, pos.) m/z : [M-Cl]⁺ calcd for C₂₆H₂₈ClIrN₃O₂S, 674.1220; found, 674.1198.

EA Anal. calcd for C₂₆H₂₈Cl₂IrN₃O₂S·2H₂O: C, 41.88%; H, 4.33%; N, 5.63%. Found: C, 41.54%; H, 4.33%; N, 5.69%.

[(cp*)Ir(5)Cl]Cl (**16**)**16**

Following procedure 2 (section 4.3.1), **16** was obtained as a pale orange-yellow solid (24 mg, 0.05 mmol, 42%).

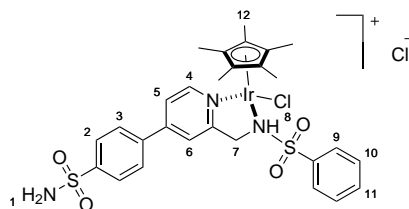
Annex spectra page: 248

¹H NMR (400 MHz, DMSO-*d*₆, 20 °C, δ): 8.73 (d, $J = 6.1$ Hz, 1H, **H**⁶), 8.22 (d, $J = 2.1$ Hz, 1H, **H**⁴), 8.09 (d, $J = 8.6$ Hz, 2H, **H**²), 8.01 (d, $J = 8.5$ Hz, 2H, **H**³), 7.90 (dd, $J = 6.2$, 2.1 Hz, 1H, **H**⁵), 7.56 (b, 1H, **H**⁸), 5.53 (q, $J = 9.3$ Hz, 1H, **H**^{8'}), 4.54 (dd, $J = 16.2$, 2.9 Hz, 1H, **H**⁷), 4.20 (dt, $J = 15.2$, 6.5 Hz, 1H, **H**^{7'}), 1.72 (s, 15H, **H**⁹).

¹³C NMR (101 MHz, DMSO-*d*₆, 20 °C, δ): 163.3, 151.7, 148.1, 145.5, 138.3, 127.8, 126.6, 123.3, 119.2, 90.1, 86.8, 52.1, 8.4.

HRMS (ESI-MS, pos.) m/z (relative intensity): [M-Cl]⁺ calcd for C₂₂H₂₇ClIrN₃O₂S, 625.1; found, 590.2 (100) [M-2Cl-H]⁺, 626.2 (81) [M-Cl]⁺.

EA Anal. calcd for C₂₂H₂₇Cl₂IrN₃O₂S · 3.3H₂O: C, 36.69%; H, 4.70%; N, 5.84%. Found: C, 36.57%; H, 4.32%; N, 5.45%.

[(cp*)Ir(6)Cl]Cl (**17**)**17**

Following procedure 2 (page: 130), **17** was obtained as a pale orange-yellow solid (24 mg, 0.05 mmol, 42%).

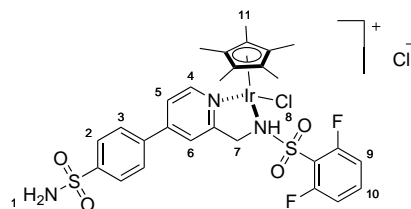
Annex spectra page: 250

$^1\text{H NMR}$ (500 MHz, DMSO- d_6 , 20 °C, δ): 8.53 (m, 1H, \mathbf{H}^4), 8.36 (t, $J = 6.3$ Hz, 1H, \mathbf{H}^{11}), 7.96 (d, $J = 8.4$ Hz, 2H, \mathbf{H}^2), 7.86 (d, $J = 8.4$ Hz, 2H, \mathbf{H}^3), 7.79 (d, $J = 6.9$ Hz, 2H, \mathbf{H}^9), 7.54 (m, 8H, $\mathbf{H}^{1,5,6,10}$), 4.22 (d, $J = 6.2$ Hz, 2H, \mathbf{H}^7), 1.63 (s, 15H, \mathbf{H}^{12}).

$^{13}\text{C NMR}$ (101 MHz, DMSO- d_6 , 20 °C, δ): 157.8, 149.6, 146.1, 144.6, 140.6, 140.3, 132.3, 129.1, 127.4, 126.5, 126.4, 120.1, 119.2, 92.1, 48.0, 8.3.

HRMS (ESI-MS, pos.) m/z : $[\text{M}-2\text{Cl}-\text{H}]^+$ calcd for $\text{C}_{28}\text{H}_{31}\text{IrN}_3\text{O}_4\text{S}_2$, 730.1; found, 730.2.

EA Anal. calcd for $\text{C}_{28}\text{H}_{31}\text{Cl}_2\text{IrN}_3\text{O}_4\text{S}_2 \cdot \frac{1}{4}\text{CH}_2\text{Cl}_2$: C, 41.28%; H, 3.86%; N, 5.11%. Found: C, 40.95%; H, 3.69%; N, 5.44%.

[(cp*)Ir(41)Cl]Cl (**18**)**18**

Following procedure 2 (section 4.3.1), K_2CO_3 (13 mg, 0.1 mmol, 1.0 eq) was added in the reaction mixture, compound **18** was obtained as a pale orange-yellow solid (24 mg, 0.05 mmol, 42%).

Annex spectra page: 252

^1H NMR (400 MHz, $\text{DMSO-}d_6$, 20 °C, δ): 8.27 (d, $J = 6.1$ Hz, 1H, H^6), 7.81 (s, 1H, H^1), 7.67 (m, 1H, H^{10}), 7.29 (b, 6H, $\text{H}^{2,3,9}$), 6.84 (d, $J = 6.8$ Hz, 1H, H^5), 5.14 (d, $J = 16.7$ Hz, 1H, H^7), 4.45 (d, $J = 16.6$ Hz, 1H, $\text{H}^{7'}$), 4.05 (s, 1H, H^8), 1.51 (s, 15H, H^{11}).

^{19}F NMR (376 MHz, $\text{DMSO-}d_6$, 20 °C, δ): 106.8.

HRMS (ESI-MS, pos.) m/z : $[\text{M-Cl}]^+$ calcd for $\text{C}_{28}\text{H}_{29}\text{ClF}_2\text{IrN}_3\text{O}_4\text{S}_2$, 766.1; found, 766.1.

EA Anal. calcd for $\text{C}_{28}\text{H}_{30}\text{Cl}_2\text{F}_2\text{IrN}_3\text{O}_4\text{S}_2 \cdot 3\text{H}_2\text{O} \cdot \text{K}_2\text{CO}_3$: C, 33.65%; H, 3.50%; N, 4.05%.

Found: C, 33.82%; H, 3.52%; N, 4.08%.

4.4 General procedure for hCA II inhibition profiling

4.4.1 Esterase activity screening assay

All steady-state measurements^[10,11] were performed in Tris-sulfate buffered solution (25 mM, pH 8.0) in the presence of 5% DMSO at 25 °C.^[12] The organic solvent ensures the solubility of the substrate (*p*-nitrophenyl acetate) as well as of the molecule used as inhibitor. The initial rates of the enzyme-catalyzed activity were measured by following the hydrolysis of the chromogenic substrate, *p*-nitrophenyl acetate, at 348 nm (25 measurements over a period of 35 minutes). Experiments were carried out in triplicate for each inhibitor. Kinetic measurements were performed in a total reaction volume of 300 μ L (in Tris-sulfate buffered solution), containing 0.5 mM *p*-nitrophenyl acetate and different concentrations of inhibitors.

The initial rates of enzyme catalysis were determined using the linear maximum slopes (first 10 min, 5 points) of the reaction traces measured by the plate reader. For comparison of the inhibition data, the initial rates were translated into % activity as a function of the inhibitor concentration. The inhibition data were analyzed via equation 4.1^[10]

$$v = \frac{v_o K_i}{K_i + \{[I]_t - 0.5(A - \sqrt{A^2 - 4[I]_t[E]_t})\}} \quad (4.1)$$

$$A = [I]_t + [E]_t + K_i$$

with v_o being the initial velocity of the enzyme-catalyzed reaction in the absence of inhibitor, K_i the inhibition constant, $[E]_t$ the total concentration of the enzyme and $[I]_t$ the total concentration of the inhibitor.

4.4.2 Competitive displacement assay

Competitive displacement of fluorescent hCA II inhibitor, dansylamide (DNSA), was used to determine the dissociation constant of strong inhibitors. DNSA is “nonfluorescent” in aqueous solution but in the presence of hCA II an increase of fluorescence signal can be observed at 470 nm. The dissociation constant (K_d) of screening hits were determined using a modification of the method proposed by Tripp.^[13-15] Black flat-bottom 96-well plates (NUNC F96 MicroWell Plates) with excitation at 280 nm, and detection at 470 nm were used. The K_d for DNSA was determined by titrating hCA II (100 nM) with DNSA (between 100 and 0.05 μ M) in a total volume of 208 μ L. The equilibrium dissociation constant for DNSA (K_{DNSA}) was then determined by fitting data to equation 4.2

$$F_{\text{tot}} = \frac{F_{\text{obs}} - F_{\text{ini}}}{F_{\text{end}} - F_{\text{ini}}} = \frac{1}{1 + (K_{\text{DNSA}}/[\text{DNSA}])} \quad (4.2)$$

where F_{tot} is the total fluorescence, F_{ini} is the initial fluorescence of hCA II in the absence of DNSA and F_{end} is the end point of fluorescence. The equilibrium dissociation constants for inhibitors were determined by competitive displacement of DNSA. A fixed concentration of DNSA (2.25 μ M) and hCA II (100 nM) was titrated against different inhibitor concentrations (from 100 μ M to 25 nM). Then the K_d value for each inhibitor was determined by fitting data to equation 4.3

$$F_{\text{tot}} = \frac{F_{\text{obs}} - F_{\text{ini}}}{F_{\text{end}} - F_{\text{ini}}} = \frac{1}{1 + (K_{\text{DNSA}}/[\text{DNSA}])(1 + [I]/K_d)} \quad (4.3)$$

where F_{tot} is the fraction of total fluorescence, F_{obs} is the fluorescence signal at each concentration of inhibitor, F_{ini} is the initial fluorescence of hCA II without DNSA and F_{end} is the end point of fluorescence.

4.5 General procedure for circular dichroism measurements

4.5.1 Sample preparation and data analysis

Each measurement were obtained at 25 °C with a time constant of 2.5 s and a step resolution of 1 nm. The ellipticity was reported as mean residue molar ellipticity ($[\Theta]$, deg cm² dmol⁻¹) calculated from equation 4.4

$$[\Theta]_{mrv} = [\Theta]_{obs}/10c_rln \quad (4.4)$$

were $[\Theta]_{obs}$ is the measured ellipticity in degrees, c_r is the protein concentration (in mol/L, hCA II=29098 g/mol), l is the optical path length of the cell (in cm) and n is the number of protein residues (259 amino acids for hCA II). For the analysis of hCA II scaffold stability in the presence of organic solvent, a quartz cell with a path length of 1 cm was used. A solution containing approximately 1 mg/mL of hCA II in 50 mM phosphate buffer (pH 7.4), with different DMSO percentages (0 to 50% (v/v)) was measured.

Circular dichroism spectra were also measured under catalysis conditions. hCA II (1 mg/mL) was dissolved (cell path length = 0.1 cm) in MOPS 1.2 mM buffer and 3 M sodium formate (pH 7.5 and 5% DMSO (v/v)).

4.6 Catalytic experiments: transfer hydrogenation

Lyophilized hCA II corresponding to 0.4 mM final concentration of free binding sites (2.5 mg) was weighed into vials. The reaction buffer (MOPS 1.2 mM buffer, 3 M sodium formate, pH 7.5, 200 μ L) was added, and the mixture was stirred until all the protein was dissolved. The metal complex stock solution was added (final concentration 0.3 mM; 0.8 equivalents [Ru] or [Ir] *vs.* hCA II free binding sites), and the mixture was stirred for 30 minutes. Finally, the substrate stock solution was added (4 μ L, final concentration 20 mM). The tubes were placed in a magnetically stirred multireactor, and were heated up to 40 °C if required.^[16]

4.7 Sample work up and analysis

4.7.1 1-Methyl-6,7-dimethoxy-3,4-dihydroisoquinoline

To the catalysis reaction an aqueous solution of NaOH (60 μ L, 20%) was added, before extraction with CH₂Cl₂ (2 x 1 mL). The extracts were dried over Na₂SO₄, and analyzed by chiral HPLC (Daicel IC 250 x 4.6 mm, 5 μ m; CH₂Cl₂/*i*PrOH/HNEt₂, 98/2/0.06, 1 mL/min, 25 °C, 280 nm). T_R 9.6 min (*R*)-6,7-dimethoxy-1-methyl-1,2,3,4-tetrahydroisoquinoline, 11.9 min 1-Methyl-6,7-dimethoxy-3,4-dihydroisoquinoline, 15.4 min (*S*)-6,7-dimethoxy-1-methyl-1,2,3,4-tetrahydroisoquinoline. The response factor used for the conversion determination is 1.9 at 280 nm.^[16]

4.7.2 1-Methyl-3,4-dihydroisoquinoline

To the catalysis reaction an aqueous solution of NaOH (60 μ L, 20%) was added, before extraction with CH₂Cl₂ (2 x 1 mL). The extracts were dried over Na₂SO₄, and analyzed by chiral HPLC (Daicel IC 250 x 4.6 mm, 5 μ m; *n*-hexane/*i*PrOH/HNEt₂, 97/3/0.06, 1 mL/min, 25 °C, 265 nm). T_R 11.0 min (*R*)-1-methyl-1,2,3,4-tetrahydroisoquinoline, 12.0 min (*S*)-1-methyl-1,2,3,4-tetrahydroisoquinoline, 18.9 min 1-methyl-3,4-dihydroisoquinoline.

4.7.3 Phenylpyrroline

To the catalysis reaction an aqueous solution of NaOH (60 μ L, 20%) was added, before extraction with CH₂Cl₂ (2 x 1 mL). The extracts were dried over Na₂SO₄, and analyzed by chiral HPLC (Daicel IC 250 x 4.6 mm, 5 μ m; *n*-hexane/*i*PrOH/HNEt₂, 98/2/0.06, 1 mL/min, 25 °C, 260 nm). T_R 8.9 min 1-phenylpyrrolidine, 10.0 min 1-phenylpyrrolidine, 11.2 min 1-phenylpyrroline. The response factor used for the conversion determination is 31.6 at 260 nm.

4.7.4 2-Cyclohexylpyrrolidine

To the catalysis reaction aq. NaOH (60 μ L, 20%) was added, before extraction with CH₂Cl₂ (1 x 1 mL). The extracts were dried over Na₂SO₄, and the conversion was determined in the crude extracts by GC-FID (Agilent J&W, 30 m x 0.32 mm, 0.25 μ M, 135 °C, isothermal, 1.7 mL/min He; injector: 250 °C; split 100; detector 240 °C). T_R 4.46 min amine, 5.06 min imine.

For *ee*-determination trifluoroacetic anhydride (TFAA, 200 μ L) was added to the GC-sample used for conversion determination, and volatiles were removed to near dryness in a gentle stream of N₂. The residue was dissolved in a small amount of CH₂Cl₂ (300 μ L), and analyzed by GC-FID on chiral stationary phase (Supelco β -DEX 325, 30 x 0.25 mm, 0.25 μ m; 115 °C isothermal; 1.7 mL/min He; injector 250 °C; split 10; detector 250 °C) T_R 44.1 (*S*), 45.6 (*R*).^[17]

4.8 Michaelis-Menten experiments

Reaction setup^[17]

Human Carbonic Anhydrase II (~2.5 mg, final concentration: 0.4 mM hCA II) was dissolved in a MOPS/formate solution (100 μL , pH 7.5, 0.4 mM and 3 M respectively) and [Ir] catalyst (8.75 μL of DMSO stock solution, final concentration: 0.35 mM [Ir]) was added. The resulting ATHase solution was mixed for 15 min at 25 °C (100 rpm).

Reactions were started by adding an appropriate volume of the substrate stock solution (100 μL , final concentration between 150 and 1 mM) to the tubes. After 20, 40 and 60 minutes, respectively, reaction aliquots (50 μL) were removed and added to a glutathione solution (40 μL , 0.25 M) to stop the catalytic reaction.

Work up and analysis

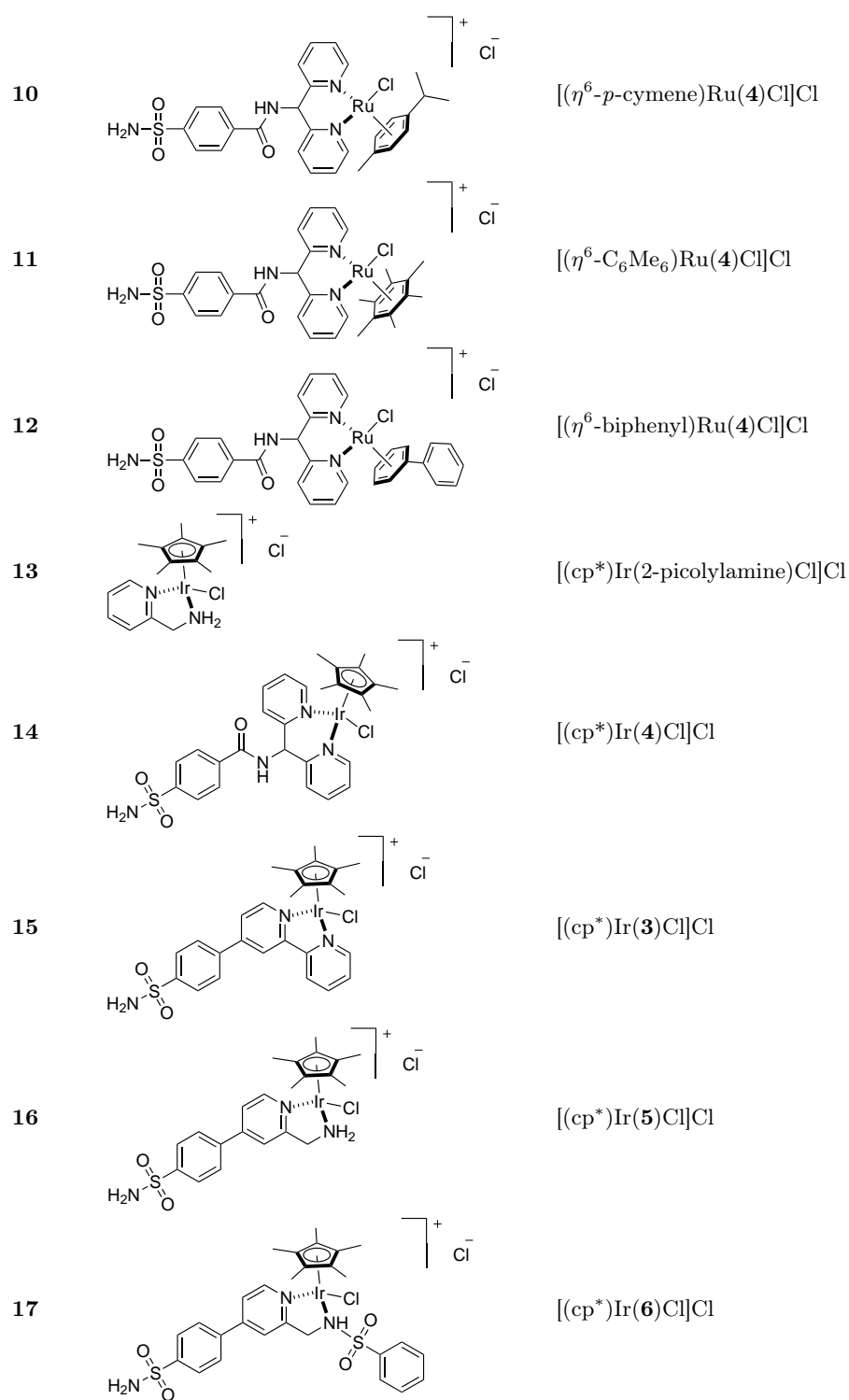
Water (300 μL) was added to aliquots, and HPLC sample were prepared by adding 200 μL of the previous solution in water (500 μL). Conversions were determined using an Eclipse XDB-C18 column (5 μm , 4.6 x 150 mm) and water/MeOH/TFA 87:13:0.1 as an eluent at a flow of 1 ml/min and 25°C (t_R 6,7-dimethoxy-1-methyl-1,2,3,4-tetrahydroisoquinoline = 11.9 min, t_R 1-methyl-6,7-dimethoxy-3,4-dihydroisoquinoline = 16.3 min.). The response factor used for the conversion determination is 1.26 at 280 nm.

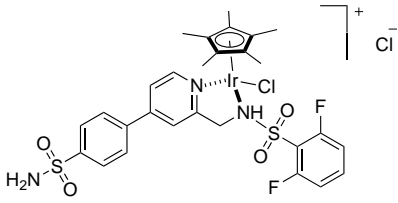
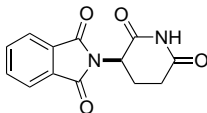
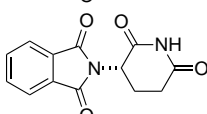
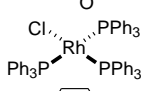
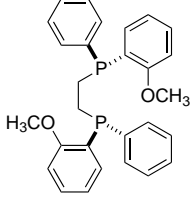
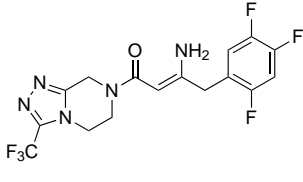
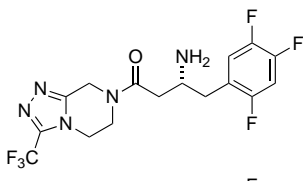
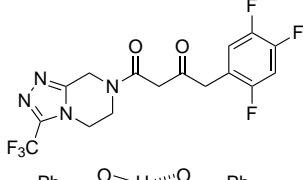
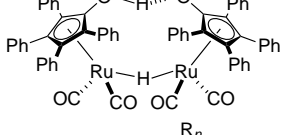
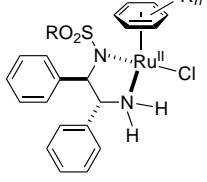
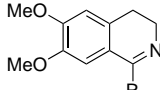
4.9 Protein purification: resin preparation

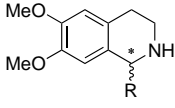
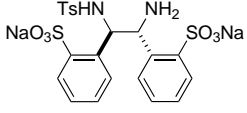
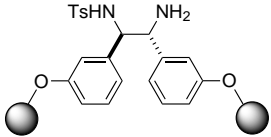
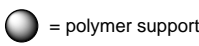
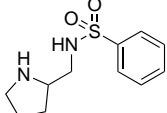
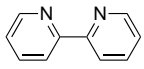
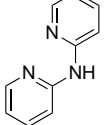
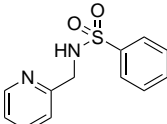
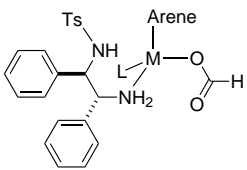
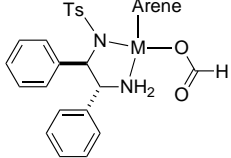
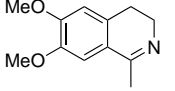
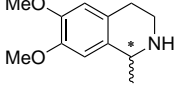
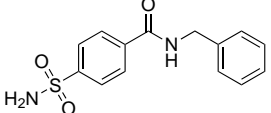
The sulfonamide ligand 4-aminomethylbenzenesulfonamide (1.5 g) was dissolved in 100 mL of 50% acetone, and added to 125 mL of CM-BioGel A that had been washed in 50% acetone. The pH was adjusted to 4.8 with HCl. EDAC (2.5 g in 5 mL of 50% acetone) was added dropwise with gentle stirring. The pH was monitored during the addition and adjusted to 4.8 as necessary during the first two hours. (The pH change is rapid at first and stabilizes after about 2 hours.) The mixture was then stirred overnight to allow coupling to complete. The coupled gel was washed thoroughly with 50% acetone to remove excess ligand, then several times with distilled water. After the final wash, the gel was resuspended in an equal volume 25 mM Tris, 0.25 M Na₂SO₄ and pH 8.3. For prolonged storage, the gel was placed at 4 °C, and NaN₃ was added to a final concentration of 0.02%. The gel was washed, and resuspended in azide free buffer before use.^[18]

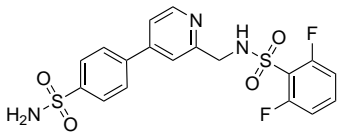
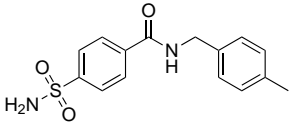
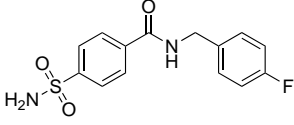
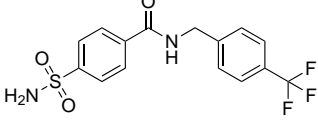
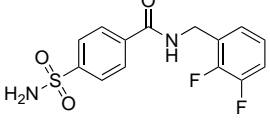
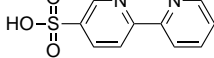
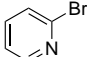
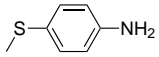
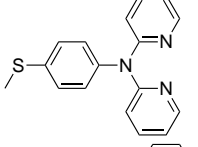
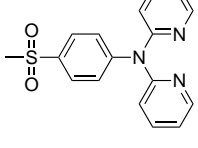
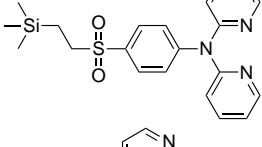
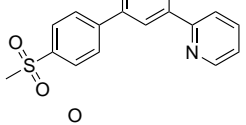
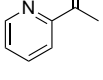
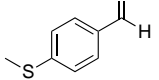
4.10 Table of molecules

Number	Structure	Name
1		2,2'-bipyridine-5-sulfonamide
2		4-(di-2-pyridinylamino)-benzenesulfonamide
3		(4-((2,2'-bipyridine)4-yl)benzenesulfonamide
4		<i>N</i> -(di(2-pyridyl)methyl)amidobenzene-4-sulfonamide
5		4-(2-(aminomethyl)pyridin-4-yl)benzenesulfonamide, TFA salt
6		<i>N</i> -((4-(4-sulfamoylphenyl)pyridin-2-yl)methyl)benzenesulfonamide,
7		1,3-dimesityl-5-((4-sulfamoylbenzamido)methyl)-4,5-dihydro-1 <i>H</i> -imidazol-3-ium
8		$[(\eta^6\text{-C}_6\text{H}_6)\text{Ru}(\mathbf{1})\text{Cl}]\text{Cl}$
9		$[(\eta^6\text{-C}_6\text{H}_6)\text{Ru}(\mathbf{4})\text{Cl}]\text{Cl}$

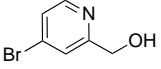
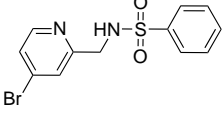
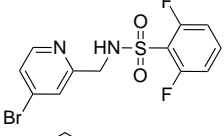
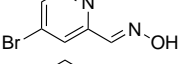
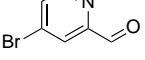
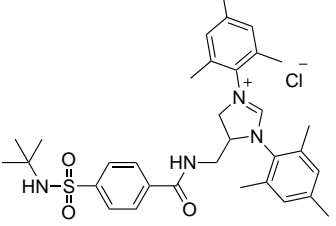
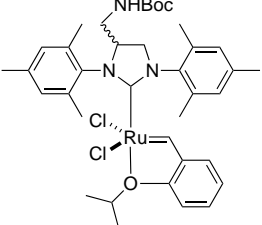
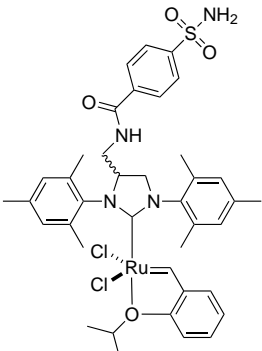
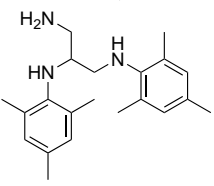
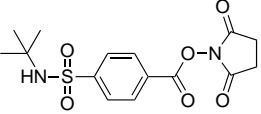


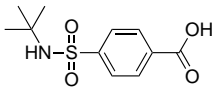
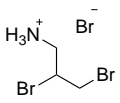
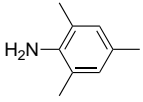
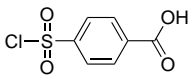
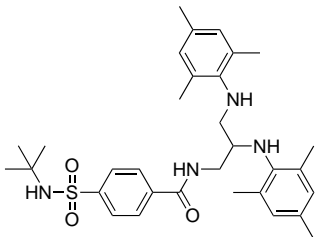
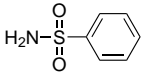
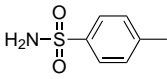
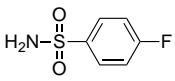
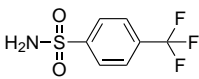
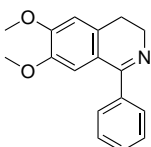
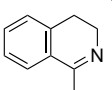
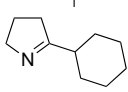
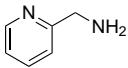
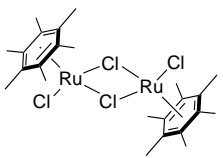
- 18  $[(cp^*)Ir(41)Cl]Cl$
- 19  (*R*)-thalidomide
- 20  (*S*)-thalidomide
- 21  Wilkinson's catalyst
- 22  DIPAMP
- 23  3-amino-1-[5,6-dihydro-3-(trifluoromethyl)-1,2,4-triazolo[4,3-a]pyrazin-7(8*H*)-yl]-4-(2,4,5-trifluorophenyl)-2-buten-1-one
- 24  sitagliptin
- 25  prositagliptin ketone
- 26  Shvo's diruthenium catalyst
- 27  Noyori's ruthenium (II) based catalyst
- 28  -

29		-
30		2,2'-[(1 <i>R</i> ,2 <i>R</i>)-1-amino-2-[[[4-methylphenyl)sulfonyl]amino]-1,2-ethanediyl]bis-benzenesulfonic acid disodium salt
31		-
		
32		<i>N</i> -(2-pyrrolidinylmethyl)-benzenesulfonamide
33		2,2'-bipyridine
34		<i>N</i> -2-pyridinyl-2-pyridinamine
35		<i>N</i> -(2-pyridinylmethyl)-benzenesulfonamide
36		-
37		-
39		6,7-diethoxy-1-methyl-3,4-dihydroisoquinoline
38		racemic salsolidine
40		<i>N</i> -benzyl-4-sulfamoylbenzamide

- 41  2,6-difluoro-*N*-((4-(4-sulfamoylphenyl)pyridin-2-yl)methyl)benzenesulfonamide
- 42  *N*-(4-methylbenzyl)-4-sulfamoylbenzamide
- 43  *N*-(4-fluorobenzyl)-4-sulfamoylbenzamide
- 44  *N*-(4-(trifluoromethyl)benzyl)-4-sulfamoylbenzamide
- 45  *N*-(2,3-difluorobenzyl)-4-sulfamoylbenzamide
- 46  2,2'-bipyridine-5-sulfonic acid
- 47  2-bromopyridine
- 48  4-(methylmercapto)aniline
- 49  *N*-(4-(methylthio)phenyl)-*N*-(pyridin-2-yl)pyridine-2-amine
- 50  *N*-(4-(methylsulfonyl)phenyl)-*N*-(pyridin-2-yl)pyridine-2-amine
- 51  *N*-(pyridine-2-yl)-*N*-(4-((2-(trimethylsilyl)ethyl)sulfonyl)phenyl)pyridin-2-amine
- 52  (4-(4-(methylthio)phenyl)-2,2'-bipyridine
- 53  2-acetylpyridine
- 54  4-(methylthio)benzaldehyde

55		(<i>E</i>)-3-(4-(methylthio)phenyl)-1-(pyridin-2-yl)prop-2-en-1-one
56		2-(6-ethoxy-4-(4-(methylthio)phenyl)-5,6-dihydro-2H-pyran-2-yl)pyridine
57		(4-(4-(methylsulfonyl)phenyl)-2,2'-bipyridine
58		(4-(4-((2-(trimethylsilyl)ethyl)sulfonyl)phenyl)-2,2'-bipyridine
59		4-carboxybenzenesulfonamide
60		bis(pyridine-2-yl)methanamine
61		2,5-dioxopyrrolidin-1-yl-4-sulfamoylbenzoate
62		di-2-pyridyl ketoxime
63		4-aminosulfonylphenylboronic acid
64		4-chloro-2-pyridinecarbonitrile
65		<i>N</i> -(<i>tert</i> -butyl)-4-(2-cyanopyridin-4-yl)benzenesulfonamide
66		<i>N</i> -(<i>tert</i> -butyl)-4-(2-(aminomethyl)pyridin-4-yl)benzenesulfonamide
67		4-bromo-2-methylpyridine
68		4-bromo-2-methylpyridine- <i>N</i> -oxide

- 69  4-bromo-2-hydroxymethylpyridine
- 70  *N*-[(4-bromopyridin-2-yl)methyl]benzenesulfonamide
- 71  *N*-[(4-bromopyridin-2-yl)methyl]-2,6-difluorobenzene-1-sulfonamide
- 72  4-bromo-2-pyridine ketoxime
- 73  4-bromo-2-pyridine aldehyde
- 74  5-((4-(*N*-(*tert*-butyl)sulfonyl)benzamido)methyl)-1,3-dimesityl-4,5-dihydro-1H-imidazol-3-ium chloride
- 75  -
- 76  -
- 77  *N,N'*-dimesitylpropane-1,2,3-triamine
- 78  2,5-dioxopyrrolidin-1-yl-4-(*N*-(*tert*-butyl)sulfonyl)benzoate

79		4-(<i>N</i> -(<i>tert</i> -butyl)sulfamoyl)benzoic acid
80		1,2-dibromo-ethanamine
81		2,4,6-trimethylaniline
82		4-(chlorosulfonyl)benzoic acid
83		<i>N</i> -(2,3-bis(mesitylamino)propyl)-4-(<i>N</i> -(<i>tert</i> -butyl)sulfamoyl)benzamide
84		benzenesulfonamide
85		<i>p</i> -toluenesulfonamide
86		4-fluorobenzenesulfonamide
87		4-(trifluoromethyl)benzenesulfonamide
88		3,4-dihydro-6,7-dimethoxy-1-phenyl-isoquinoline
89		3,4-dihydro-1-methyl-isoquinoline
90		5-cyclohexyl-3,4-dihydro-2 <i>H</i> -pyrrole
91		2-picolyamine
92		$[(\eta^6\text{-C}_6\text{Me}_6)\text{RuCl}_2]_2$

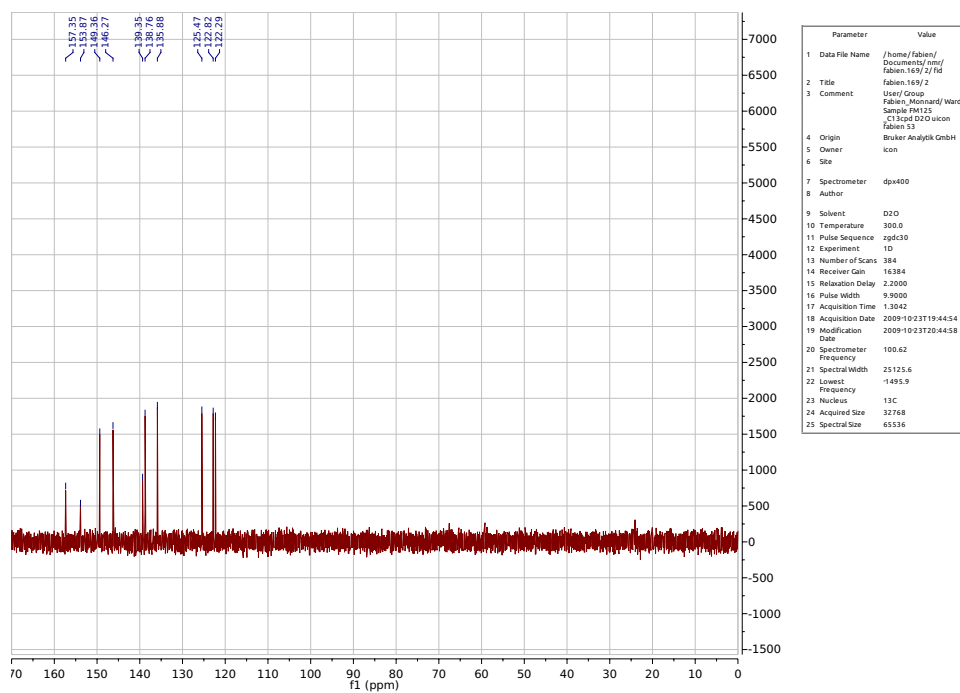
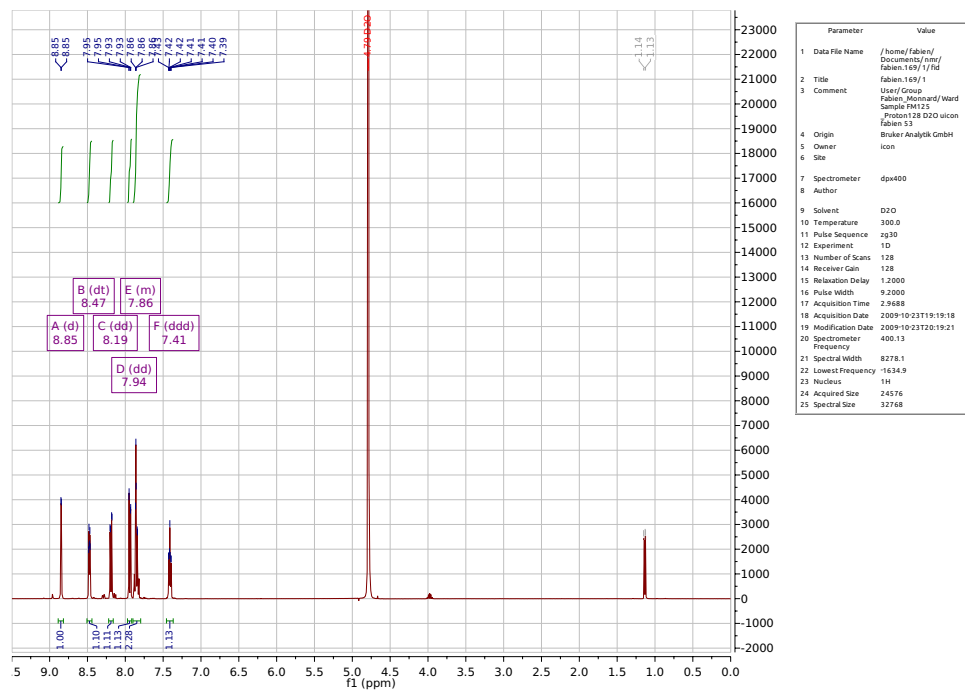
4.11 References

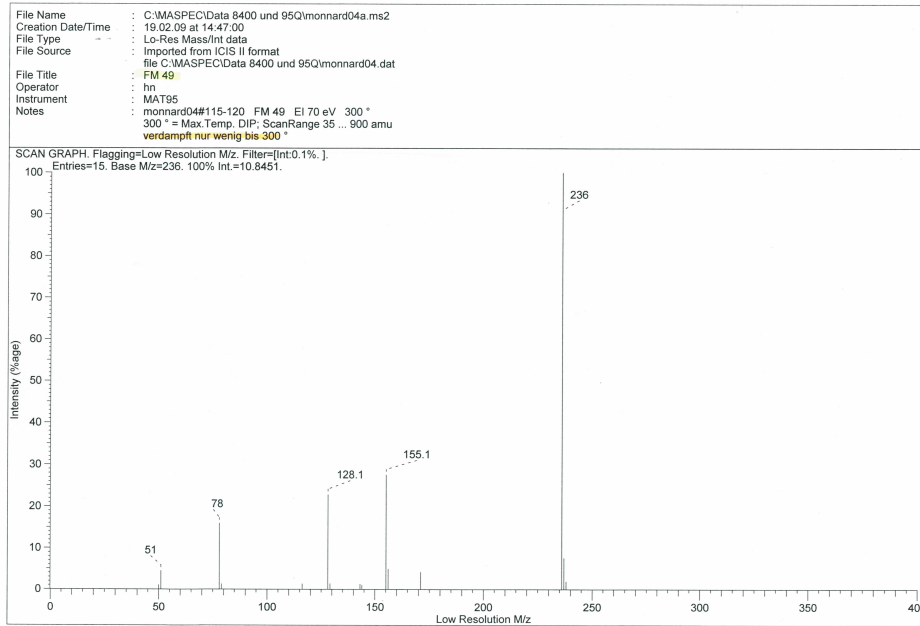
- [1] Williams, T.; Kelley, C.; many others, “Gnuplot 4.4: an interactive plotting program”, <http://gnuplot.sourceforge.net/>, 2010.
- [2] Herrmann, W. A.; Thiel, W. R.; Kuchler, J. G. *Chem. Ber.* **1990**, *123*, 1953.
- [3] Renz, M.; Hemmert, C.; Meunier, B. *Eur. J. Org. Chem.* **1998**, *1998*, 1271.
- [4] Jain, A.; Huang, S. G.; Whitesides, G. M. *J. Am. Chem. Soc.* **1994**, *116*, 5057.
- [5] Kim, C. Y.; Chang, J. S.; Doyon, J.; Jr, T. T. B.; Fierke, C. A.; Jain, A.; Christianson, D. W. *J. Am. Chem. Soc.* **2000**, *122*, 12125.
- [6] Lo, C.; Ringenberg, M. R.; Gnanndt, D.; Wilson, Y.; Ward, T. R. *Chem. Commun.* **2011**, *47*, 12065.
- [7] Freedman, D. A.; Evju, J. K.; Pomije, M. K.; Mann, K. R. *Inorg. Chem.* **2001**, *40*, 5711.
- [8] Günnaz, S.; Özdemir, N.; Dayan, S.; Dayan, O.; Çetinkaya, B. *Organometallics* **2011**, *30*, 4165.
- [9] Bennett, M. A.; Huang, T.-N.; Matheson, T. W.; Smith, A. K. *Inorganic Synthesis* **2007**, *21*, 74.
- [10] Srivastava, D. K.; Jude, K. M.; Banerjee, A. L.; Haldar, M.; Manokaran, S.; Kooren, J.; Mallik, S.; Christianson, D. W. *J. Am. Chem. Soc.* **2007**, *129*, 5528.
- [11] Nair, S. K.; Calderone, T. L.; Christianson, D. W.; Fierke, C. A. *J. Biol. Chem.* **1991**, *266*, 17320.
- [12] Vullo, D.; Franchi, M.; Gallori, E.; Antel, J.; Scozzafava, A.; Supuran, C. *J. Med. Chem.* **2004**, *47*, 1272.
- [13] Iyer, R.; Barrese III, A. A.; Parakh, S.; Parker, C. N.; Tripp, B. C. *J. Biomol. Screening* **2006**, *11*, 782.
- [14] Baird Jr, T. T.; Waheed, A.; Okuyama, T.; Sly, W. S.; Fierke, C. A. *Biochemistry* **1997**, *36*, 2669.
- [15] Wang, S. C.; Zamble, D. B. *Biochem. Mol. Biol. Educ.* **2006**, *34*, 364.
- [16] Dürrenberger, M. *et al. Angew. Chem. Int. Ed.* **2011**, *50*, 3026.
- [17] Köhler, V.; Wilson, Y. M.; M., D.; Ghislieri, D.; Churakova, E.; Quinto, T.; L., K.; Häussinger, D.; Hollmann, F.; Turner, N. J.; Ward, T. R. *Nat. Chem.* In press.
- [18] Bering, C. L.; Kuhns, J. J.; Rowlett, R. *J. Chem. Educ.* **1998**, *75*, 1021.

Part III

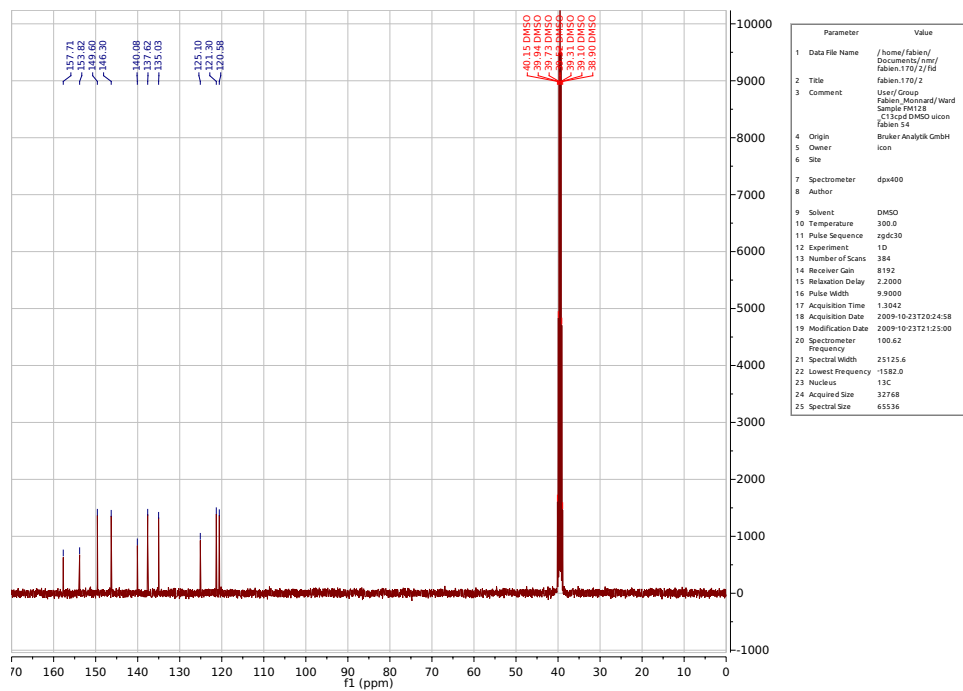
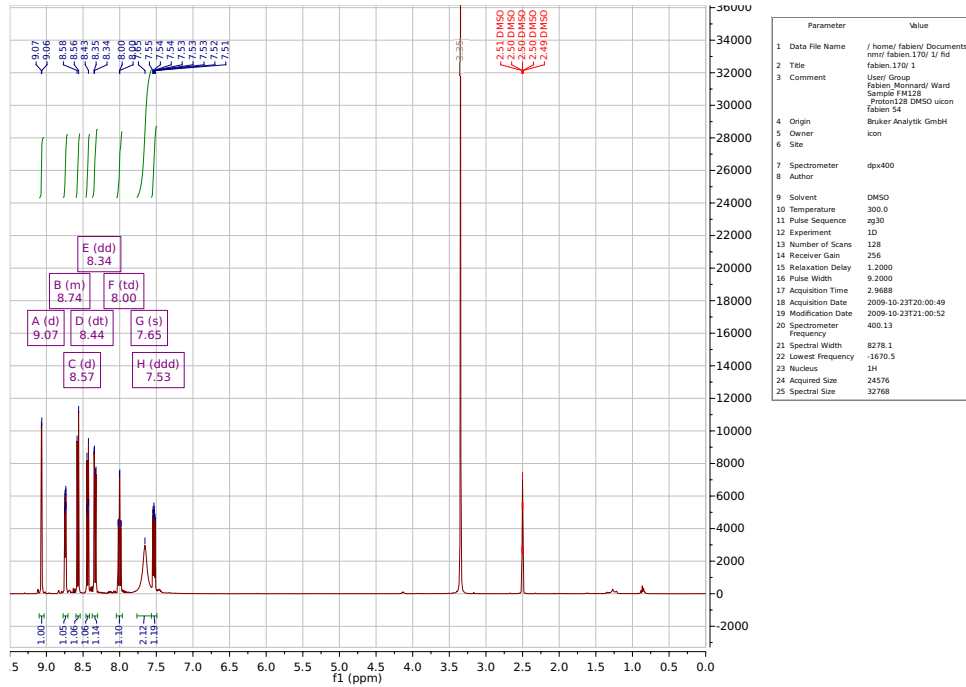
Annexes

2,2'-Bipyridine-5-sulfonic acid (46)





2,2'-Bipyridine-5-sulfonamide (1)



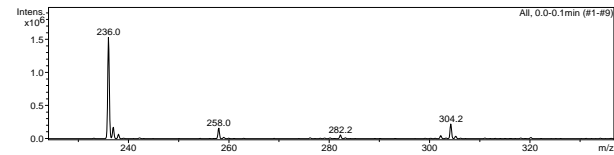
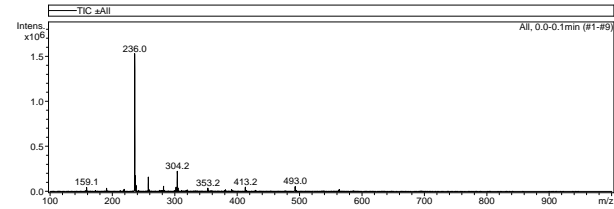
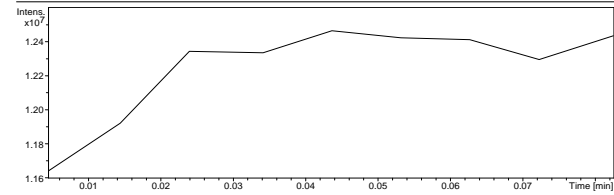
Display Report

Analysis Info

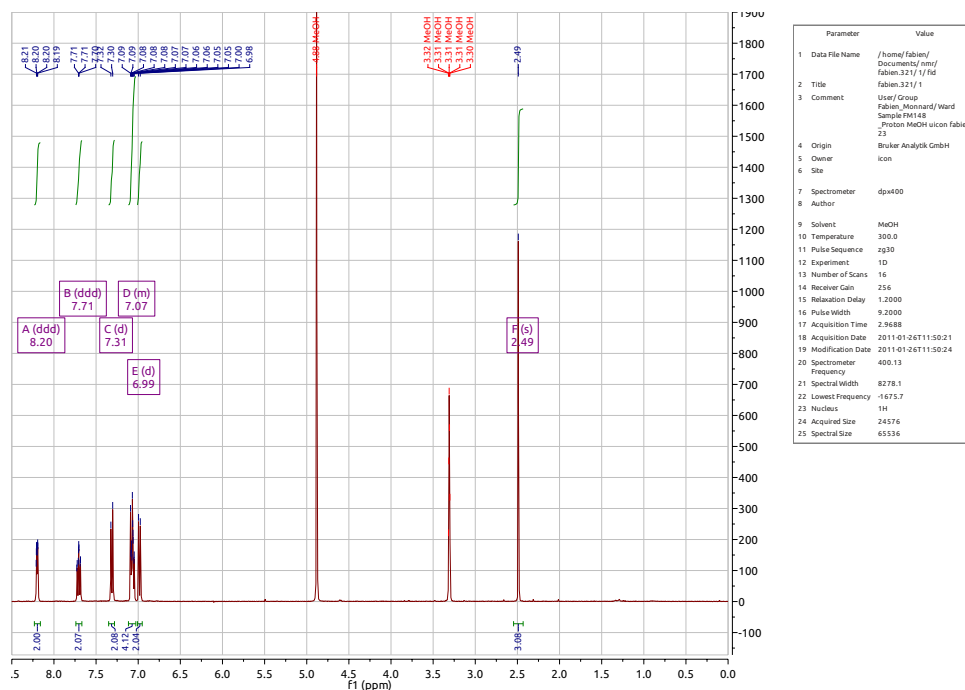
Analysis Name FM000097.d Acquisition Date 10/26/09 08:40:23
Method Copy of DEFAULT.MS Operator Administrator
Sample Name FM128 Instrument esquire3000plus_01096
Comment

Acquisition Parameter

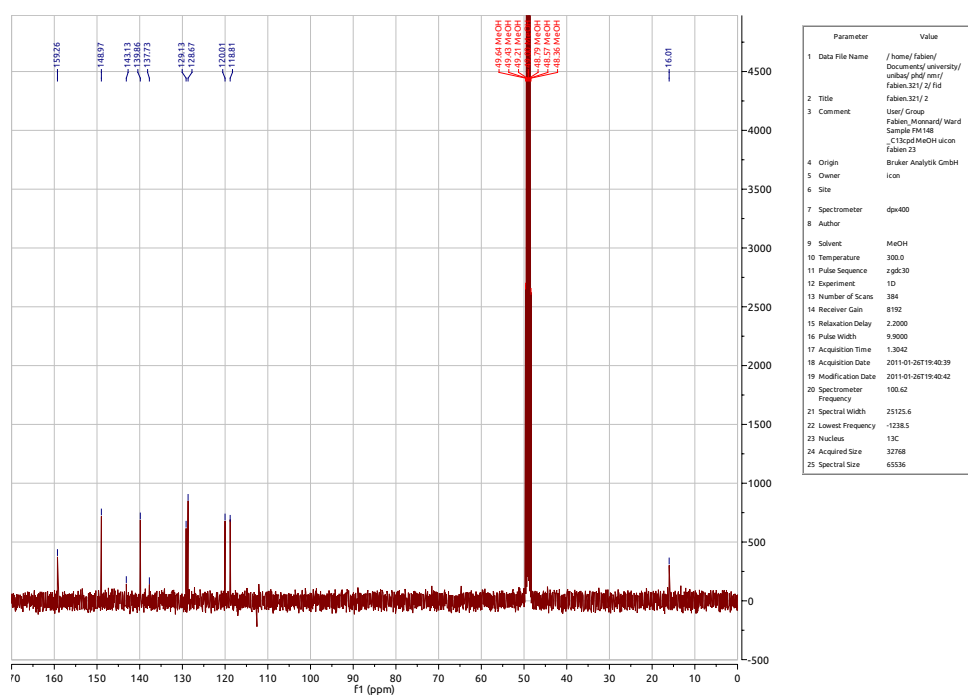
Ion Source Type	ESI	Ion Polarity	Positive	Alternating Ion Polarity	off
Mass Range Mode	Std/Normal	Scan Begin	100 m/z	Scan End	1000 m/z
Capillary Exit	108.6 Volt	Skim 1	40.0 Volt	Trap Drive	34.1
Accumulation Time	796 µs	Averages	5 Spectra	Auto MS/MS	off



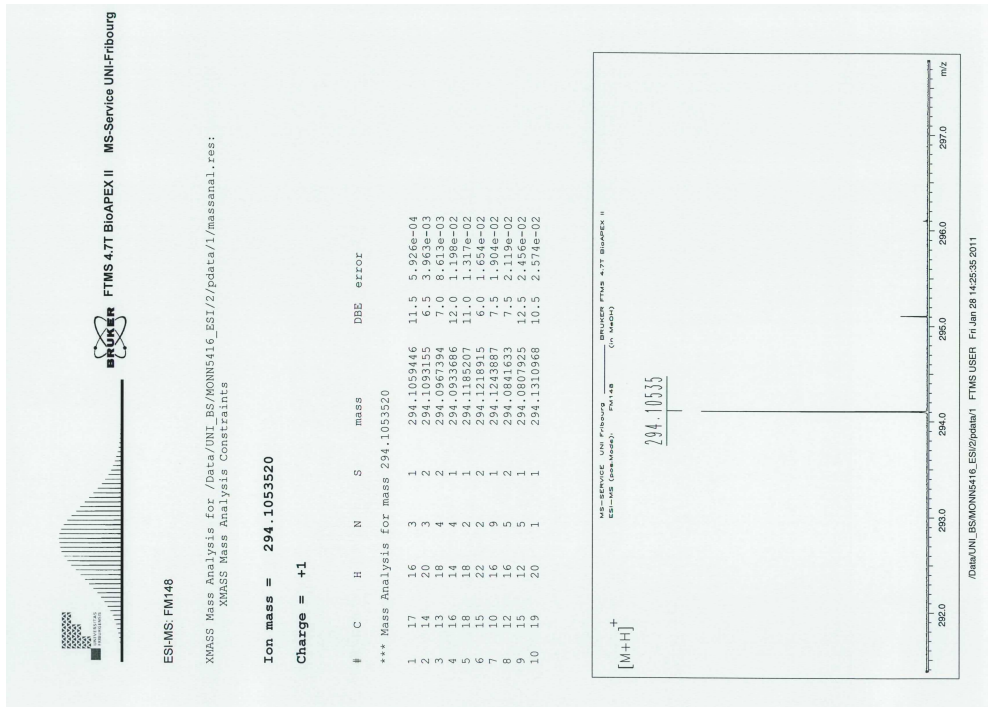
N-(4-(Methylthio)phenyl)-*N*-(pyridin-2-yl)pyridine-2-amine (49)



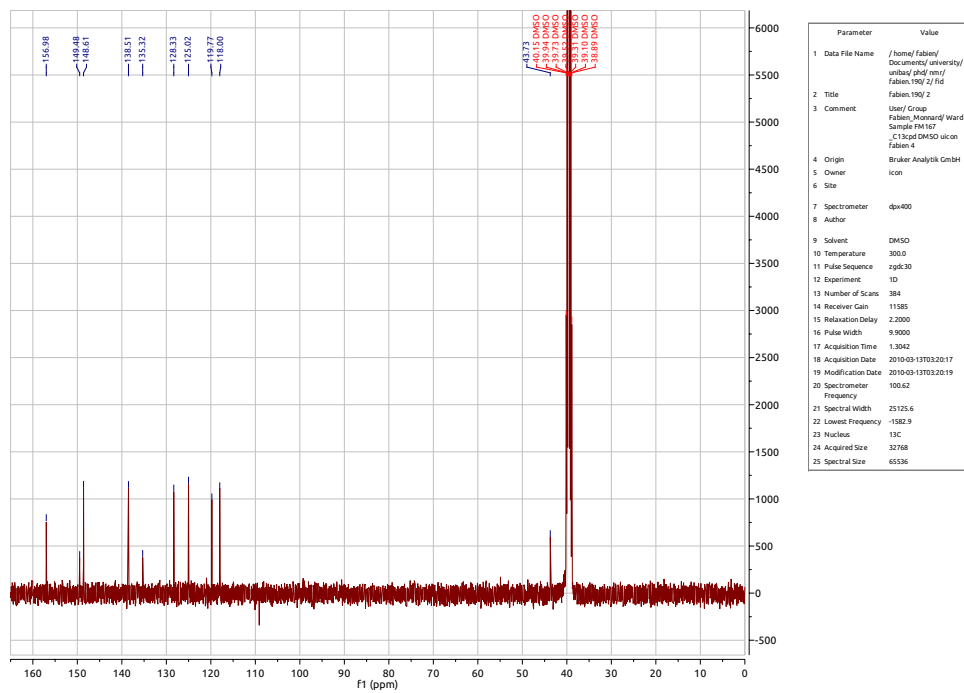
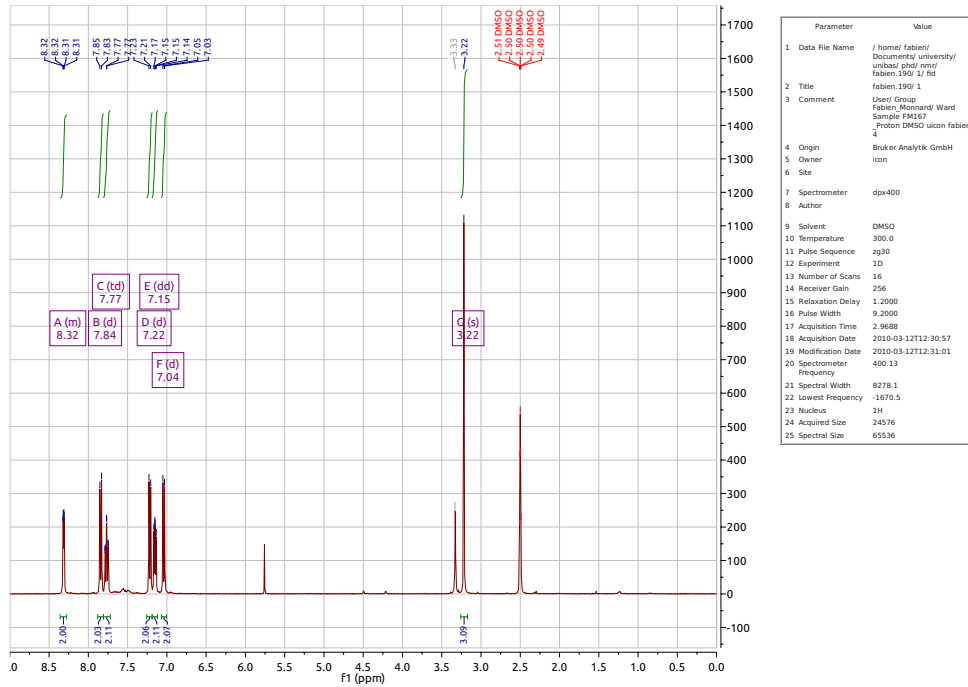
Parameter	Value
1 Data File Name	/home/fabien/ Documents/ rmy/ Fabien.321/ 1/ f6d
2 Title	Fabien.321/ 1
3 Comment	User/ Group Fabien, Monnard/ Ward Sample 94148 _Proton MeOH uicon Fabien 23
4 Origin	Bruker Analytik GmbH
5 Owner	icon
6 Site	
7 Spectrometer	dp400
8 Author	
9 Solvent	MeOH
10 Temperature	300.0
11 Pulse Sequence	zg30
12 Experiment	1D
13 Number of Scans	16
14 Receiver Gain	256
15 Relaxation Delay	1.2000
16 Pulse Width	9.2000
17 Acquisition Time	2.3688
18 Acquisition Date	2011-01-26T11:50:21
19 Modification Date	2011-01-26T11:50:24
20 Spectrometer Frequency	400.13
21 Spectral Width	8278.1
22 Lowest Frequency	-1675.7
23 Nucleus	1H
24 Acquired Size	24576
25 Spectral Size	65536

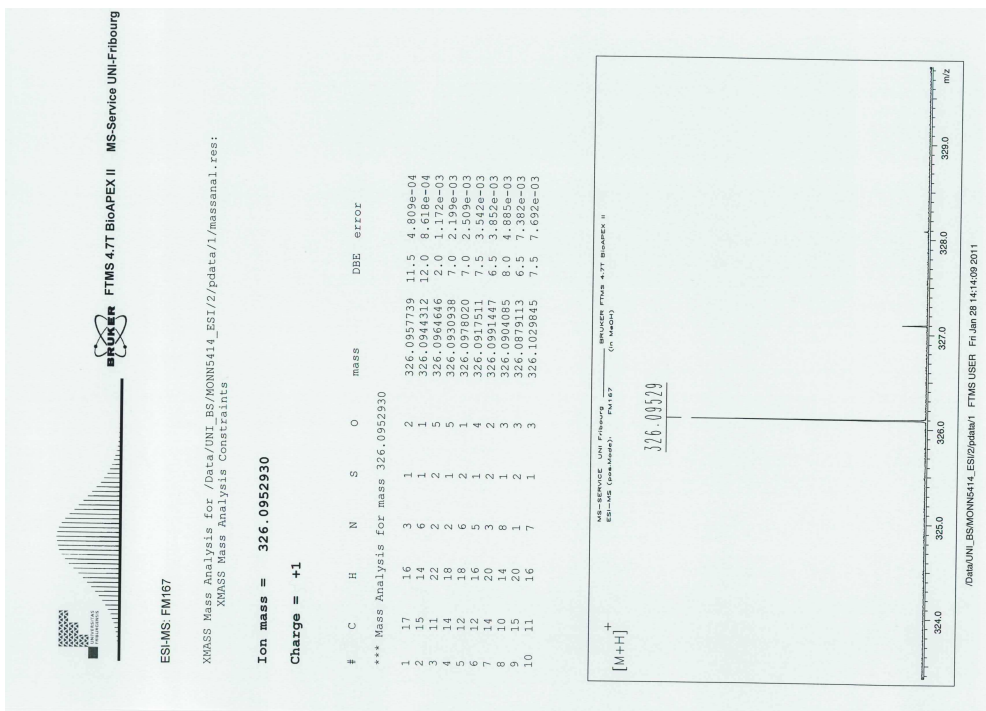


Parameter	Value
1 Data File Name	/home/fabien/ Documents/ university/ unbauf/ zhaf/ rmy/ Fabien.321/ 2/ f6d
2 Title	Fabien.321/ 2
3 Comment	User/ Group Fabien, Monnard/ Ward Sample 94148 _C13cpd MeOH uicon Fabien 23
4 Origin	Bruker Analytik GmbH
5 Owner	icon
6 Site	
7 Spectrometer	dp400
8 Author	
9 Solvent	MeOH
10 Temperature	300.0
11 Pulse Sequence	zgdc30
12 Experiment	1D
13 Number of Scans	384
14 Receiver Gain	8192
15 Relaxation Delay	2.2000
16 Pulse Width	9.9000
17 Acquisition Time	1.3042
18 Acquisition Date	2011-01-26T19:40:39
19 Modification Date	2011-01-26T19:40:42
20 Spectrometer Frequency	100.62
21 Spectral Width	25125.6
22 Lowest Frequency	-1238.5
23 Nucleus	13C
24 Acquired Size	32768
25 Spectral Size	65536

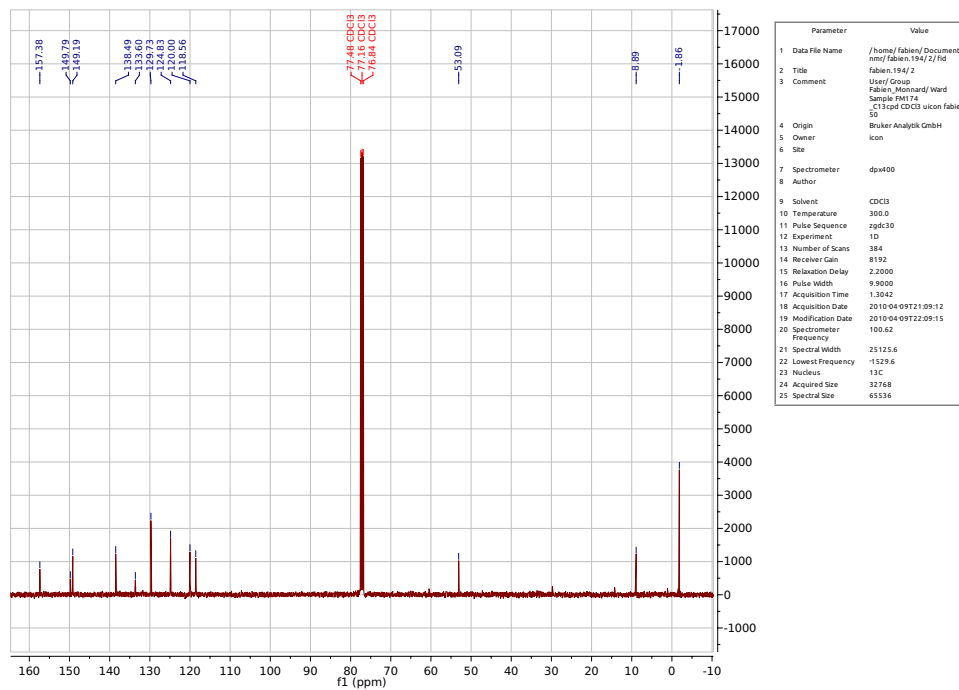
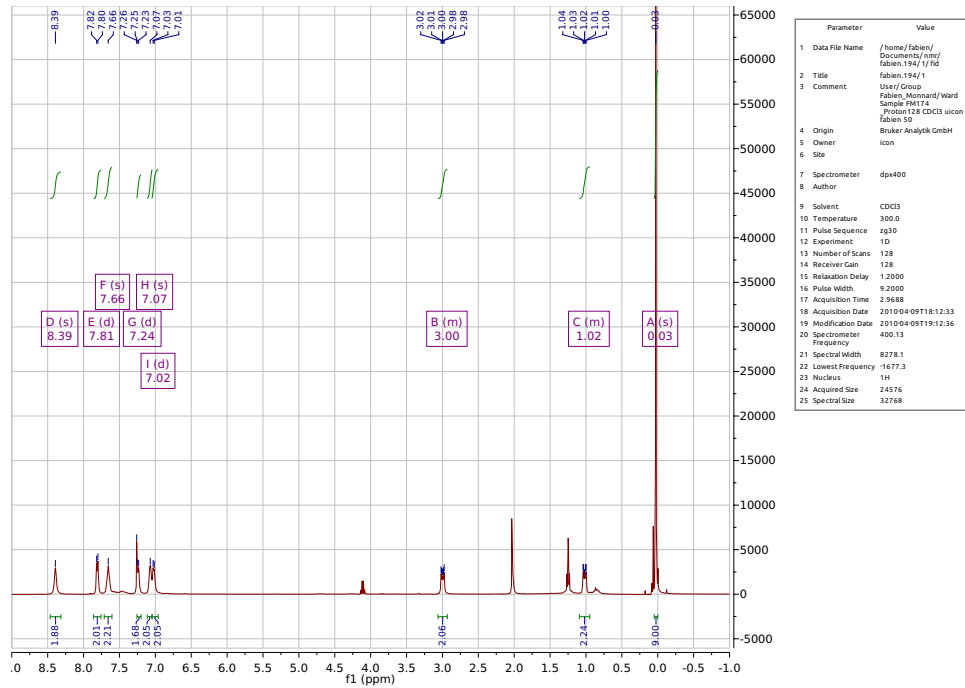


N-(4-(Methylsulfonyl)phenyl)-*N*-(pyridin-2-yl)pyridine-2-amine (**50**)





N-(Pyridine-2-yl)-*N*-(4-((2-(trimethylsilyl)ethyl)sulfonyl)phenyl)pyridin-2-amine (51)





BRUKER FTMS 4.7T BioAPEX II MS-Service UNI-Fribourg

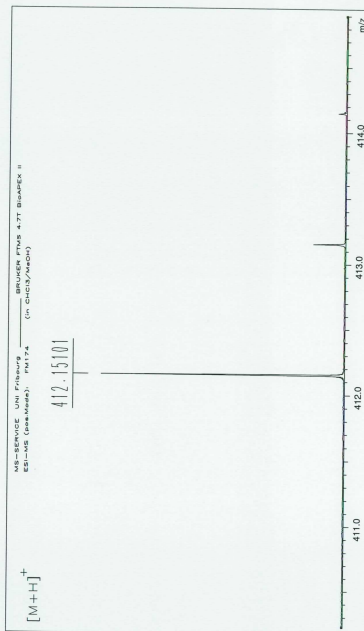
ESI-MS: FM174

XMSS Mass Analysis for /Data/UNI_BS/MONN5445_ESI/10/pdata/1/massanal.res:
 XMSS Mass Analysis Constraints

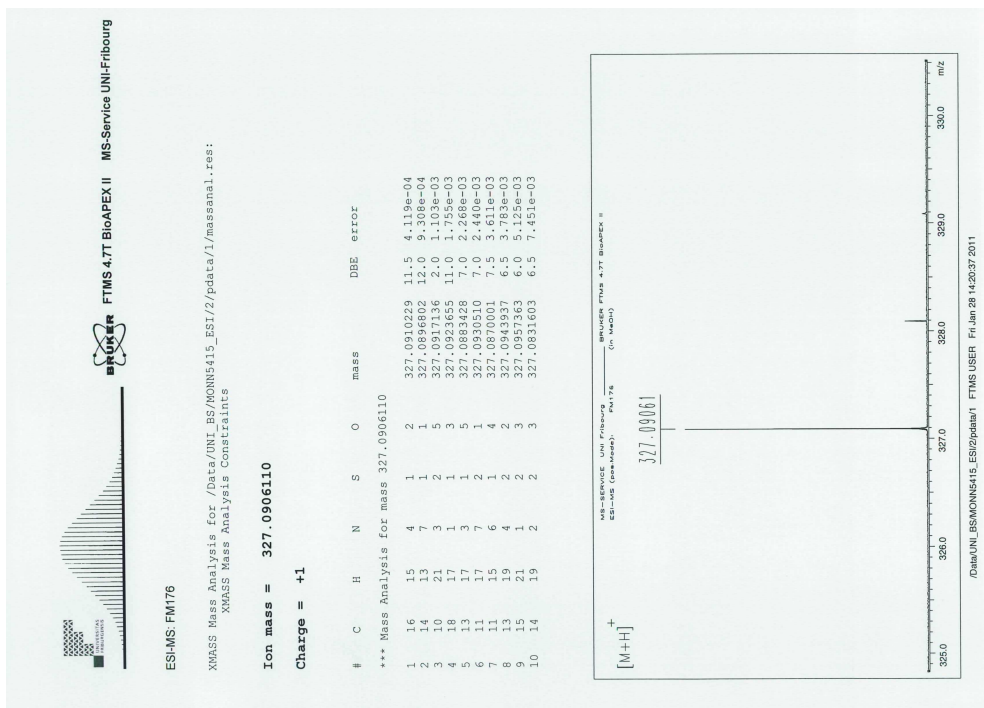
Ion mass = 412.1510130

Charge = +1

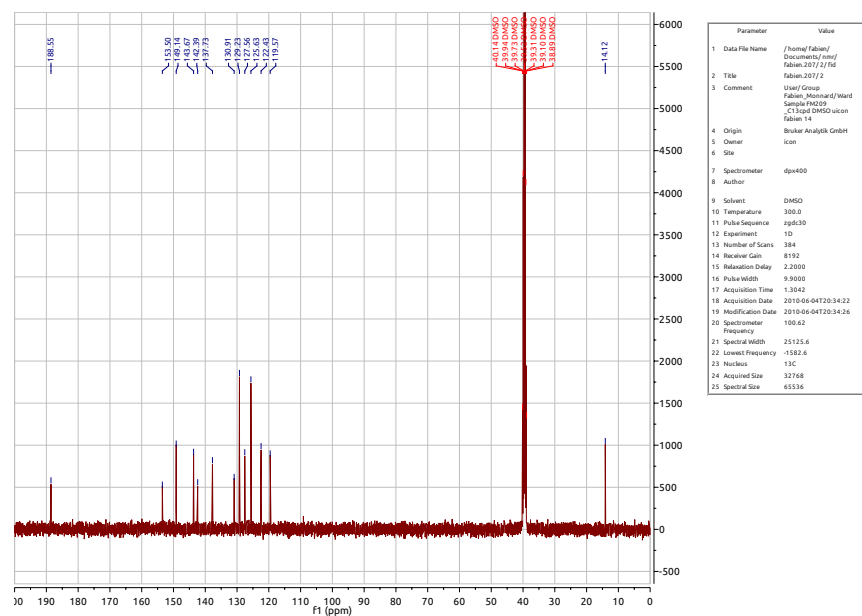
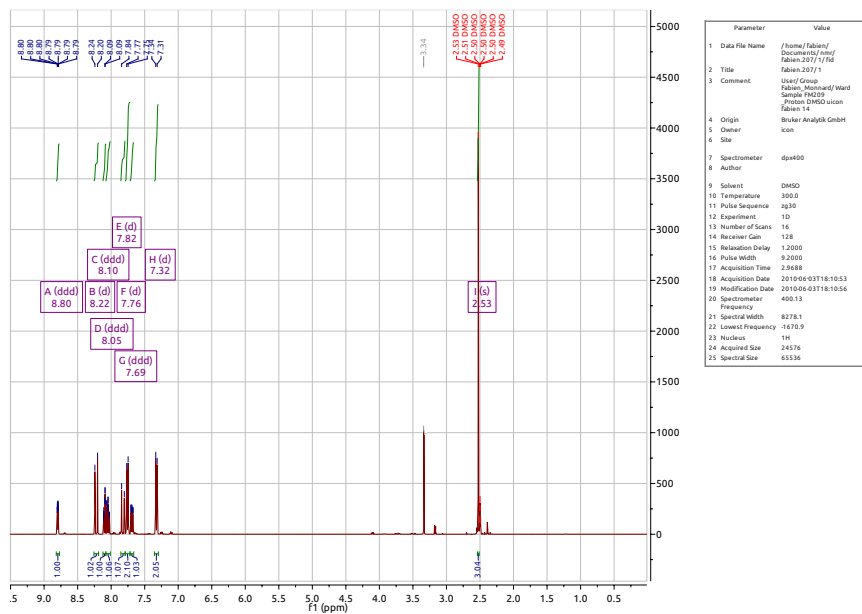
#	C	H	N	O	S	SI	mass	DBE	error
*** Mass Analysis for mass 412.1510130									
1	21	26	3	2	1	1	412.1509507	11.5	6.226e-05
2	14	32	5	1	1	2	412.1510130	2.0	3.989e-04
3	14	32	2	6	1	2	412.1514119	2.0	3.989e-04
4	15	32	2	5	2	1	412.1516415	2.0	6.285e-04
5	13	30	5	4	2	1	412.1502988	2.5	7.142e-04
6	12	30	5	5	1	2	412.1502988	2.5	9.437e-04
7	14	36	2	2	2	3	412.1520508	1.0	1.038e-03
8	19	24	6	1	1	1	412.1496081	12.0	1.405e-03
9	15	28	6	3	1	2	412.1526012	7.0	1.786e-03
10	9	30	5	3	1	1	412.1526012	-1.5	1.786e-03

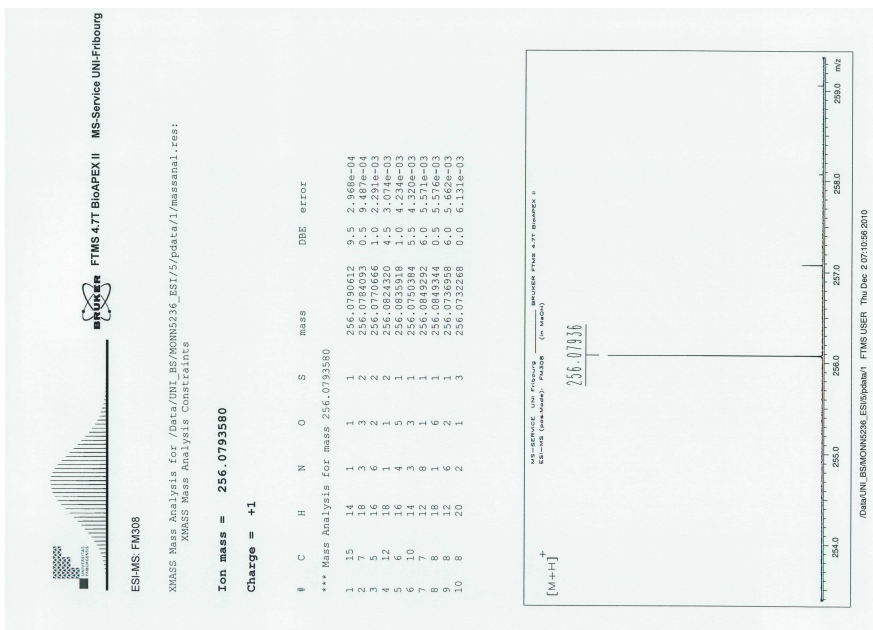


/Data/UNI_BS/MONN5445_ESI/10/pdata/1 FTMS USER Wed Feb 9 14:25:30 2011

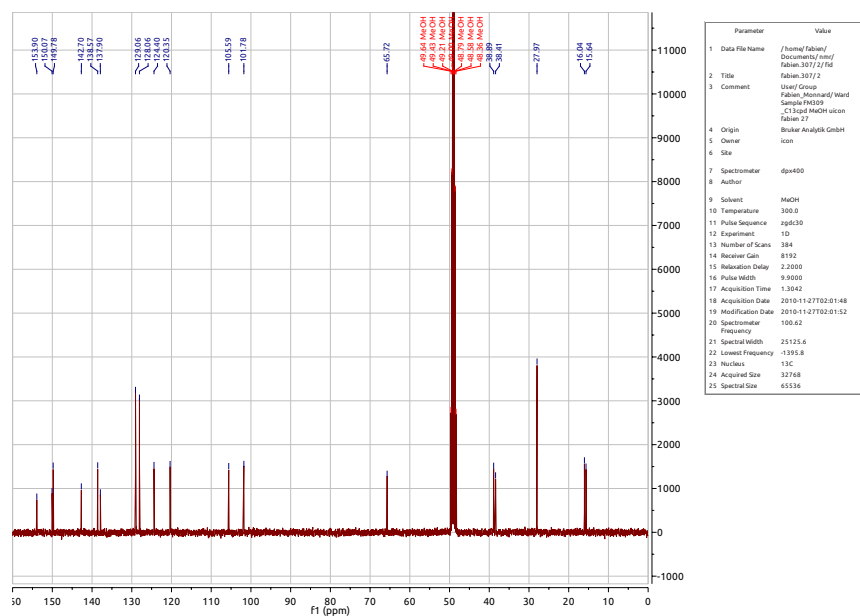
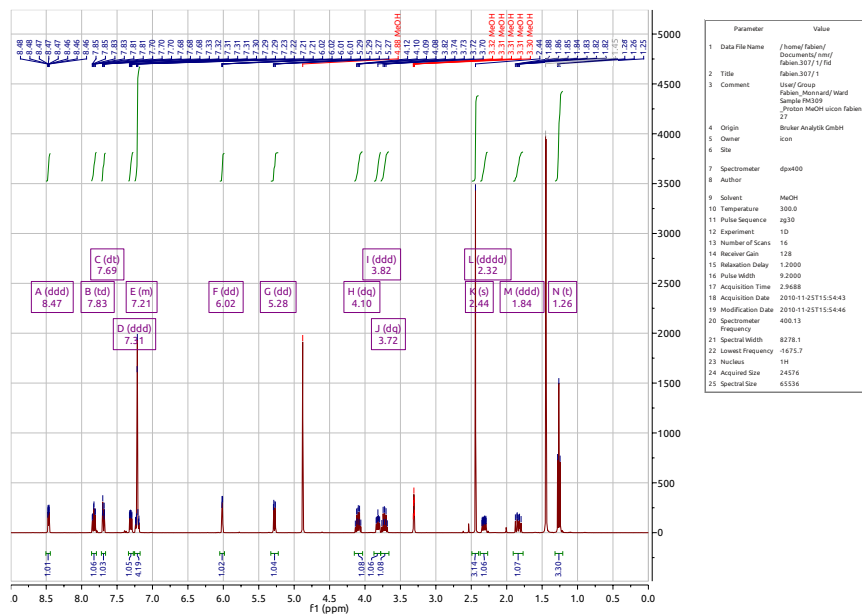


(*E*)-3-(4-(Methylthio)phenyl)-1-(pyridin-2-yl)prop-2-en-1-one (55)





2-(6-Ethoxy-4-(4-(methylthio)phenyl)-5,6-dihydro-2H-pyran-2-yl)pyridine (**56**)



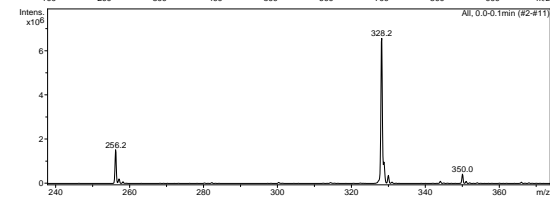
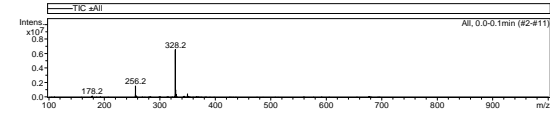
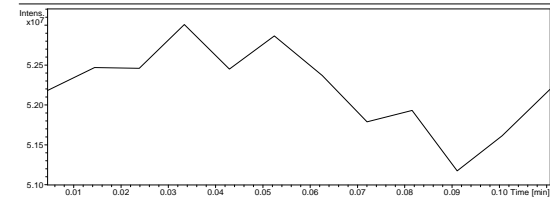
Display Report

Analysis Info

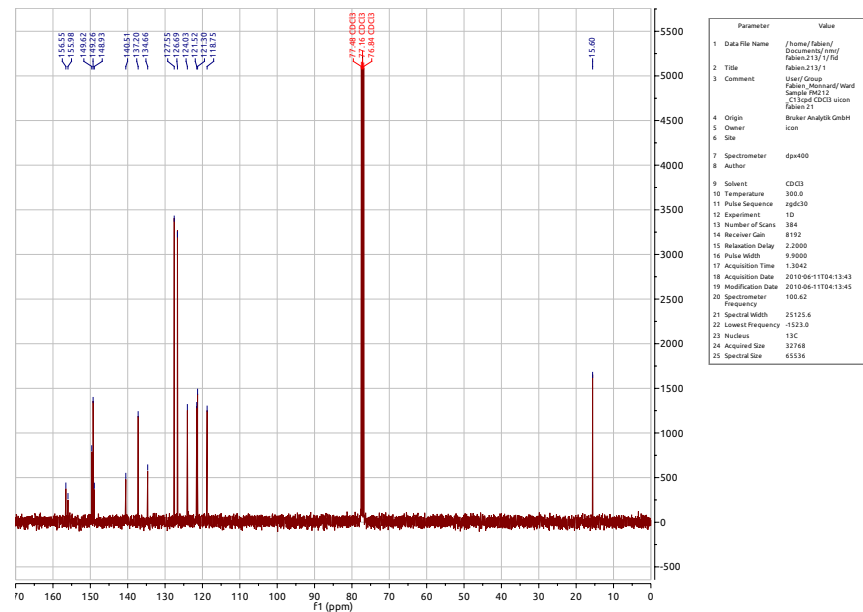
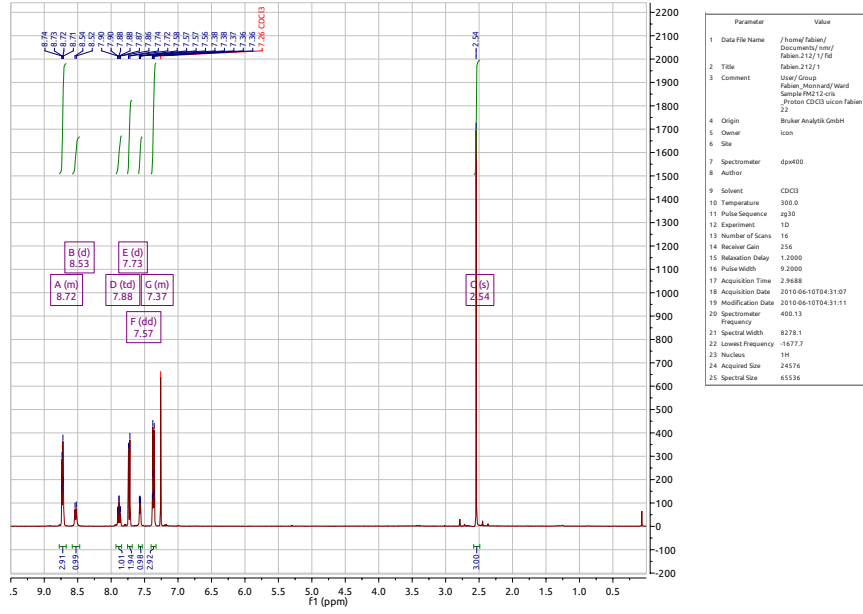
Analysis Name	FM000171.d	Acquisition Date	06/14/10 17:01:36
Method	Copy(2) of E3Kp Default.ms	Operator	Administrator
Sample Name	FM196	Instrument	esquire3000plus_01096
Comment			

Acquisition Parameter

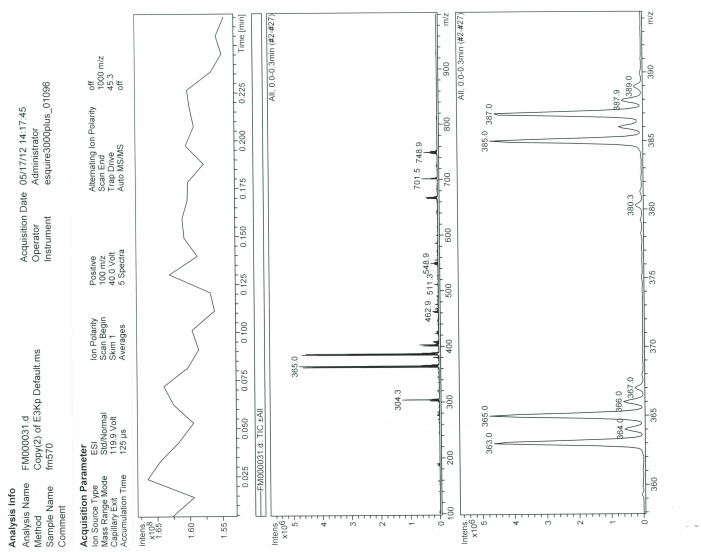
Ion Source Type	ESI	Ion Polarity	Positive	Alternating Ion Polarity	off
Mass Range Mode	Std/Normal	Scan Begin	100 m/z	Scan End	1000 m/z
Capillary Exit	113.5 Volt	Scan 1	40.0 Volt	Trap Drive	38.9
Accumulation Time	388 μ s	Averages	5 Spectra	Auto MS/MS	off



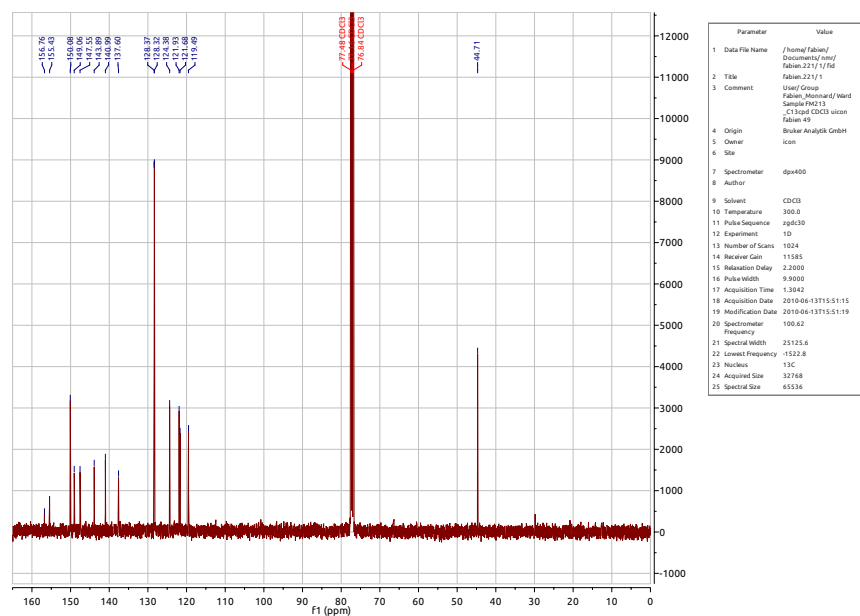
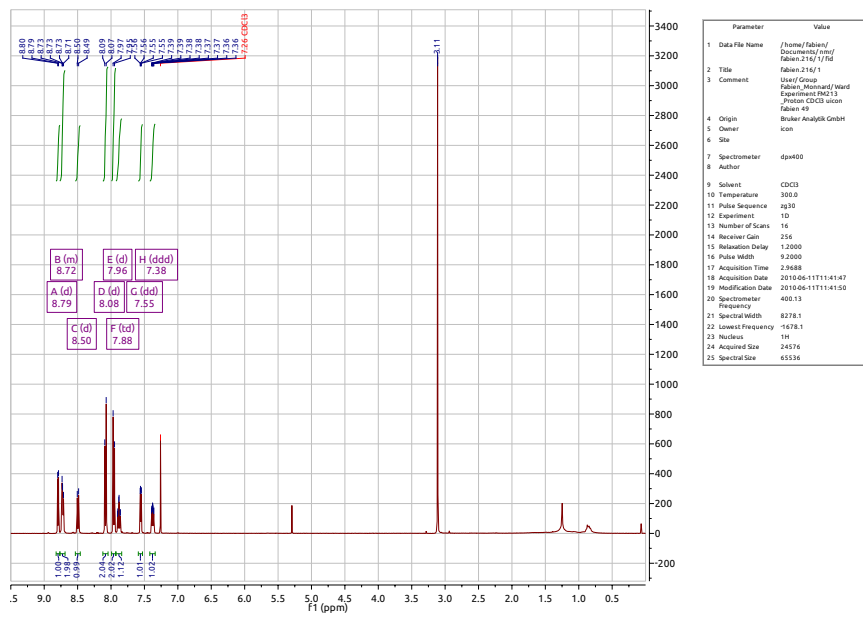
(4-(4-(Methylthio)phenyl)-2,2'-bipyridine (52)



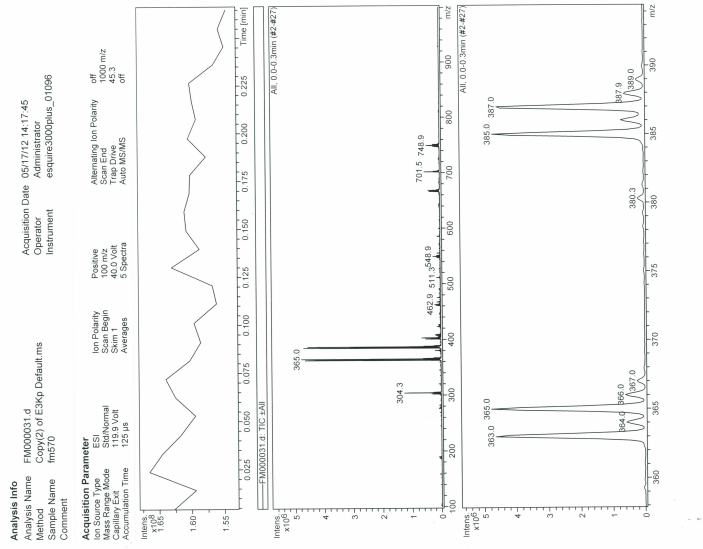
Display Report



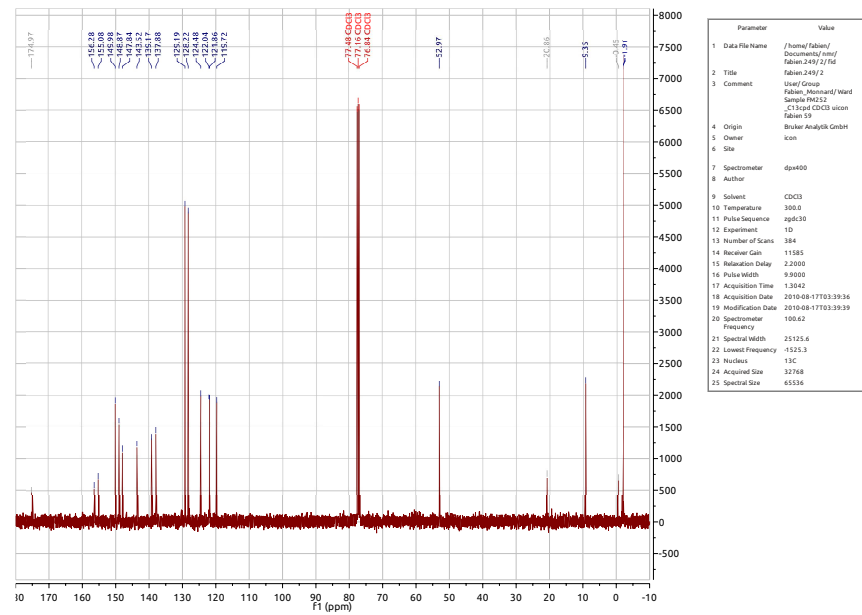
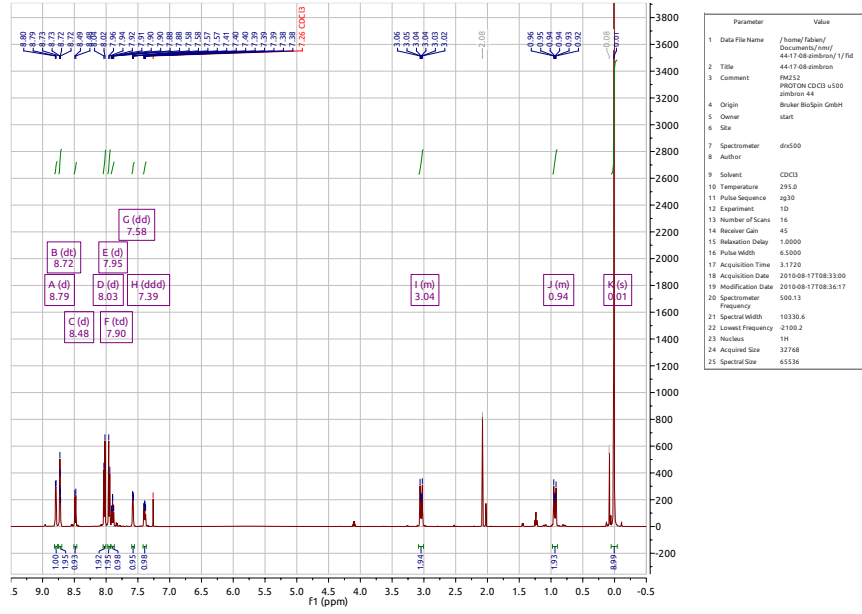
(4-(4-(Methylsulfonyl)phenyl)-2,2'-bipyridine (57)

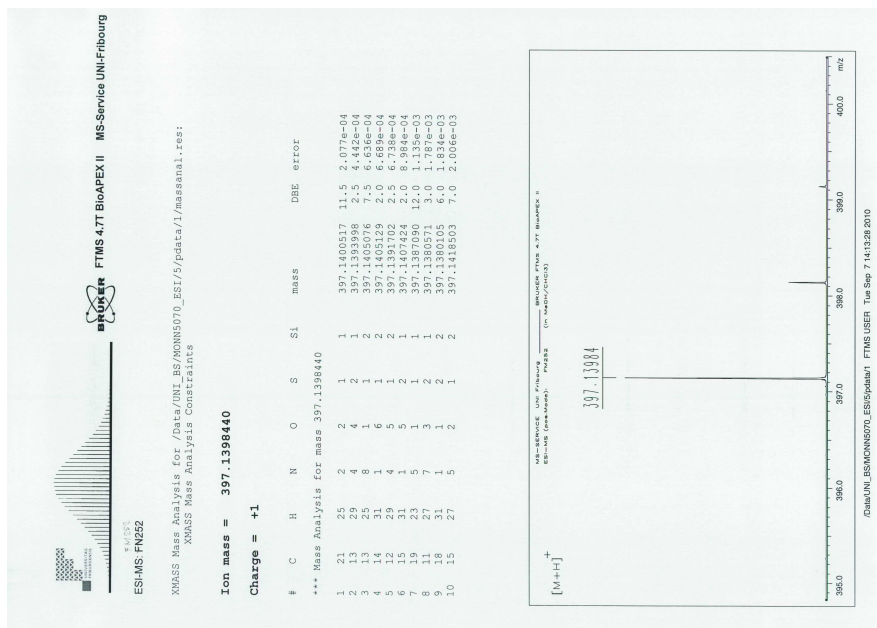


Display Report

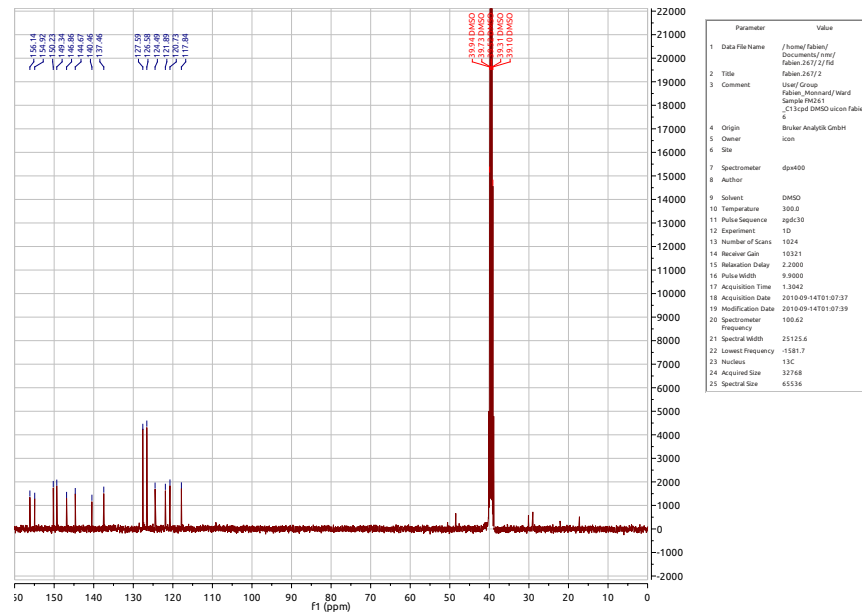
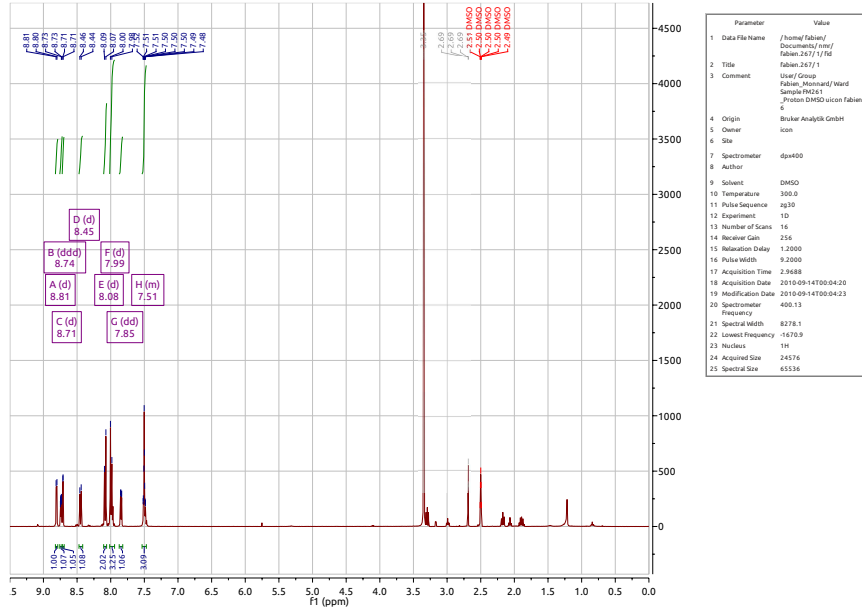


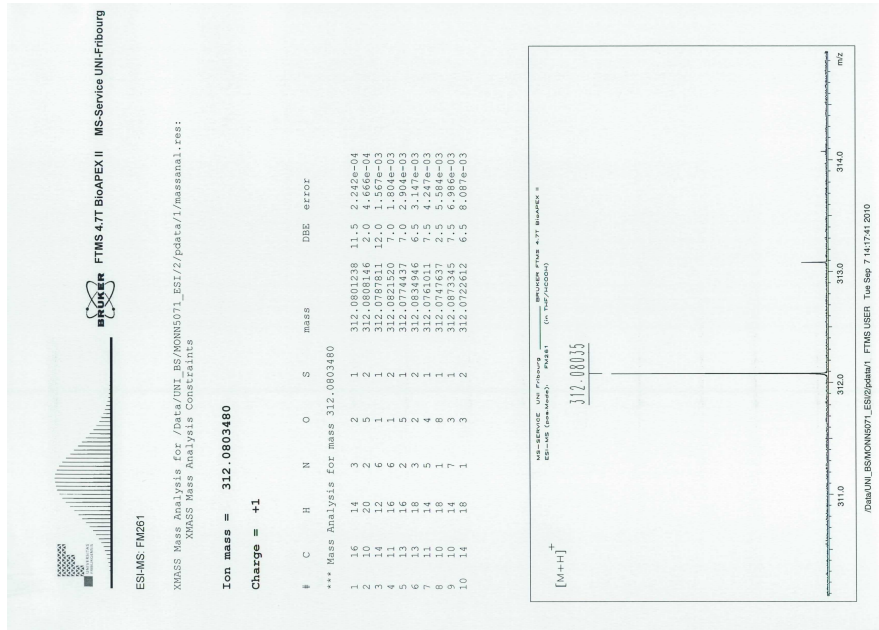
(4-(4-((2-(Trimethylsilyl)ethyl)sulfonyl)phenyl)-2,2'-bipyridine (58)



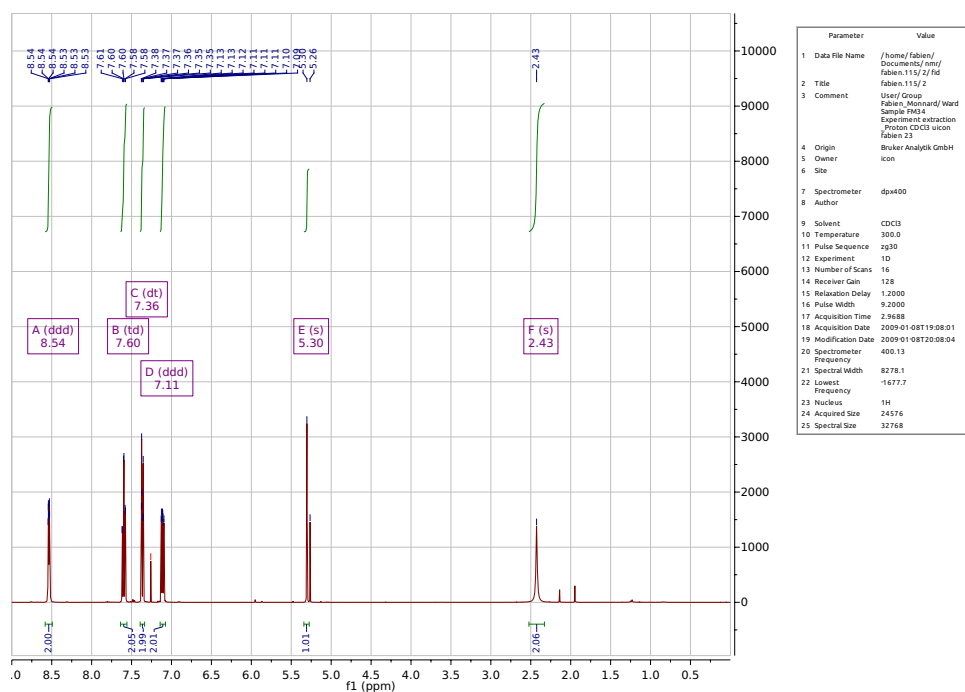


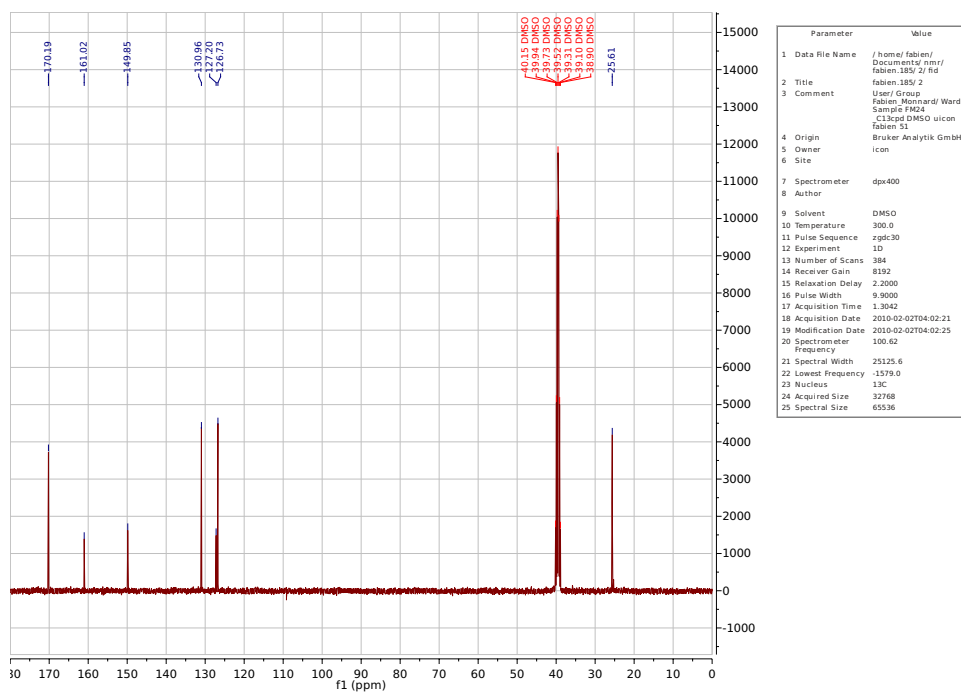
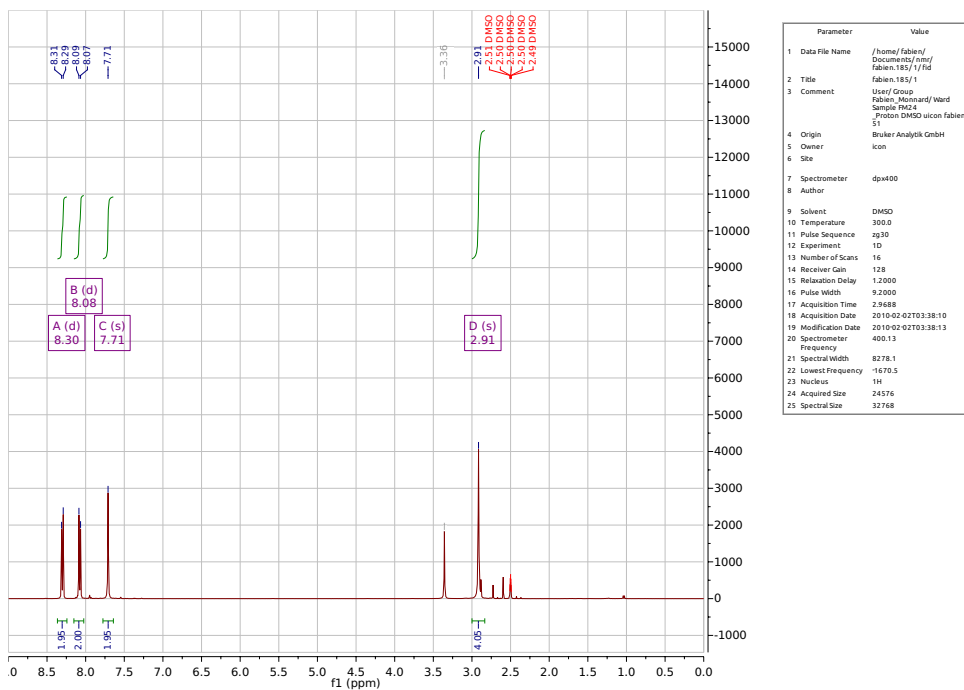
(4-((2,2'-Bipyridine)4-yl)benzenesulfonamide (**3**)

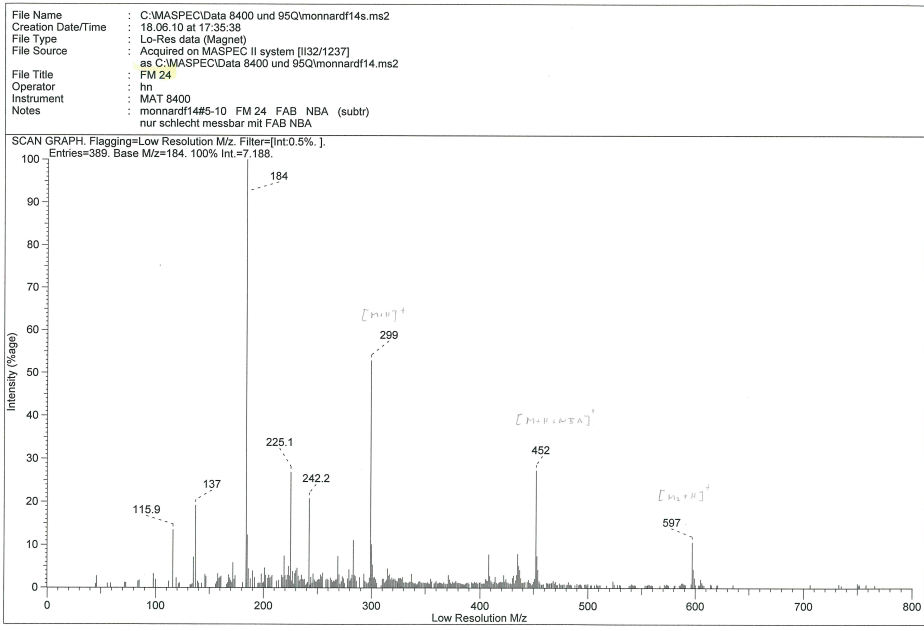




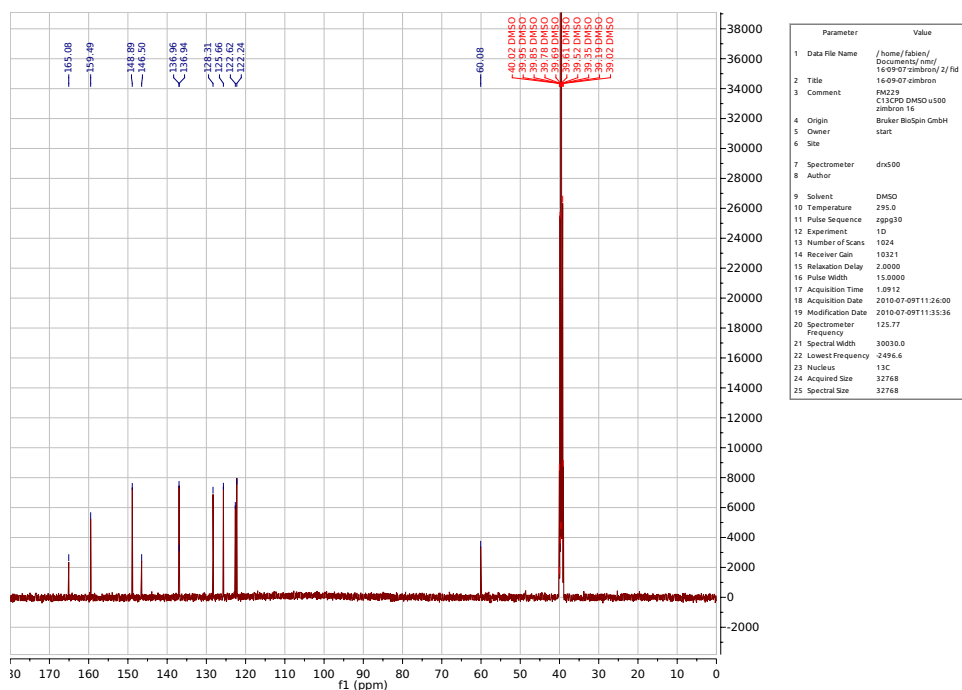
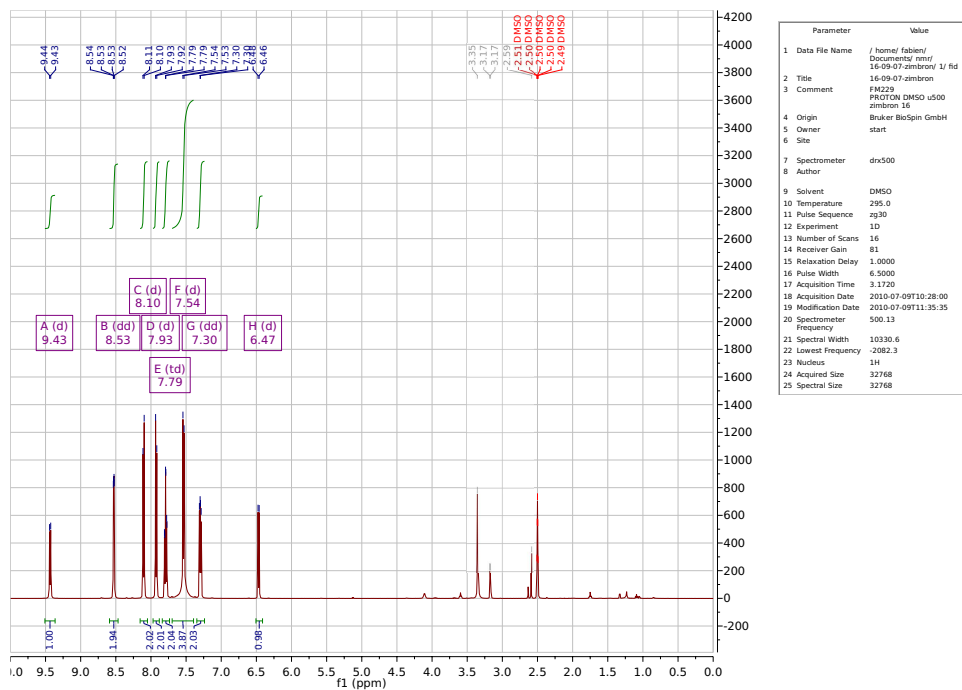
Bis(pyridine-2-yl)methanamine (60)



N-(Di(2-pyridyl)methyl)-amidobenzene-4-sulfonamide (**61**)

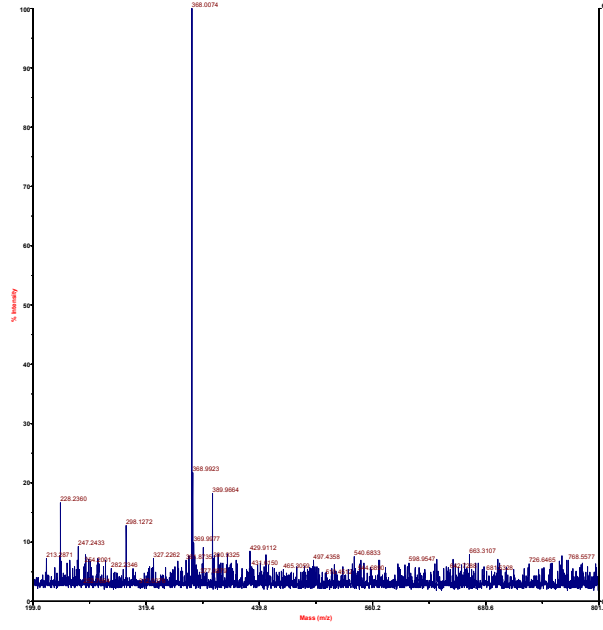


N-(Di(2-pyridyl)methyl)-amidobenzene-4-sulfonamide (4)



13 march SN 6181

Voyager Spec #1(BP = 368.0, 648)



Mode of operation: Reflector
Extraction mode: Delayed
Polarity: Positive
Acquisition control: Manual

Accelerating voltage: 20000 V
Grid voltage: 75%
Mirror voltage ratio: 1.12
Guide wire Ø: 0.1%
Extraction delay time: 50 nsec

Acquisition mass range: 200 -- 800 Da
Number of laser shots: 200/spectrum
Laser intensity: 1730
Laser Rep. Rate: 20.0 Hz
Calibration type: External -- D:\giese\user\Calibration\porph_pos.cal
Calibration matrix: 2,5-Dihydroxybenzoic acid
Low mass gate: Off
Timed ion selector: Off

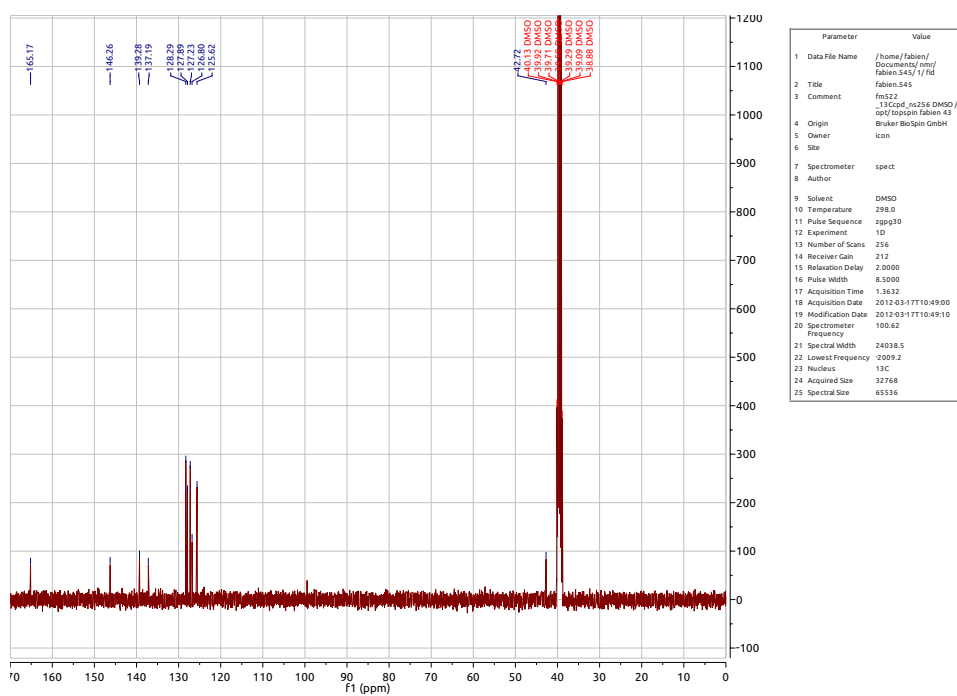
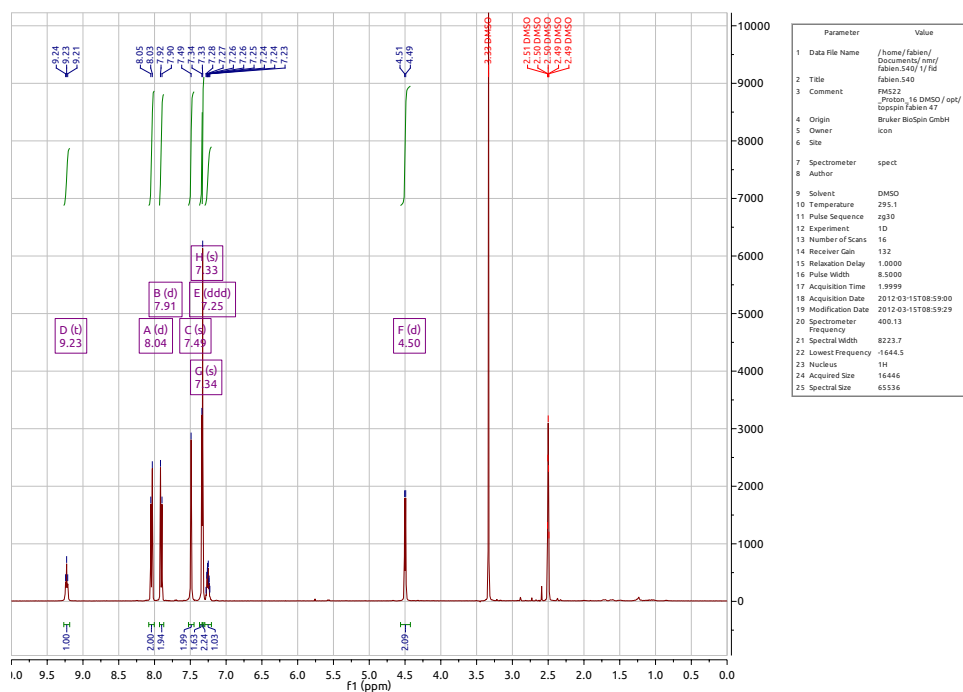
Digitizer start time: 14.3005
Bin size: 0.5 nsec
Number of data points: 28303
Vertical scale Ø: 500 mV
Vertical offset: 0.5%
Input bandwidth Ø: 500 MHz

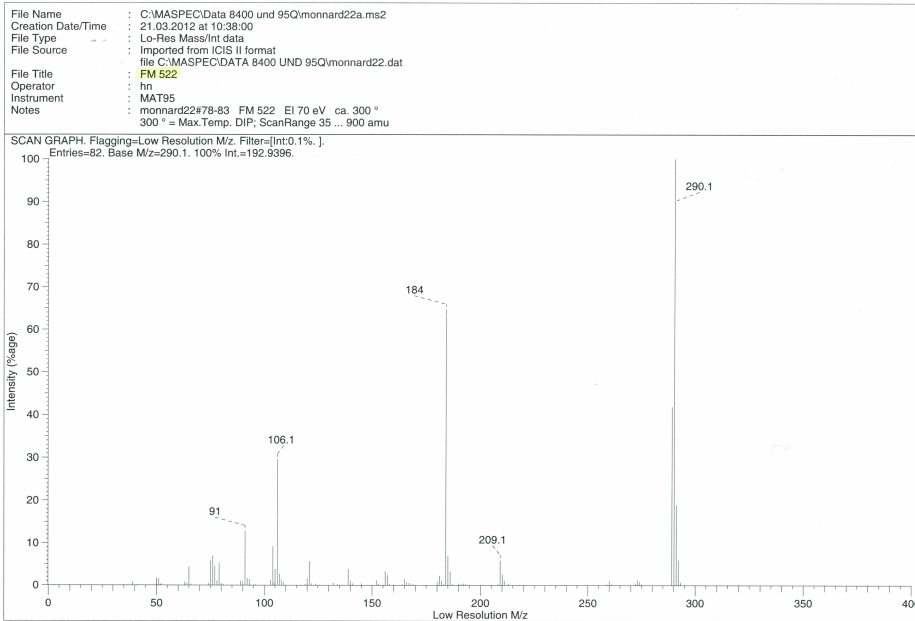
Sample well: 34
Plate ID: PLATE1
Serial number: 6181
Instrument name: Voyager-DE PRO
Plate type filename: C:\VOYAGER\100 well plate.pit
Lab name: Dep. Chemie

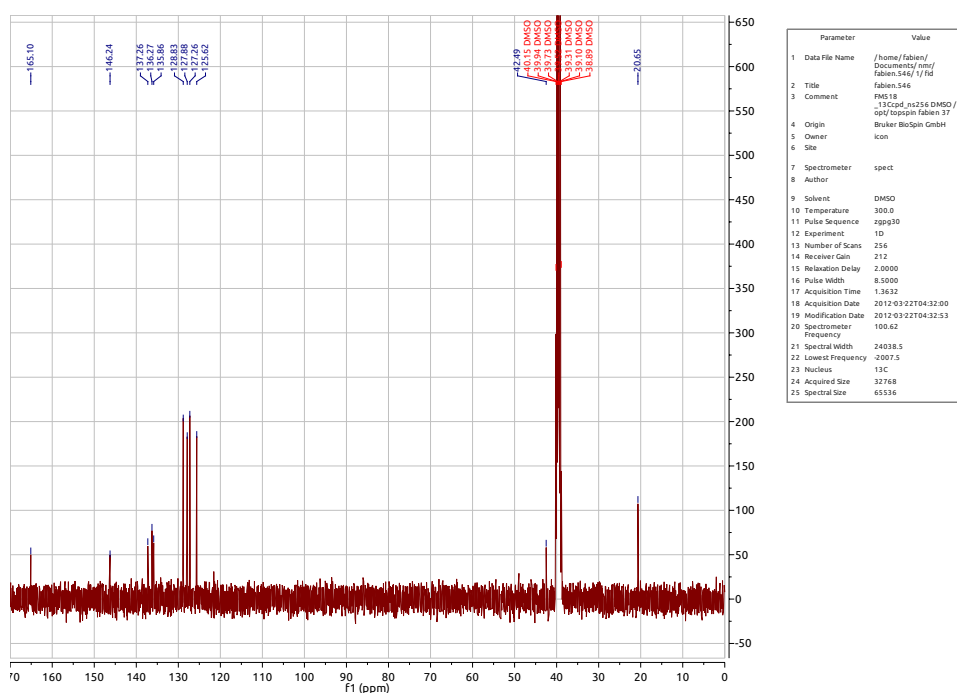
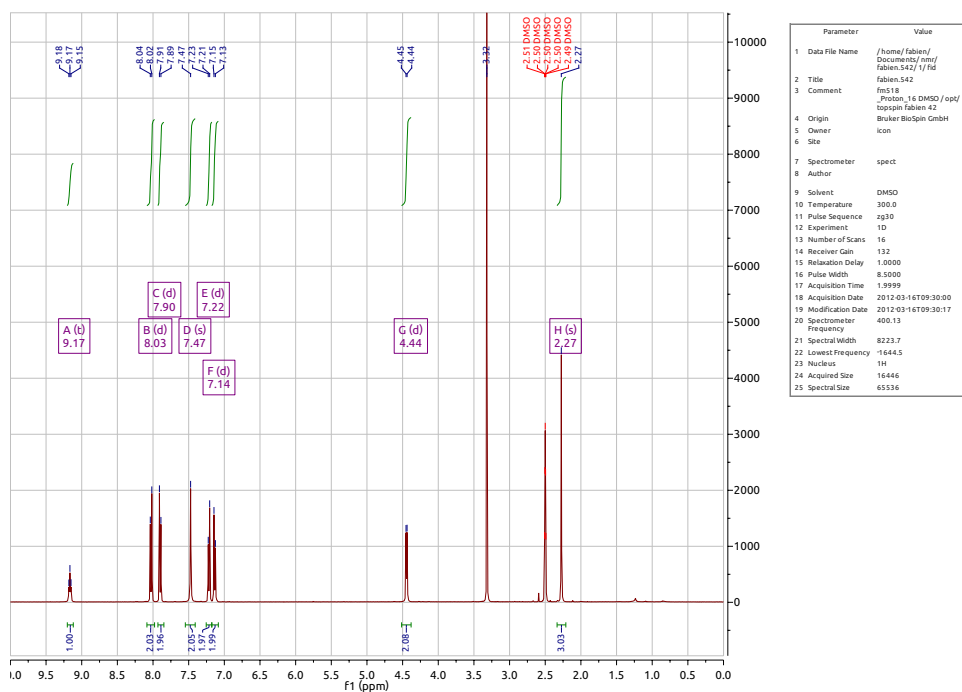
Absolute x-position: 17834
Absolute y-position: 33060.5
Relative x-position: 1106.48
Relative y-position: 992.96
Shots in spectrum: 200
Source pressure: 8.146e-007
Mirror pressure: 2.583e-007
TCZ pressure: 0.006484
TIS gate width: 8
TIS flight length: 687.7

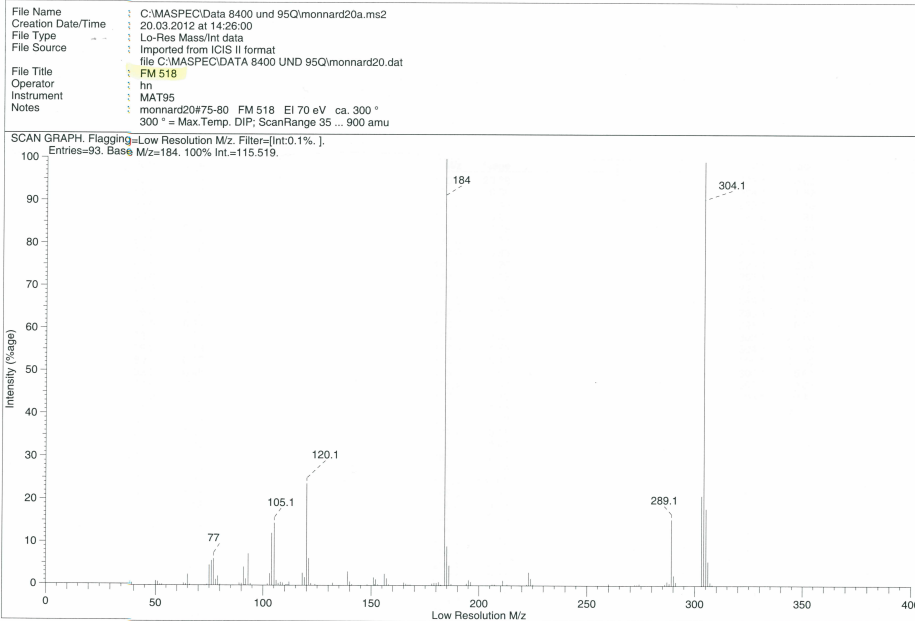
Acquired: 10:18:00, July 09, 2010
D:\giese\user\Ward\Fabien\fm229_0001.dat

Printed: 10:21, July 09, 2010

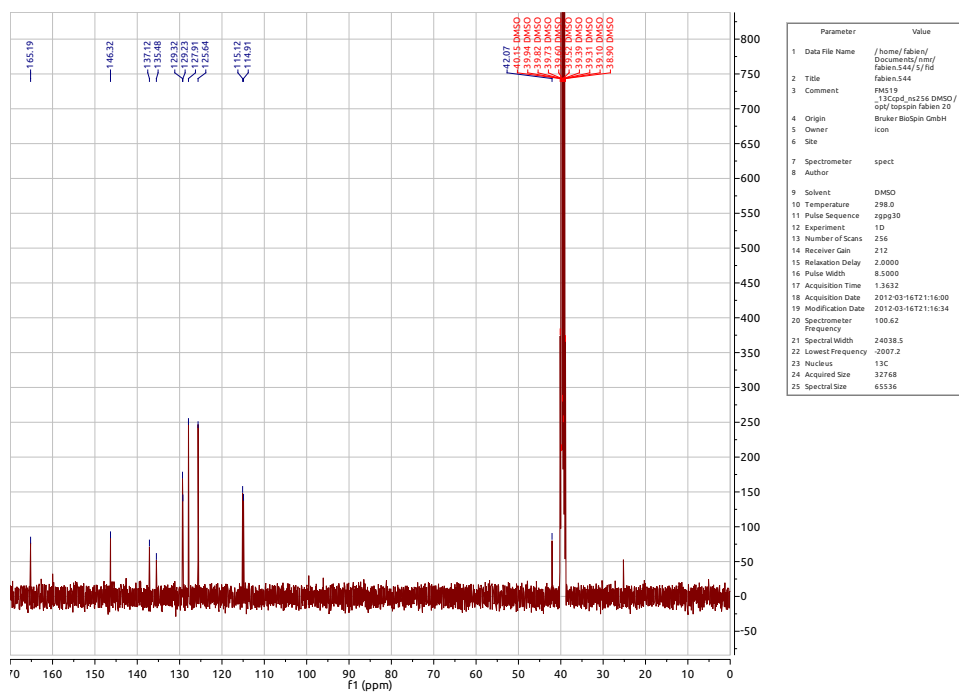
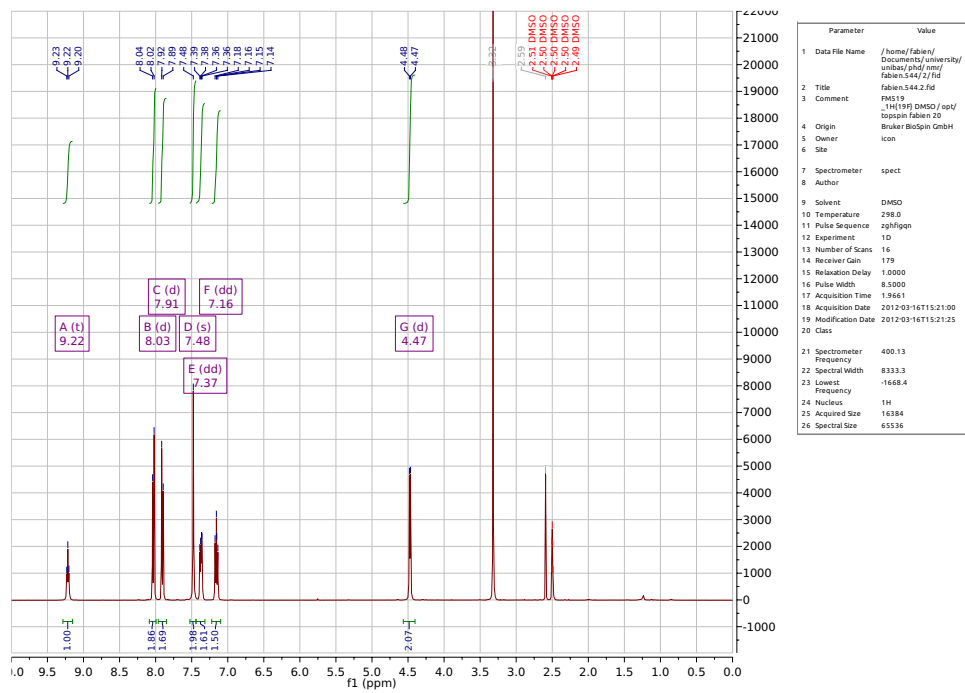
N-Benzyl-4-sulfamoylbenzamide (40)

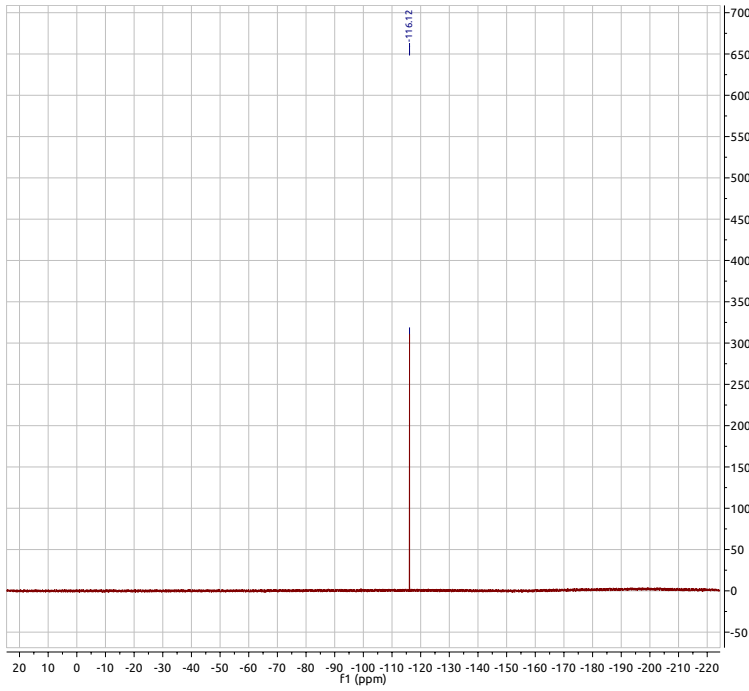


N-(4-Methylbenzyl)-4-sulfamoylbenzamide (**42**)



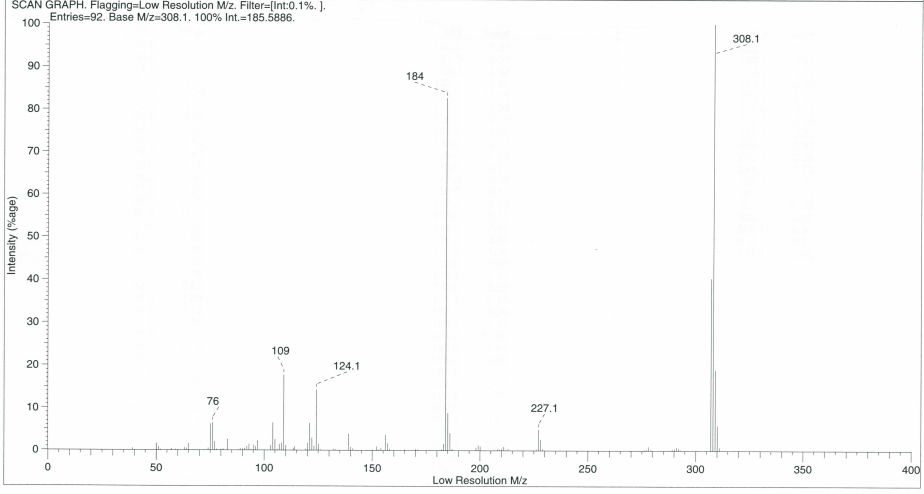
N-(4-Fluorobenzyl)-4-sulfamoylbenzamide (**43**)

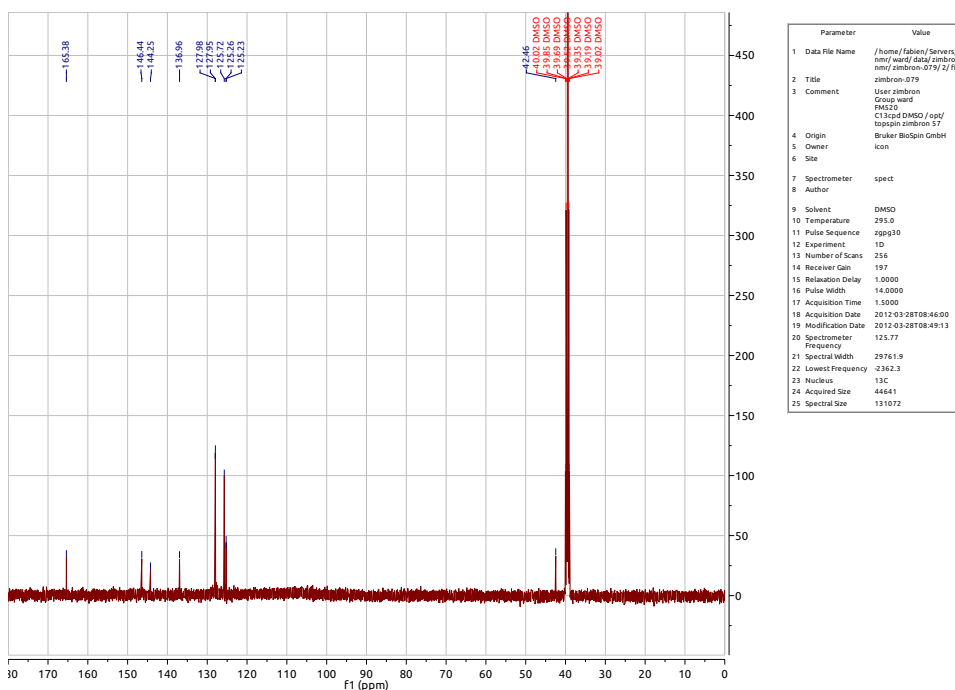
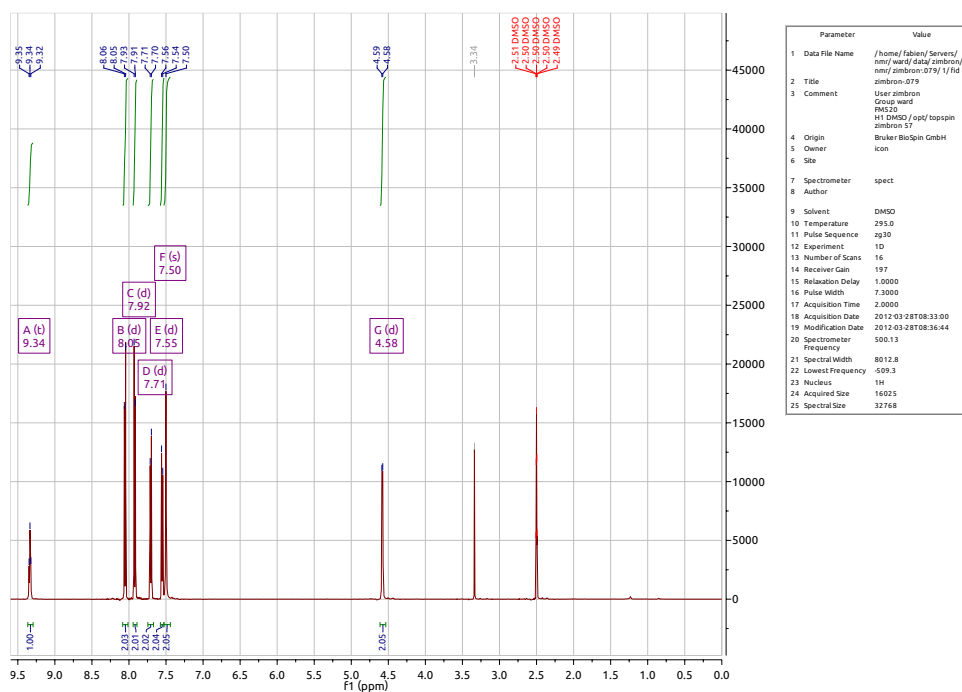


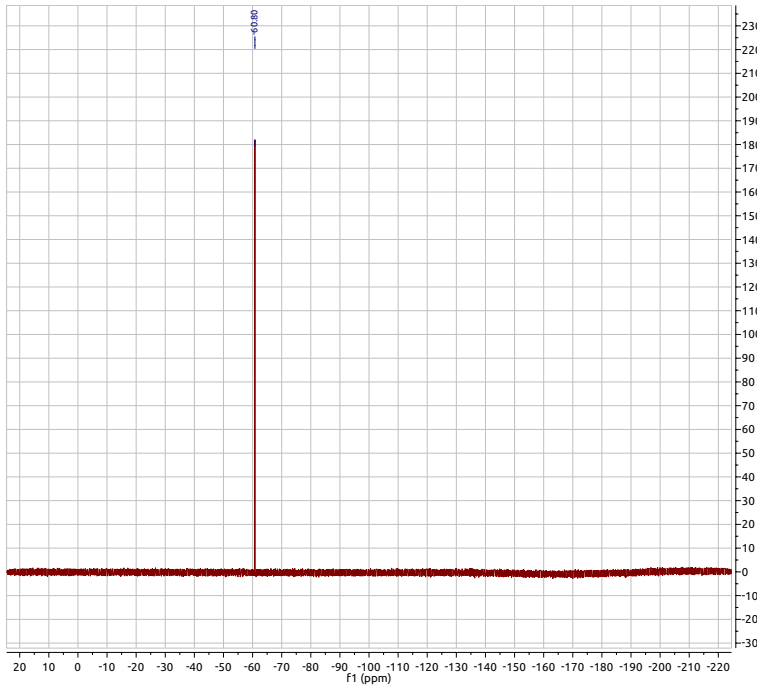


Parameter	Value
1 Data File Name	/home/fabien/Documents/fabien.544/1d
2 Title	Fabien.544
3 Comment	FM519
4 Origin	319F1H DMSO / opt / topspin Fabien 20
5 Owner	Bruker BioSpin GmbH
6 Site	kon
7 Spectrometer	spect
8 Author	
9 Solvent	DMSO
10 Temperature	298.1
11 Pulse Sequence	zgpgpgn.2
12 Experiment	1D
13 Number of Scans	16
14 Receiver Gain	212
15 Relaxation Delay	1.5000
16 Pulse Width	13.0000
17 Acquisition Time	1.3982
18 Acquisition Date	2012-03-16T15:23:00
19 Modification Date	2012-03-16T15:23:30
20 Spectrometer Frequency	376.46
21 Spectral Width	93750.0
22 Lowest Frequency	-86324.8
23 Nucleus	1H
24 Acquired Size	131072
25 Spectral Size	262144

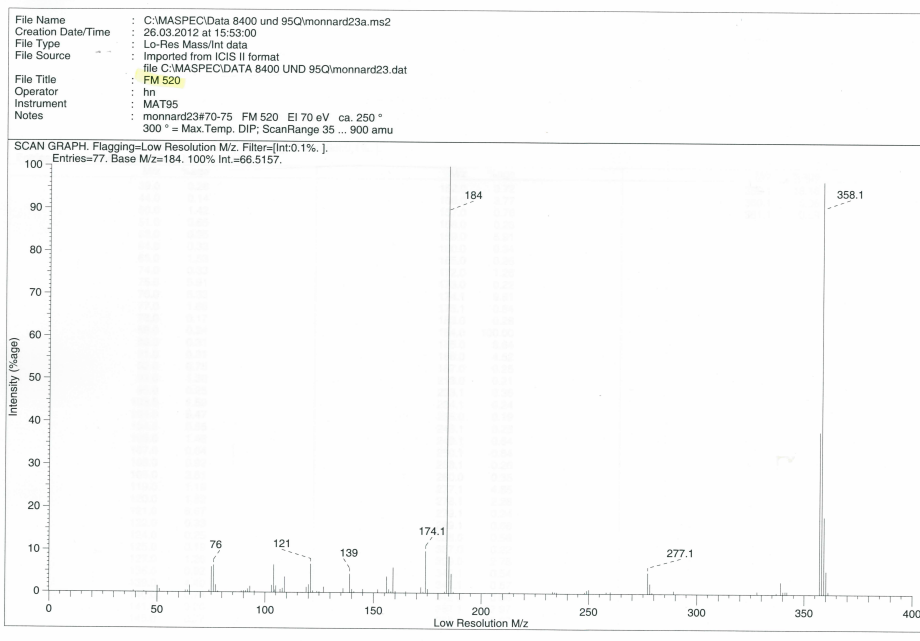
File Name : C:\MASPEC\Data 8400 und 95Q\monnard21a.ms2
 Creation Date/Time : 20.03.2012 at 14:52:00
 File Type : Lo-Res Mass/Int data
 File Source : Imported from ICIS II format
 file C:\MASPEC\DATA 8400 UND 95Q\monnard21.dat
 File Title : FM 519
 Operator : hn
 Instrument : MAT95
 Notes : monnard21#75-80 FM 519 EI 70 eV ca. 300 °
 300 ° = Max.Temp. DIP; ScanRange 35 ... 900 amu

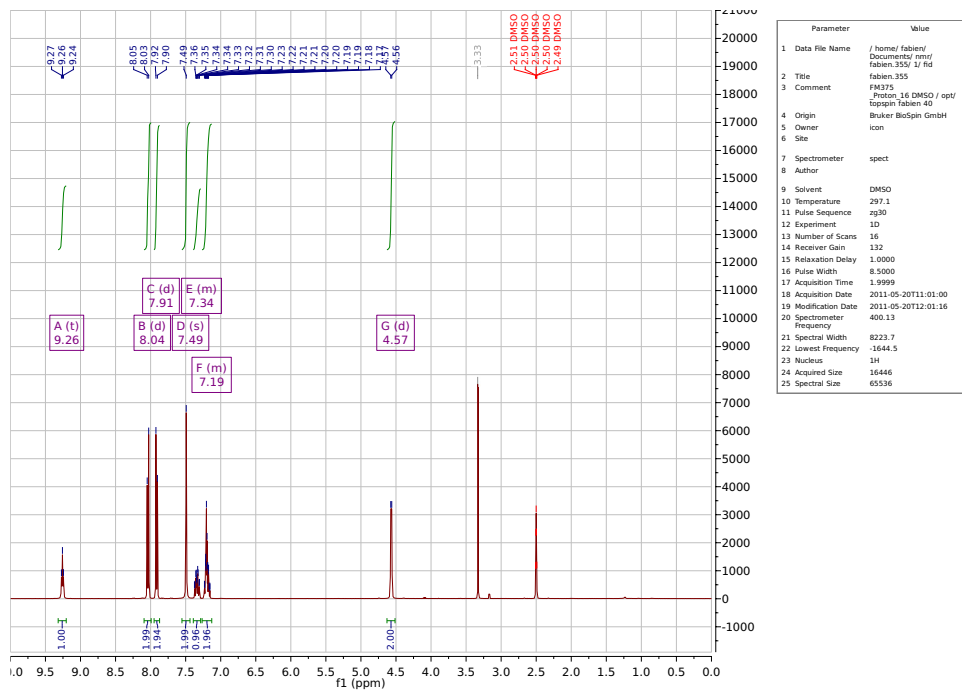


N-(4-(Trifluoromethyl)benzyl)-4-sulfamoylbenzamide (44)

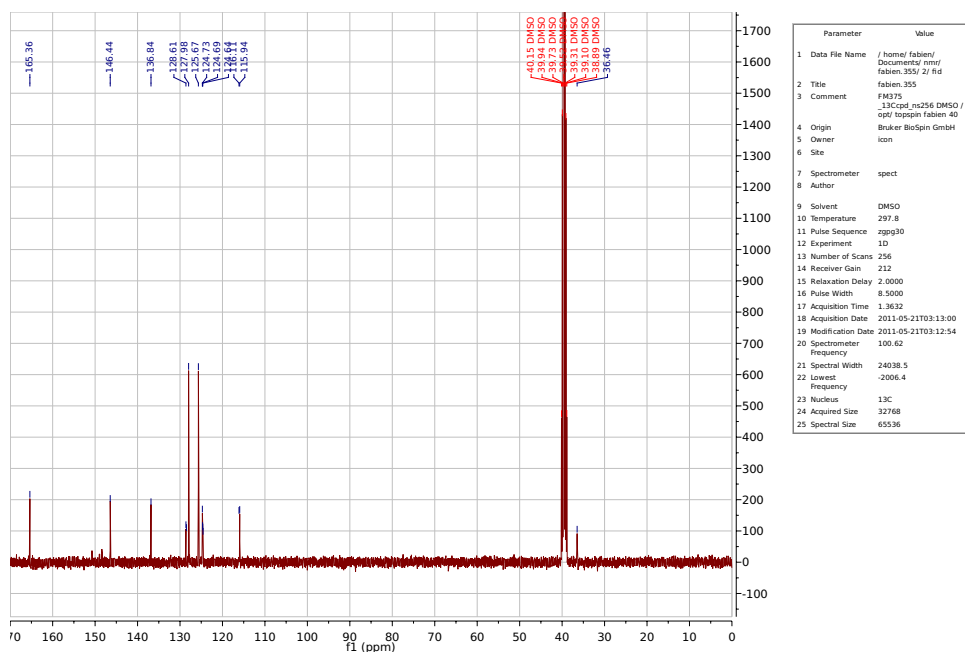


Parameter	Value
1 Data File Name	/home/fabien/Documents/nmr/fabien.552/zf/fd
2 Title	fabien.552
3 Comment	FM520 19F(1H) DMSO /op/ topspin fabien 4
4 Origin	Brüker BioSpin GmbH
5 Owner	icon
6 Size	
7 Spectrometer	spect
8 Author	
9 Solvent	DMSO
10 Temperature	300.0
11 Pulse Sequence	zgpg30g2
12 Experiment	1D
13 Number of Scans	16
14 Receiver Gain	212
15 Relaxation Delay	1.5000
16 Pulse Width	13.0000
17 Acquisition Time	1.3892
18 Acquisition Date	2012-03-23T15:42:00
19 Modification Date	2012-03-23T15:42:35
20 Spectrometer Frequency	376.46
21 Spectral Width	93750.0
22 Lowest Frequency	84524.8
23 Nucleus	19F
24 Acquired Size	131072
25 Spectral Size	262144



N-(2,3-Difluorobenzyl)-4-sulfamoylbenzamide (45)

Parameter	Value
1 Data File Name	/home/fabien/Documents/renu/fabien.355/1/rd
2 Title	fabien.355
3 Comment	FM375
4 Origin	Proton_16 DMSO / opt/
5 Owner	topspin fabien.40
6 Site	icon
7 Spectrometer	spect
8 Author	
9 Solvent	DMSO
10 Temperature	297.1
11 Pulse Sequence	zg30
12 Experiment	1D
13 Number of Scans	16
14 Receiver Gain	132
15 Relaxation Delay	1.0000
16 Pulse Width	8.5000
17 Acquisition Time	1.9999
18 Acquisition Date	2011-05-20T11:01:00
19 Modification Date	2011-05-20T12:01:16
20 Spectrometer Frequency	400.13
21 Spectral Width	8223.7
22 Lowest Frequency	1644.5
23 Nucleus	1H
24 Acquired Size	16446
25 Spectral Size	65536



Parameter	Value
1 Data File Name	/home/fabien/Documents/renu/fabien.355/2/rd
2 Title	fabien.355
3 Comment	FM375
4 Origin	13Cced, ns256 DMSO /
5 Owner	opt/ topspin fabien.40
6 Site	icon
7 Spectrometer	spect
8 Author	
9 Solvent	DMSO
10 Temperature	297.8
11 Pulse Sequence	zgpg30
12 Experiment	1D
13 Number of Scans	256
14 Receiver Gain	212
15 Relaxation Delay	2.0000
16 Pulse Width	8.5000
17 Acquisition Time	1.3632
18 Acquisition Date	2011-05-21T03:13:00
19 Modification Date	2011-05-21T03:12:54
20 Spectrometer Frequency	100.62
21 Spectral Width	24038.5
22 Lowest Frequency	-2006.4
23 Nucleus	13C
24 Acquired Size	32768
25 Spectral Size	65536

¹³C NMR (101 MHz, DMSO) δ 165.36, 146.44, 136.84, 128.61, 128.49, 127.98, 125.67, 124.73, 124.69, 124.64, 124.57, 116.11, 115.94, 40.15, 39.94, 39.73, 39.52, 39.31, 39.10, 38.89, 36.46.



BRUKER FTMS 4.7T BioAPEX II MS-Service UNI-Fribourg

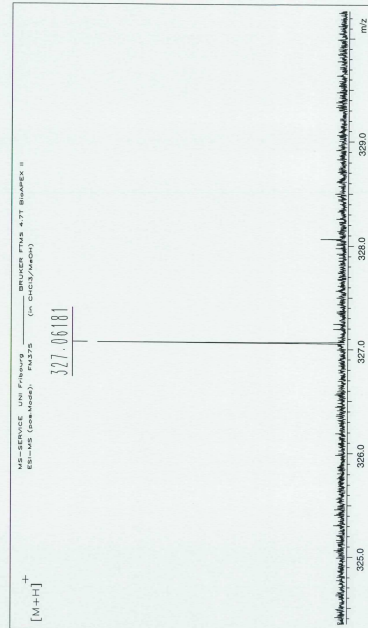
ESI/MS: FM375

XMSS Mass Analysis for /Data/UNI_BS/MONN5756_ESI/3/pdata/1/massanal.res:
 XMSS Mass Analysis Constraints

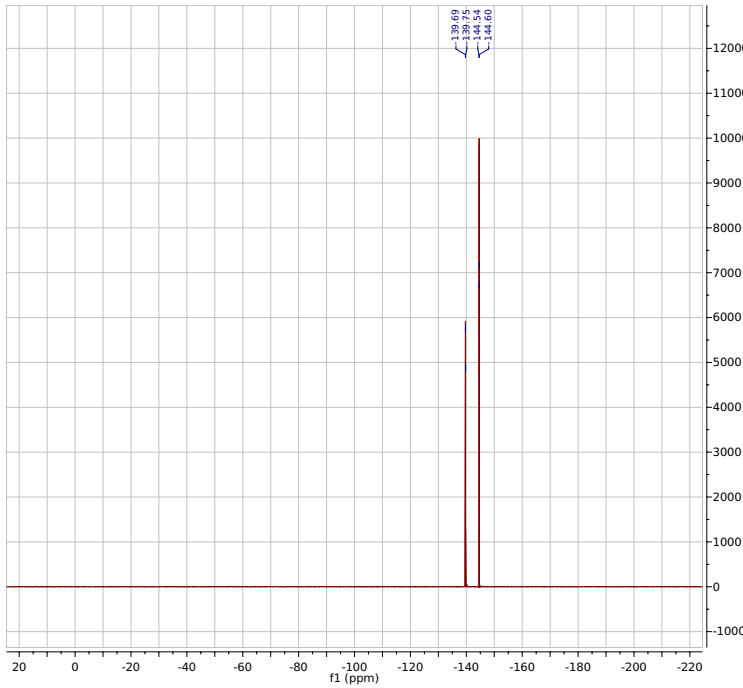
Ion mass = 327.0618140

Charge = +1

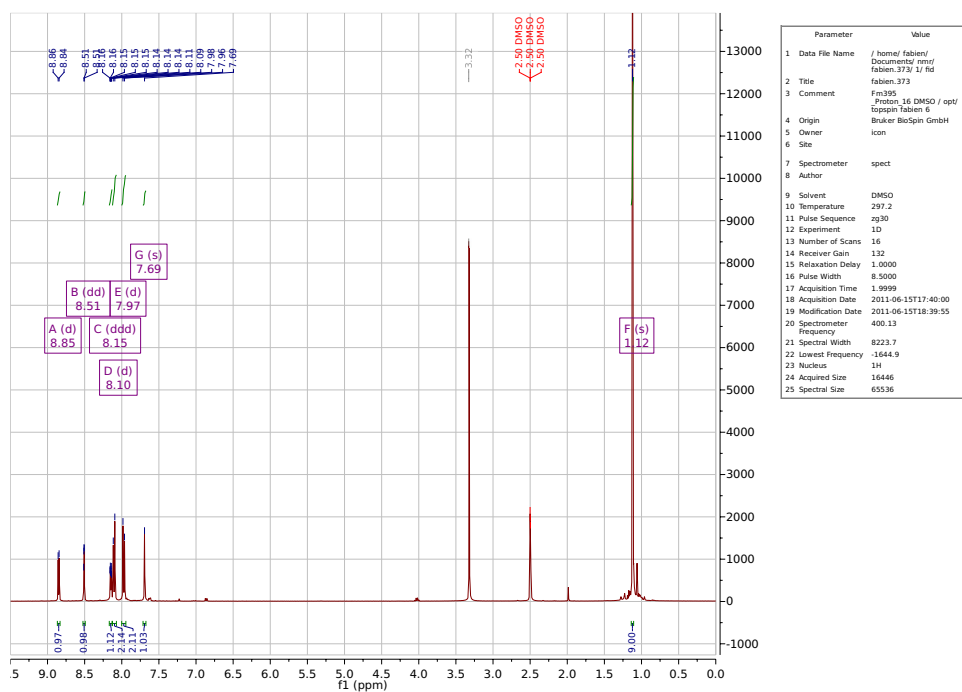
#	C	H	F	N	O	S	mass	DBE	error
*** Mass Analysis for mass 327.0618140									
1	14	13	2	2	3	1	327.0609458	8.5	8.682e-04
2	1	1	1	2	2	2	327.0631738	7.5	1.360e-03
3	17	12	1	2	2	2	327.0631738	13.5	2.18e-03
4	11	17	2	2	3	2	327.0643166	13.5	2.18e-03
5	9	16	1	4	4	2	327.0591510	3.5	2.663e-03
6	12	19	2	1	1	3	327.0591341	3.0	2.680e-03
7	12	12	1	4	4	1	327.0557802	8.5	6.034e-03
8	15	15	2	1	1	2	327.0557633	8.0	6.542e-03
9	13	14	1	3	4	1	327.0683563	8.0	6.542e-03
10	7	19	2	3	3	3	327.0593114	-1.0	6.702e-03



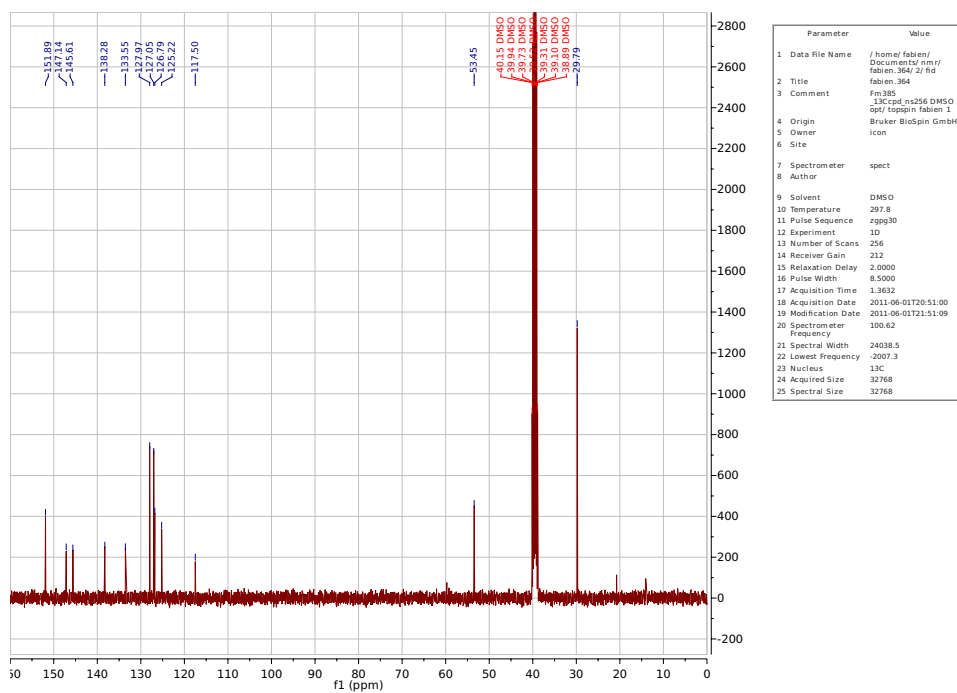
/Data/UNI_BS/MONN5756_ESI/3/pdata/1/ FTMS USER Mon May 30 15:36:34 2011



Parameter	Value
1 Data File Name	/home/fabien/Documents/mri/fabien_359_41.res
2 Title	fabien.355
3 Comment	FM375
4 Origin	39F (H) DMSO / opt/
5 Owner	topspin fabien.40
6 Site	Bruker Biospin GmbH
7 Spectrometer	kon
8 Author	spect
9 Solvent	DMSO
10 Temperature	297.4
11 Pulse Sequence	zgpg30g.2
12 Experiment	1D
13 Number of Scans	16
14 Receiver Gain	212
15 Relaxation Delay	1.5000
16 Pulse Width	13.0000
17 Acquisition Time	1.3982
18 Acquisition Date	2011-05-21T03:17:00
19 Modification Date	2011-05-21T04:16:56
20 Spectrometer Frequency	376.46
21 Spectral Width	93750.0
22 Lowest Frequency	-84524.8
23 Nucleus	19F
24 Acquired Size	131072
25 Spectral Size	6536

N-(*tert*-Butyl)-4-(2-cyanopyridin-4-yl)benzenesulfonamide (65)

Parameter	Value
1 Data File Name	/home/fabien/Document/reny/fabien_373/1/fid
2 Title	fabien_373
3 Comment	Fm395 Proton_16 DMSO / opt/ Toppin fabien 6
4 Origin	Bruker BioSpin GmbH
5 Owner	icon
6 Site	
7 Spectrometer	spect
8 Author	
9 Solvent	DMSO
10 Temperature	291.2
11 Pulse Sequence	zg30
12 Experiment	1D
13 Number of Scans	16
14 Receiver Gain	132
15 Relaxation Delay	1.0000
16 Pulse Width	8.5000
17 Acquisition Time	1.9999
18 Acquisition Date	2011-06-15T17:40:00
19 Modification Date	2011-06-15T18:39:55
20 Spectrometer Frequency	400.13
21 Spectral Width	8223.7
22 Lowest Frequency	-1644.9
23 Nucleus	1H
24 Acquired Size	16446
25 Spectral Size	65536



Parameter	Value
1 Data File Name	/home/fabien/Document/reny/fabien_364/2/fid
2 Title	fabien_364
3 Comment	Fm385 13C-CPD, m256 DMSO / opt/ Toppin fabien 1
4 Origin	Bruker BioSpin GmbH
5 Owner	icon
6 Site	
7 Spectrometer	spect
8 Author	
9 Solvent	DMSO
10 Temperature	297.8
11 Pulse Sequence	zgpg30
12 Experiment	1D
13 Number of Scans	256
14 Receiver Gain	212
15 Relaxation Delay	2.0000
16 Pulse Width	8.5000
17 Acquisition Time	1.9632
18 Acquisition Date	2011-06-01T20:51:00
19 Modification Date	2011-06-01T21:51:09
20 Spectrometer Frequency	100.62
21 Spectral Width	24038.5
22 Lowest Frequency	-2007.3
23 Nucleus	13C
24 Acquired Size	32768
25 Spectral Size	32768



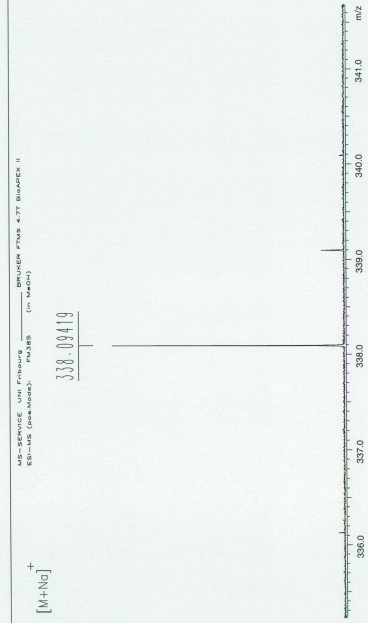
ESI-MS: FM385

XMSS Mass Analysis for /Data/UNI_BS/MONN5822_ESI/2/pdata/1/massanal.res:
XMSS Mass Analysis Constraints

Ion mass = 338.0941890

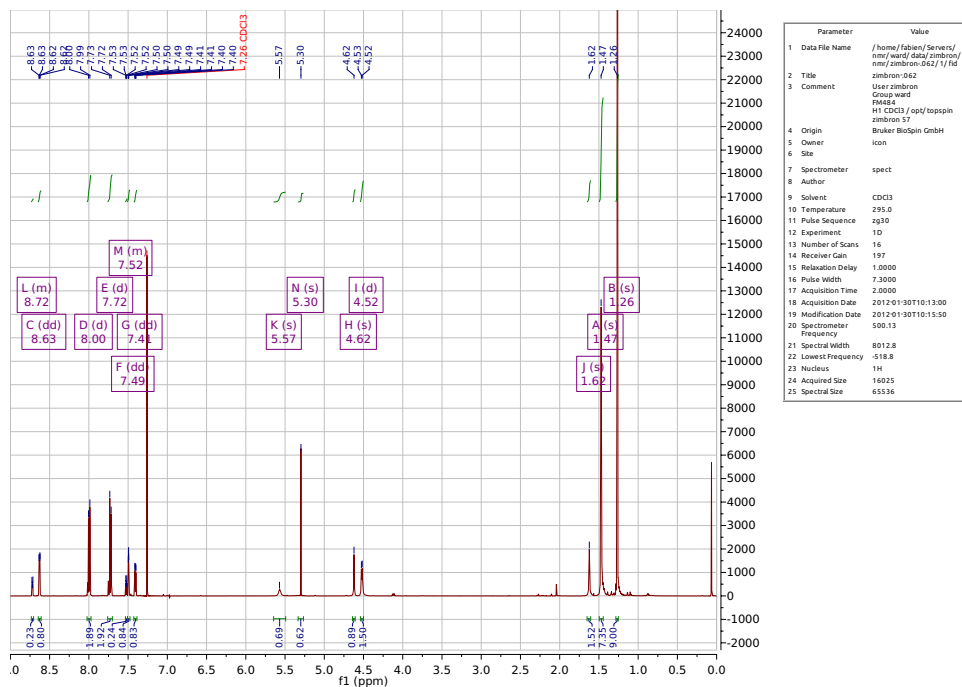
Charge = +1

#	C	H	N	O	S	Na	mass	DBE	error
*** Mass Analysis for mass 338.0941890									
1	16	17	3	2	1	1	338.0933686	9.5	8.204e-04
2	10	20	5	4	2	0	338.0951220	3.5	9.330e-04
3	18	16	3	2	1	0	338.0957719	12.5	1.585e-03
4	13	26	5	2	1	0	338.0963861	6.5	2.450e-03
5	14	25	4	2	1	0	338.0965334	6.5	2.450e-03
6	13	24	1	3	3	0	338.0912821	2.5	2.907e-03
7	11	22	4	2	3	0	338.0899395	3.0	4.250e-03
8	11	17	5	4	1	1	338.0893458	5.5	4.843e-03
9	15	20	3	2	2	0	338.0991447	7.5	4.956e-03
10	11	25	1	3	3	1	338.0888768	-0.5	5.312e-03

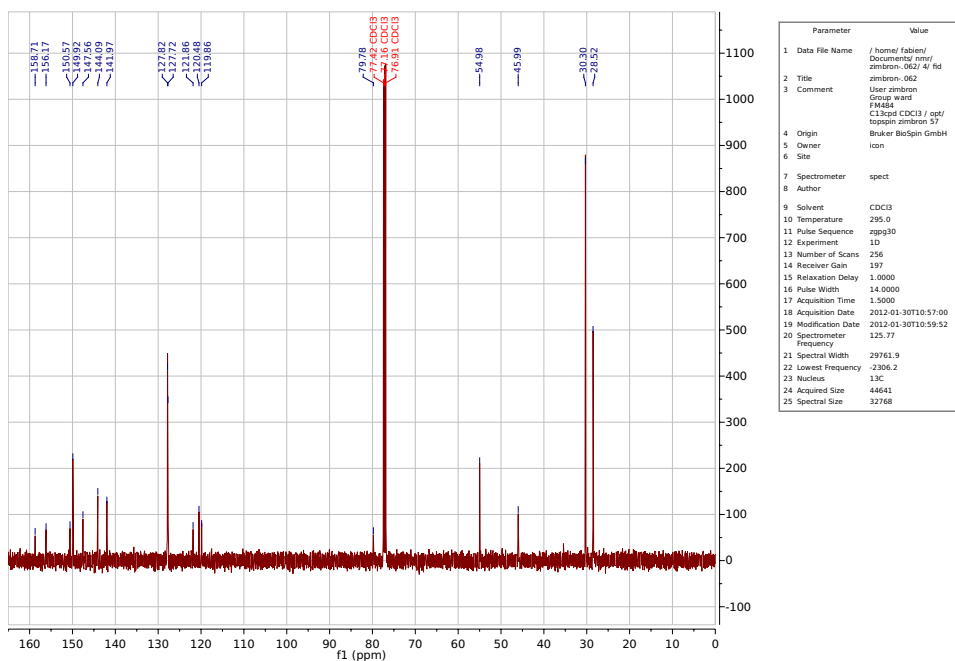


/Data/UNI_BS/MONN5822_ESI/2/pdata/1 FTMS USER Wed Jun 22 11:03:51 2011

N-(*tert*-Butyl)-4-(2-(aminomethyl)pyridin-4-yl)benzenesulfonamide (**66**)



Parameter	Value
1 Data File Name	/home/fabien/Servers/nmr/wesol_data/zimbron/nmr/zimbron-062/1/f1d
2 Title	zimbron-062
3 Comment	User zimbron Group ward FM484 H1 CDCl3 / opt/topspin zimbron 57
4 Origin	Bruker BioSpin GmbH
5 Owner	icon
6 Site	
7 Spectrometer	spect
8 Author	
9 Solvent	CDCl3
10 Temperature	295.0
11 Pulse Sequence	zgpg30
12 Experiment	1D
13 Number of Scans	16
14 Receiver Gain	197
15 Relaxation Delay	1.0000
16 Pulse Width	7.3000
17 Acquisition Time	2.0000
18 Acquisition Date	2012-01-30T10:13:00
19 Modification Date	2012-01-30T16:15:50
20 Spectrometer	500.13
21 Frequency	
22 Spectral Width	8012.8
23 Lowest Frequency	-518.8
24 Nucleus	1H
25 Acquired Size	16025
26 Spectral Size	6536



Parameter	Value
1 Data File Name	/home/fabien/Documents/nmr/zimbron-062/4/f1d
2 Title	zimbron-062
3 Comment	User zimbron Group ward FM484 C13cpd CDCl3 / opt/topspin zimbron 57
4 Origin	Bruker BioSpin GmbH
5 Owner	icon
6 Site	
7 Spectrometer	spect
8 Author	
9 Solvent	CDCl3
10 Temperature	295.0
11 Pulse Sequence	zgpg30
12 Experiment	1D
13 Number of Scans	256
14 Receiver Gain	197
15 Relaxation Delay	1.0000
16 Pulse Width	14.0000
17 Acquisition Time	1.5000
18 Acquisition Date	2012-01-30T10:57:00
19 Modification Date	2012-01-30T10:59:52
20 Spectrometer	125.77
21 Frequency	
22 Spectral Width	29761.9
23 Lowest Frequency	-2306.2
24 Nucleus	13C
25 Acquired Size	44641
26 Spectral Size	32768

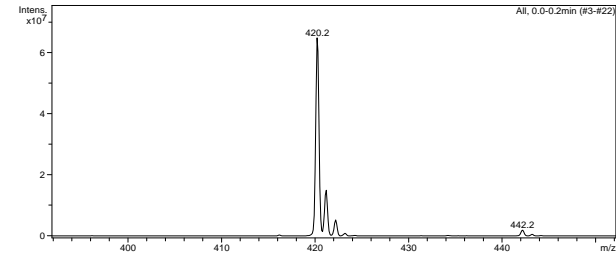
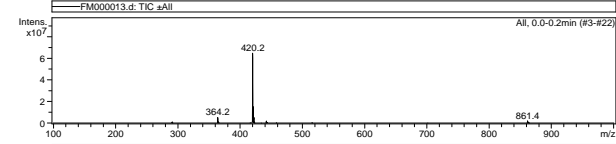
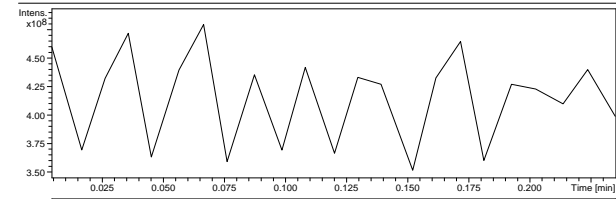
Display Report

Analysis Info

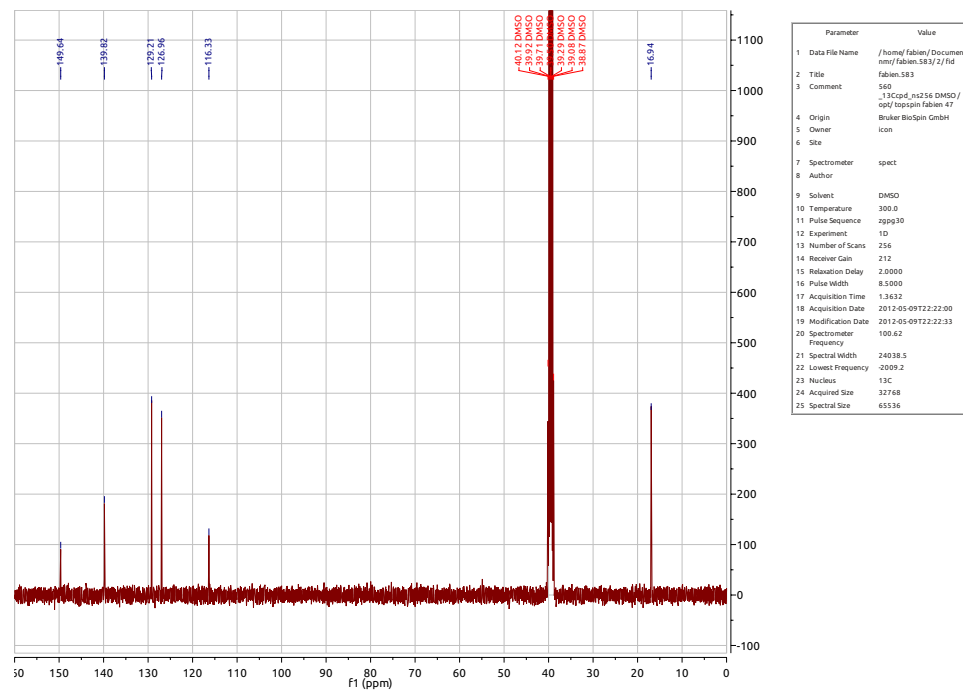
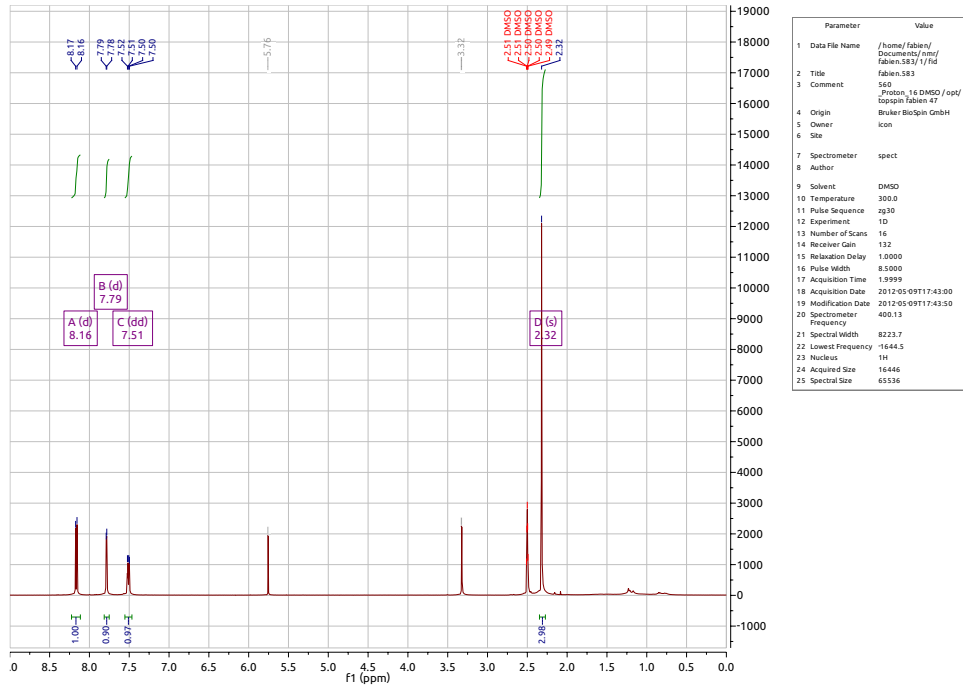
Analysis Name FM000013.d Acquisition Date 01/25/12 13:43:40
Method Copy(2) of E3Kp Default.ms Operator Administrator
Sample Name fm484 Instrument esquire3000plus_01096
Comment

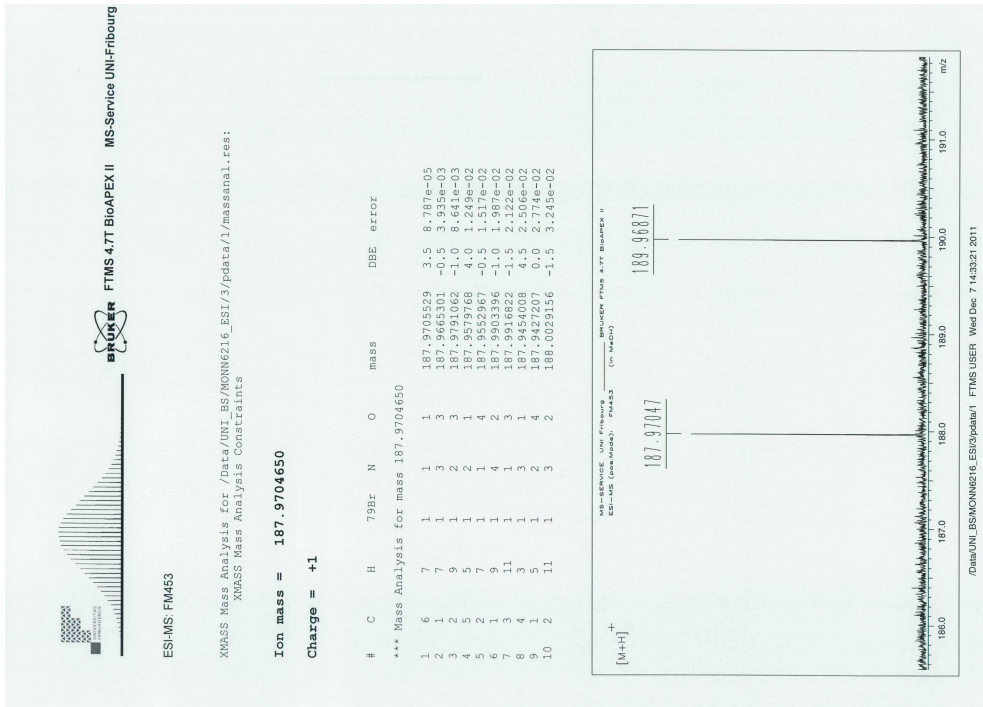
Acquisition Parameter

Ion Source Type	ESI	Ion Polarity	Positive	Alternating Ion Polarity	off
Mass Range Mode	Std/Normal	Scan Begin	100 m/z	Scan End	1000 m/z
Capillary Exit	122.4 Volt	Skim 1	40.0 Volt	Trap Drive	47.8
Accumulation Time	36 μ s	Averages	5 Spectra	Auto MS/MS	off

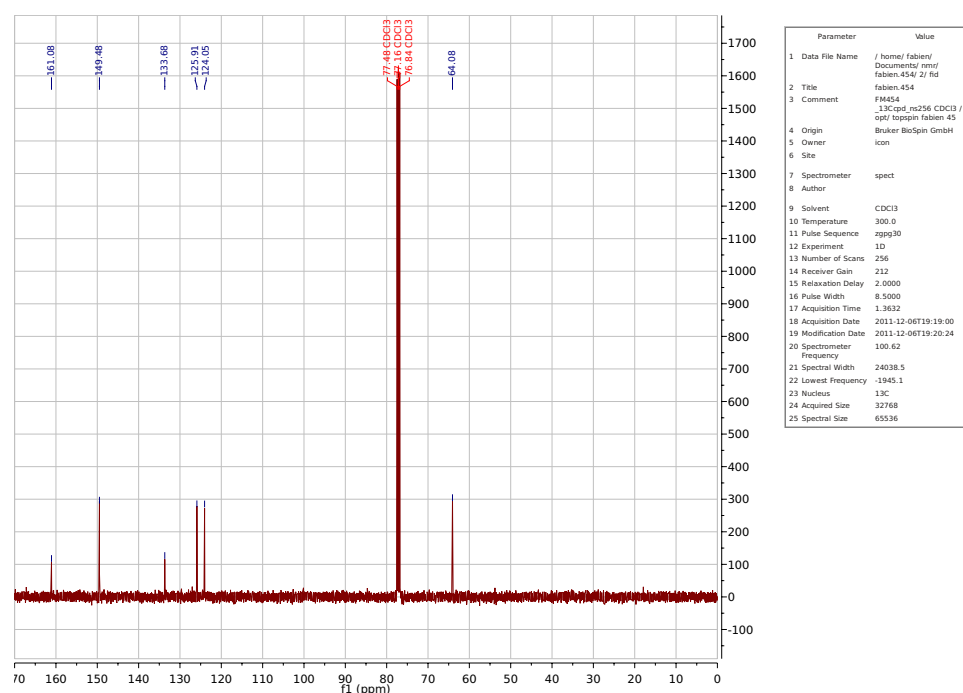
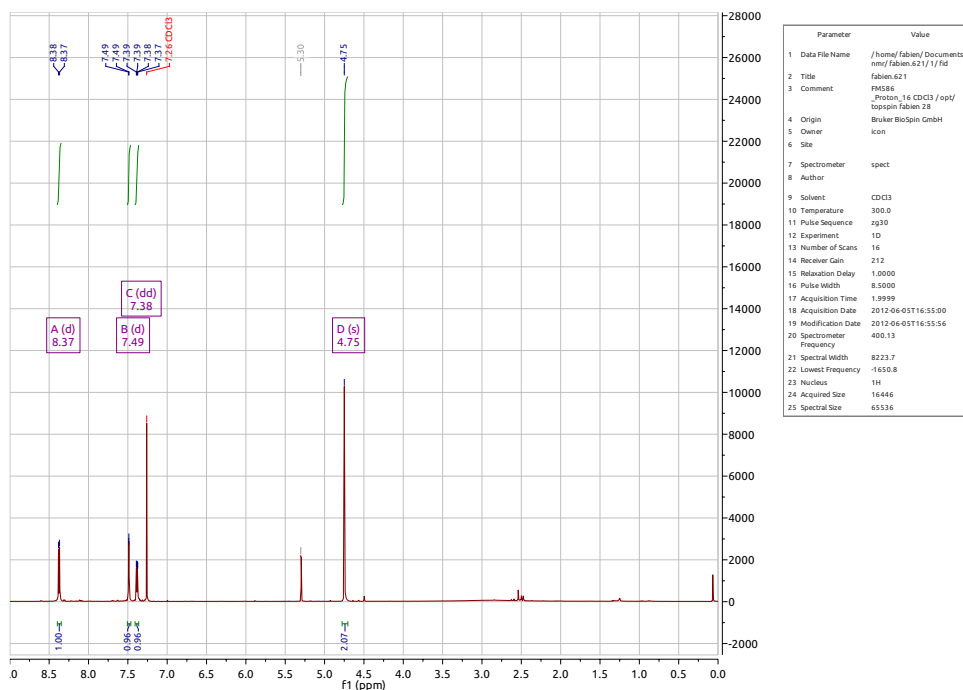


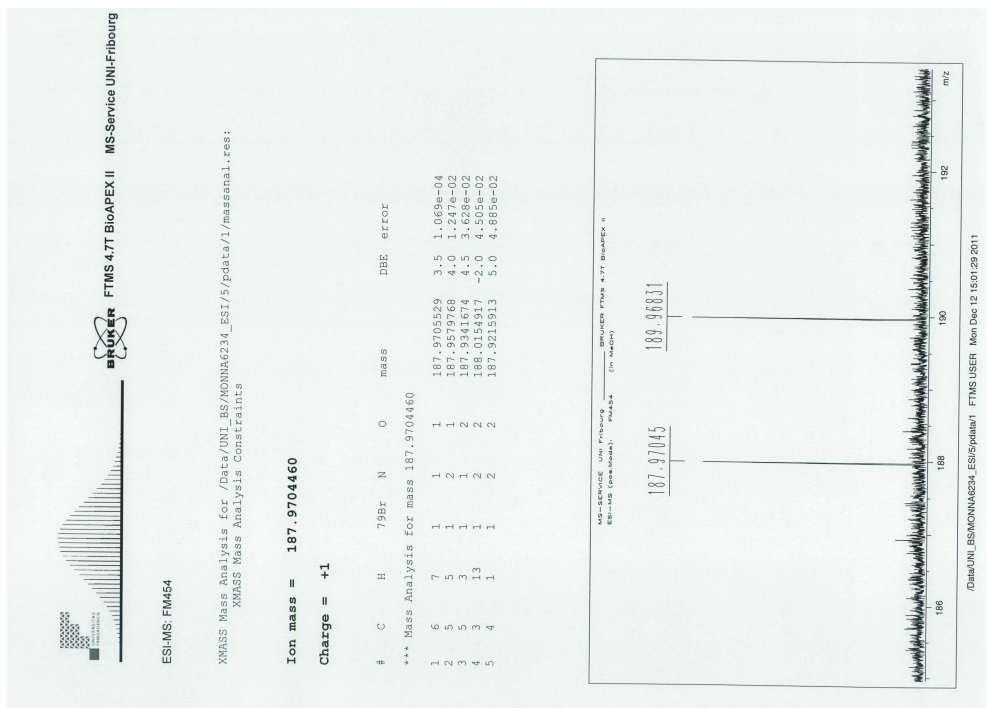
4-Bromo-2-methylpyridine-*N*-oxide (68)



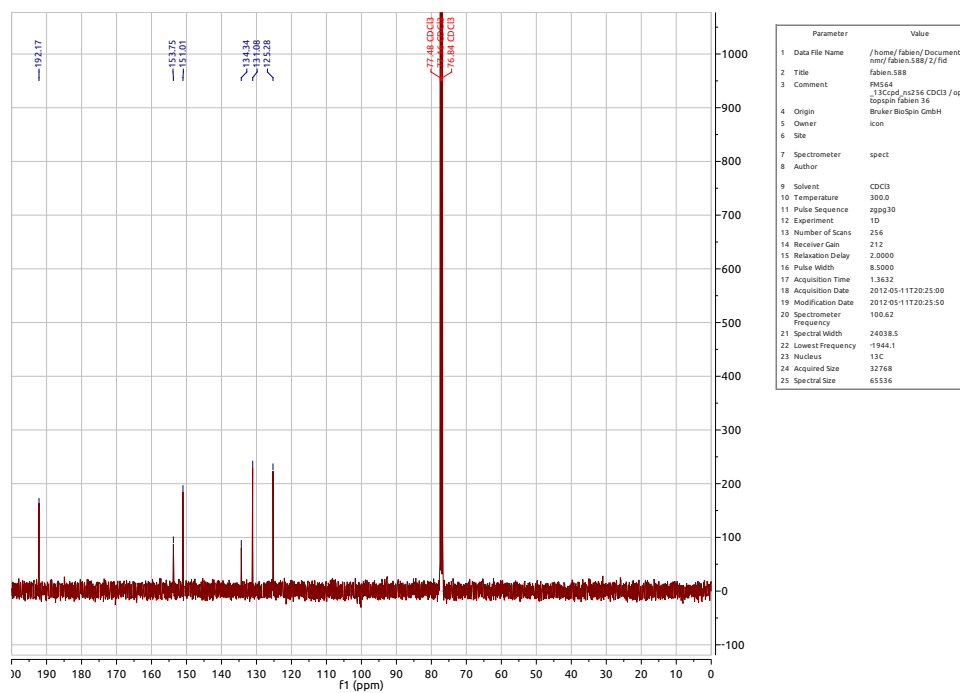
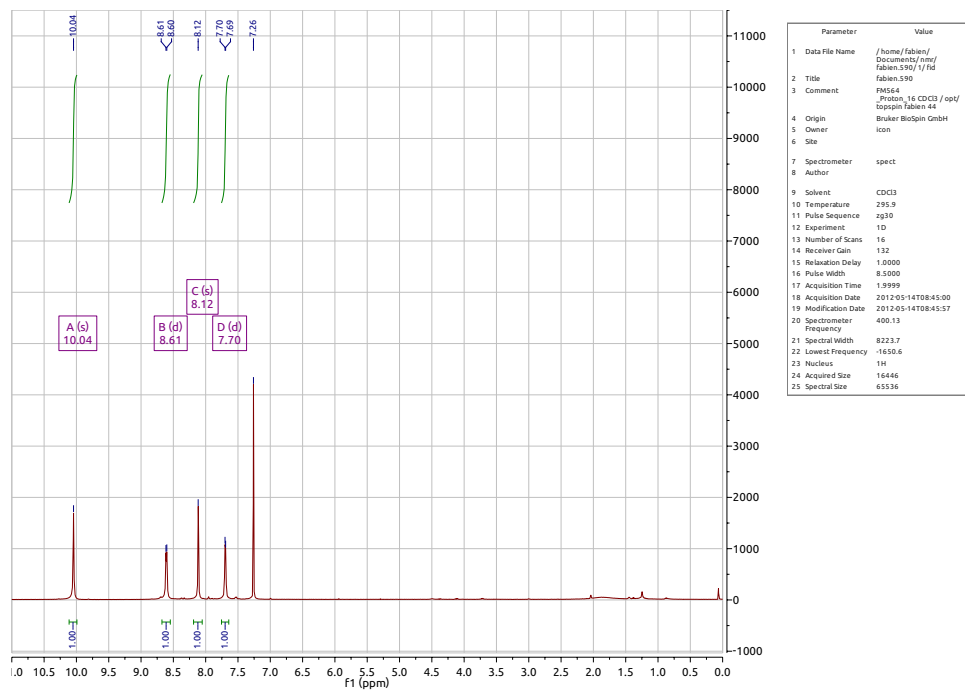


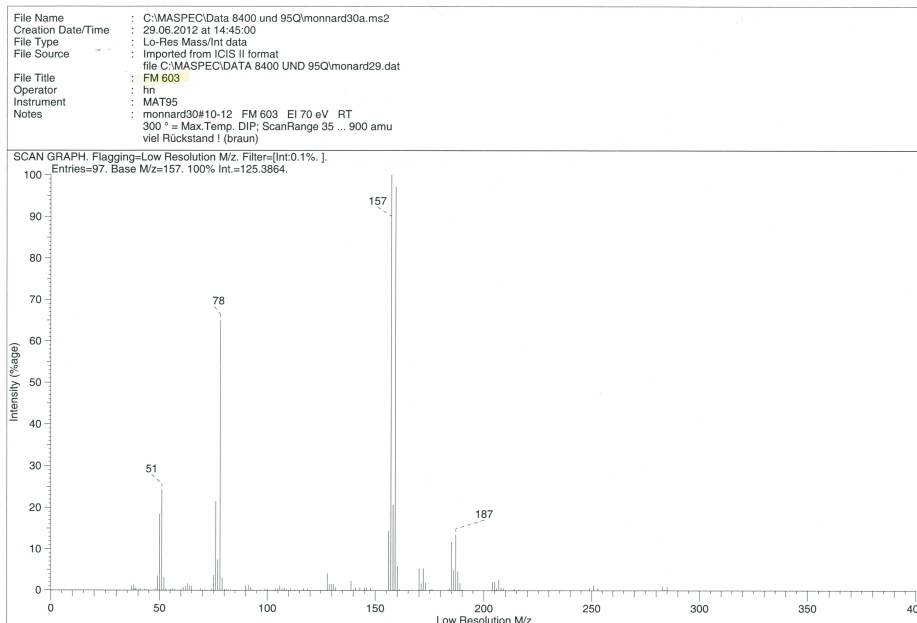
4-Bromo-2-hydroxymethylpyridine (69)



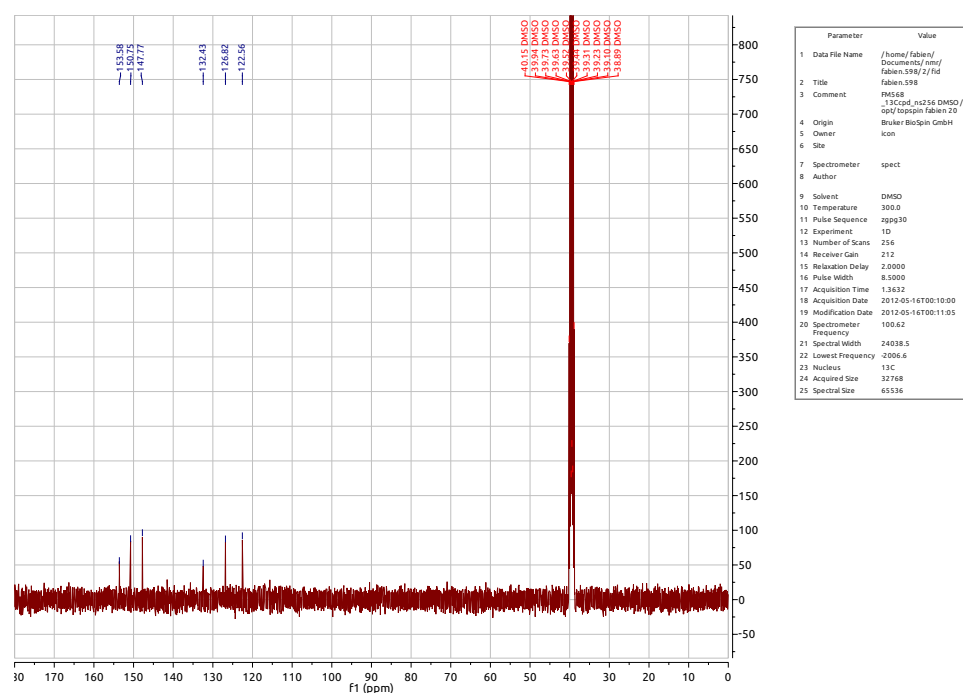
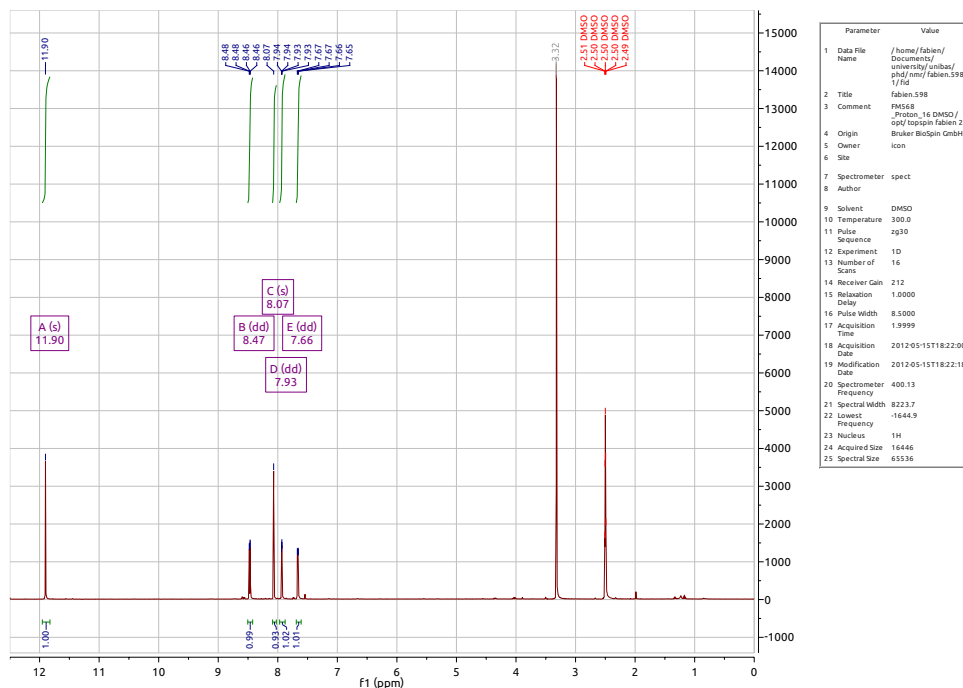


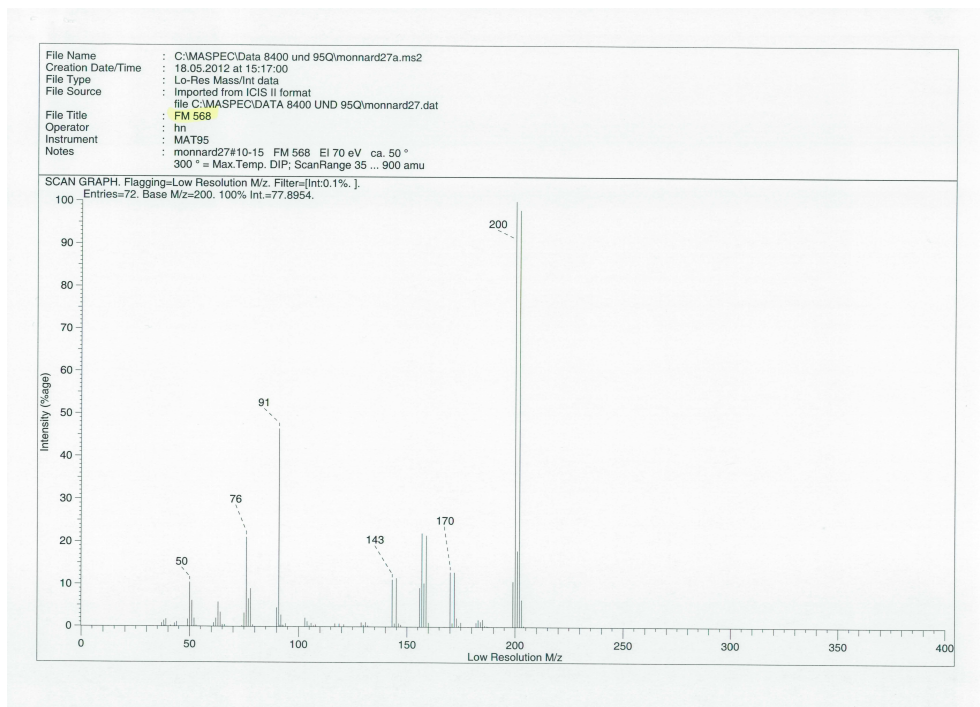
4-Bromo-2-pyridine aldehyde (73)



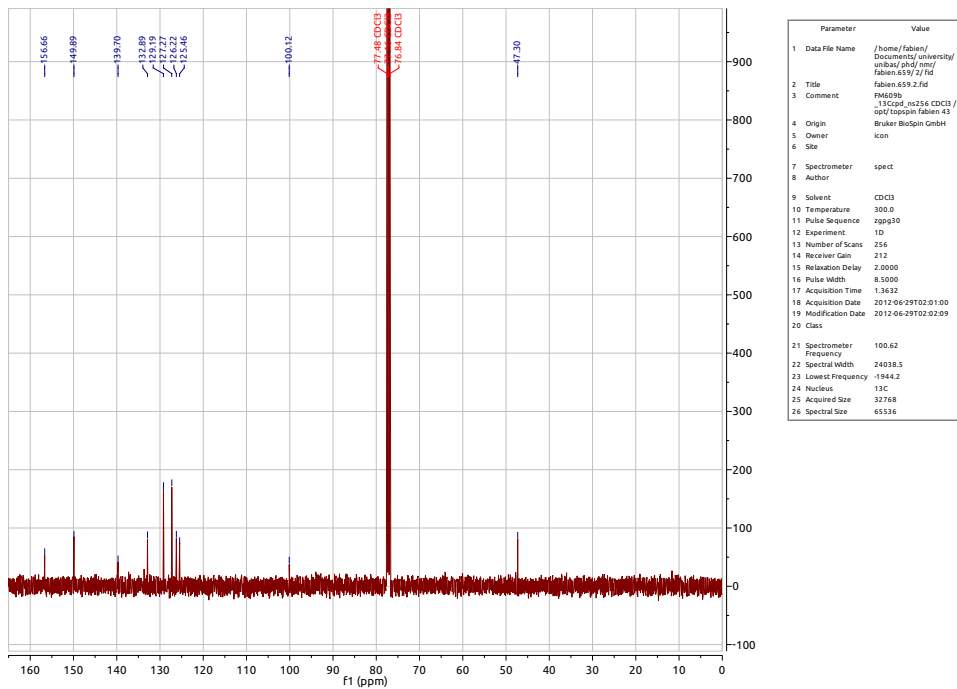
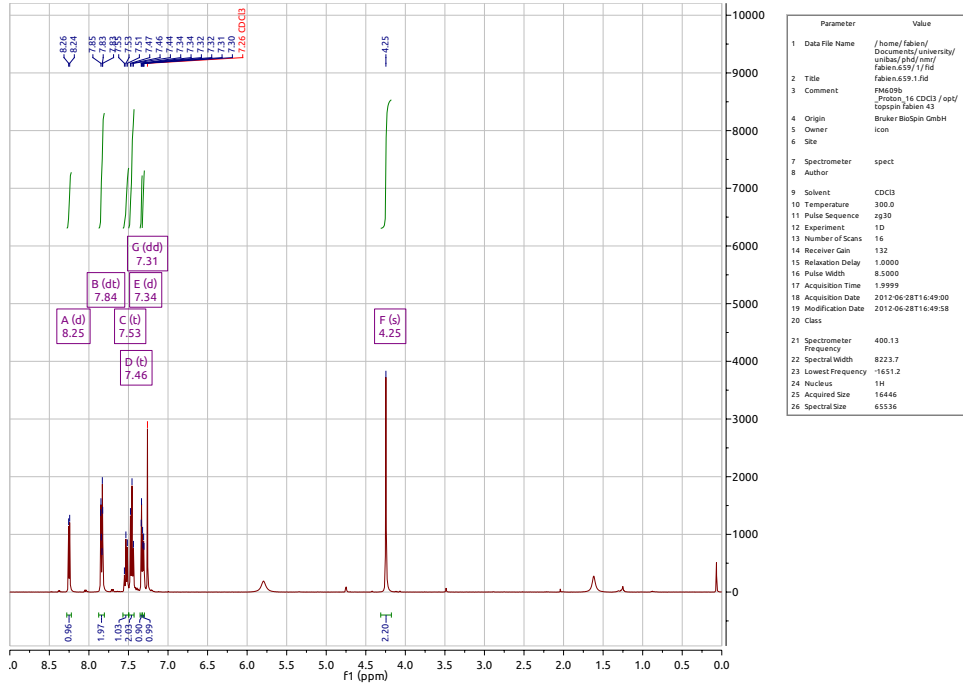


4-Bromo-2-pyridine ketoxime (72)





N-[(4-Bromopyridin-2-yl)methyl]benzenesulfonamide (**70**)



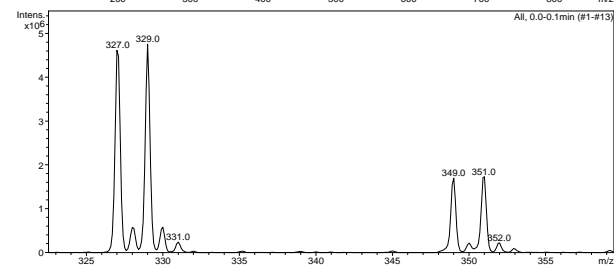
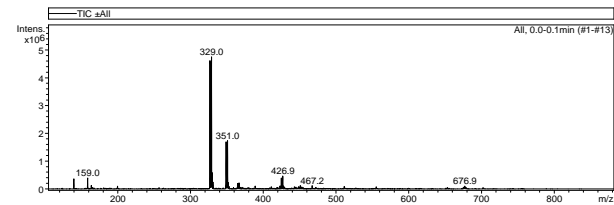
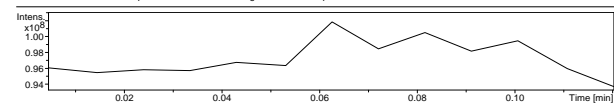
Display Report

Analysis Info

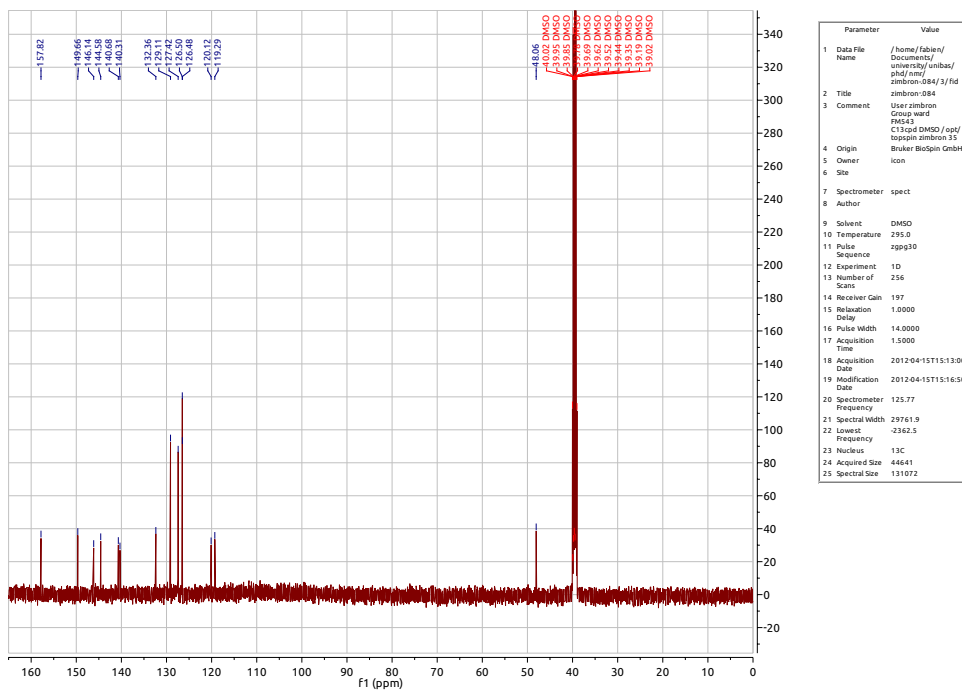
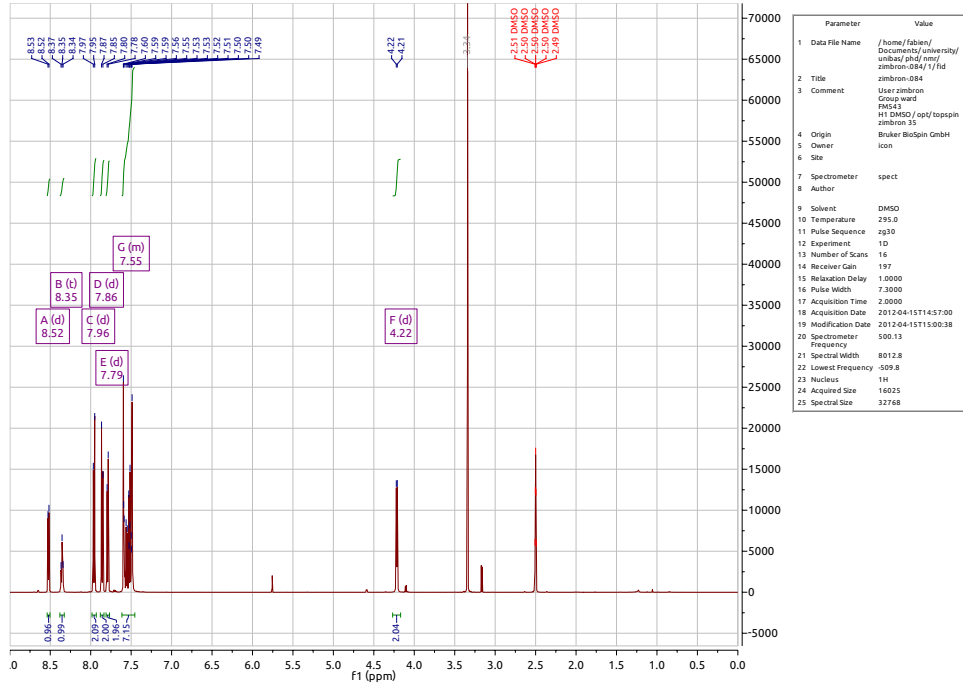
Analysis Name	FM000038.d	Acquisition Date	06/28/12 15:25:13
Method	Copy(2) of E3Kp Default.ms	Operator	Administrator
Sample Name	fm609	Instrument	esquire3000plus_01096
Comment			

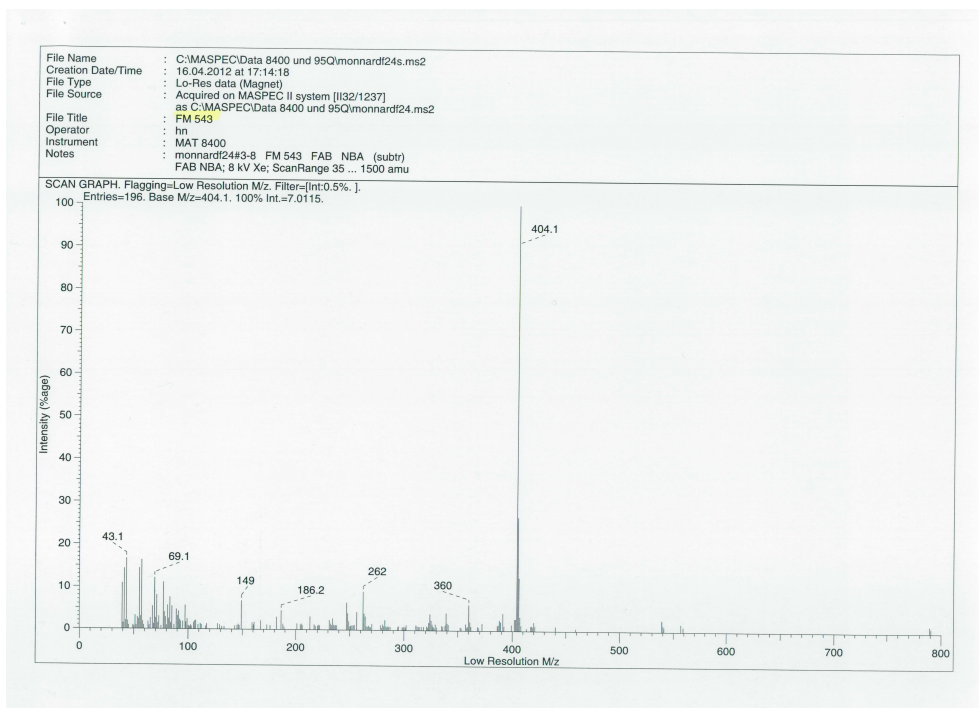
Acquisition Parameter

Ion Source Type	ESI	Ion Polarity	Positive	Alternating Ion Polarity	off
Mass Range Mode	Std/Normal	Scan Begin	100 m/z	Scan End	1000 m/z
Capillary Exit	115.7 Volt	Skim 1	40.0 Volt	Trap Drive	41.1
Accumulation Time	201 μ s	Averages	5 Spectra	Auto MS/MS	off

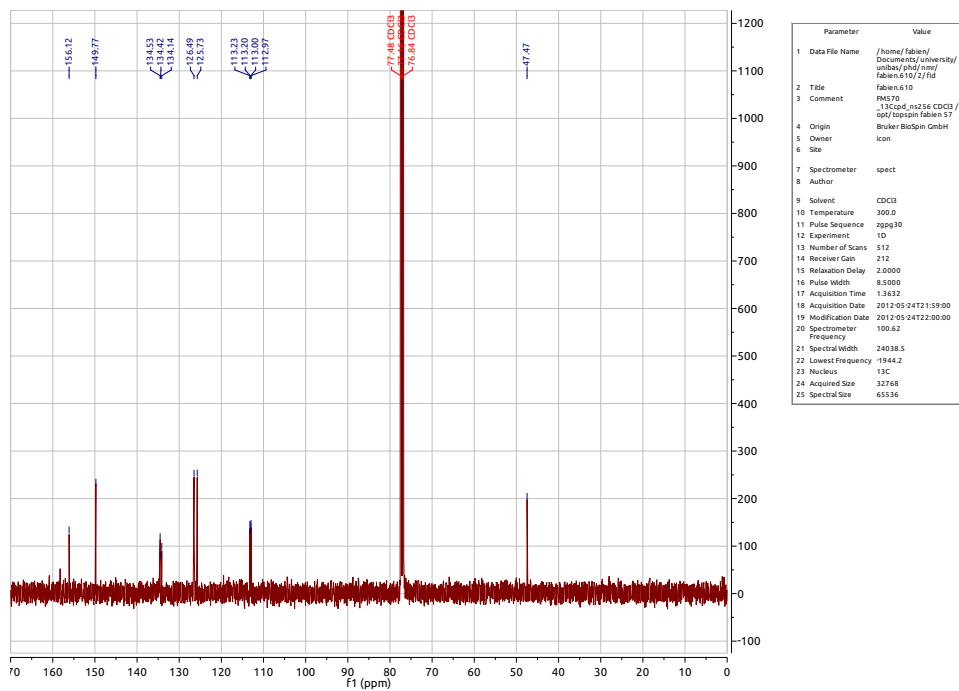
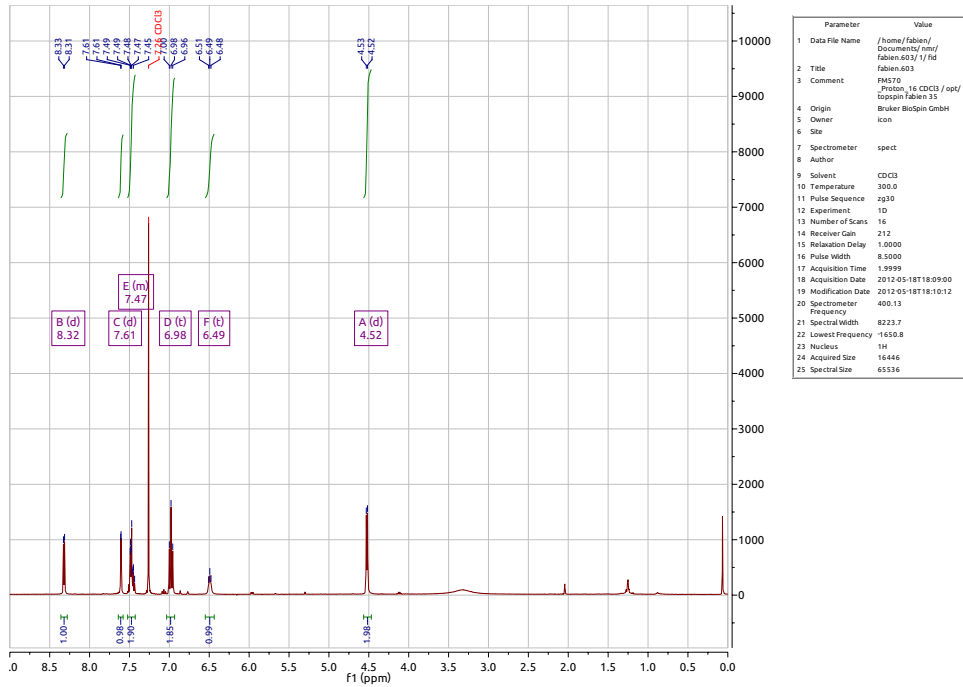


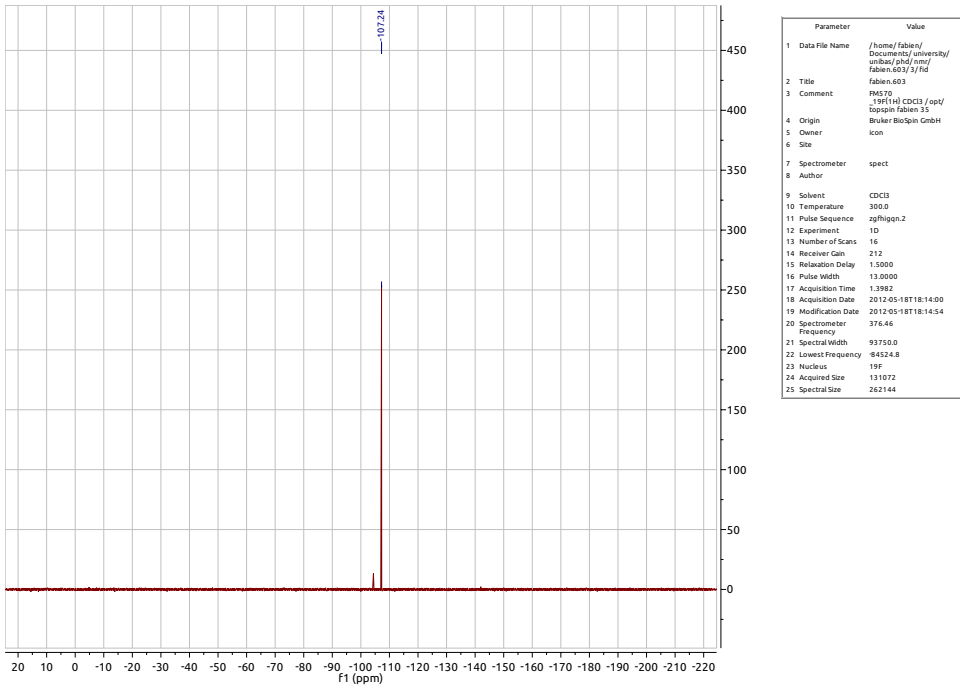
N-((4-(4-Sulfamoylphenyl)pyridin-2-yl)methyl)benzenesulfonamide (**6**)





N-[(4-Bromopyridin-2-yl)methyl]-2,6-difluorobenzene-1-sulfonamide (**71**)



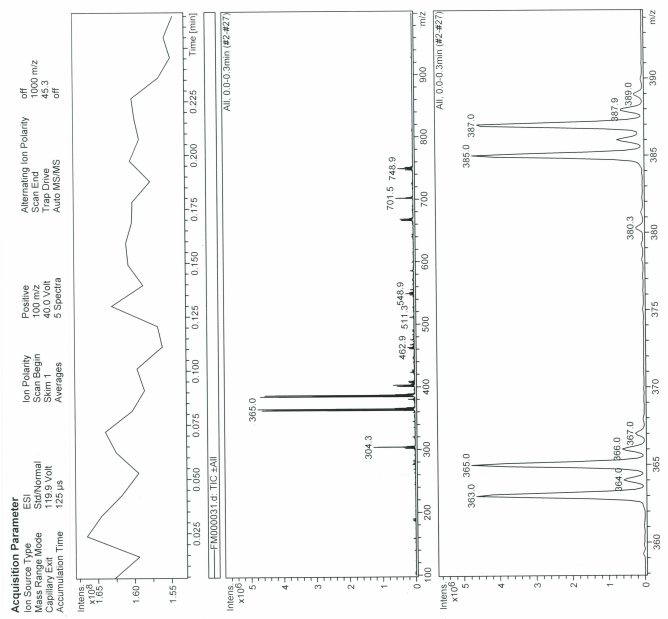


Parameter	Value
1 Data File Name	/home/fabien/Documents/universite/uniba/pha/rtm/fabien.603.3.fid
2 Title	fabien.603
3 Comment	FM570 31951H) CDC13 / opt/ topspin fabien 35
4 Origin	Bruker BioSpin GmbH
5 Owner	kon
6 Site	
7 Spectrometer	spect
8 Author	
9 Solvent	CDC13
10 Temperature	300.0
11 Pulse Sequence	zgpgpgn.2
12 Experiment	1D
13 Number of Scans	16
14 Receiver Gain	212
15 Relaxation Delay	1.5000
16 Pulse Width	13.0000
17 Acquisition Time	1.3982
18 Acquisition Date	2012-05-18T18:14:00
19 Modification Date	2012-05-18T18:14:54
20 Spectrometer	376.46
21 Frequency	
22 Spectral Width	93750.0
23 Lowest Frequency	64524.8
24 Nucleus	19F
25 Acquired Size	131072
26 Spectral Size	262144

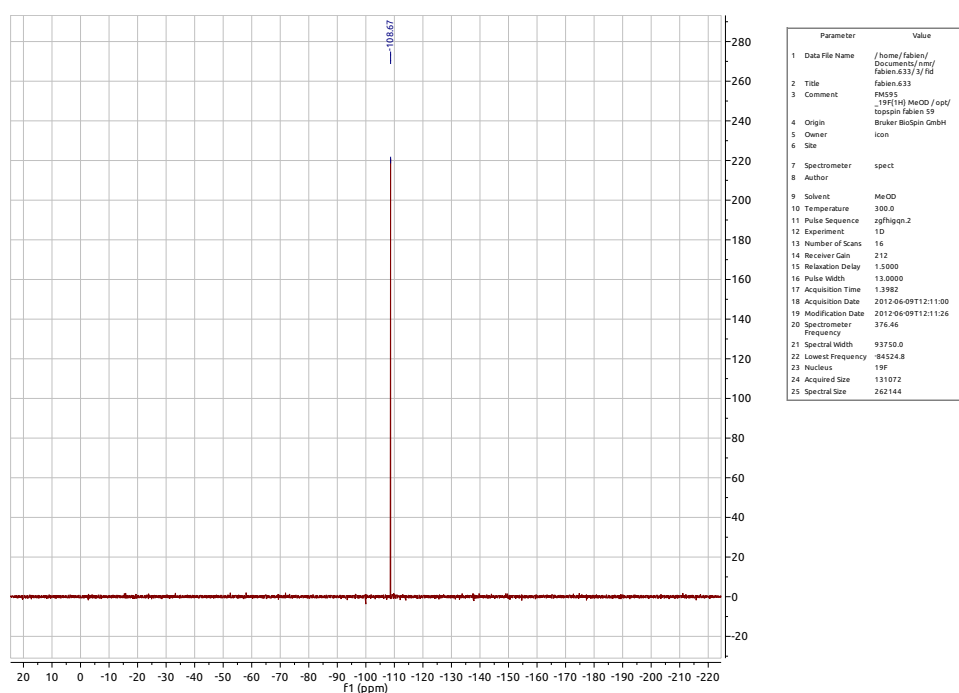
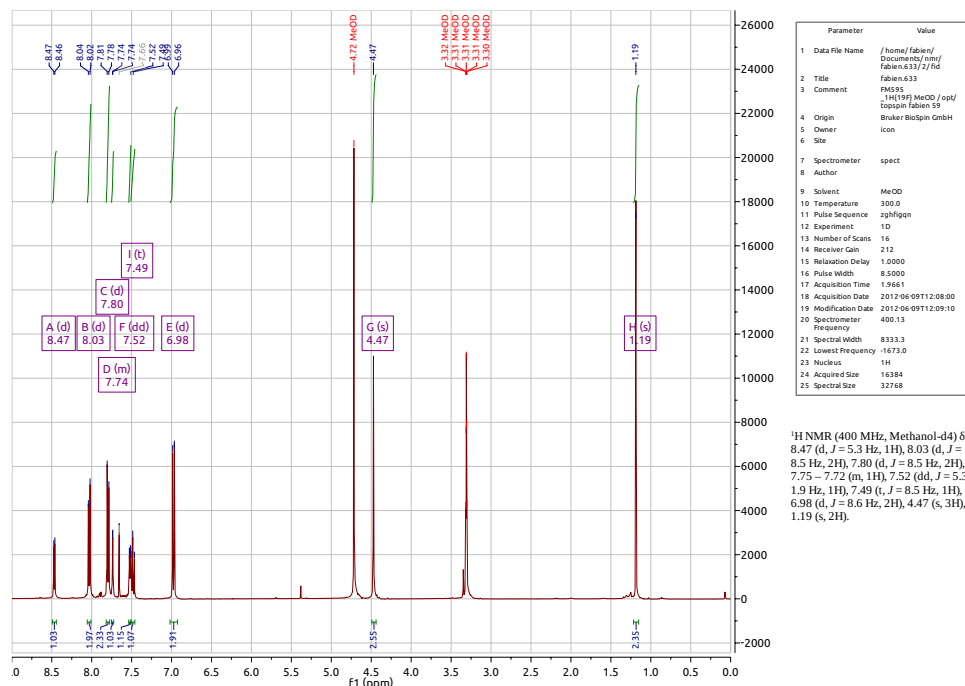
Display Report

Analysis Info
 Analysis Name: FM000031.d
 Method: Copy(2) of E3kp Default.ms
 Sample Name: fms70
 Comment:

Acquisition Parameters
 Acquisition Date: 05/17/12 14:17:45
 Operator: Administrator
 Instrument: esquire3000plus_01096



2,6-Difluoro-*N*-((4-(4-sulfamoylphenyl)pyridin-2-yl)methyl)benzenesulfonamide (41)



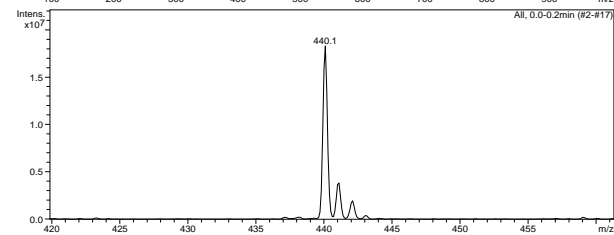
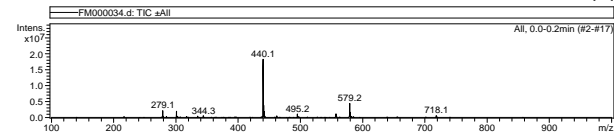
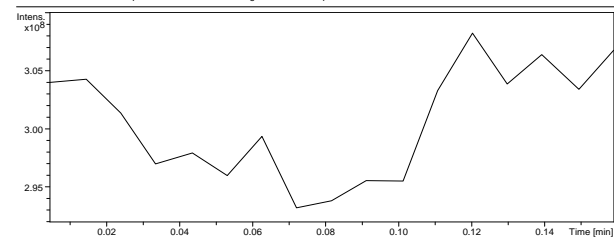
Display Report

Analysis Info

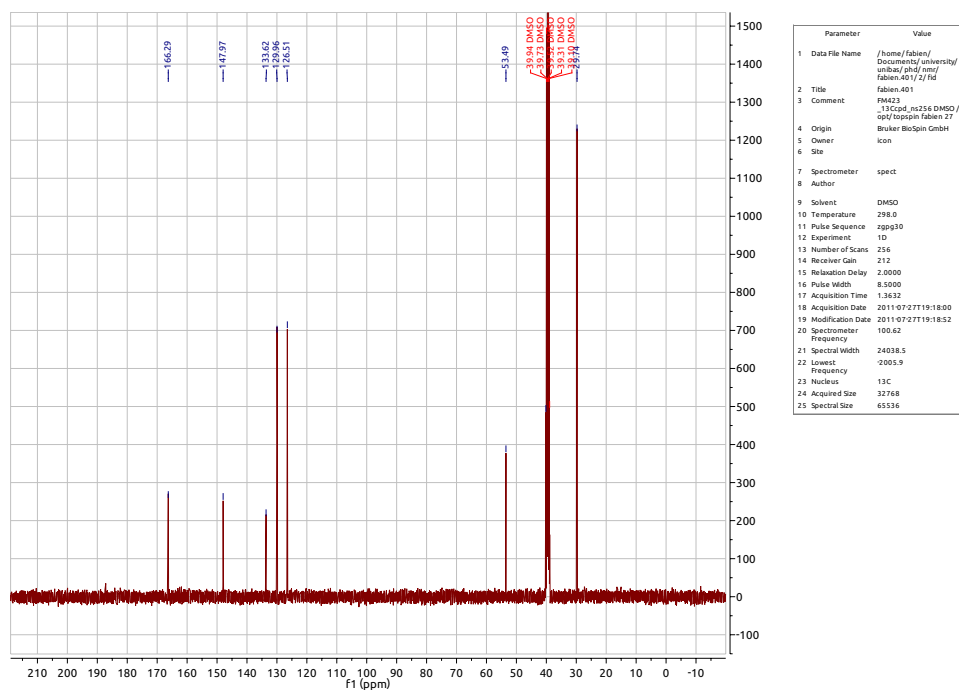
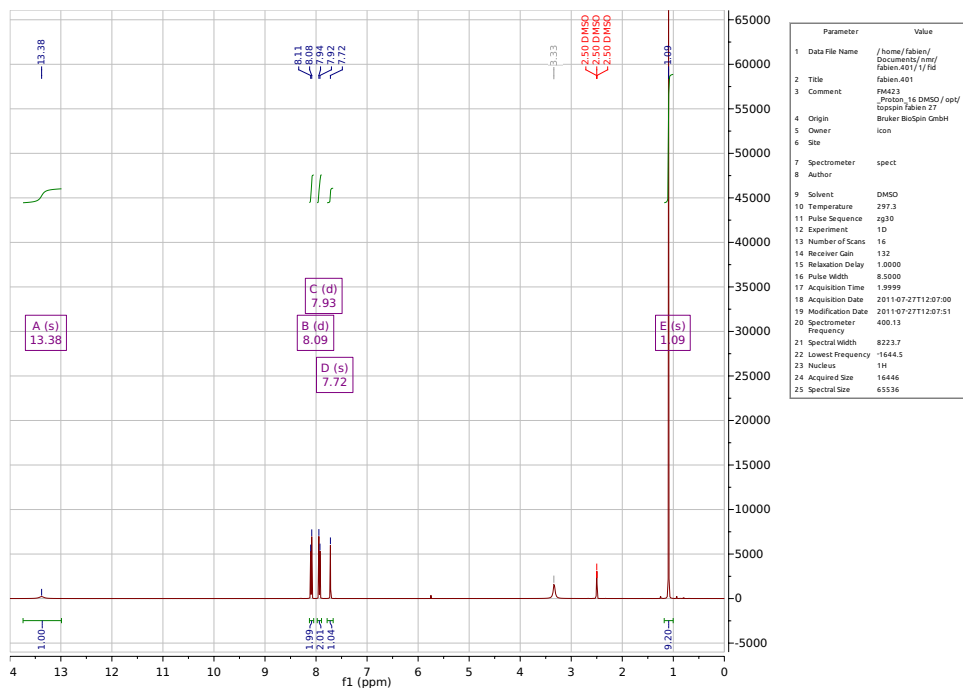
Analysis Name	FM000034.d	Acquisition Date	06/08/12 11:53:57
Method	Copy of wdw127-4.MS	Operator	Administrator
Sample Name	FM592	Instrument	esquire3000plus_01096
Comment			

Acquisition Parameter

Ion Source Type	ESI	Ion Polarity	Positive	Alternating Ion Polarity	off
Mass Range Mode	Std/Normal	Scan Begin	100 m/z	Scan End	1000 m/z
Capillary Exit	123.9 Volt	Skim 1	40.0 Volt	Trap Drive	49.3
Accumulation Time	71 μ s	Averages	5 Spectra	Auto MS/MS	off



4-(*N*-(*tert*-Butyl)sulfamoyl)benzoic acid (**79**)





ESI-MS FM422

BRUKER FTMS 4.7T BioAPEX II MS-Service UNI-Fribourg

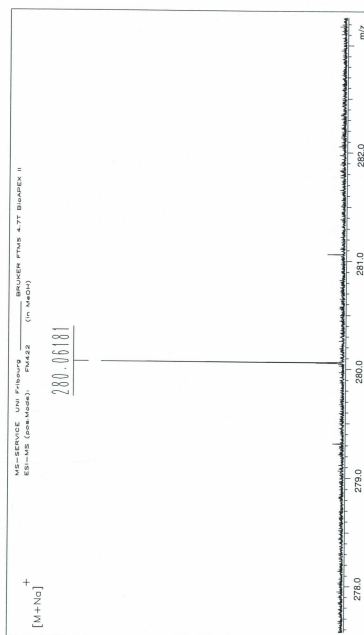
XMAS Mass Analysis For /Data/UNI_BS/MONN5983_ESI/5/pdata/1/massanal.res:
 XMAS Mass Analysis Constraints

Ion mass = 280.0618090

Charge = +1

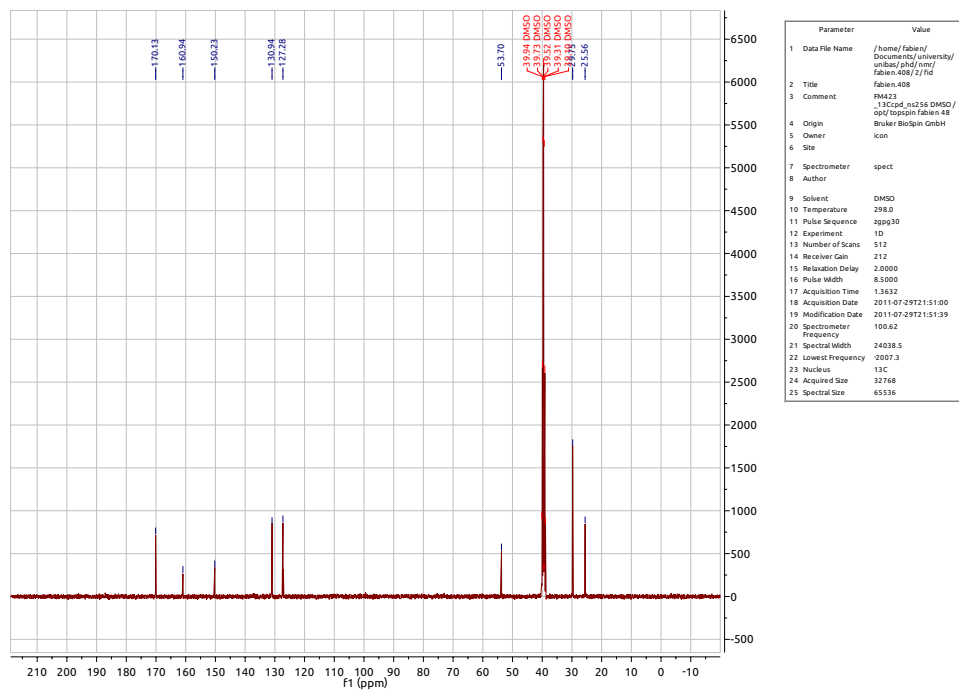
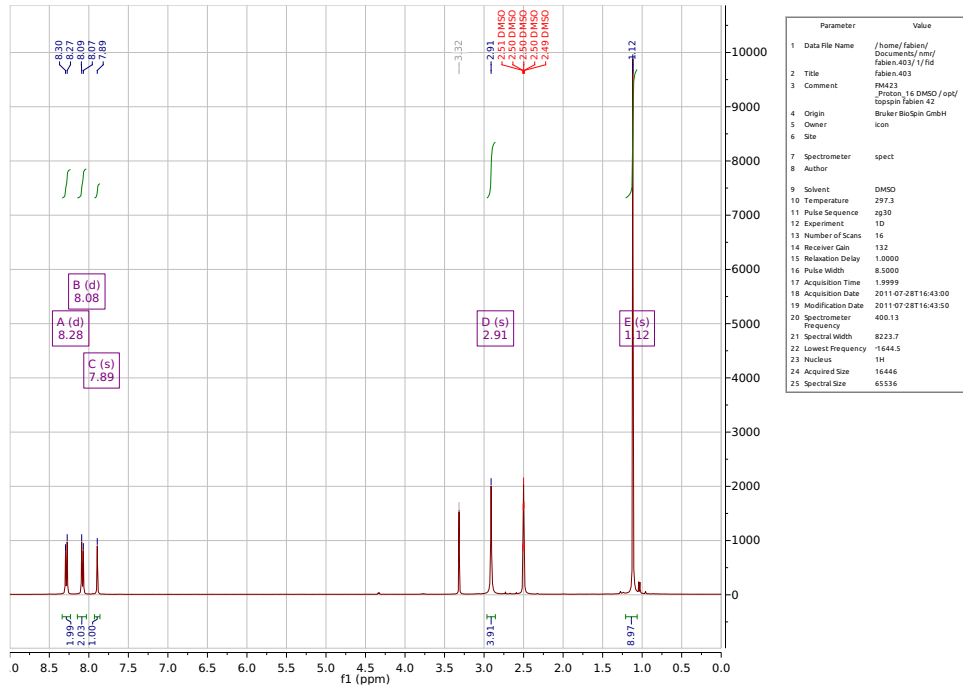
280.0618

#	C	H	N	O	S	Na	mass	DBE	error
*** Mass Analysis for mass 280.0618090									
1	11	15	1	4	1	1	280.0613998	4.5	4.092e-04
2	11	12	4	3	1	0	280.0624624	8.0	6.534e-04
3	6	17	4	3	2	0	280.0631531	-1.5	1.344e-03
4	6	17	4	3	2	1	280.0631531	1.5	1.344e-03
5	9	13	4	3	1	1	280.0620571	5.0	1.759e-03
6	13	14	1	4	1	0	280.0638051	7.5	1.996e-03
7	8	14	3	6	1	0	280.0597823	3.5	2.027e-03
8	14	13	2	1	1	1	280.0640788	9.0	2.271e-03
9	8	19	1	4	2	1	280.0647706	-0.5	2.962e-03
10	8	16	4	3	2	0	280.0638332	3.0	4.024e-03



/Data/UNI_BS/MONN5983_ESI/5/pdata/1 FTMS USER Fri Aug 19 16:54:01 2011

2,5-Dioxopyrrolidin-1-yl-4-(*N*-(*tert*-butyl)sulfamoyl)benzoate (78)





ESI-MS: FMM23

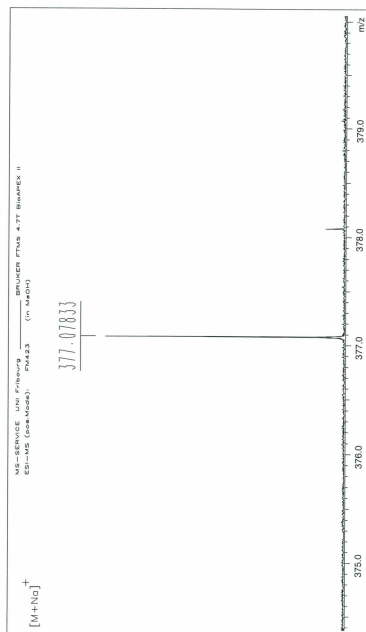
XMass Mass Analysis for /Data/UNI_BS/MONN985_ESI/5/pdata/1/massanal.res:
XMass Mass Analysis Constraints

Ion mass = 377.0783250

Charge = +1

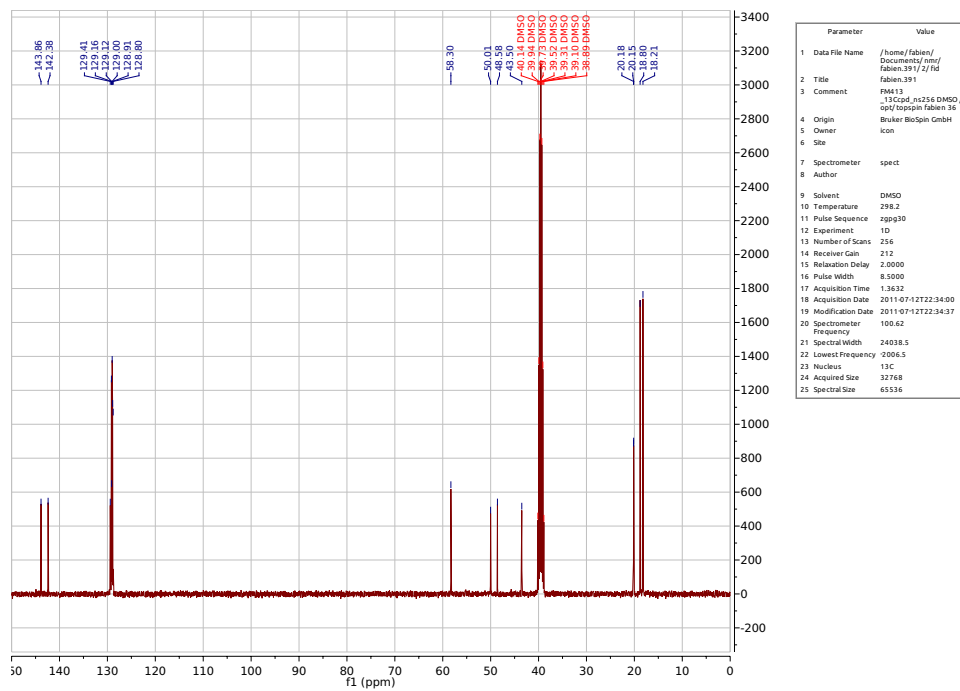
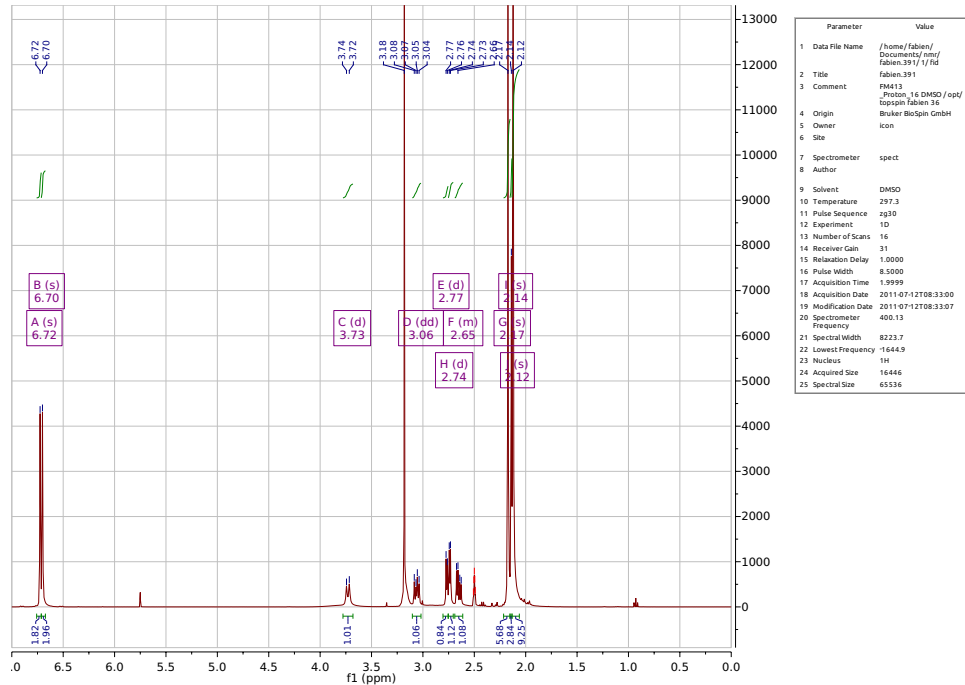
377.0783

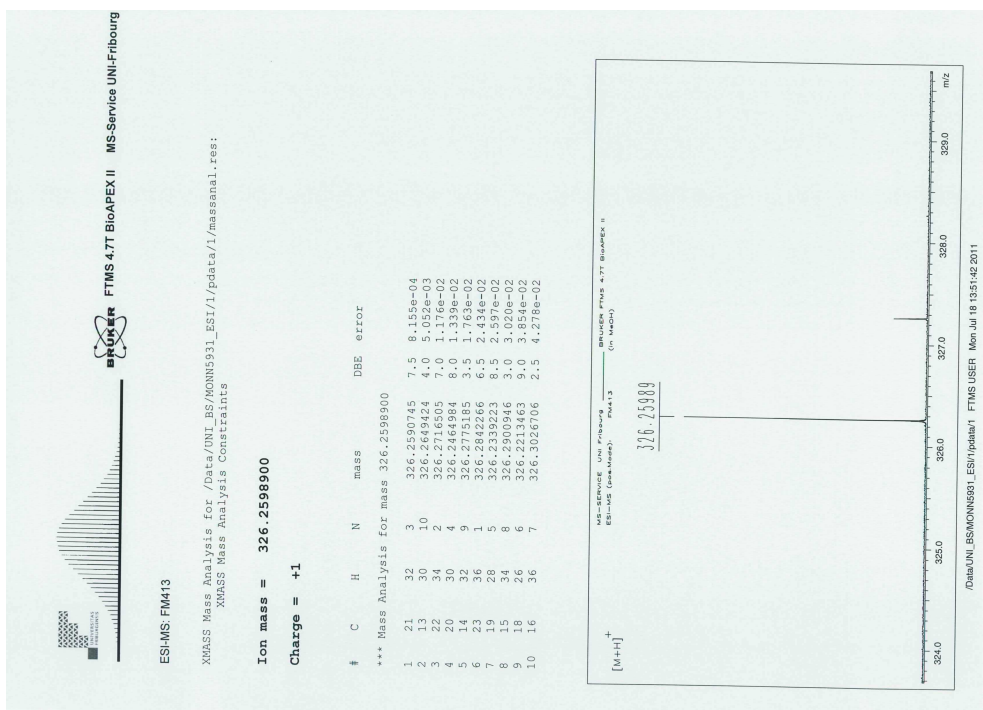
#	C	H	N	O	S	Na	mass	DBE	error
*** Mass Analysis for mass 377.0783250									
1	15	18	2	6	1	1	377.077781	7.5	5.469e-04
2	18	19	1	4	2	0	377.080064	10.5	1.858e-03
3	18	19	1	4	2	0	377.0725956	7.0	5.729e-03
4	16	20	1	4	2	1	377.0709782	6.0	7.347e-03
5	13	19	3	6	2	0	377.0685729	3.0	9.752e-03
6	11	20	3	6	2	1	377.0890115	7.5	1.069e-02
7	14	18	4	5	1	1	377.0876073	11.0	1.072e-02
8	16	15	3	6	1	1	377.0903542	7.0	1.203e-02
9	16	20	4	5	1	0	377.0914169	10.5	1.309e-02
10	16	17	4	5	1	0			



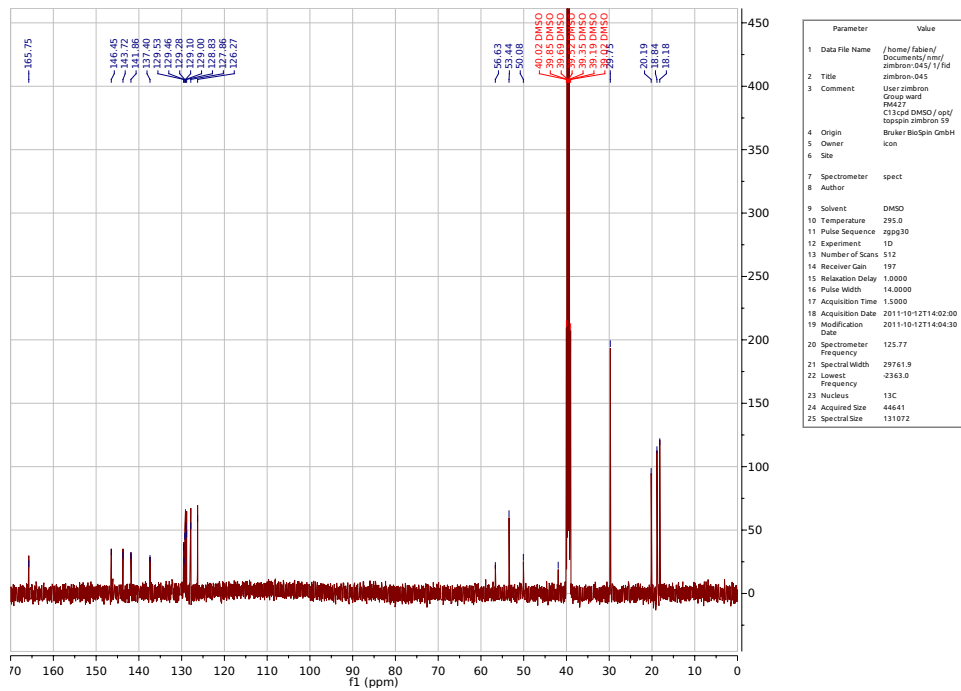
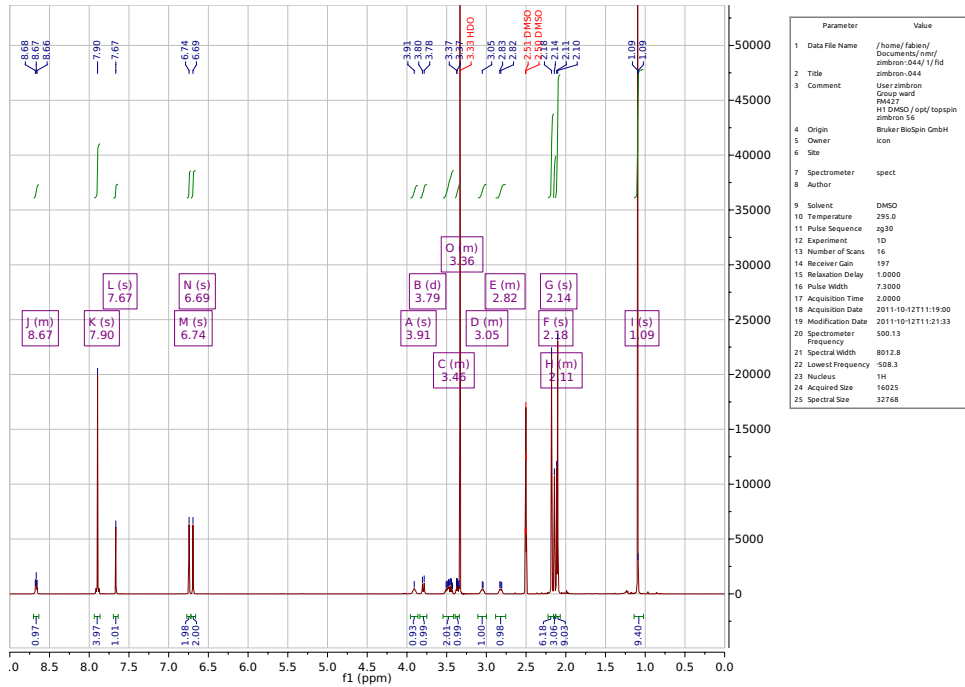
/Data/UNI_BS/MONN985_ESI/5/pdata/1 FTMS USER Fri Aug 19 16:40:59 2011

N,N'-Dimethylpropane-1,2,3-triamine (77)

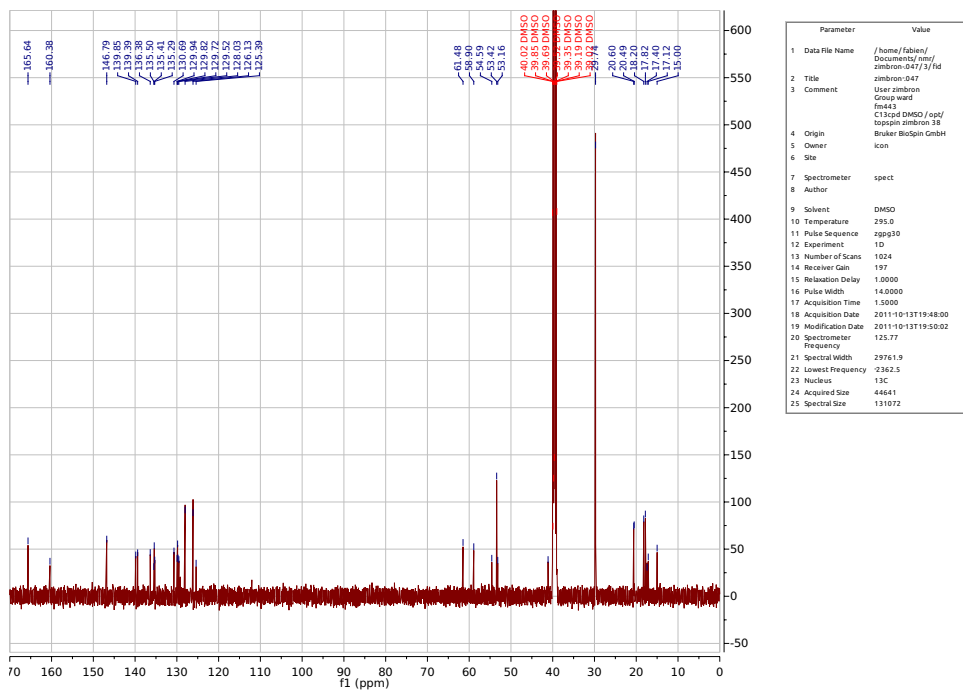
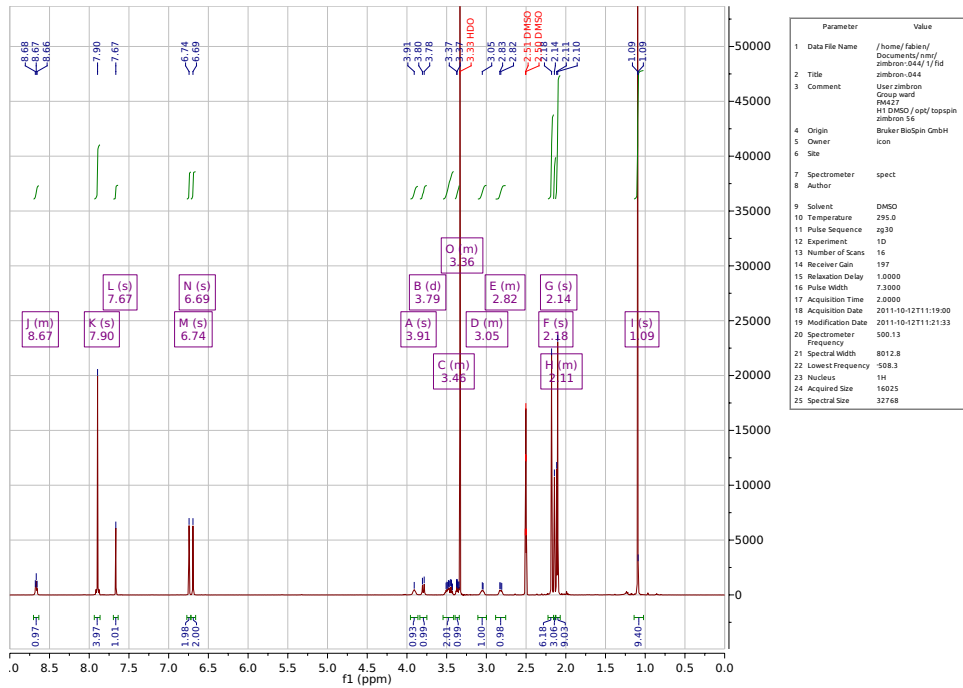


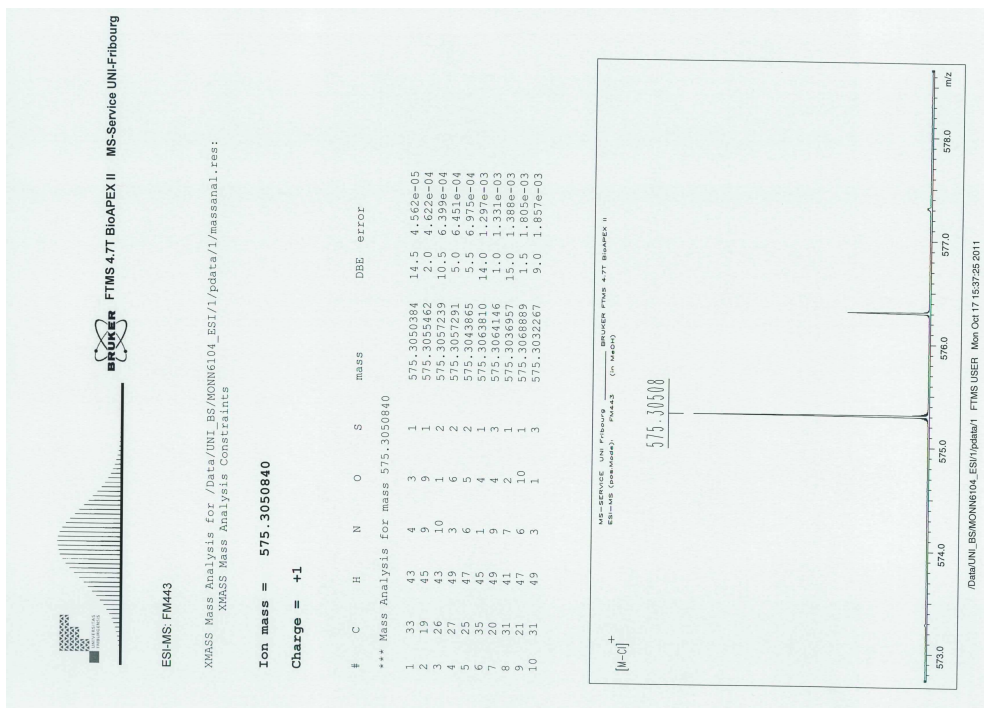


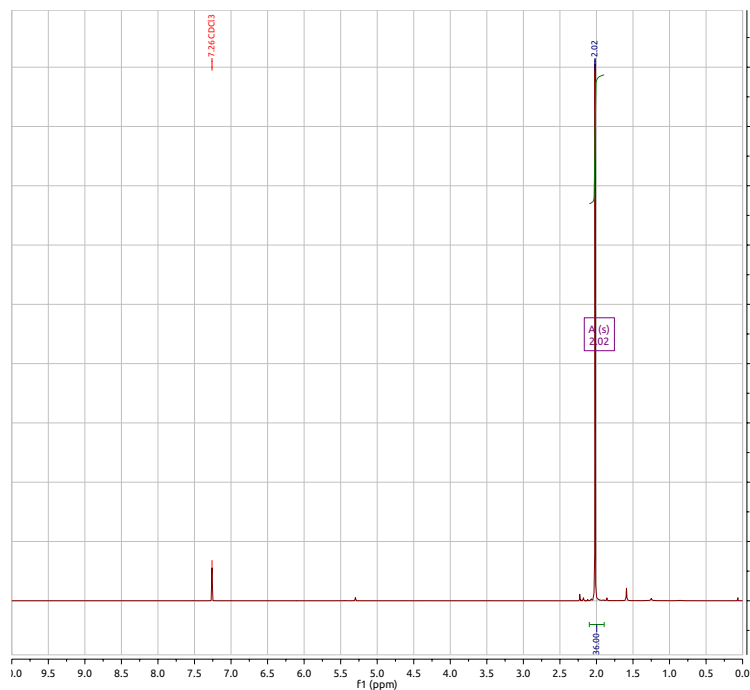
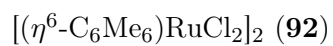
N-(2,3-Bis(mesitylamino)propyl)-4-(*N*-(*tert*-butyl)sulfamoyl)benzamide (**83**)



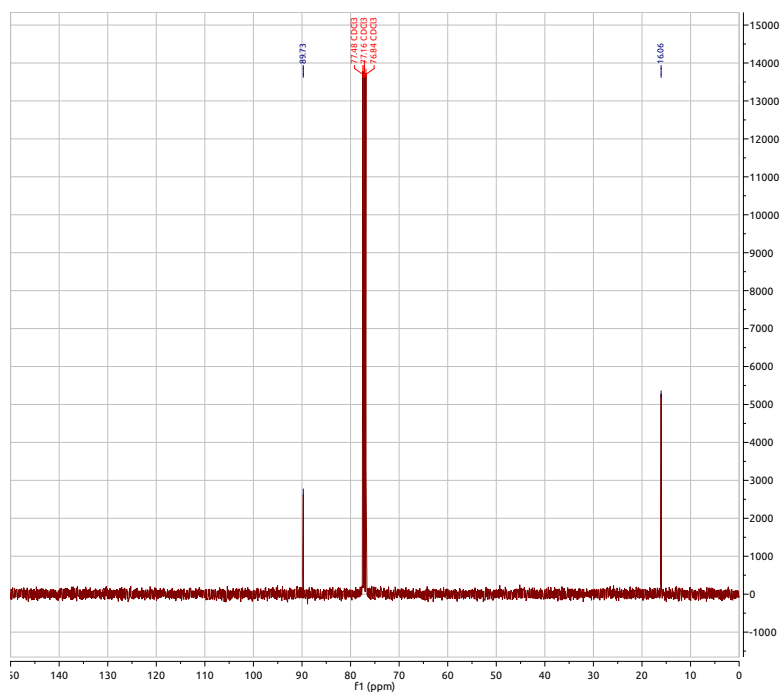
5-((4-(*N*-(*tert*-Butyl)sulfamoyl)benzamido)methyl)-1,3-dimesityl-4,5-dihydro-1H-imidazol-3-ium chloride (**74**)







Parameter	Value
1 Data File Name	/home/fabry/ Documents/ university/ uniba/ phd/ mmf/ Fabien 178/ 1/ fid
2 Title	Fabien 178/ 1
3 Comment	User/ Group Fabien_Monard/ Ward Sample RW136
4 Origin	Bruker Analytik GmbH
5 Owner	icon
6 Site	
7 Spectrometer	dpx400
8 Author	
9 Solvent	CDCl3
10 Temperature	300.0
11 Pulse Sequence	zg30
12 Experiment	1D
13 Number of Scans	16
14 Receiver Gain	258
15 Relaxation Delay	1.2000
16 Pulse Width	9.2000
17 Acquisition Time	2.9688
18 Acquisition Date	2009-12-08T09:02:52
19 Modification Date	2009-12-08T09:02:55
20 Spectrometer Frequency	400.13
21 Spectral Width	8278.1
22 Lowest Frequency	-1677.3
23 Nucleus	1H
24 Acquired Size	24576
25 Spectral Size	65536



Parameter	Value
1 Data File Name	/home/fabry/ Documents/ university/ uniba/ phd/ mmf/ Fabien 178/ 2/ fid
2 Title	Fabien 178/ 2
3 Comment	User/ Group Fabien_Monard/ Ward Sample RW136
4 Origin	Bruker Analytik GmbH
5 Owner	icon
6 Site	
7 Spectrometer	dpx400
8 Author	
9 Solvent	CDCl3
10 Temperature	300.0
11 Pulse Sequence	zgpg30
12 Experiment	1D
13 Number of Scans	384
14 Receiver Gain	16384
15 Relaxation Delay	2.2000
16 Pulse Width	9.9000
17 Acquisition Time	1.3042
18 Acquisition Date	2009-12-09T06:08:05
19 Modification Date	2009-12-09T06:08:08
20 Spectrometer Frequency	100.62
21 Spectral Width	25125.6
22 Lowest Frequency	-1521.4
23 Nucleus	13C
24 Acquired Size	32768
25 Spectral Size	65536

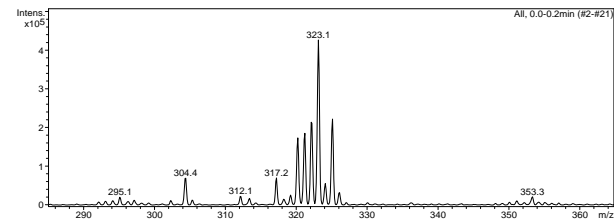
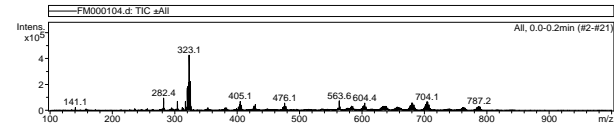
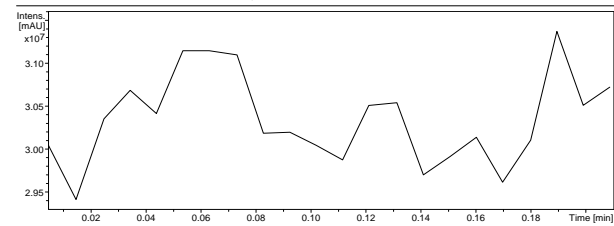
Display Report

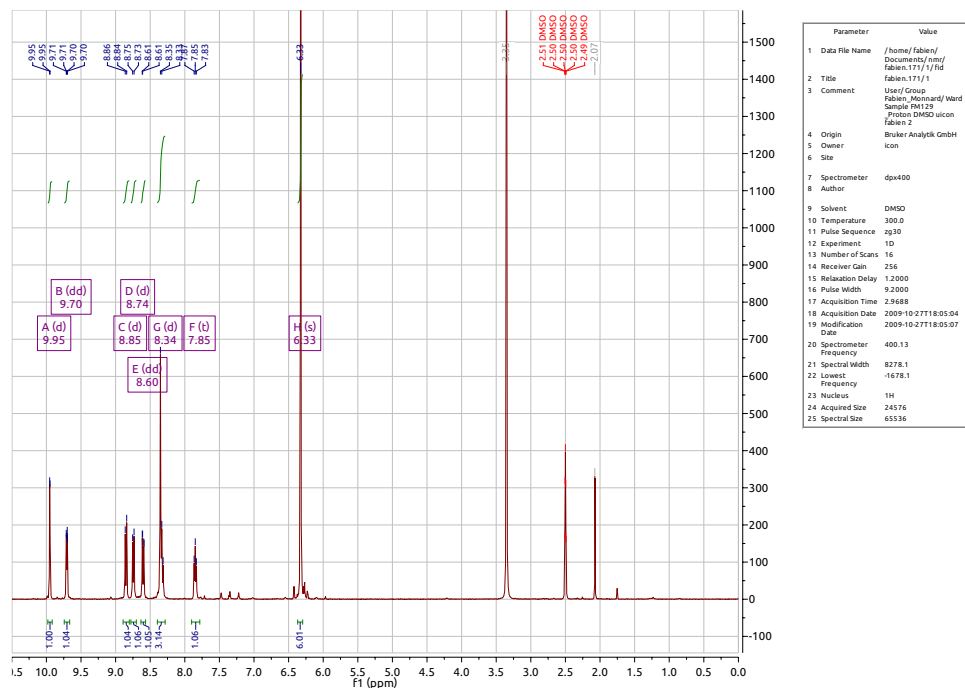
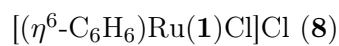
Analysis Info

Analysis Name	FM000104.d	Acquisition Date	12/07/09 18:55:16
Method	Copy of DEFAULT.MS	Operator	Carsten
Sample Name	FM134	Instrument	esquire3000plus_01096
Comment			

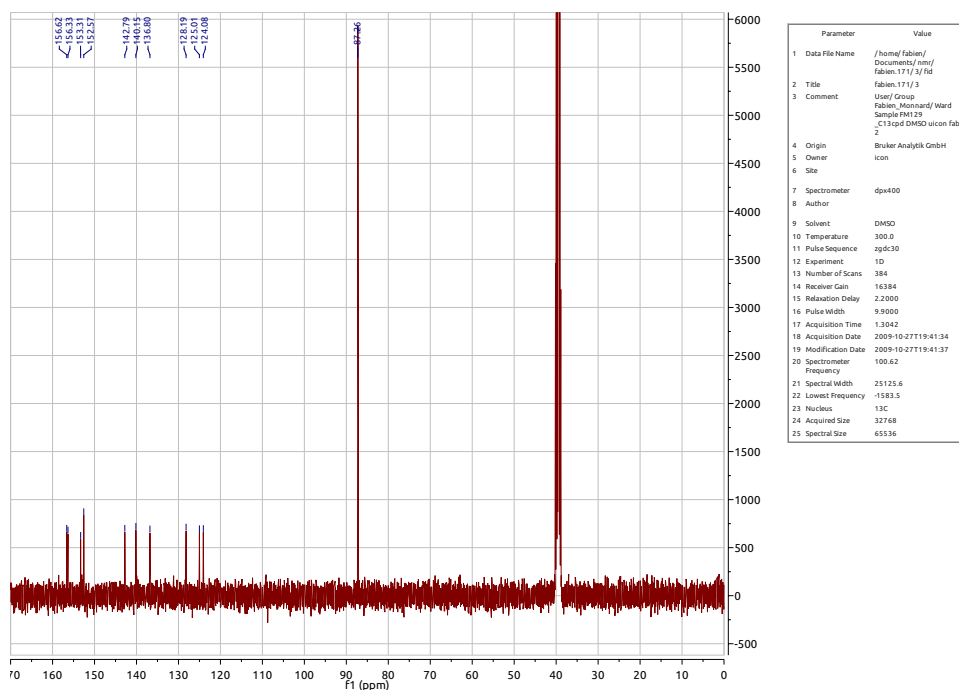
Acquisition Parameter

Ion Source Type	ESI	Ion Polarity	Positive	Alternating Ion Polarity	off
Mass Range Mode	Std/Normal	Scan Begin	100 m/z	Scan End	1000 m/z
Capillary Exit	141.1 Volt	Skim 1	40.0 Volt	Trap Drive	66.1
Accumulation Time	706 µs	Averages	5 Spectra	Auto MS/MS	off





Parameter	Value
1 Data File Name	/home/fabien/Documents/nmr/fabien.171/1
2 Title	Fabien.171/1
3 Comment	User/Group Fabien_Monnard/Ward Sample PA129 Proton DMSO uicon Fabien.2
4 Origin	Bruker Analytik GmbH
5 Owner	icon
6 Site	
7 Spectrometer	dpx400
8 Author	
9 Solvent	DMSO
10 Temperature	300.0
11 Pulse Sequence	zg30
12 Experiment	1D
13 Number of Scans	16
14 Receiver Gain	256
15 Relaxation Delay	1.2000
16 Pulse Width	3.2000
17 Acquisition Time	2.9688
18 Acquisition Date	2009-10-27T18:05:04
19 Modification Date	2009-10-27T18:05:07
20 Spectrometer Frequency	400.13
21 Spectral Width	8278.1
22 Lowest Frequency	-1678.1
23 Nucleus	1H
24 Acquired Size	24576
25 Spectral Size	65336



Parameter	Value
1 Data File Name	/home/fabien/Documents/nmr/fabien.171/3/fid
2 Title	Fabien.171/3
3 Comment	User/Group Fabien_Monnard/Ward Sample PA129 _C13cpd DMSO uicon fabien.2
4 Origin	Bruker Analytik GmbH
5 Owner	icon
6 Site	
7 Spectrometer	dpx400
8 Author	
9 Solvent	DMSO
10 Temperature	300.0
11 Pulse Sequence	zgpg30
12 Experiment	1D
13 Number of Scans	384
14 Receiver Gain	16384
15 Relaxation Delay	2.2000
16 Pulse Width	9.9000
17 Acquisition Time	1.3042
18 Acquisition Date	2009-10-27T19:41:34
19 Modification Date	2009-10-27T19:41:37
20 Spectrometer Frequency	100.62
21 Spectral Width	25125.6
22 Lowest Frequency	-1583.5
23 Nucleus	13C
24 Acquired Size	32168
25 Spectral Size	65536

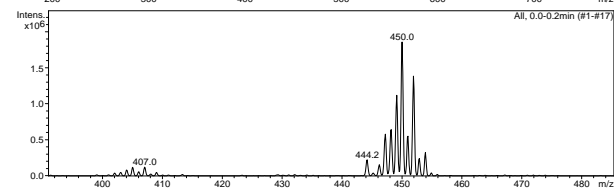
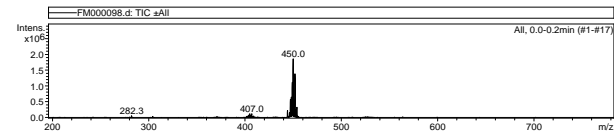
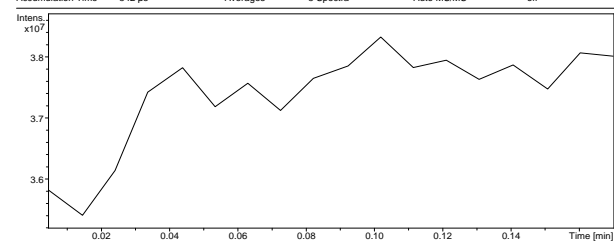
Display Report

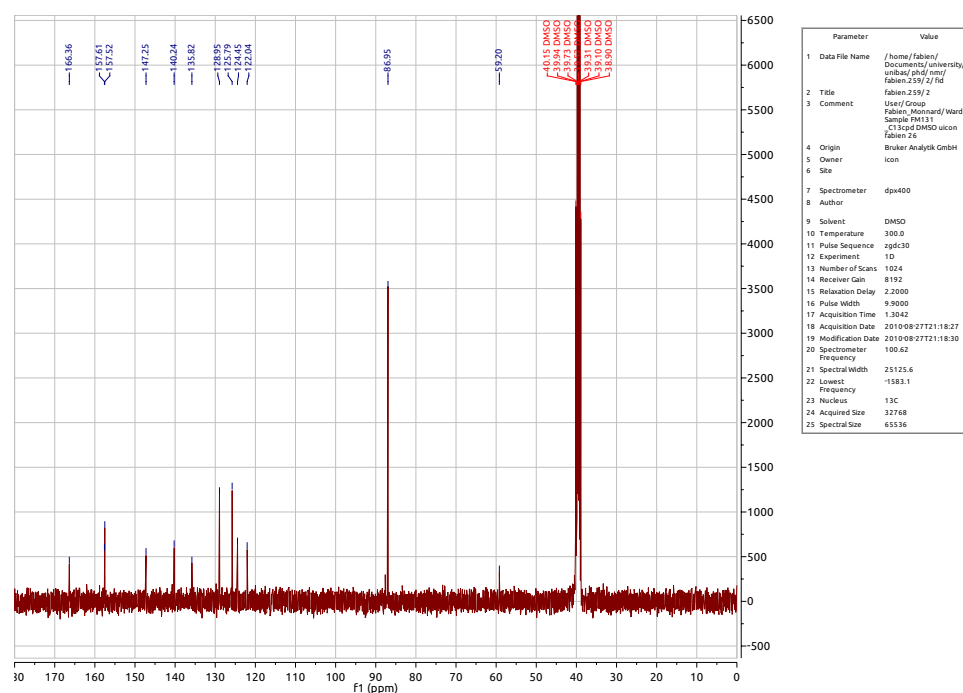
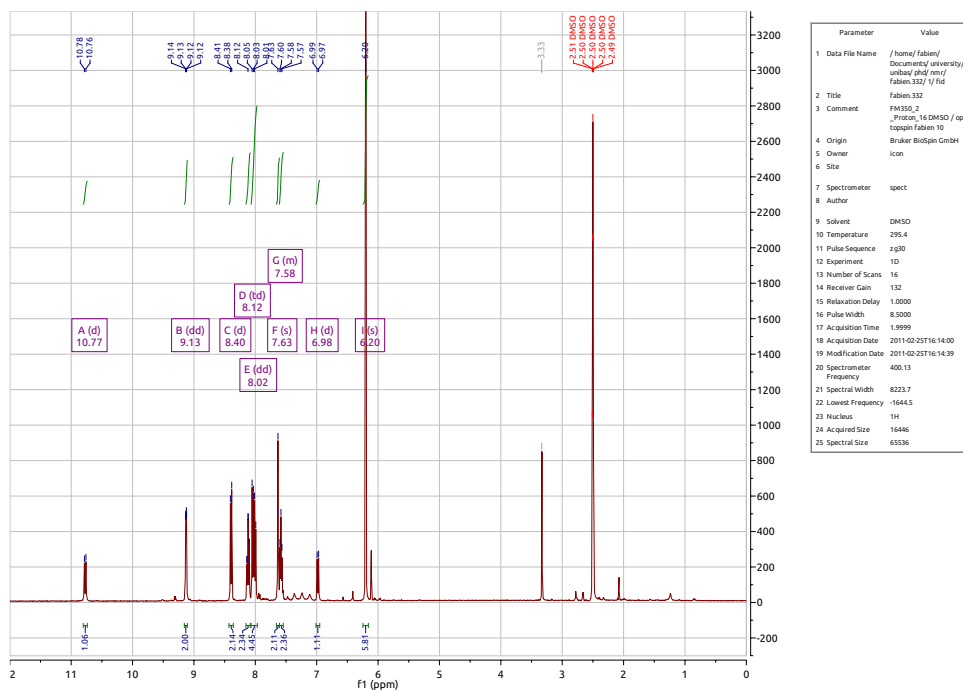
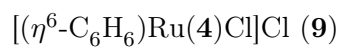
Analysis Info

Analysis Name	FM000098.d	Acquisition Date	10/26/09 18:36:23
Method	Copy of DEFAULT.MS	Operator	Eaton
Sample Name	FM129	Instrument	esquire3000plus_01096
Comment			

Acquisition Parameter

Ion Source Type	ESI	Ion Polarity	Positive	Alternating Ion Polarity	off
Mass Range Mode	Std/Normal	Scan Begin	100 m/z	Scan End	1000 m/z
Capillary Exit	124.8 Volt	Skim 1	40.0 Volt	Trap Drive	50.0
Accumulation Time	542 μ s	Averages	5 Spectra	Auto MS/MS	off





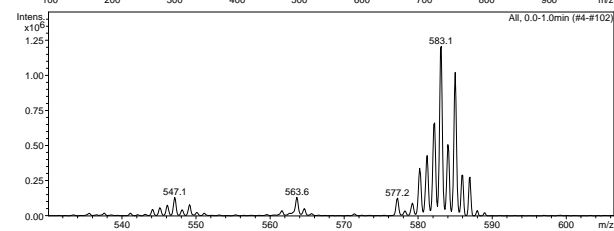
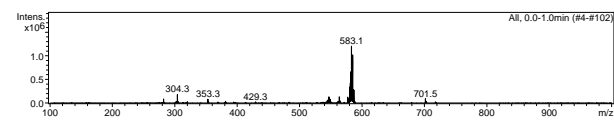
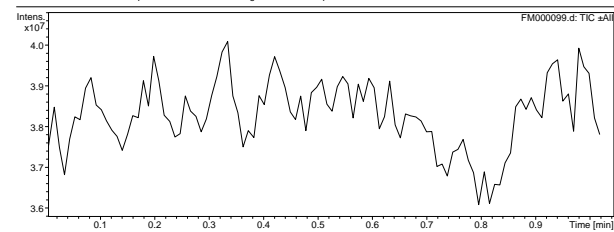
Display Report

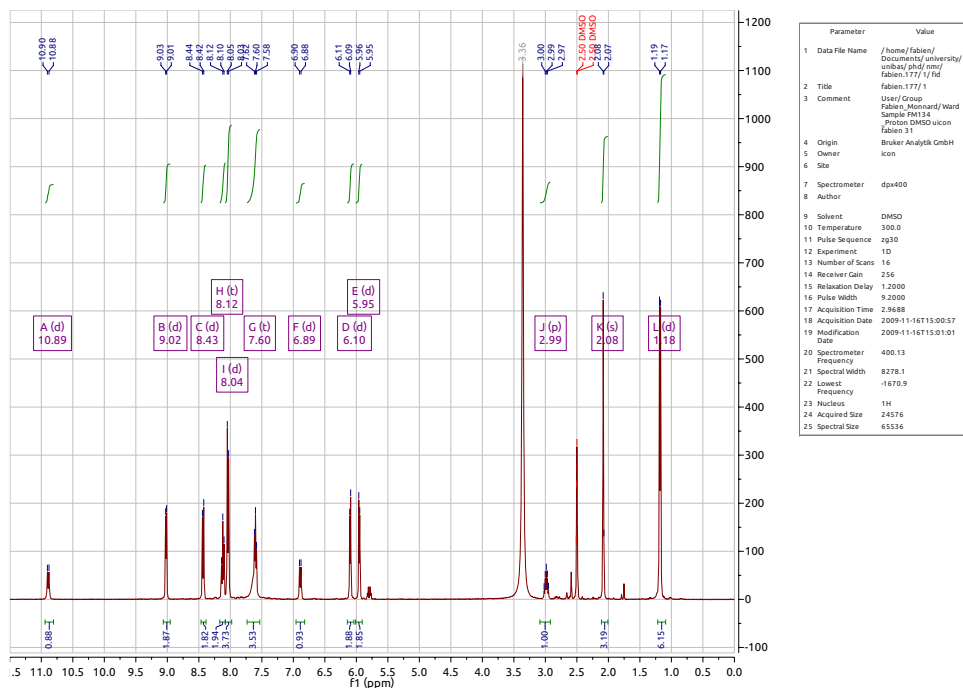
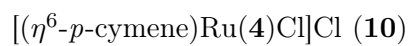
Analysis Info

Analysis Name	FM000099.d	Acquisition Date	11/04/09 09:24:54
Method	Copy of E3Kp Default.ms	Operator	Administrator
Sample Name	FM131	Instrument	esquire3000plus_01096
Comment			

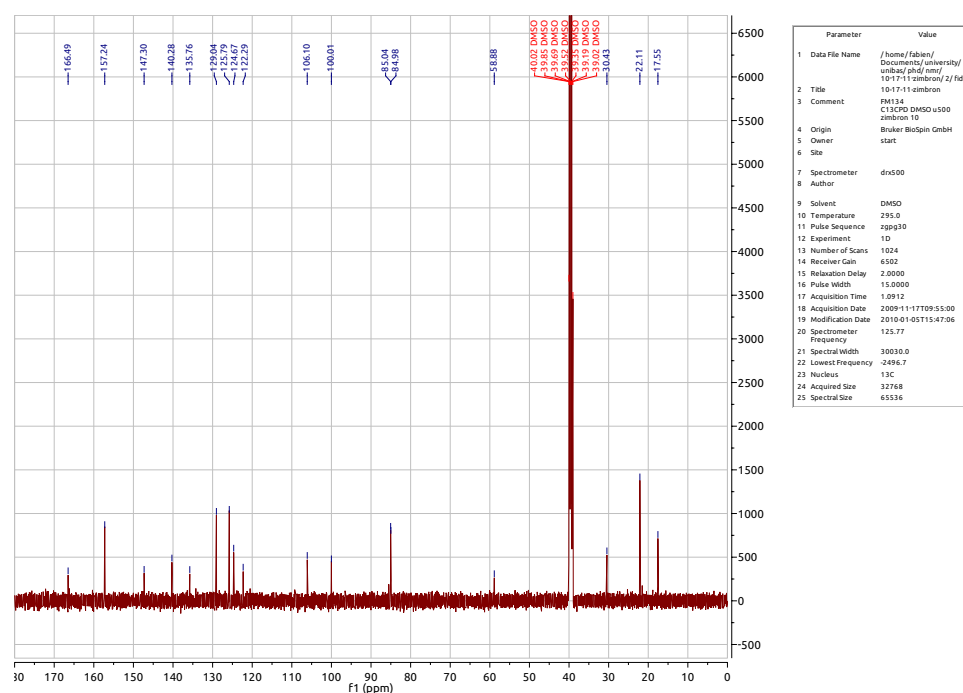
Acquisition Parameter

Ion Source Type	ESI	Ion Polarity	Positive	Alternating Ion Polarity	off
Mass Range Mode	Std/Normal	Scan Begin	100 m/z	Scan End	1000 m/z
Capillary Exit	134.3 Volt	Skim 1	40.0 Volt	Trap Drive	59.4
Accumulation Time	544 μ s	Averages	5 Spectra	Auto MS/MS	off





Parameter	Value
1 Data File Name	/home/fabien/Documents/uniba/phi/ru/10-17-11/fid
2 Title	fabien.177/1
3 Comment	User/Group fabien_Moscard/Ward Sample PA134 Piston DMSO uicon Fabien 31
4 Origin	Bruker Analytik GmbH
5 Owner	icon
6 Site	
7 Spectrometer	dp400
8 Author	
9 Solvent	DMSO
10 Temperature	300.0
11 Pulse Sequence	zg30
12 Experiment	1D
13 Number of Scans	16
14 Receiver Gain	255
15 Relaxation Delay	1.2000
16 Pulse Width	9.2000
17 Acquisition Time	2.3668
18 Acquisition Date	2009-11-16T15:00:57
19 Modification Date	2009-11-16T15:01:01
20 Spectrometer Frequency	400.13
21 Spectral Width	8278.1
22 Lowest Frequency	-1576.9
23 Nucleus	1H
24 Acquired Size	25676
25 Spectral Size	65536



Parameter	Value
1 Data File Name	/home/fabien/Documents/uniba/phi/ru/10-17-11/zimbrony/2/fid
2 Title	10-17-11 zimbrony
3 Comment	PA134 C13CPD DMSO u500 zimbrony 10
4 Origin	Bruker BioSpin GmbH
5 Owner	start
6 Site	
7 Spectrometer	drx500
8 Author	
9 Solvent	DMSO
10 Temperature	255.0
11 Pulse Sequence	zgpg30
12 Experiment	1D
13 Number of Scans	1024
14 Receiver Gain	6502
15 Relaxation Delay	2.0000
16 Pulse Width	15.0000
17 Acquisition Time	1.0912
18 Acquisition Date	2009-11-17T09:55:00
19 Modification Date	2010-01-05T15:47:06
20 Spectrometer Frequency	125.77
21 Spectral Width	30030.0
22 Lowest Frequency	-2496.7
23 Nucleus	13C
24 Acquired Size	32768
25 Spectral Size	65536

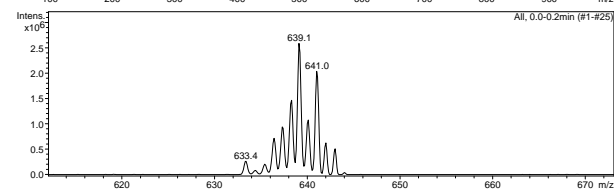
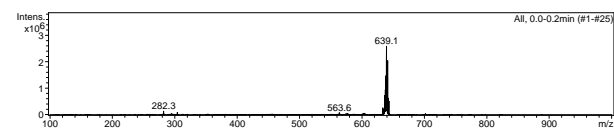
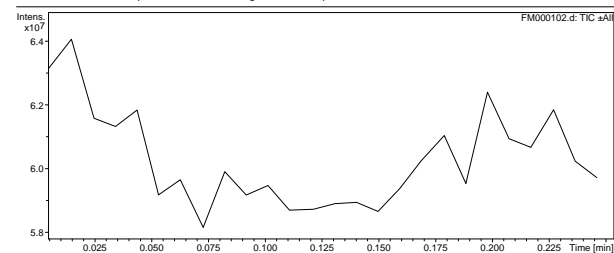
Display Report

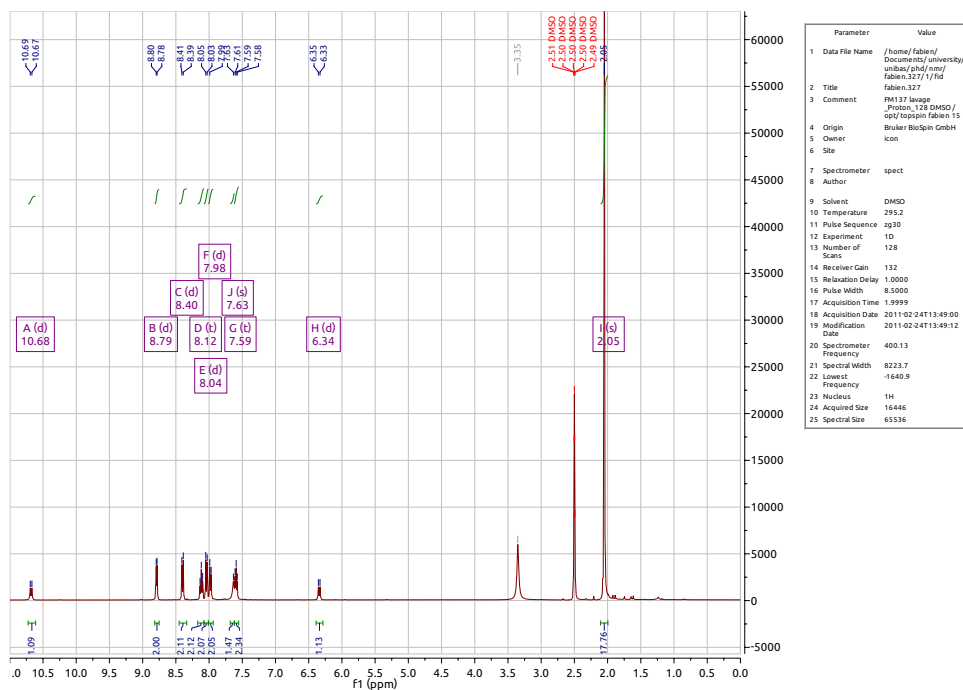
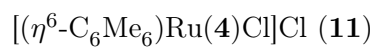
Analysis Info

Analysis Name	FM000102.d	Acquisition Date	11/16/09 08:36:42
Method	Copy of E3Kp Default.ms	Operator	Sabina
Sample Name	FM134	Instrument	esquire3000plus_01096
Comment			

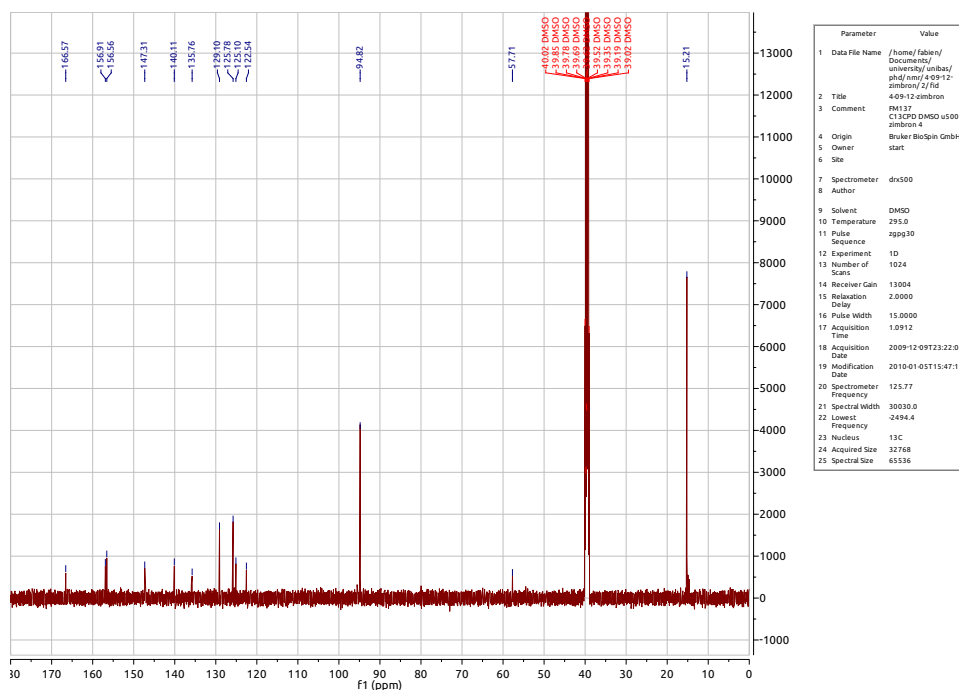
Acquisition Parameter

Ion Source Type	ESI	Ion Polarity	Positive	Alternating Ion Polarity	off
Mass Range Mode	Std/Normal	Scan Begin	100 m/z	Scan End	1000 m/z
Capillary Exit	138.9 Volt	Skim 1	40.0 Volt	Trap Drive	64.0
Accumulation Time	330 μ s	Averages	5 Spectra	Auto MS/MS	off





Parameter	Value
1 Data File Name	/home/fabian/Documents/uniba/chemistry/fabian/phi4/nmy/4-09-12-zimbon4
2 Title	phi4/nmy/4-09-12-zimbon4
3 Comment	PM137 average
4 Origin	Proton, 128 DMSO / opf/topspin fabian 15
5 Owner	Bruker Biospin GmbH
6 Site	icon
7 Spectrometer	spect
8 Author	
9 Solvent	DMSO
10 Temperature	295.2
11 Pulse Sequence	zg30
12 Experiment	1D
13 Number of Scans	128
14 Receiver Gain	132
15 Relaxation Delay	1.0000
16 Pulse Width	8.5000
17 Acquisition Time	1.9999
18 Acquisition Date	2011-02-24T13:49:00
19 Modification Date	2011-02-24T13:49:12
20 Spectrometer Frequency	400.13
21 Spectral Width	8233.7
22 Lowest Frequency	-1640.9
23 Nucleus	^1H
24 Acquired Size	16446
25 Spectral Size	65536



Parameter	Value
1 Data File Name	/home/fabian/Documents/uniba/chemistry/fabian/phi4/nmy/4-09-12-zimbon4
2 Title	phi4/nmy/4-09-12-zimbon4
3 Comment	PM137
4 Origin	C13CPD DMSO d500 zimbon 4
5 Owner	Bruker Biospin GmbH
6 Site	start
7 Spectrometer	dmx500
8 Author	
9 Solvent	DMSO
10 Temperature	295.0
11 Pulse Sequence	zgpg30
12 Experiment	1D
13 Number of Scans	1024
14 Receiver Gain	13004
15 Relaxation Delay	2.0000
16 Pulse Width	15.0000
17 Acquisition Time	1.0912
18 Acquisition Date	2009-12-09T23:22:00
19 Modification Date	2010-01-05T15:47:15
20 Spectrometer Frequency	125.77
21 Spectral Width	30030.0
22 Lowest Frequency	-2494.4
23 Nucleus	^{13}C
24 Acquired Size	32768
25 Spectral Size	65536

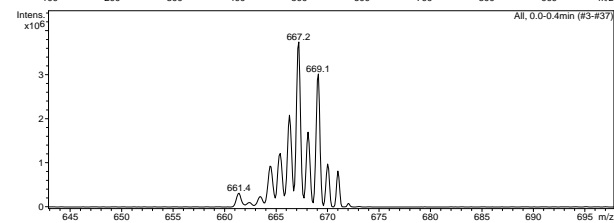
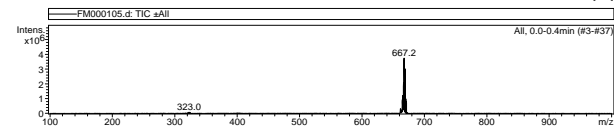
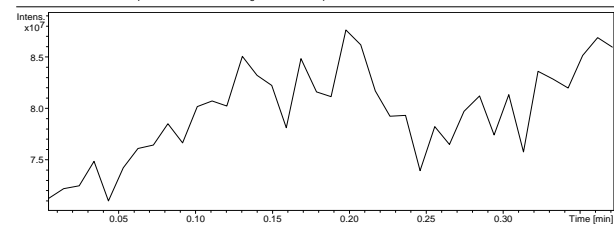
Display Report

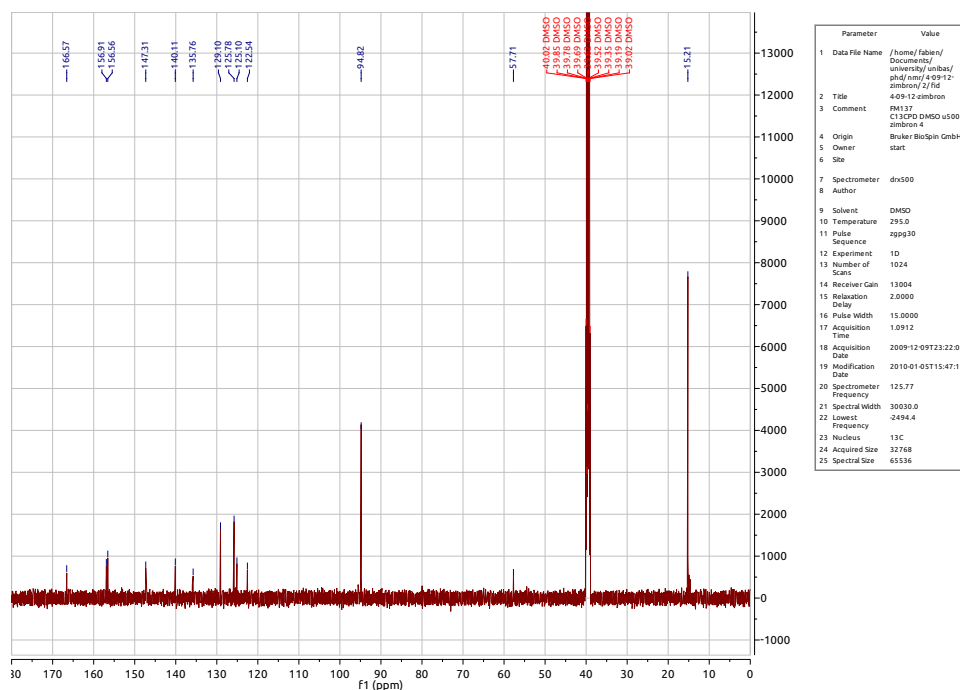
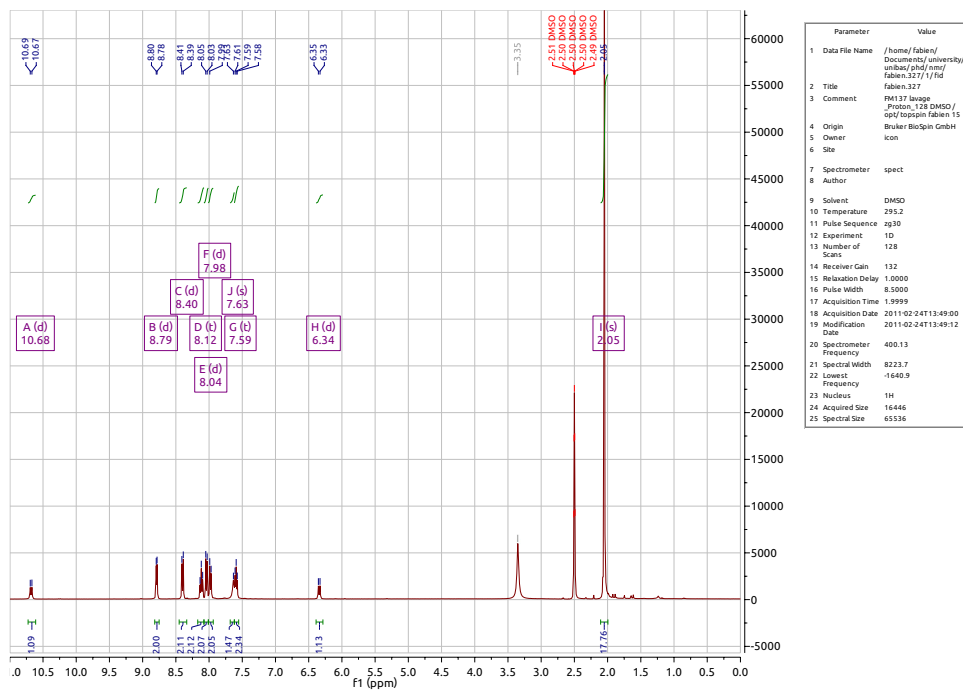
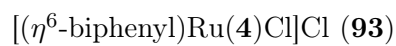
Analysis Info

Analysis Name	FM000105.d	Acquisition Date	12/08/09 15:26:02
Method	Copy(2) of E3Kp Default.ms	Operator	Carsten
Sample Name	FM137	Instrument	esquire3000plus_01096
Comment			

Acquisition Parameter

Ion Source Type	ESI	Ion Polarity	Positive	Alternating Ion Polarity	off
Mass Range Mode	Std/Normal	Scan Begin	100 m/z	Scan End	1000 m/z
Capillary Exit	141.0 Volt	Skim 1	40.0 Volt	Trap Drive	66.0
Accumulation Time	270 μ s	Averages	5 Spectra	Auto MS/MS	off





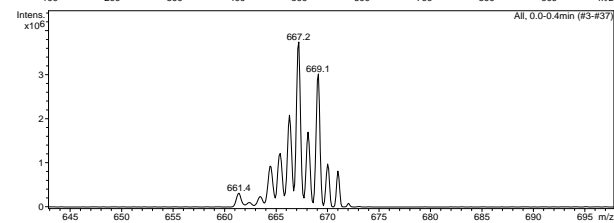
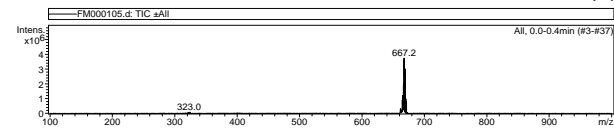
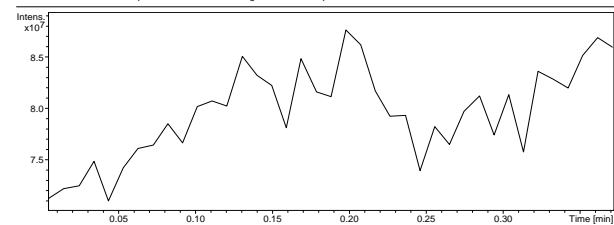
Display Report

Analysis Info

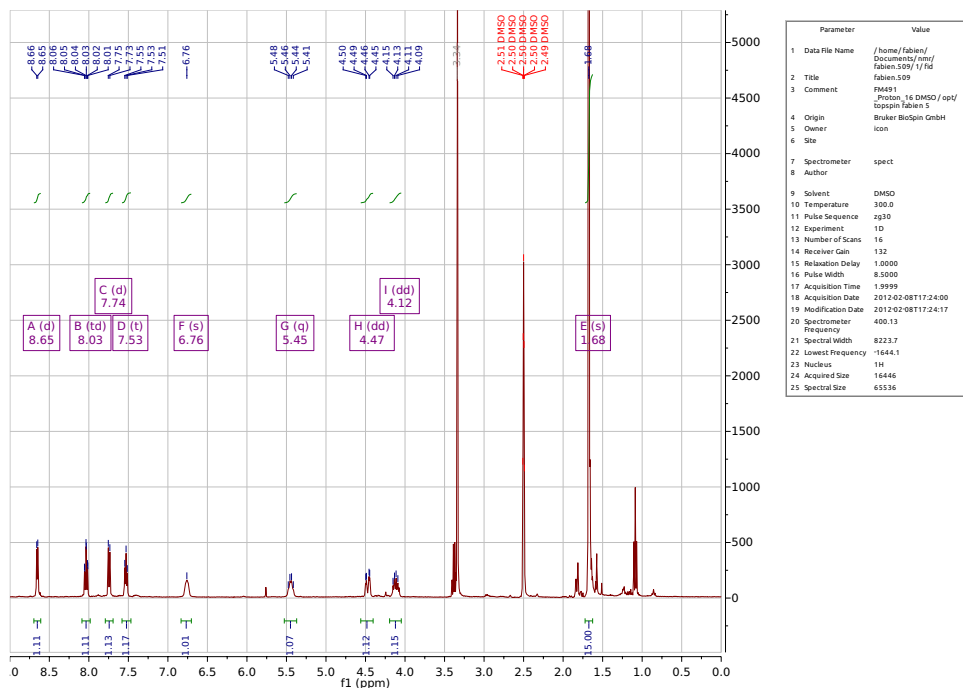
Analysis Name	FM000105.d	Acquisition Date	12/08/09 15:26:02
Method	Copy(2) of E3Kp Default.ms	Operator	Carsten
Sample Name	FM137	Instrument	esquire3000plus_01096
Comment			

Acquisition Parameter

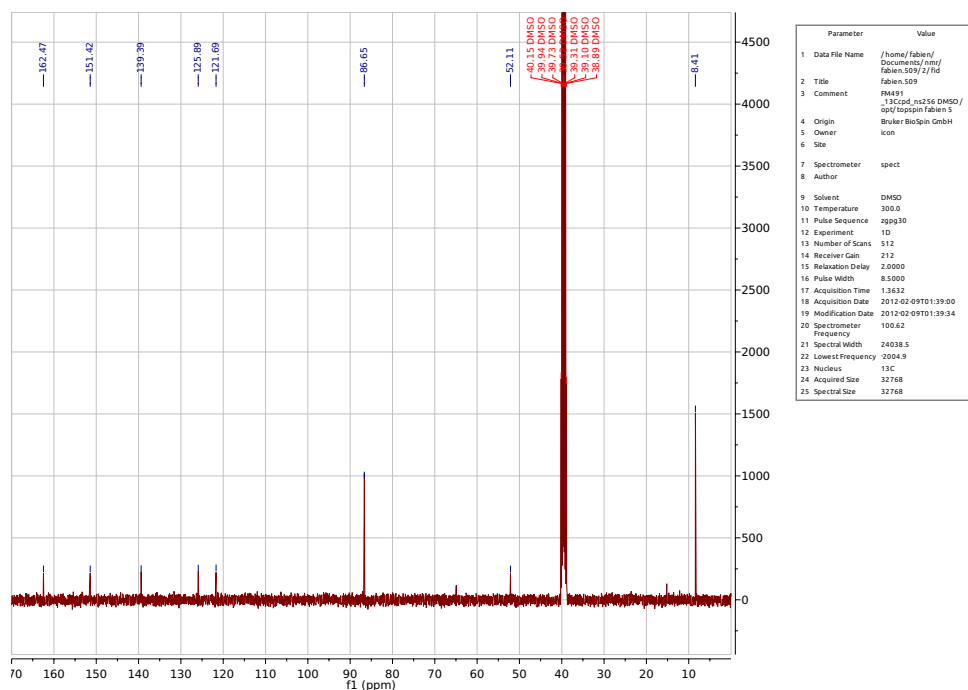
Ion Source Type	ESI	Ion Polarity	Positive	Alternating Ion Polarity	off
Mass Range Mode	Std/Normal	Scan Begin	100 m/z	Scan End	1000 m/z
Capillary Exit	141.0 Volt	Skim 1	40.0 Volt	Trap Drive	66.0
Accumulation Time	270 μ s	Averages	5 Spectra	Auto MS/MS	off



$[(cp^*)Ir(2\text{-picolyamine})Cl]Cl$ (**13**)



Parameter	Value
1 Data File Name	/home/fabien/Documents/nmr/Fabien.509/1/H2
2 Title	Fabien.509
3 Comment	RM491 Pipon 16 DMSO / opt/ topspin Fabien 5
4 Origin	Bruker BioSpin GmbH
5 Owner	icon
6 Site	
7 Spectrometer	spect
8 Author	
9 Solvent	DMSO
10 Temperature	300.0
11 Pulse Sequence	zg30
12 Experiment	1D
13 Number of Scans	16
14 Receiver Gain	132
15 Relaxation Delay	1.0000
16 Pulse Width	8.5000
17 Acquisition Time	1.9999
18 Acquisition Date	2012-02-08T17:24:00
19 Modification Date	2012-02-08T17:24:17
20 Spectrometer Frequency	400.13
21 Spectral Width	8223.7
22 Lowest Frequency	1644.1
23 Nucleus	1H
24 Acquired Size	16446
25 Spectral Size	65536



Parameter	Value
1 Data File Name	/home/fabien/Documents/nmr/Fabien.509/2/H2
2 Title	Fabien.509
3 Comment	RM491 13Ccpn 16.258 DMSO/ Sp4/topspin Fabien 5
4 Origin	Bruker BioSpin GmbH
5 Owner	icon
6 Site	
7 Spectrometer	spect
8 Author	
9 Solvent	DMSO
10 Temperature	300.0
11 Pulse Sequence	zgpg30
12 Experiment	1D
13 Number of Scans	212
14 Receiver Gain	212
15 Relaxation Delay	2.0000
16 Pulse Width	8.5000
17 Acquisition Time	1.3632
18 Acquisition Date	2012-02-09T01:39:00
19 Modification Date	2012-02-09T01:39:34
20 Spectrometer Frequency	100.62
21 Spectral Width	24038.5
22 Lowest Frequency	2004.9
23 Nucleus	13C
24 Acquired Size	32768
25 Spectral Size	32768

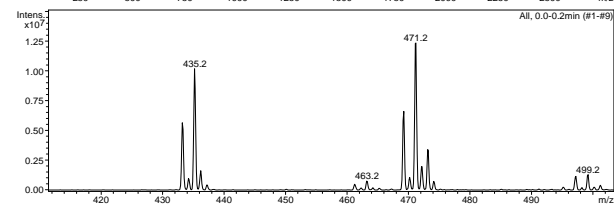
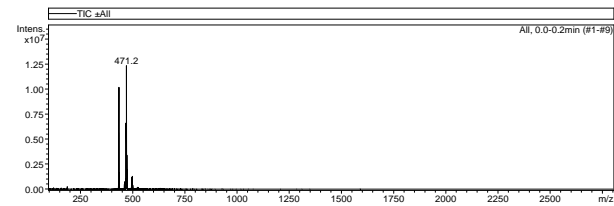
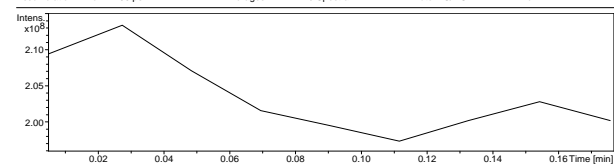
Display Report

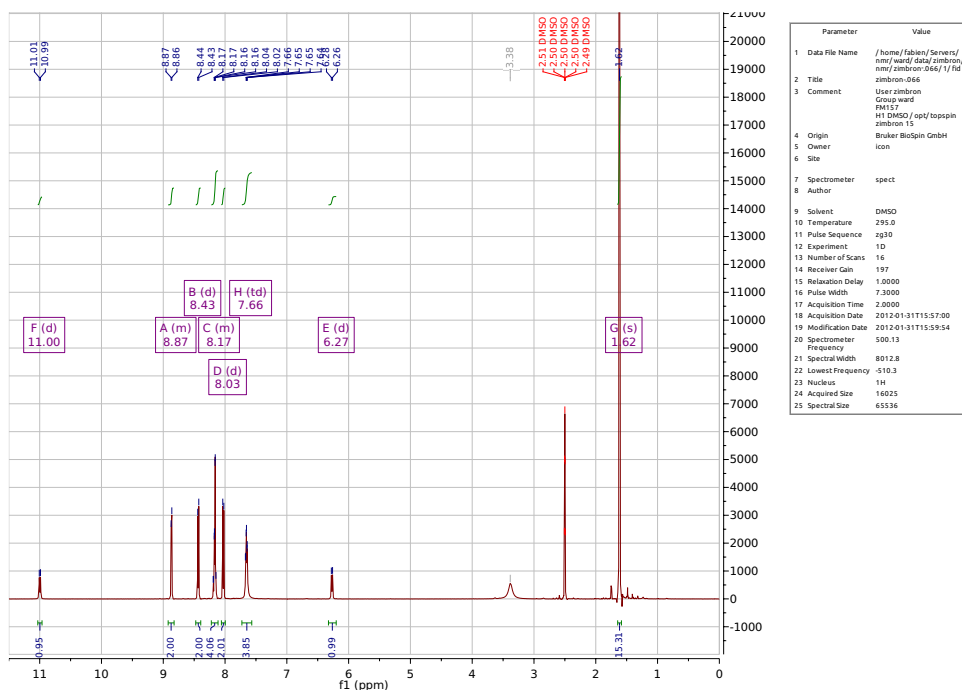
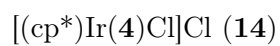
Analysis Info

Analysis Name	FM000019.d	Acquisition Date	02/08/12 17:54:37
Method	Copy of DEFAULT.MS	Operator	Administrator
Sample Name	FM491	Instrument	esquire3000plus_01096
Comment			

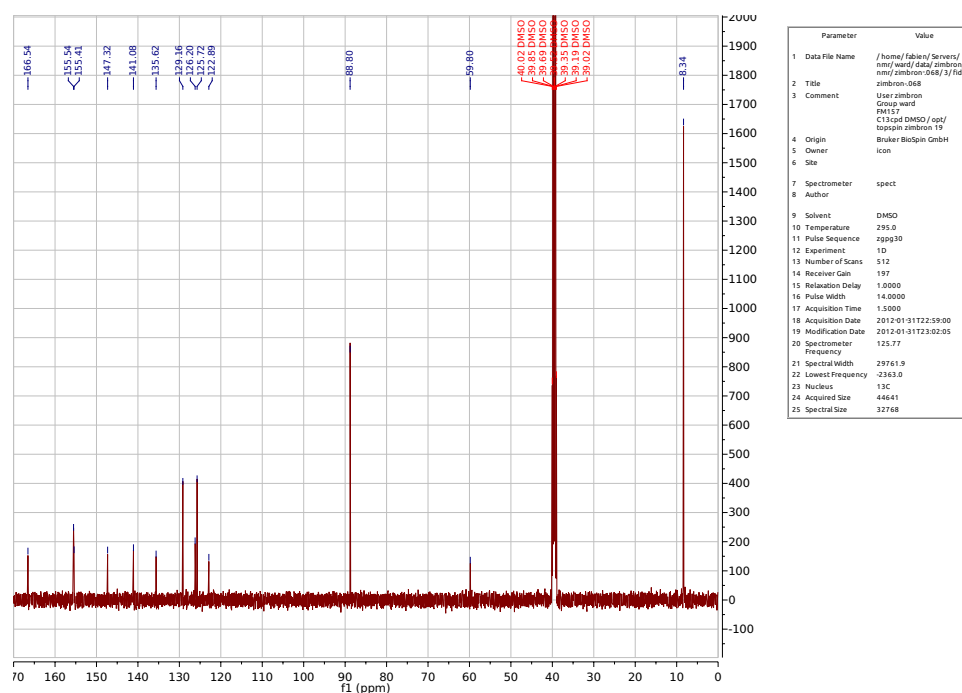
Acquisition Parameter

Ion Source Type	ESI	Ion Polarity	Positive	Alternating Ion Polarity	off
Mass Range Mode	Std/Normal	Scan Begin	100 m/z	Scan End	2900 m/z
Capillary Exit	126.3 Volt	Skim 1	40.0 Volt	Trap Drive	51.6
Accumulation Time	96 μ s	Averages	5 Spectra	Auto MS/MS	off





Parameter	Value
1 Data File Name	/home/fabian/Server/nmr/zimbron/066/17/rd/zimbron-066
2 Title	User zimbron
3 Comment	Group ward RM153 H1 DMSO-d6/ppp/topspin/zimbron 15
4 Origin	Bruker Biospin GmbH
5 Owner	icon
6 Site	
7 Spectrometer	spect
8 Author	
9 Solvent	DMSO
10 Temperature	295.0
11 Pulse Sequence	zg30
12 Experiment	1d
13 Number of Scans	16
14 Receiver Gain	197
15 Relaxation Delay	1.0000
16 Pulse Width	7.0000
17 Acquisition Time	2.5000
18 Acquisition Date	2012-01-31T15:57:00
19 Modification Date	2012-01-31T15:59:54
20 Spectrometer Frequency	500.13
21 Spectral Width	8012.8
22 Lowest Frequency	-510.3
23 Nucleus	1H
24 Acquired Size	16025
25 Spectral Size	65536



Parameter	Value
1 Data File Name	/home/fabian/Server/nmr/zimbron/066/17/rd/zimbron-066
2 Title	User zimbron
3 Comment	Group ward RM153 C13cp DMSO-d6/ppp/topspin/zimbron 19
4 Origin	Bruker Biospin GmbH
5 Owner	icon
6 Site	
7 Spectrometer	spect
8 Author	
9 Solvent	DMSO
10 Temperature	295.0
11 Pulse Sequence	zgpg30
12 Experiment	1d
13 Number of Scans	512
14 Receiver Gain	197
15 Relaxation Delay	1.0000
16 Pulse Width	14.0000
17 Acquisition Time	1.5000
18 Acquisition Date	2012-01-31T22:59:00
19 Modification Date	2012-01-31T23:02:05
20 Spectrometer Frequency	125.77
21 Spectral Width	29761.9
22 Lowest Frequency	-2365.0
23 Nucleus	13C
24 Acquired Size	44641
25 Spectral Size	32768

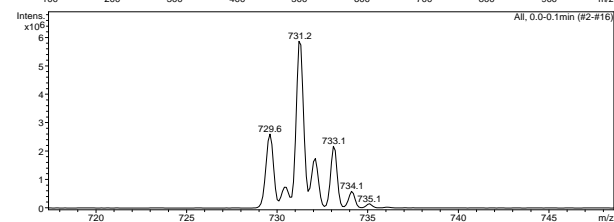
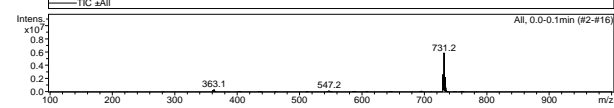
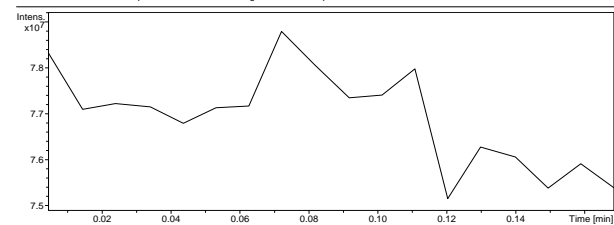
Display Report

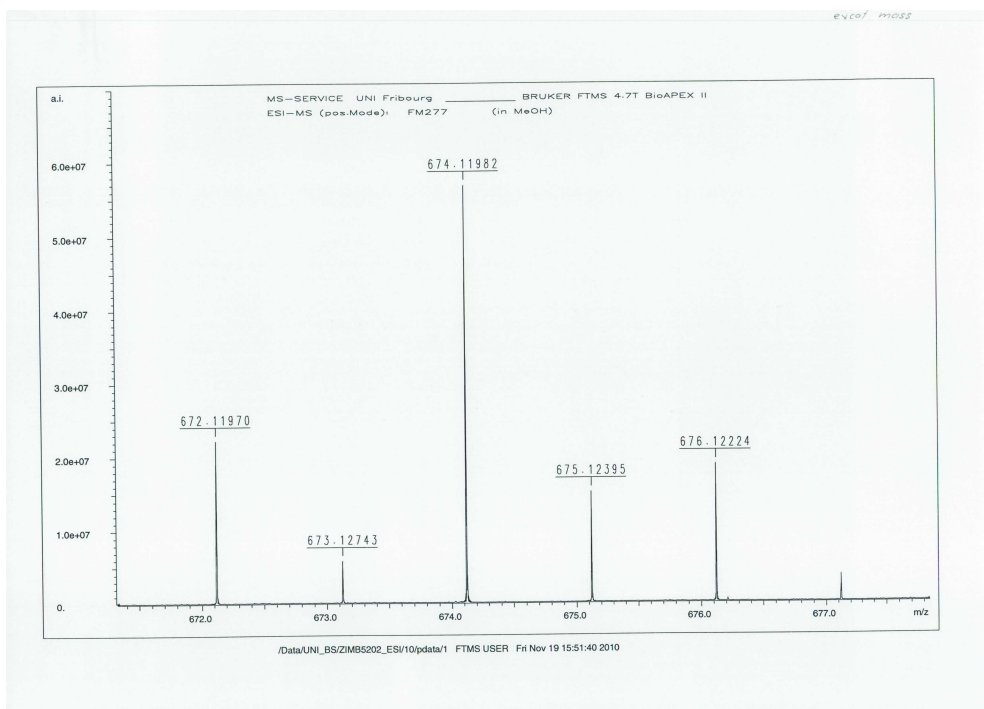
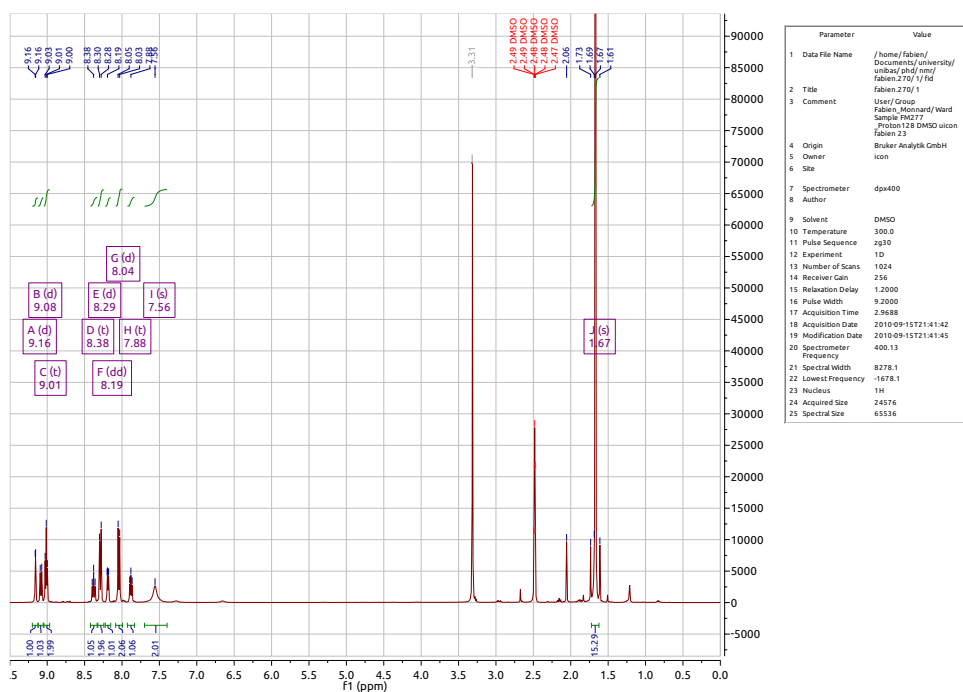
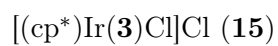
Analysis Info

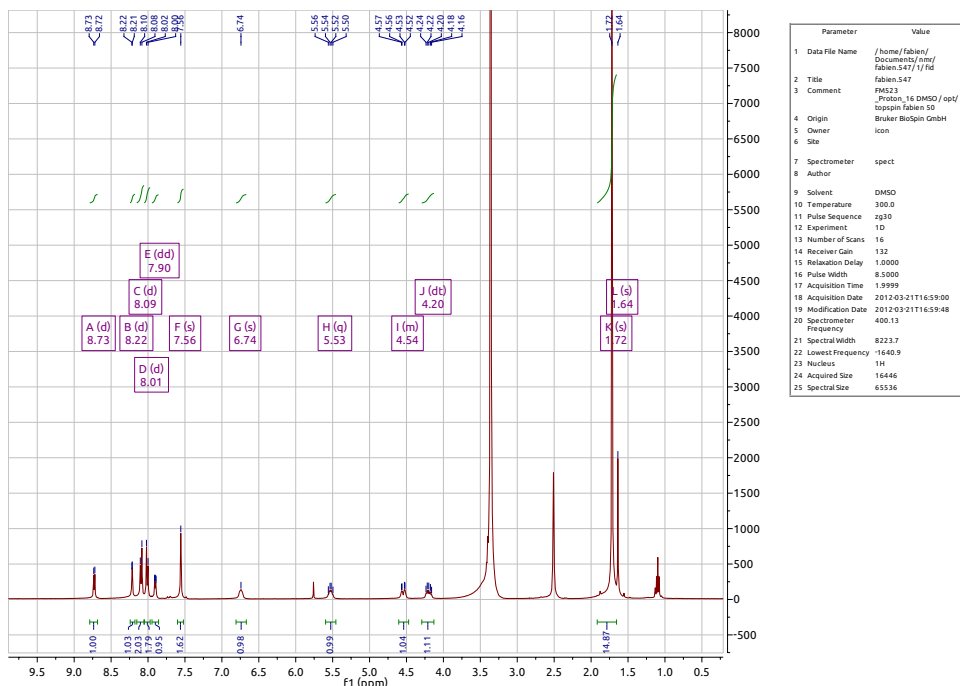
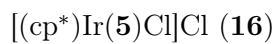
Analysis Name	Fm000150.d	Acquisition Date	02/18/10 17:00:39
Method	Copy(2) of E3Kp Default.ms	Operator	Sandro
Sample Name	7FM15	Instrument	esquire3000plus_01096
Comment			

Acquisition Parameter

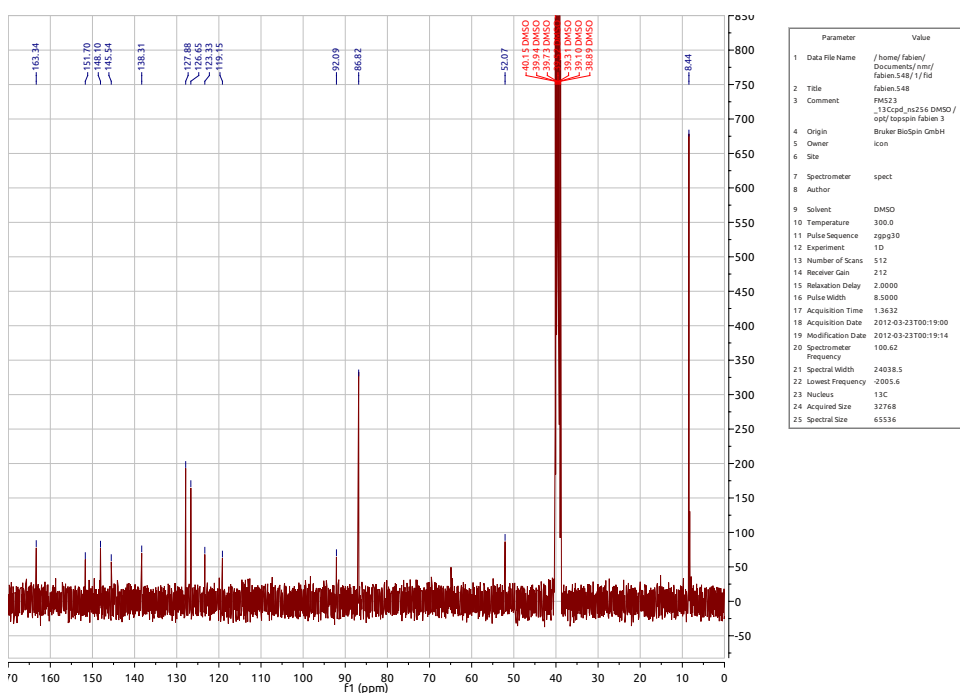
Ion Source Type	ESI	Ion Polarity	Positive	Alternating Ion Polarity	off
Mass Range Mode	Std/Normal	Scan Begin	100 m/z	Scan End	1000 m/z
Capillary Exit	145.8 Volt	Skim 1	40.0 Volt	Trap Drive	70.8
Accumulation Time	297 μ s	Averages	5 Spectra	Auto MS/MS	off







Parameter	Value
1 Data File Name	/home/fabien/Documents/fmf/fabien.547/1/fd
2 Title	fabien.547
3 Comment	FM523
4 Origin	_Proton, 16 DMSO/epf/
5 Owner	brspn fabien 50
6 Site	Brucker BioSpin GmbH
7 Spectrometer	icon
8 Author	spect
9 Solvent	DMSO
10 Temperature	300.0
11 Pulse Sequence	zg30
12 Experiment	10
13 Number of Scans	16
14 Receiver Gain	132
15 Relaxation Delay	1.0000
16 Pulse Width	8.5000
17 Acquisition Time	1.9999
18 Acquisition Date	2012-03-21T16:59:00
19 Modification Date	2012-03-21T16:59:48
20 Spectrometer Frequency	400.12
21 Spectral Width	8223.7
22 Lowest Frequency	15402.9
23 Nucleus	1H
24 Acquired Size	16446
25 Spectral Size	65336



Parameter	Value
1 Data File Name	/home/fabien/Documents/fmf/fabien.548/1/fd
2 Title	fabien.548
3 Comment	FM523
4 Origin	_13Cppl_m256 DMSO /
5 Owner	0907 brspn fabien 3
6 Site	Brucker BioSpin GmbH
7 Spectrometer	icon
8 Author	spect
9 Solvent	DMSO
10 Temperature	300.0
11 Pulse Sequence	zgpg30
12 Experiment	10
13 Number of Scans	512
14 Receiver Gain	212
15 Relaxation Delay	2.0000
16 Pulse Width	8.5000
17 Acquisition Time	1.3632
18 Acquisition Date	2012-03-23T00:19:14
19 Modification Date	2012-03-23T00:19:14
20 Spectrometer Frequency	100.62
21 Spectral Width	24038.5
22 Lowest Frequency	-2005.6
23 Nucleus	13C
24 Acquired Size	33768
25 Spectral Size	65336

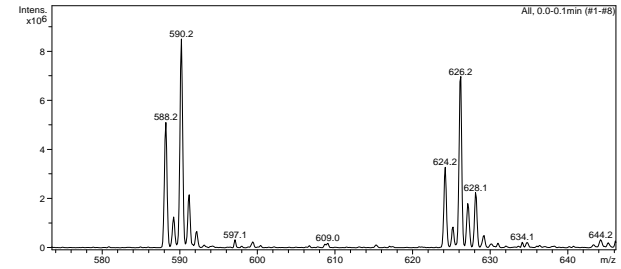
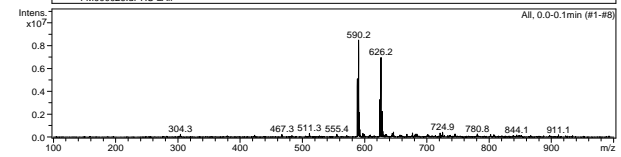
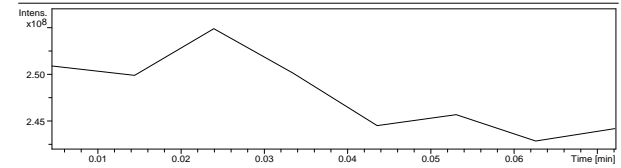
Display Report

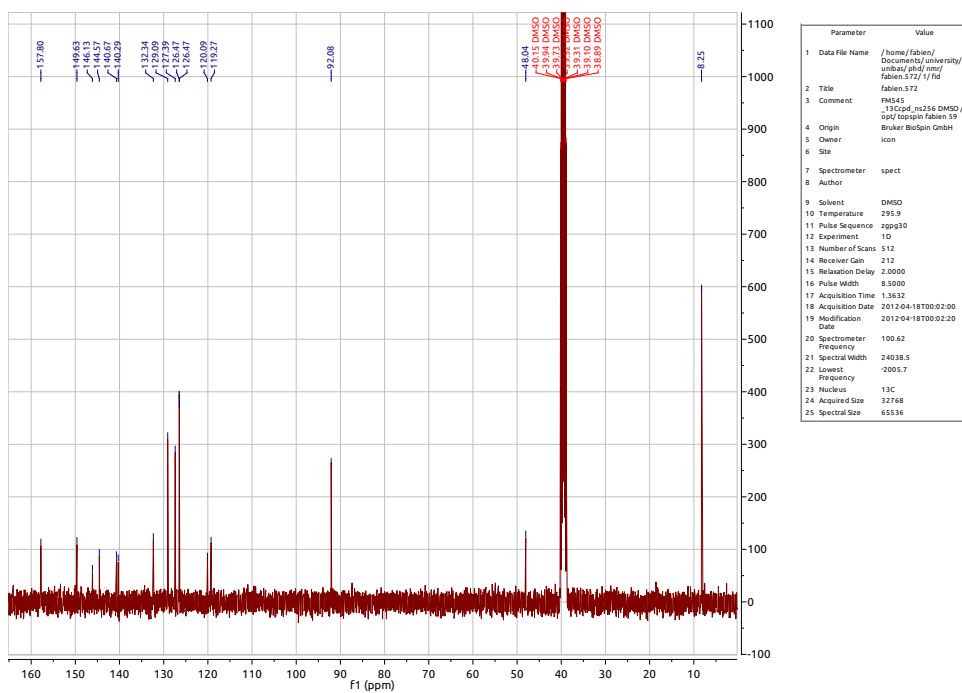
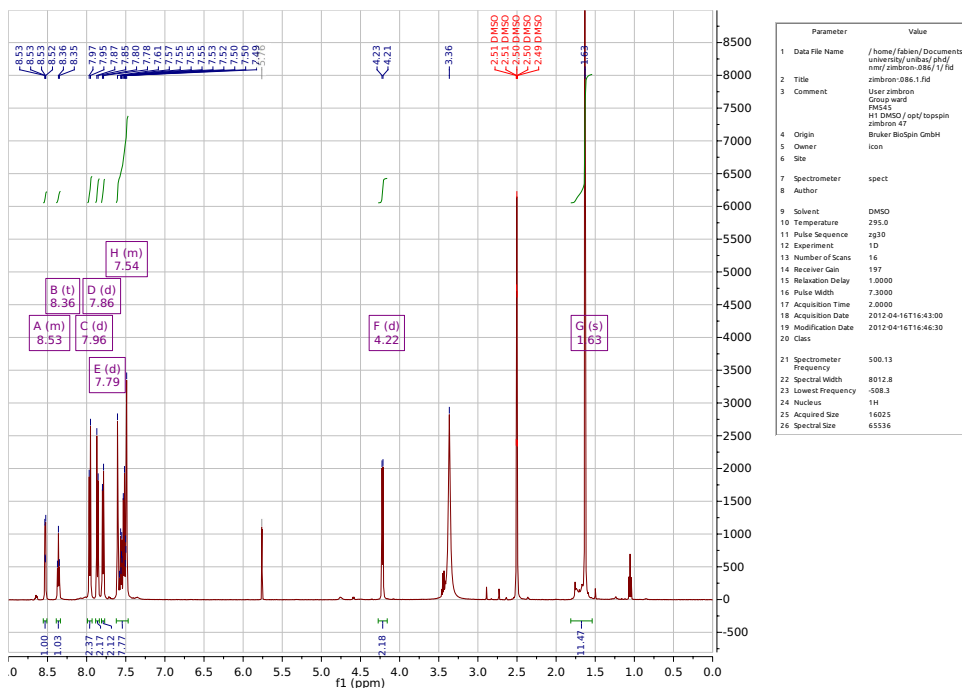
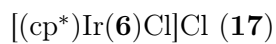
Analysis Info

Analysis Name	FM000026.d	Acquisition Date	03/22/12 08:45:39
Method	Copy of DEFAULT.MS	Operator	Malika
Sample Name	FM523	Instrument	esquire3000plus_01096
Comment			

Acquisition Parameter

Ion Source Type	ESI	Ion Polarity	Positive	Alternating Ion Polarity	off
Mass Range Mode	Std/Normal	Scan Begin	100 m/z	Scan End	1000 m/z
Capillary Exit	140.5 Volt	Skim 1	40.0 Volt	Trap Drive	65.6
Accumulation Time	84 μ s	Averages	5 Spectra	Auto MS/MS	off





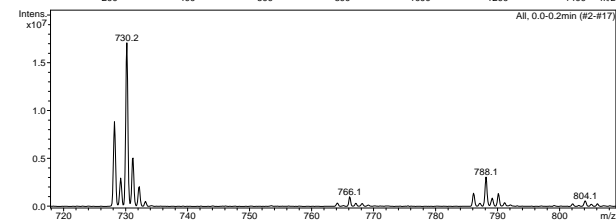
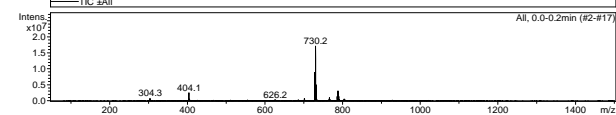
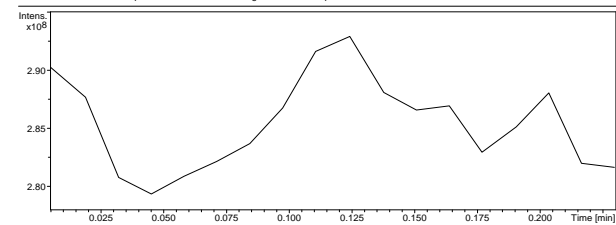
Display Report

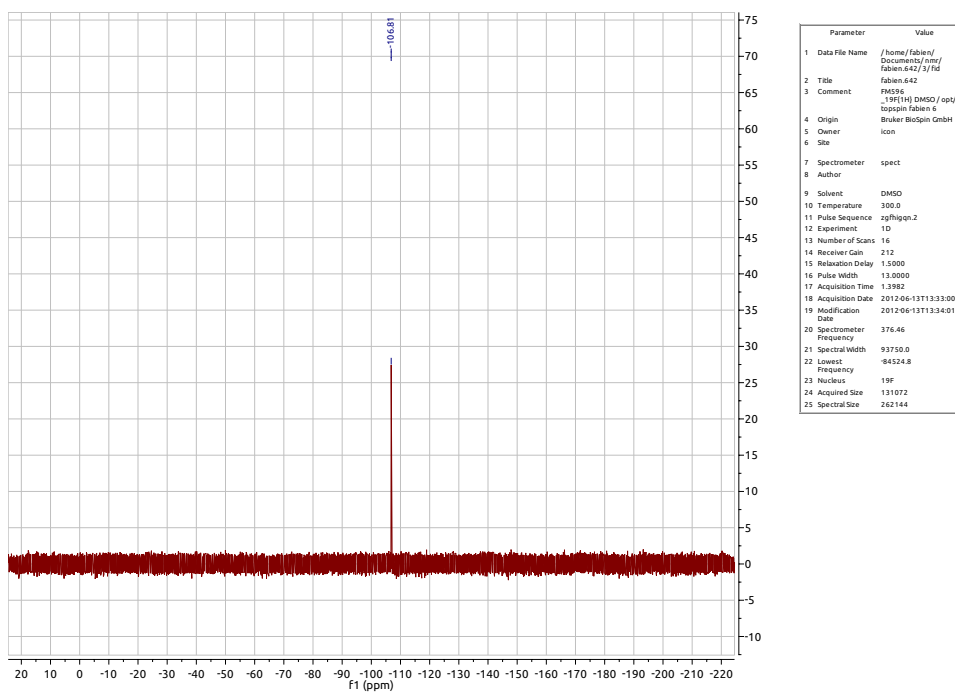
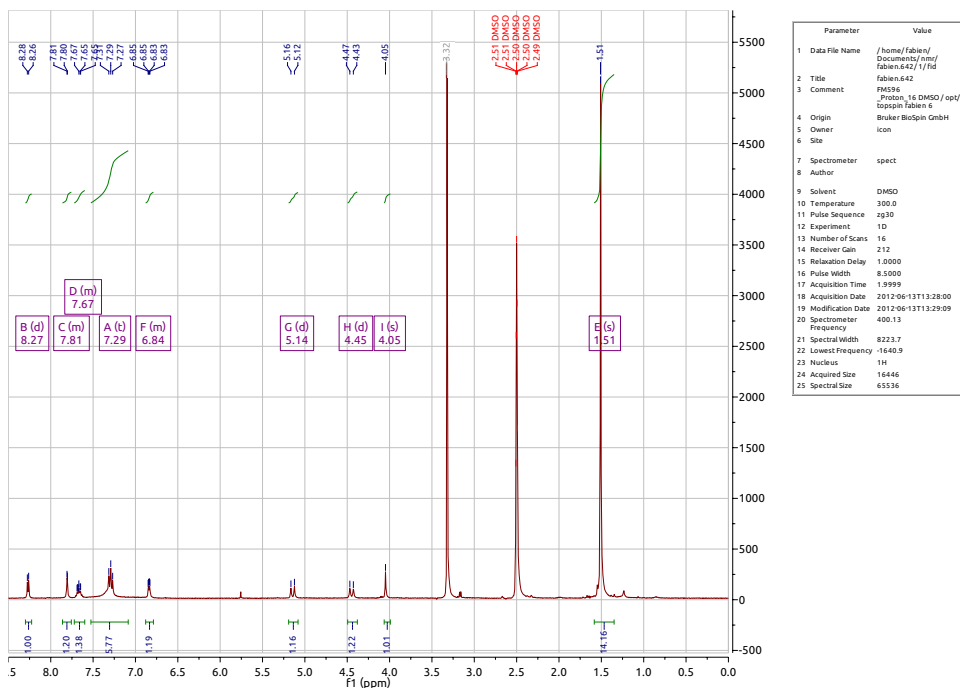
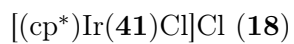
Analysis Info

Analysis Name	FM000027.d	Acquisition Date	04/16/12 17:00:21
Method	Copy(2) of E3Kp Default.ms	Operator	Administrator
Sample Name	fm545	Instrument	esquire3000plus_01096
Comment			

Acquisition Parameter

Ion Source Type	ESI	Ion Polarity	Positive	Alternating Ion Polarity	off
Mass Range Mode	Std/Normal	Scan Begin	50 m/z	Scan End	1500 m/z
Capillary Exit	134.3 Volt	Skim 1	40.0 Volt	Trap Drive	78.9
Accumulation Time	72 μ s	Averages	5 Spectra	Auto MS/MS	off





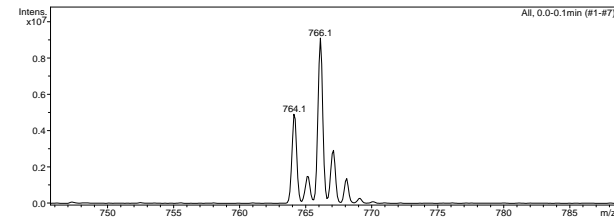
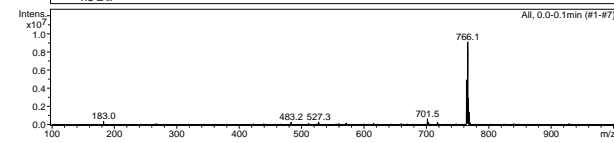
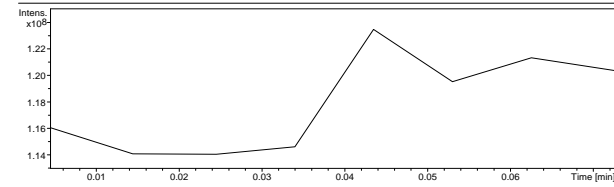
Display Report

Analysis Info

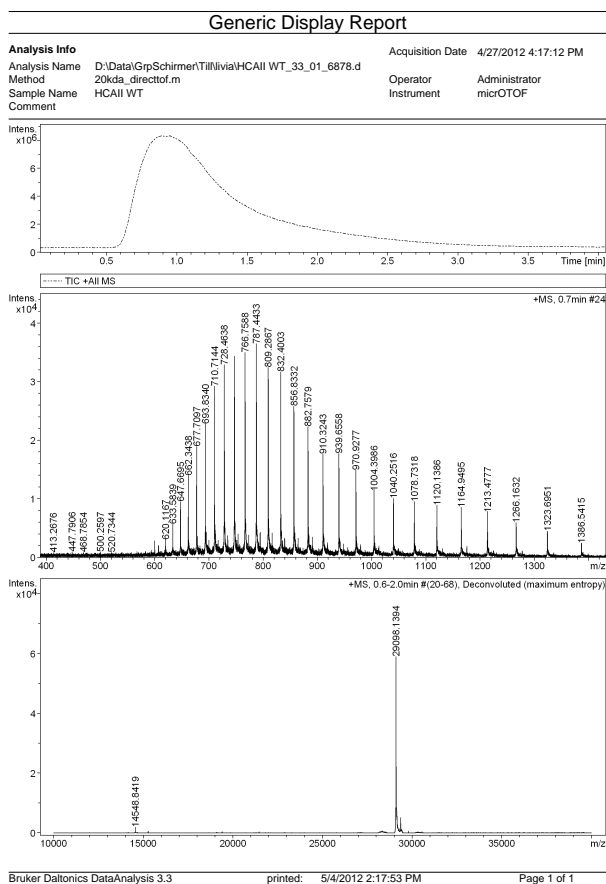
Analysis Name	FM000036.d	Acquisition Date	06/13/12 14:13:24
Method	Copy of wdw130-1.MS	Operator	Administrator
Sample Name	FM596	Instrument	esquire3000plus_01096
Comment			

Acquisition Parameter

Ion Source Type	ESI	Ion Polarity	Positive	Alternating Ion Polarity	off
Mass Range Mode	Std/Normal	Scan Begin	100 m/z	Scan End	1000 m/z
Capillary Exit	148.4 Volt	Skim 1	40.0 Volt	Trap Drive	73.5
Accumulation Time	162 μ s	Averages	5 Spectra	Auto MS/MS	off

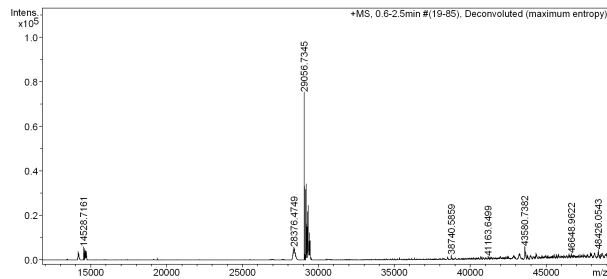
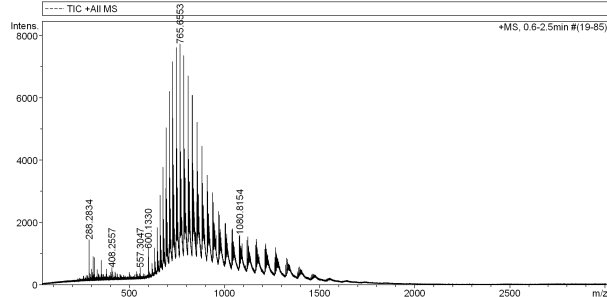
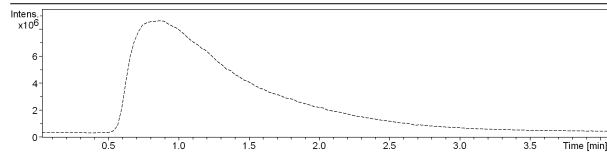


Human Carbonic Anhydrase II isozymes



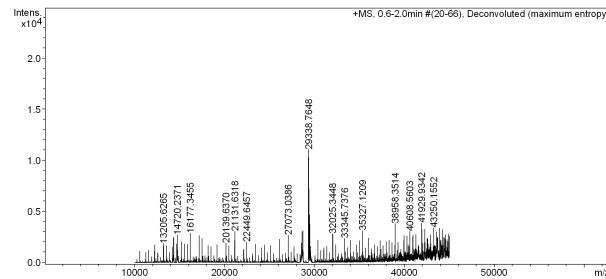
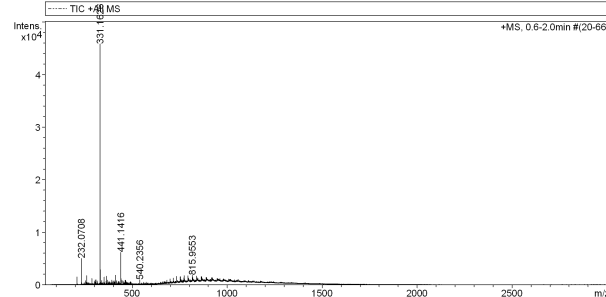
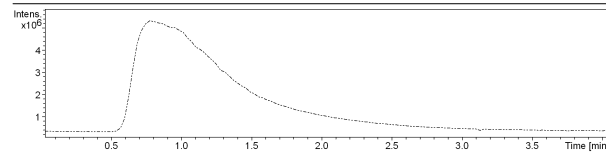
Generic Display Report

Analysis Info
 Analysis Name D:\Data\GrpSchimer\Tilfelisah\CAII 191A_27_01_6899.d
 Method 20kda_directof.m
 Sample Name hCAII 191A
 Comment
 Acquisition Date 5/16/2012 10:29:38 AM
 Operator Administrator
 Instrument micrOTOF



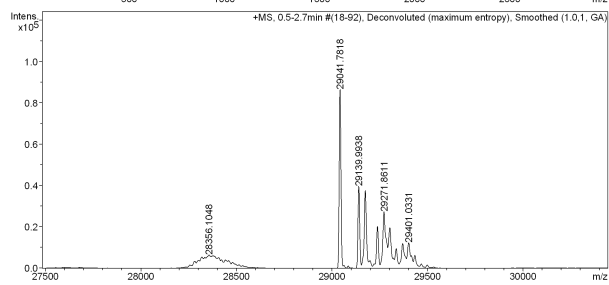
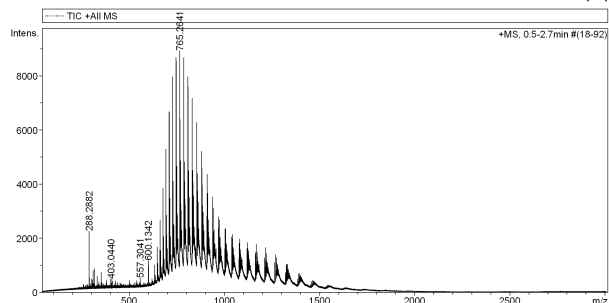
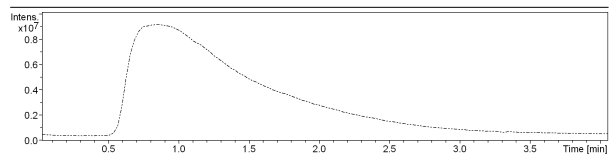
Generic Display Report

Analysis Info
 Analysis Name D:\Data\GrpSchimer\Tilfelisah\CAII H64A_24_01_6896.d
 Method 20kda_directof.m
 Sample Name hCAII H64A
 Comment
 Acquisition Date 5/16/2012 10:12:23 AM
 Operator Administrator
 Instrument micrOTOF



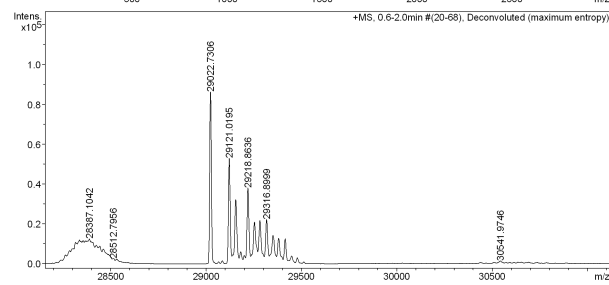
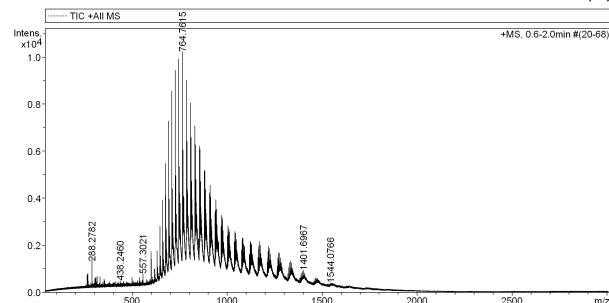
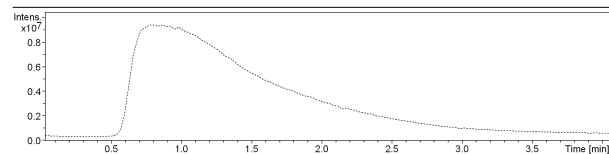
Generic Display Report

Analysis Info
 Analysis Name D:\Data\GrpSchirmer\Tilfelisa\hCAII K170A_31_01_6903.d
 Method 20kda_directof.m
 Sample Name hCAII K170A
 Comment
 Acquisition Date 5/16/2012 10:52:49 AM
 Operator Administrator
 Instrument micrOTOF



Generic Display Report

Analysis Info
 Analysis Name D:\Data\GrpSchirmer\Tilfelisa\hCAII F131A_30_01_6902.d
 Method 20kda_directof.m
 Sample Name hCAII F131A
 Comment
 Acquisition Date 5/16/2012 10:47:04 AM
 Operator Administrator
 Instrument micrOTOF



Curriculum vitae

Nationality: Swiss

Date of birth: 30th of September, 1984

Education

- **Oct. 2008 - Sep. 2012:** Ph.D. candidate in Inorganic Chemistry, Basel/Switzerland
> **Supervisor:** Prof. Dr. Thomas R. Ward
- **Oct. 2006 - Dec. 2007:** M.Sc. in Chemistry, Basel/Switzerland
> **Supervisor:** Prof. Dr. Helma Wennemers
- **Oct. 2003 - Oct. 2006:** B.Sc. in Chemistry, Neuchâtel/Switzerland
- **June 2003:** Certificat de Maturité, La Chaux-de-Fonds/Switzerland

Professional experience

- **March 2008:** Training Course, Basel/Switzerland
> **Supervisor:** Dr. Jessica Bernard
Clariant Analytical Services MuttENZ, Clariant AG, Basel/Switzerland
- **April 2008 - Sep. 2008:** Training Course, Basel/Switzerland
> **Supervisor:** Dr. René Hermatschweiler
Van Bearle AG, Basel/Switzerland

Other skills

- **September 2011:** 31th REGIO-Symposium, Sornetan/Switzerland
> Main Organiser
- **Oct. 2008 - Sep. 2012:** Teaching assistant
> First year Pharmaceutical Science students

The following lecturers contributed to my education:

University of Neuchâtel: Prof. Dr. Robert Deschenaux, Prof. Dr. Reinhard Neier, Prof. Dr. Thomas R. Ward, Prof. Dr. Georg Süss-Fink, Prof. Dr. Raphael Tabacchi, Prof. Dr. Thomas Bürgi, Prof. Dr. Fritz Stoeckli, Prof. Dr. Helen Stoeckli-Evans, Prof. Dr. Piero Martinoli, Prof. Dr. François Sigrist, Prof. Dr. Martin Burkhard, Prof. Dr. Bruno Betschart, Dr. Claude Saturnin, Dr. Sylvain Burger, M. Marc Heyraud.

University of Basel: Prof. Dr. Helma Wennemers, Prof. Dr. Markus Meuwly, Prof. Dr. Matthias Hamburger, Prof. Dr. Angelo Vedani, Prof. Dr. Karl Gademann, Prof. Dr. Edwin Constable, Prof. Dr. Andreas Pfaltz, Prof. Dr. Wolfgang Meier, Prof. Dr. Giese Bernd, Prof. Dr. Thomas R. Ward, PD Dr. Daniel Häusinger.

Cover picture: X-ray structure of [(cp*)Ir(**6**)Cl]Cl \subset WT hCA II, PDB code 3ZP9.